HEINRICH HEINE
UNIVERSITÄT DÜSSELDORF

Regulation and assembly of the cytochrome bc_1-aa_3 supercomplex in *Corynebacterium glutamicum*

Inaugural dissertation

for the attainment of the title of doctor
in the Faculty of Mathematics and Natural Sciences
at the Heinrich Heine University Düsseldorf

presented by

Cedric-Farhad Davoudi

born in Iserlohn

Jülich, February 2019

The thesis in hand has been conducted at the Institute of Bio- and Geosciences IBG-1: Biotechnology, Forschungszentrum Jülich, from December 2015 until February 2019 under the supervision of Prof. Dr. Michael Bott and Dr. Meike Baumgart.

Published by permission of the
Faculty of Mathematics and Natural Sciences at
Heinrich Heine University Düsseldorf.

Supervisor: Prof. Dr. Michael Bott
Institute of Bio- and Geosciences
IBG-1: Biotechnology
Forschungszentrum Jülich GmbH

Co-supervisor: Prof. Dr. Georg Groth
Institute of Biochemical Plant Physiology and Bioeconomy
Science Center (BioSC)
Heinrich Heine University Düsseldorf

Date of oral examination: 16.05.2019

Results described in this dissertation have been published in the following original publications or are summarized in manuscripts which are submitted or will be submitted soon:

Morosov, X.*, **Davoudi, C.-F.***, Baumgart, M., Brocker, M. and Bott, M. (2018) The copper-deprivation stimulon of *Corynebacterium glutamicum* comprises proteins for biogenesis of the actinobacterial cytochrome bc_1-aa_3 supercomplex. *J. Biol. Chem.*
doi.org/10.1074/JBC.RA118.004117
*Shared first author

Davoudi, C.-F., Baumgart, M. and Bott, M. (2019) Identification of Surf1 as an assembly factor of the cytochrome bc_1-aa_3 supercomplex of *Actinobacteria*. *Biochim. Biophys. Acta, Bioenerg., Submitted*

Keppel, M.*, **Davoudi, C.-F.*,** Filipchyk, A. *, Viets, U., Pfeifer, E., Polen, T., Baumgart, M., Bott, M. and Frunzke, J. (2019) HrrSA orchestrates a systemic response to heme and determines prioritisation of terminal cytochrome oxidases. *To be submitted*
*Shared first author

Abbreviations

Δ	Deletion
a.u.	Arbitrary units
ATCC	American Type Culture Collection
ATP	Adenosine triphosphate
BCS	Bathocuproine disulfonate
Bp	Base pairs
BHI(S)	Brain Heart Infusion (+Sorbitol)
CA	Catalytic domain
DHp	Dimerization and histidine phosphotransfer domain
Da	Dalton
ECF	Extracytoplasmic function
et al.	*et alii*
EMSA	Electrophoretic mobility shift assay
HK	Histidine kinase
IPTG	Isopropyl-β-D-thiogalactopyranoside
Kan^R	Kanamycin resistant
K_D	Dissociation constant
LB	Lysogeny Broth
M	Molar (mol/l)
NAD+/NADH	Nicotinamide adenine dinucleotide, oxidized/reduced
OCS	One-component system
OD_{600}	Optical density at 600 nm
PBS	Phosphate-buffered saline
PMF	Proton motive force
RBS	Ribosome binding site
REC	Receiver domain
RNAP	RNA polymerase
ROS	Reactive oxygen species
rpm	Revolutions per minute
RR	Response regulator
STP	Signal transduction protein
TCS	Two-component system
TMD	Transmembrane domain
TPM	Transcripts per million
v/v	Volume per volume
wt	Wild type
w/v	Weight per volume

Further abbreviations not included in this section are according to international standards, as, for example listed in the author guidelines of the *FEBS Journal*.

Content

1 Summary

1.1 Summary English

The synthesis of aerobic respiratory chains requires cofactors such as heme and copper and chaperones involved in the biogenesis of the enzyme complexes. The Gram-positive soil bacterium *Corynebacterium glutamicum* possesses a branched aerobic respiratory chain comprising, besides several dehydrogenases reducing menaquinone to menaquinol, a copper-dependent cytochrome bc_1-aa_3 supercomplex and cytochrome *bd* quinol oxidase. The cytochrome bc_1-aa_3 supercomplex is characteristic for aerobic *Actinobacteria* and the major generator of proton-motive force, but knowledge on its assembly or regulation is very limited. In this thesis, assembly factors involved in copper and heme insertion and regulatory proteins involved in expression control of respiratory chain components were identified and characterized. The following results were obtained:

(i) Identification of the copper-deprivation stimulon led to the discovery of the two proteins Cg2699 (***c***opper ***t***ransport and ***i***nsertion ***p***rotein, CtiP) and Cg1884 (CopC). CtiP contains 16 predicted transmembrane helices and shows sequence similarity to the copper-transporter CopD and the cytochrome biogenesis chaperone CtaG. Deletion of *ctiP* resulted in a strong growth defect in standard glucose minimal medium (CGXII) resembling a cytochrome aa_3 oxidase-deficient strain. Furthermore, the Δ*ctiP* strain exhibited an increased copper-tolerance, suggesting a copper-transporting function. Transcriptome analysis revealed an induction of the copper-deprivation stimulon in the Δ*ctiP* strain under copper sufficiency. CopC is a secreted protein with a C-terminal transmembrane helix and harbors a Cu(II)-binding site. Deletion of *copC* resulted in a growth defect in BHI complex medium and improved growth under copper excess, also suggesting an involvement in copper-transport. The lack of either CtiP or CopC prevented co-purification of the subunits of the supercomplex, indicating a crucial role of both CtiP and CopC in the correct assembly of the supercomplex.

(ii) The search for further assembly factors of the bc_1-aa_3 supercomplex led to the discovery of Cg2460, a homologue of the heme *a* insertion chaperone Surf1. Loss of Surf1 caused a strong growth defect, comparable to the Δ*ctiP* strain, which could be complemented by several actinobacterial Surf1 homologues. Furthermore, the Δ*surf1* strain exhibited an increased copper sensitivity. Cytochrome measurements showed a reduction of cytochromes *c* and *a*, but an increase of cytochrome *d*. Analysis of membranes of the Δ*surf1* strain revealed the complete loss of cytochrome *c* oxidase activity. Lack of Surf1 prevented co-purification of the subunits of the supercomplex, indicating a crucial role in the correct assembly of the supercomplex. Transcriptome analysis revealed an induction of the copper-deprivation stimulon in the Δ*surf1* strain, suggesting an intertwined regulation of copper and heme homeostasis.

(iii) To assess the global cellular response towards heme, a genome-wide target profiling of the heme-sensing two-component system HrrSA was performed. Time-resolved ChAP-Seq analyses to follow DNA-binding by the response regulator HrrA encoded on a plasmid was coupled with time-resolved RNA-Seq analyses comparing a Δ*hrrA* strain with the wild type. This approach revealed 272 affected genes upon a 4 µM heme pulse under iron-starvation conditions. These targets include genes encoding proteins involved in heme biosynthesis, oxidative stress, cell envelope remodeling and the respiratory chain. Furthermore, HrrA-mediated repression of *sigC*, encoding the extracytoplasmic function sigma factor σ^C, which activates the cytochrome *bd* oxidase genes, leads to prioritised heme distribution to the cytochrome bc_1-aa_3 branch under heme sufficiency.

1.2 Summary German

Die Synthese aerober Atmungsketten erfordert Kofaktoren wie Häm und Kupfer sowie Chaperone, die an der Biogenese der Enzymkomplexe beteiligt sind. Das Gram-positive Bodenbakterium *Corynebacterium glutamicum* besitzt eine verzweigte aerobe Atmungskette, die neben mehreren Dehydrogenasen, die Menachinon zu Menachinol reduzieren, einen kupferabhängigen Cytochrom bc_1-aa_3-Superkomplex und eine Cytochrom *bd*-Chinoloxidase umfasst. Der Cytochrom bc_1-aa_3-Superkomplex ist für aerobe Actinobakterien charakteristisch und der Hauptgenerator der Protonen-motorischen Kraft. Das Wissen über dessen Assemblierung und Regulation ist sehr begrenzt. In dieser Arbeit wurden Assemblierungsfaktoren, die an der Insertion von Kupfer und Häm beteiligt sind, sowie regulatorische Proteine, die an der Expressionskontrolle von Komponenten der Atmungskette beteiligt sind, identifiziert und charakterisiert. Dabei wurden folgende Ergebnisse erzielt:

(i) Die Identifikation des Kupfermangel-Stimulons führte zur Entdeckung der beiden Proteine Cg2699 (***c**opper **t**ransport and **i**nsertion **p**rotein*, CtiP) und Cg1884 (CopC). CtiP enthält 16 vorhergesagte Transmembranhelices und weist Sequenzähnlichkeit zu dem Kupfer-Transporter CopD aus *Pseudomonas syringae* und dem Cytochrom-Biogenese-Chaperon CtaG aus *Bacillus subtilis* auf. Eine Deletion von *ctiP* resultierte in einem starken Wachstumsdefekt in Standard-Glukose-Minimal-Medium (CGXII), welcher dem eines aa_3-Oxidase-defizienten Stamm ähnelte. Darüber hinaus wies der Δ*ctiP*-Stamm eine erhöhte Kupfertoleranz auf, was auf eine Kupfer-transportierende Funktion hindeutet. Eine Transkriptom-Analyse offenbarte die Induktion des Kupfer-Mangel-Stimulons im Δ*ctiP*-Stamm trotz eines ausreichenden Kupfergehaltes im Medium. CopC ist ein sekretiertes Protein mit einer C-terminalen Transmembranhelix und besitzt eine Cu(II)-Bindestelle. Deletion von *copC* führte zu einem Wachstumsdefekt in BHI-Komplexmedium und verbessertem Wachstum unter Kupferstress, was ebenfalls auf eine Beteiligung am Kupfertransport hindeutet. Das Fehlen von CtiP oder CopC verhinderte die Ko-Aufreinigung von bc_1-aa_3-Supercomplex-Untereinheiten, was auf eine wichtige Rolle von CtiP und CopC bei der korrekten Assemblierung des Supercomplexes hindeutet.

(ii) Die Suche nach weiteren Biogenese-Chaperonen führte zur Identifizierung von Cg2460, einem Homolog des Häm-*a*-Insertions-Chaperons Surf1 aus *Paracoccus denitrificans*. Der Verlust von Surf1 führte zu einem starken Wachstumsdefekt in *C. glutamicum*, vergleichbar mit einem Δ*ctiP*-Stamm, welcher durch verschiedene aktinobakterielle Surf1-Homologe komplementiert werden konnte. Zudem wies der Δ*surf1*-Stamm eine erhöhte Kupfersensitivität auf. Messungen der Cytochrome zeigten eine Reduktion von Cytochrom *c* und *a*, jedoch eine Erhöhung von Cytochrom *d*. Analysen von Membranen des Δ*surf1*-Stamms zeigten den kompletten Verlust der Cytochrom *c*-Oxidase-Aktivität. Das Fehlen von Surf1 verhinderte die Ko-Aufreinigung der Untereinheiten des bc_1-aa_3-Superkomplexes, was auf eine wichtige Rolle bei der korrekten Assemblierung hindeutet. Eine Transkriptom-Analyse ergab die Induktion des Kupfer-Mangel-Stimulons im Δ*surf1*-Stamm, was für eine Kopplung von Häm- und Kupfer-Homöostase spricht.

(iii) Um die globale zelluläre Häm-Antwort zu charakterisieren, wurde eine Genom-weite Zielgen-Untersuchung des Häm-wahrnehmenden Zwei-Komponenten-Systems HrrSA durchgeführt. Zeitaufgelöste ChAP-Seq-Analysen zur Analyse der DNA-Bindung durch den auf einem Plasmid kodierten Antwortregulator HrrA wurden mit zeitaufgelösten RNA-Seq-Analysen gekoppelt, bei denen ein Δ*hrrA*-Stamm mit dem Wildtyp verglichen wurde. Dieser Ansatz offenbarte 272 beeinflusste Zielgene als Antwort auf einen 4 µM Häm-Puls unter Eisen-Mangel-Bedingungen. Die durch diese Zielgene kodierten Proteine sind beteiligt an der Häm-Biosynthese, an der Antwort auf oxidativen Stress, an der Remodellierung der Zellhülle sowie an der Atmungskette. Darüber hinaus führt die HrrA-vermittelte Repression von *sigC*, das für den *extracytoplasmic function σ factor* σ^C kodiert, der u.a. die Expression der Cytochrom *bd*-Oxidase-Gene aktiviert, zu einer Priorisierung der Häm-Verteilung in Richtung des Cytochrom bc_1-aa_3-Zweigs der Atmungskette bei ausreichender Häm-Versorgung.

2 Introduction

2.1 Aerobic respiration in bacteria

Aerobic chemoheterotrophic bacteria oxidize organic material, such as glucose, with oxygen as terminal electron acceptor (Baron, 1996; Simon *et al.*, 2008). Initially, the carbon sources are oxidized e.g. in glycolysis and the tricarboxylic acid (TCA) cycle to carbon dioxide and the resulting reducing equivalents are transferred to oxygen *via* the membrane-bound respiratory chain (Baron, 1996). In the first steps, the reducing equivalents (e.g. NADH) are transferred *via* various dehydrogenases to quinones, either ubiquinone or menaquinone (Figure 1). Reoxidation of the reduced quinones is catalyzed either by quinol oxidases, such as cytochrome bo_3 oxidase or cytochrome *bd* oxidase, or by a cytochrome bc_1 complex and a cytochrome *c* oxidase (Figure 1) (Trumpower, 1990; Trumpower and Gennis, 1994; Yap *et al.*, 2010). Several enzymes of the respiratory chain can couple electron transfer to the generation of proton motive force (PMF) by transferring protons from the cytoplasm to the extracytoplasmic space (Simon *et al.*, 2008). The PMF then serves as driving force for many active transport processes and for the generation of ATP by the F_1F_0-ATP synthase (Mitchell, 1961; Poole, 2000). Most aerobic bacteria possess two or even more terminal oxidases with different properties, allowing adaption to changing environmental conditions (Richardson, 2000).

In the context of this thesis, three respiratory enzymes are of particular interest, the cytochrome bc_1 complex, cytochrome *c* oxidase, and cytochrome *bd* oxidase (Capaldi, 1990; Trumpower, 1990; Borisov *et al.*, 2011). All of these are multisubunit complexes with several different cofactors and prosthetic groups. The bc_1 complex contains two heme *b* groups, one heme c_1 group, and a 2Fe-2S cluster (Trumpower, 1990). Cytochrome *c* oxidase typically contains a Cu_A center with two copper ions, one heme *a* group, and the heme a_3/Cu_B catalytic center, where oxygen is reduced to water (Capaldi, 1990). Dedicated assembly proteins guide the insertion of these cofactors and heme groups into the apo-proteins, such as the Surf1 protein initially identified in mammals and described to be involved in heme a_3 insertion (Zhu *et al.*, 1998; Smith *et al.*, 2005; Hannappel *et al.*, 2012).

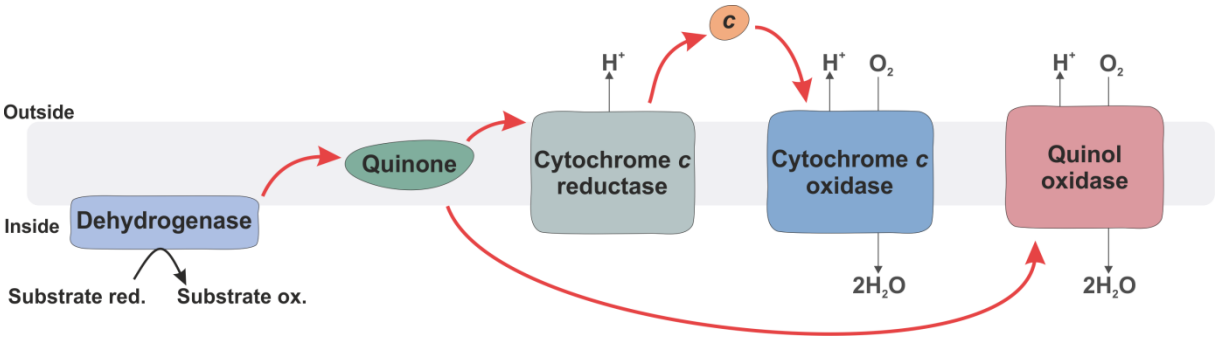

Figure 1: Schematic overview of a respiratory chain with O_2 as terminal electron acceptor. Depicted is the initial electron transfer from substrate-oxidizing dehydrogenases to quinones, which distribute the electrons towards a cytochrome *c* reductase and cytochrome *c* oxidase or a quinol oxidase. The terminal oxidases use these electrons for reduction of O_2 to $2H_2O$ and the generation of a electrochemical proton gradient over the membrane (proton motive force, PMF). Electron transfer is indicated by red arrows. *c* indicates soluble cytochrome *c*.

2.2 The respiratory chain of *C. glutamicum*

Corynebacterium glutamicum is a Gram-positive soil bacterium and a member of the *Actinobacteria*, one of the largest phyla of bacteria consisting of 57 families. These include many medically important human pathogens such as *Mycobacterium tuberculosis*, *Mycobacterium smegmatis* and *Corynebacterium diphtheriae* (Kinoshita *et al.*, 1957; Stackebrandt *et al.*, 1997; Gao and Gupta, 2012; Lewin *et al.*, 2016) as well as various biotechnologically relevant species, such as antibiotics-producing Streptomycetes (de Lima Procópio *et al.*, 2012). As *C. glutamicum* is used for production of about five million tons of amino acids annually, predominantly L-glutamate and L-lysine (Becker *et al.*, 2011; Wendisch *et al.*, 2014), it has high industrial relevance and has become a model organism for white biotechnology (Eggeling and Bott, 2005; Burkovski, 2008; Yukawa and Inui, 2013; Burkovski, 2015). Understanding of the energy metabolism of *Actinobacteria* is not only important for biotechnological production purposes, but has become an important medical research topic as proteins involved in respiration and oxidative phosphorylation are interesting targets for antibiotics (Andries *et al.*, 2005; Balemans *et al.*, 2012; Bald *et al.*, 2017; Berube and Parish, 2017).

Although aerobic conditions are favored, the facultative anaerobic *C. glutamicum* exhibits limited growth without oxygen using nitrate respiration or mixed-acid fermentation (Nishimura *et al.*, 2007; Takeno *et al.*, 2007; Michel *et al.*, 2015). For aerobic respiration *C. glutamicum* uses a branched respiratory chain, with one branch composed of a

cytochrome bc_1 complex and an aa_3 oxidase and the second branch consisting of a cytochrome *bd* quinol oxidase (Figure 2) (Bott and Niebisch, 2003). The only respiratory quinones present in *C. glutamicum* are menaquinones (MK), of which MK-9 is the most abundant one, receiving electrons from donors such as malate:quinone oxidoreductase or NADH dehydrogenase (Figure 2) (Collins *et al.*, 1977; Bott and Niebisch, 2003). A unique feature first identified in *C. glutamicum* and later found to be characteristic of all aerobic *Actinobacteria* is the presence of a bc_1-aa_3 supercomplex with a diheme cytochrome c_1, which is the only *c*-type cytochrome in this organism (Bott and Niebisch, 2003; Niebisch and Bott, 2003; Kao *et al.*, 2016). Based on proton translocation numbers the bc_1-aa_3 supercomplex ($6H^+/2e^-$) is more efficient compared to the cytochrome *bd* oxidase ($2H^+/2e^-$) (Bott and Niebisch, 2003). Purification of the supercomplex revealed the following subunits of the bc_1 complex: QcrA (Rieske iron-sulfur protein), QcrB (cytochrome *b*), and QcrC (cytochrome c_1) and of the aa_3 oxidase: CtaC (subunit II), CtaD (subunit I), CtaE (subunit III) and CtaF (subunit IV) (Bott and Niebisch, 2003; Niebisch and Bott, 2003). Additionally, proteins co-purified with the supercomplex could be identified, namely Cg2949 (secreted lipoprotein), Cg2211 (integral membrane protein), and Cg2444 (cytosolic protein) (Niebisch and Bott, 2003).

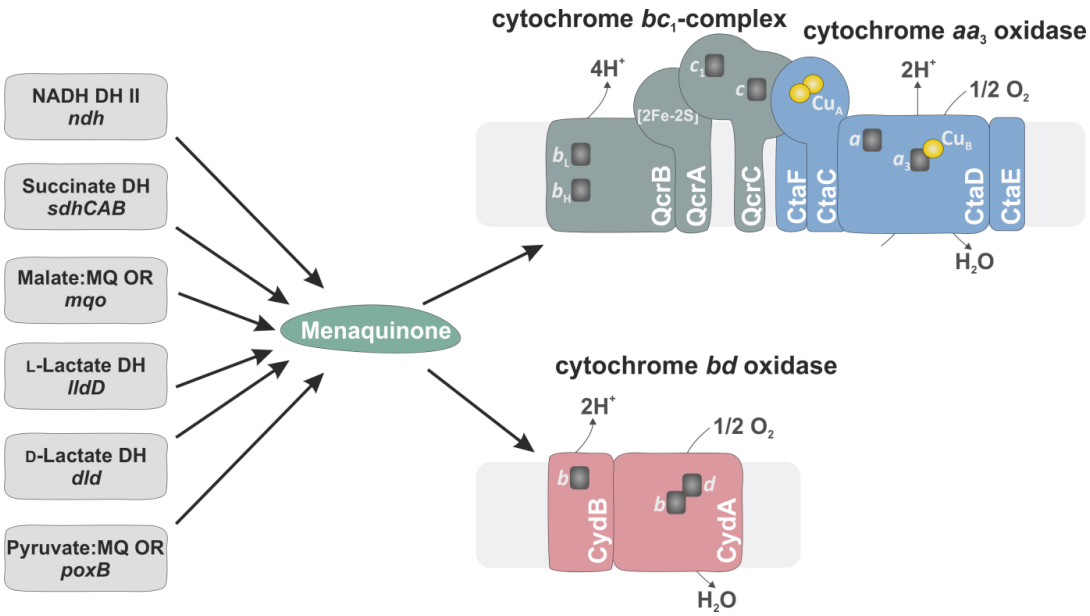

Figure 2: Composition of the aerobic respiratory chain of *C. glutamicum*. The schematic representation illustrates the components involved in electron transport towards O_2-reducing terminal oxidases, consisting of the cytochrome bc_1-aa_3 branch and the cytochrome *bd* branch (modified after (Bott and Niebisch, 2003)). Dark gray squares indicate heme groups, yellow circles indicate copper ions. Electron routes are represented by black arrows. MQ: menaquinone, DH: dehydrogenase, OR: oxidoreductase.

Due to a lacking growth phenotype of strains in which the genes for the co-purified proteins were deleted, an involvement of these proteins in supercomplex biogenesis can be excluded and their function is unknown at present. In contrast, the deletion of the *qcr* operon encoding bc_1 complex subunits or deletion of the *ctaD* gene encoding subunit I of the aa_3 oxidase led to a strong growth defect in glucose minimal medium and in complex medium, resulting not only in a decreased growth rate but also in a lower final optical density (Niebisch and Bott, 2001). This growth phenotype could be attributed to the lack of a functional bc_1-aa_3 supercomplex (Niebisch and Bott, 2003). Furthermore, deletion of *ctaD* was found to cause a significant decrease of the H^+/O ratio and a 14% lower cell yield in complex medium (Kabashima *et al.*, 2009). Likewise, loss of CtaD resulted in a similar growth defect in *M. smegmatis* indicating that the bc_1-aa_3 branch is the main route in *Actinobacteria* (Bott and Niebisch, 2003; Matsoso *et al.*, 2005; Kabashima *et al.*, 2009; Kao *et al.*, 2016). Analysis of the redox potentials of prosthetic groups of the supercomplex in *C. glutamicum* showed that whereas electron transfer rates from *c* hemes to Cu_A lasted 0.1 – 1 ms, the time constant for oxidation of the *b* hemes was 6.5 ms, thereby representing the rate-limiting step for the overall oxidations (Graf *et al.*, 2016).

Recent interest in the structure of the supercomplex resulted not only in the appearance of models based on homology and electron microscopy (EM) (Kao *et al.*, 2016), but also solved cryogenic electron microscopy (cryo-EM) structures of the supercomplex of *M. smegmatis* (Figure 3) (Gong *et al.*, 2018; Wiseman *et al.*, 2018). In two separate studies, these cryo-EM structures revealed the dimerized architecture of the supercomplex (Gong *et al.*, 2018; Wiseman *et al.*, 2018) and confirmed the association of homologues of Cg2211 (PRSAF1) and Cg2949 (LpqE) (Gong *et al.*, 2018). Additionally, the association of a periplasmic superoxide dismutase (SOD) to cytochrome *b* was found in both structures (Figure 3). A homologue of this SOD could not be found in *C. glutamicum*. It was postulated, that SOD enables detoxification of superoxide radicals formed by the bc_1 complex (Gong *et al.*, 2018; Wiseman *et al.*, 2018). Furthermore, one of the structures revealed two conformations of cytochrome c_1, one connecting and one disconnecting electron transfer from the bc_1 complex to the aa_3 oxidase (Figure 3) (Wiseman *et al.*, 2018). This conformational change was postulated to regulate supercomplex activity during growth phases (Wiseman *et al.*, 2018).

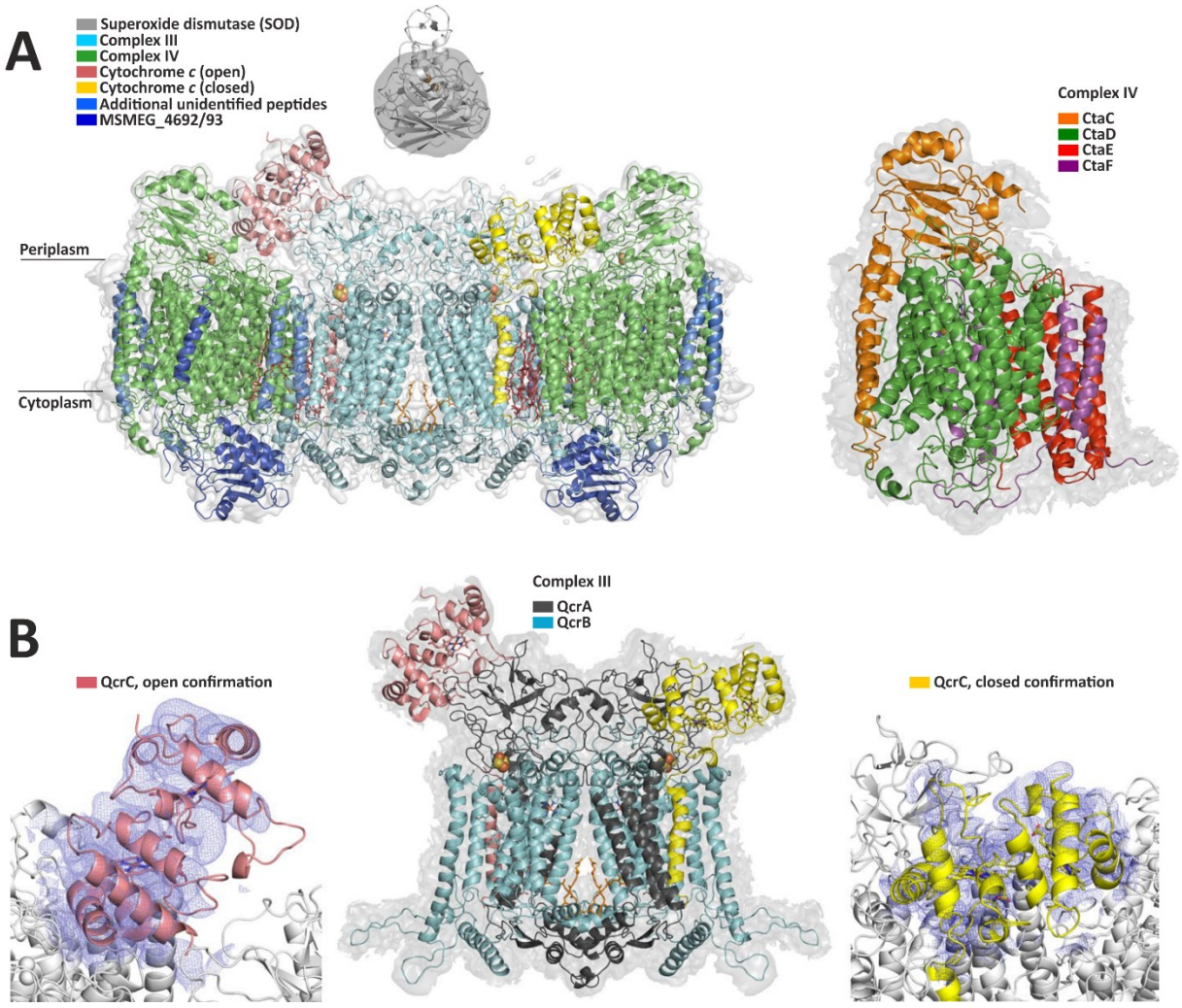

Figure 3: Structure of the cytochrome bc_1-aa_3 supercomplex of *M. smegmatis*. (A) The side view cryo-EM map depicts the overall architecture of the complex III-complex IV dimer including accessory proteins (left) and a detailed overview of complex IV (right). (B) Complex III is shown as a dimer (middle) harboring the diheme cytochrome c_1 domain in the open (left) and closed (right) conformation, respectively (modified after (Wiseman *et al.*, 2018)).

The alternative cytochrome *bd* oxidase can directly oxidize menaquinol and is encoded by the *cydABDC* operon of which two genes code for subunits of the oxidase (*cydA*, *cydB*) and two genes encode an ABC transporter necessary for biogenesis of the oxidase (Bott and Niebisch, 2003; Kalinowski *et al.*, 2003). Although, as described above, the *bd* oxidase is less efficient in proton translocation and generation of PMF, it has a higher oxygen affinity compared to the bc_1-aa_3 supercomplex and is therefore described to play an important role under oxygen deprivation (Bott and Niebisch, 2003; Kabus *et al.*, 2007). The deletion of the *cydAB* genes in *C. glutamicum* did not have an impact on the growth rate, but resulted in a 40% lower biomass yield compared to the wild type (wt) (Kabus *et al.*, 2007; Kabashima *et al.*, 2009). Overexpression of the *cydABDC* operon results in a decreased growth rate (45%)

and biomass yield (65%), suggesting a rerouting of electrons to the less efficient cytochrome *bd* branch (Kabus *et al.*, 2007). A *C. glutamicum* strain lacking both the bc_1 complex genes and *bd* oxidase genes, named DOOR (devoid of oxygen respiration), exhibited a very strong growth defect in aerobic glucose minimal medium, which could partially be overcome by the addition of peptone (Koch-Koerfges *et al.*, 2013). Although the DOOR strain was incapable of respiration, indicating a lack of further oxidases, the PMF was only decreased by 30% compared to the wild type. It was postulated that the generation of PMF could occur *via* the succinate:menaquinone oxidoreductase by reducing fumarate with MKH_2 or through the F_1F_0-ATP synthase by coupling ATP hydrolysis to proton export (Koch-Koerfges *et al.*, 2013).

2.3 Environmental stimulus perception in *C. glutamicum*

In nature, nutrient supply fluctuates and as a prerequisite for a functioning respiratory chain microorganisms have to identify altering growth conditions. As a soil bacterium, *C. glutamicum* further has to be able to recognize substrates and differentiate them from toxins. This capability is crucial for survival and therefore bacteria have evolved various mechanisms for perceiving stimuli in their environment. Basis for these systems are signal transduction proteins (STPs) sensing the environment followed by a rapid cellular response, usually in the form of expression level changes.

2.3.1 One-component systems

One-component systems (OCS) represent the simplest signal transduction systems and are composed of a receiver domain responsible for stimulus perception and a transmitter domain typically consisting of a helix-turn-helix DNA-binding domain to repress or activate transcription of target genes (Ulrich *et al.*, 2005). The first regulator described for *C. glutamicum* was LysG, which activates the expression of the lysine exporter gene *lysE* upon binding of the effector molecule L-lysine or L-arginine (Bellmann *et al.*, 2001). Since then, computational predictions stated 158 potential regulators, constituting 5.3 % of the predicted protein-coding regions in the genome of *C. glutamicum* (Brinkrolf *et al.*, 2007). Of these, 70 OCSs (excluding σ factors) with knowledge about regulatory interactions have been described, comprising 60 activators and repressors with additional 10 regulators possessing a dual regulatory function (Brinkrolf *et al.*, 2010).

2.3.2 Extracytoplasmic function σ factors

Another variation of these single protein regulators are extracytoplasmic function (ECF) σ factors. This subfamily of σ^{70} factors is also a component of the RNA polymerase holoenzyme and represents a large group of alternative σ factors. However, the composition differs as ECF σ factors lack two of the four conserved σ^{70} subunits and only consist of σ_2 and σ_4 necessary for RNA polymerase core enzyme binding and promoter recognition (Österberg *et al.*, 2011). ECF σ factors are usually bound by their cognate anti-σ factor, which upon stimulus detection dissociates, thereby releasing the ECF σ factor to bind to a target promoter and assemble with the RNA polymerase core enzyme (Helmann, 1999; Staron *et al.*, 2009; Österberg *et al.*, 2011; Mascher, 2013). Due to the displacement of an already bound σ factor the ECF σ factors can redirect the RNA polymerase to target promoters (Helmann, 1999; Helmann, 2002; Paget, 2015). The number of ECF σ factors within a species varies from 0 (e.g. Chlamydiae) to over 30 (e.g. *Streptomyces* spp.) (Staron *et al.*, 2009). *C. glutamicum* possesses five ECF σ factors: σ^C, σ^D, σ^E, σ^H and σ^M (Kim *et al.*, 2005; Nakunst *et al.*, 2007; Park *et al.*, 2008; Ehira *et al.*, 2009; Ikeda *et al.*, 2009). σ^M regulates the expression of 23 genes, including the *suf* operon involved in the assembly of iron-sulfur clusters, thioredoxins, chaperones, and genes involved in the heat shock response (Nakunst *et al.*, 2007). In contrast to σ^M, for σ^E (surface stress response) and σ^H (oxidative and heat stress response) cognate anti-σ factors have been described (CseE and RshA, respectively), encoded downstream of their corresponding ECF σ factor gene (Kim *et al.*, 2005; Park *et al.*, 2008; Ehira *et al.*, 2009; Busche *et al.*, 2012). Recently, the regulon of σ^D was uncovered for *C. glutamicum* strains ATCC13032 and R, consisting of genes involved in cell wall integrity (Taniguchi *et al.*, 2017; Toyoda and Inui, 2018). The regulon of σ^C comprises genes for heme biosynthesis, respiratory chain components, copper-dependent genes, and iron-regulated genes (Toyoda and Inui, 2016). Although the stimulus of σ^C is not known it was postulated that oxidative stress could induce the σ^C response (Toyoda and Inui, 2016).

2.3.3 Two-component systems

Although OCFs still are the most abundant form of signal-transduction in prokaryotes they are usually only capable of sensing cytoplasmic stimuli (Ulrich *et al.*, 2005). A more complex mode of signal perception is the two-component system (TCS), which separates the receiver and transmitter domain of OCFs. TCSs are typically composed of a membrane-bound sensor

kinase or histidine kinase (HK), which perceives stimuli, and a cognate response regulator (RR) responsible for signal transmission (Figure 4) usually resulting in transcriptional regulation of target genes (Hoch and Silhavy, 1995; Inouye and Dutta, 2003).

The architecture of a typical HK consists of an N-terminal transmembrane sensor domain (TMD) and a C-terminal cytoplasmic transmitter domain harboring a kinase core. Whereas the sensor domain can vary and is highly specialized, the kinase domain is conserved and consists of a dimerization and histidine-phosphotransfer domain (DHp; HisKA in PFAM database) and a C-terminal catalytical and ATP binding domain (CA; HATPase_c domain in PFAM) (Figure 4) (Punta *et al.*, 2012; Finn *et al.*, 2014). Additional domains such as PAS, HAMP or GAF can be located between the TMD and DHp domain (Galperin *et al.*, 2001). The composition of a classical RR consists of an N-terminal receiver domain (REC) (response_reg domain in PFAM) and a C-terminal effector or output domain (OPD). Stimulus perception leads to autophosphorylation of the HK which is caused by the CA domain binding ATP and transferring the γ-phosphoryl group of the ATP to the conserved histidine residue in the DHp domain of the second monomer (Stock *et al.*, 2000). Subsequent transfer of this phosphoryl group to a conserved aspartate residue within the REC domain of the RR leads to a conformational change and (in most cases) activates the RR leading to a stimulus-specific activation or repression of target genes (Figure 4) (Stock *et al.*, 2000; Mascher *et al.*, 2006).

To ensure pathway specificity in signal transduction, TCS have evolved several mechanisms. One is molecular recognition which relies on co-evolved interface residues in HKs and RRs conferring HKs the ability to discriminate between cognate and foreign RRs (Skerker *et al.*, 2008; Capra and Laub, 2012; Podgornaia and Laub, 2013). A different method to avoid cross-talk between TCSs is substrate competition that is based on a higher stoichiometry of RR to HK and therefore outnumbering non-cognate RRs (Siryaporn and Goulian, 2008; Groban *et al.*, 2009). HKs can have the ability to not only phosphorylate RRs but also very specifically dephosphorylate their cognate RR (Huynh and Stewart, 2011). This bifunctionality of HKs was also observed for the two TCSs HrrSA and ChrSA of *C. glutamicum*, which albeit both sensing heme differ in their output as one is used for heme utilization and the other for heme detoxification (see 2.5) (Frunzke *et al.*, 2011; Heyer *et al.*, 2012; Hentschel *et al.*, 2014). Due to the similarity between these homologous TCSs HrrS and ChrS exhibited dephosphorylation solely of their cognate RR HrrA and ChrA, preventing cross-talk between the TCSs (Hentschel *et al.*, 2014).

Moreover, *C. glutamicum* possesses the two TCSs CopSR, responsible for the copper-stress response (see 2.4), and CgtSR5, whose function could not yet be discerned (Schelder *et al.*, 2011; Bott and Brocker, 2012). Similar to HrrSA and ChrSA, these TCSs share a high sequence identity (CopS/CgtS5 56%; CopR/CgtR5 62%) and presumably resulted from a gene duplication. Moreover, nine additional TCSs are present in the genome of *C. glutamicum* of which some have been further characterized. These include CitAB, regulating citrate utilization, MrtBA, responsible for osmoregulation and cell wall stress and PhoSR, involved in the response to phosphate starvation (Schaaf and Bott, 2007; Brocker *et al.*, 2009; Brocker *et al.*, 2011; Bott and Brocker, 2012).

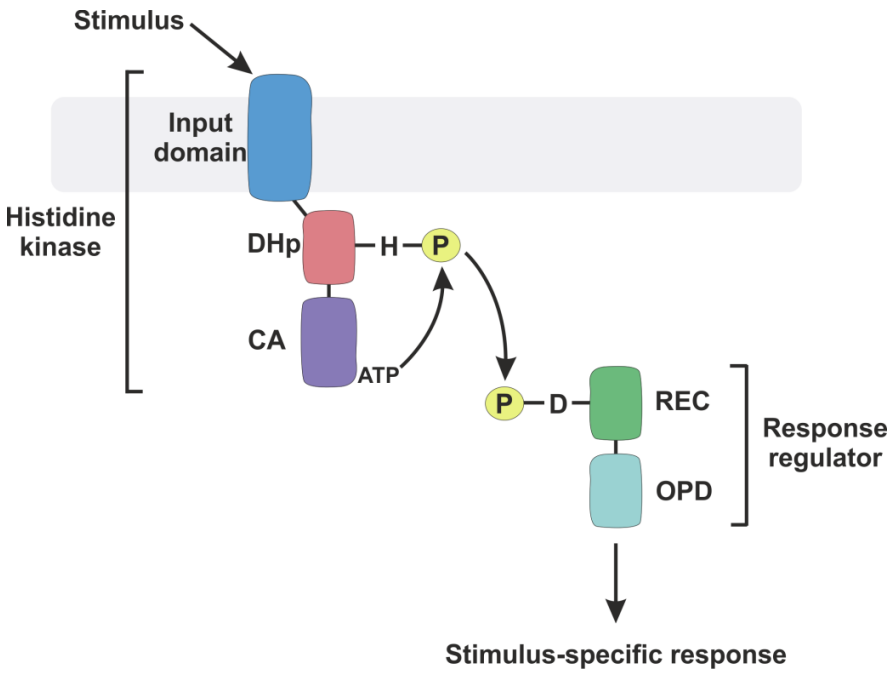

Figure 4: Overview of a TCS signal transduction system. Stimulus recognition by the input domain of an often membrane-bound histidine kinase triggers the phosphorylation of a specific histidine residue in the dimerization and histidine phosphotransfer domain (DHp). This transfer of a phosphoryl group is mediated by the catalytic and ATP-binding domain (CA) of a second monomer. The phosphoryl group is subsequently transferred to a conserved aspartate residue in the receiver domain (REC) of the cognate response regulator. In this active form the output domain (OPD) can initiate a stimulus-specific response (modified after (Jensen *et al.*, 2002)).

2.4 Transcriptional regulation of terminal oxidases in *C. glutamicum*

The knowledge about transcriptional regulation of both the bc_1-aa_3 supercomplex and *bd* oxidase genes is still very limited and only a small number of involved regulators is known.

Under iron-limitation and presence of heme, a major activator for the *ctaE-qcrCAB* operon and *ctaD* gene is the response regulator HrrA of the two-component system HrrSA (see 2.3.3) (Figure 5) (Frunzke *et al.*, 2011). Furthermore, binding sites of the global regulator GlxR were found in the promoter regions of *ctaD* and *ctaCF*, which were tested by electrophoretic mobility shift assays and promoter-reporter analyses, confirming binding and transcriptional activation by the cAMP-binding GlxR regulator (Figure 5) (Toyoda *et al.*, 2011). The expression of the alternative cytochrome *bd* oxidase genes is dependent on OxyR, an oxidative-stress sensing regulator, which represses the operon (Teramoto *et al.*, 2013; Milse *et al.*, 2014). Expression is relieved under conditions of oxidative stress, when OxyR loses its DNA-binding ability. The only known activator for the *bd* oxidase branch genes is the ECF sigma factor σ^C (see 2.3.2), which activates the *cydABDC* operon and additionally functions as a repressor of the *ctaE-qcrCAB* operon (Figure 5) (Toyoda and Inui, 2016).

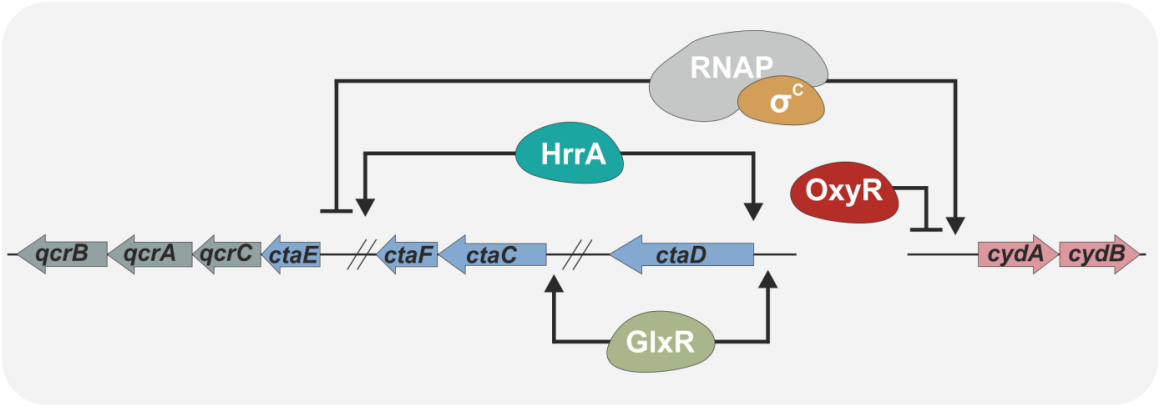

Figure 5: Transcriptional regulation of terminal oxidases in *C. glutamicum*. Depicted is the genomic composition of genes encoding subunits of the cytochrome bc_1 complex (gray), cytochrome aa_3 oxidase (blue) and cytochrome *bd* oxidase (pink), as well as their known regulators.

2.5 Heme and copper homeostasis in *C. glutamicum*

Metal ions are crucial components of respiratory pathways as several enzymes are strictly dependent on metal ions for functionality (Merchant and Helmann, 2012). Iron, mostly in the form of heme and iron-sulfur clusters, and copper are essential cofactors in the respiratory chain (see 2.1). Simultaneously, these metal ions represent toxic compounds for the cell as they lead to the formation of highly reactive oxygen species (ROS) causing cellular damage by reacting with DNA, proteins, and lipids (Yoshida *et al.*, 1993; Pierre and

Fontecave, 1999; Andrews *et al.*, 2003; Magnani and Solioz, 2007). Copper ions were even described to compete with and replace iron ions in enzymes, resulting in loss of functionality (Macomber and Imlay, 2009). Therefore, acquisition of iron and copper ions has to be strictly regulated.

The master regulator for iron homeostasis in *C. glutamicum* is DtxR which under conditions of iron sufficiency binds Fe^{2+} and in this form inhibits iron acquisition by repressing genes coding for several iron, heme, and siderophore importers (Brune *et al.*, 2006; Wennerhold and Bott, 2006). DtxR is also involved in iron preservation by activating genes coding for iron storage proteins ferritin and Dps (Brune *et al.*, 2006). Furthermore, DtxR represses several transcriptional regulator genes, such as *ripA*, encoding a repressor of genes for iron-containing proteins, and *hrrA*, encoding the above-mentioned response regulator of the TCS HrrSA crucial for heme utilization. Another direct target is *hmuO*, encoding a heme oxygenase, which is also repressed by DtxR (Wennerhold *et al.*, 2005; Wennerhold and Bott, 2006; Frunzke *et al.*, 2011). Repression of *hrrA* leads to the upregulation of heme biosynthesis genes which are direct targets of HrrA (Frunzke *et al.*, 2011; Heyer *et al.*, 2012). Iron-starvation conditions lead to the dissociation of Fe^{2+} from DtxR and thus its inactivation, resulting in derepression of the repressed target genes, such as *hrrA*, allowing the expression of heme utilization genes such as *hmuO*, which is directly activated by HrrA (Wennerhold and Bott, 2006). The homologous TCS ChrSA interferes with HrrSA in a heme-dependent manner and controls heme resistance by activation of *hrtBA*, encoding an ABC transporter responsible for heme export and thus detoxification (Heyer *et al.*, 2012; Hentschel *et al.*, 2014).

C. glutamicum possesses a number of iron- and heme-dependent proteins, however comparative genomics revealed only four cuproproteins: CtaC and CtaD (cytochrome aa_3 oxidase) and two multicopper oxidases (Cg1080, CopO) (Ridge *et al.*, 2008; Zhang and Gladyshev, 2010). A visible growth defect in *C. glutamicum* due to copper excess is apparent starting from 20 µM $CuSO_4$ (Schelder *et al.*, 2011). To ensure copper homeostasis, the organism harbors two characterized mechanisms for stringent copper-dependent gene regulation. Under copper excess conditions the TCS CopSR activates the expression of the copper detoxification system, including *copB*, coding for a copper-transporting ATPase, and *copO*, encoding a multicopper oxidase responsible for extracellular oxidation of Cu^{+} to the less toxic Cu^{2+} (Bott and Brocker, 2012). The other characterized regulator in *C. glutamicum*

involved in the establishment of copper homeostasis is the OCS CsoR (Schelder, 2011; Teramoto *et al.*, 2012). During absence of copper CsoR of *C. glutamicum* R acts as a repressor towards *copA* and *copB*, encoding P_{1B}-type ATPases (Teramoto *et al.*, 2012). Further targets have been described in *C. glutamicum* ATCC 13032 comprising copper chaperone genes (cg3402, cg3411), the cg3282-*copB* operon and a putative copper exporter gene (*ctpV*) (Schelder, 2011). Perception of copper results in the dissociation of CsoR from its targets, thereby activating them and conferring copper resistance to the organism (Schelder, 2011; Teramoto *et al.*, 2012).

2.6 Aims of this thesis

In contrast to eukaryotes and α-proteobacteria, information about cytochrome biogenesis of Actinobacteria is scarce. Therefore, the first part of this thesis was dedicated to the identification and characterization of proteins involved in the biogenesis of the cytochrome bc_1-aa_3 supercomplex of *C. glutamicum* with a specific focus on copper and heme. In a preceding study, copper starvation conditions had been used to identify candidates potentially involved in the assembly of the copper ions into the aa_3 oxidase. These studies led to the identification of two membrane proteins, Cg2699 (CtiP) and Cg1884 (CopC) and their initial characterization. In this thesis, these proteins were further analyzed with respect to their role in bc_1-aa_3 supercomplex assembly by analyzing cytochrome spectra, purification of the supercomplex, and cytochrome *c* oxidase activity measurements. Additionally, to find further proteins involved in the biogenesis of the bc_1-aa_3 supercomplex, individual deletion strains of all other genes found to be upregulated under copper starvation were constructed and analyzed with respect to growth under different copper conditions.

BLAST analyses led to the discovery of the potential Surf1 homologue Cg2460. Surf1 was previously shown to function as a heme *a* insertion chaperone in α-proteobacteria but had never been reported in Gram-positive bacteria including Actinobacteria. The second part of this thesis was therefore dedicated to the analysis of Cg2460, named Surf1 in the following. For this purpose, a *surf1* deletion strain was constructed and investigated with respect to growth behavior, global gene expression, influence on bc_1-aa_3 supercomplex assembly and cytochrome *c* oxidase activity. Furthermore, the conservation of Surf1 in other

actinobacterial species was analyzed and selected homologs were tested for conserved functionality.

A third part of this thesis involved experiments aiming at a detailed analysis of the characteristics of HrrA-dependent transcriptional regulation by time-resolved genome-wide target profiling using ChAP-Seq and RNA-Seq approaches.

3 Results

The major topic of this doctoral thesis was the investigation of biogenesis and regulation of the cytochrome bc_1-aa_3 supercomplex in *C. glutamicum*. The results of these studies have been summarized in a publication and two manuscripts, one of which has been submitted for publication and one of which will be submitted soon.

In the publication "The copper-deprivation stimulon of *Corynebacterium glutamicum* comprises proteins for biogenesis of the actinobacterial cytochrome bc_1-aa_3 supercomplex" the genome-wide analysis of genes with altered expression under copper starvation (copper-starvation stimulon) is described. The further characterization of this stimulon led to the discovery of the two proteins Cg2699 (CtiP) and Cg1884 (CopC). CtiP possesses 16 predicted transmembrane helices and shows sequence similarity to the copper-importer CopD of *Pseudomonas syringae* and to the cytochrome maturation chaperone CtaG of *Bacillus subtilis*. Deletion of *ctiP* resulted in a strong growth defect comparable to a *ctaD* deletion strain and simultaneously enabled higher resistance towards copper excess. In the *ctiP* deletion strain the copper-deprivation stimulon was induced under copper-sufficiency. CopC is a secreted protein harboring a C-terminal transmembrane domain and a Cu(II)-binding site. A *copC* deletion strain exhibited a growth defect on BHI agar plates and in liquid BHI medium but a higher resistance towards copper excess. Both the *ctiP* and *copC* deletion strain negatively impacted the assembly of the cytochrome bc_1-aa_3 supercomplex discernable by the disturbed co-purification of supercomplex subunits.

The manuscript "Identification of Surf1 as an assembly factor of the cytochrome bc_1-aa_3 supercomplex of *Actinobacteria*" describes the characterization of Cg2460, a homologue of the putative heme *a* insertion protein Surf1 previously only described in eukaryotes and Gram-negative bacteria. Deletion of *surf1* resulted in a strong growth defect, again comparable to strains lacking a functional bc_1-aa_3 supercomplex, which could be complemented using homologous genes of several actinobacterial species. Analysis of supercomplex formation exhibited loss of co-purified subunits, similar to the *ctiP* deletion. Cytochrome *c* oxidase activity measurements using isolated membranes of the *surf1*

deletion strain revealed complete loss of enzyme activity. Transcriptome analysis resulted in the upregulation of the copper-starvation stimulon in the *surf1* deletion.

The investigation of a genome-wide target profiling of the TCS HrrSA is described in the manuscript entitled “HrrSA orchestrates a systemic response to heme and determines prioritisation of terminal cytochrome oxidases”. Utilization of time-resolved omics methods (ChAP-Seq and RNA-Seq analysis) resulted in the identification of 272 genomic targets of HrrA under iron limitation and in the presence of 4 µM heme. This approach exposed a dynamic regulation of genes encoding for proteins in heme biosynthesis, oxidative stress, cell wall remodeling and the respiratory chain. Further, repression of *sigC*, encoding the ECF σ^C which was shown to activate cytochrome *bd* oxidase genes, reveals the prioritisation of the cytochrome bc_1-aa_3 branch *via* HrrA.

3.1 Author contributions

Morosov, X.*, Davoudi, C.-F.*, Baumgart, M., Brocker, M., and Bott, M. (2018). The copper-deprivation stimulon of *Corynebacterium glutamicum* comprises proteins for biogenesis of the actinobacterial cytochrome bc_1-aa_3 supercomplex *J. Biol. Chem.*
doi.org/10.1074/JBC.RA118.004117
*Shared first author

XM, CD, MBr, MBa, and MBo designed the study and analyzed the data. The experimental work was performed by XM and CD. XM performed the DNA microarray experiments, constructed the *C. glutamicum* Δ*ctiP*, Δ*copC*, Δcg1883 and Δ*ctaD*Δ*ctiP* deletion strains, performed growth experiments on agar plates, and performed $CtaD_{St}$-purification experiments in the wild type and the Δ*ctaD*, Δ*ctaD*Δ*ctiP* and Δ*copC* strain background. CD constructed the *C. glutamicum* deletion strains lacking cg0569, cg1744, cg1832, cg1883, cg2566, and cg2750 of the copper-starvation stimulon, performed the growth experiments of all mutant strain in media with different copper content, performed $QcrB_{St}$ purification experiments in the Δ*qcr* and Δ*qcr*Δ*ctiP* strain background and contributed to the manuscript preparation. XM and CD prepared the figures, MBo wrote and revised the final manuscript.
Overall contribution CD: 40%

Davoudi, C.-F., Baumgart, M. and Bott, M. (2019) Identification of Surf1 as an assembly factor of the cytochrome bc_1-aa_3 supercomplex of *Actinobacteria*. *Biochim. Biophys. Acta, Bioenerg., Submitted*

CD, MBa and MBo designed the study, which was supervised by MBa and MBo. CD performed all experimental work (construction of deletion strains, cultivation experiments, protein purification, DNA microarray studies, measurement of cytochrome spectra and enzyme activities). CD, MBa and MBo analyzed the data. CD prepared the figures, CD and MBo wrote the manuscript.
Overall contribution CD: 80%.

Keppel, M.*, Davoudi, C.-F.*, Filipchyk, A. *, Viets, U., Pfeifer, E., Polen, T., Baumgart, M., Bott, M. and Frunzke, J. (2019) HrrSA orchestrates a systemic response to heme and determines prioritisation of terminal cytochrome oxidases. *To be submitted*
*Shared first author

MK, CD, AF, MBo and JF designed the study, which was supervised by MBa, MBo and JF. MK, CD and UV performed the experiments. MK constructed the *hrrA* expression plasmid and was involved in conducting the ChAP-Seq and RNA-Seq experiments. UV performed the ChAP-Seq and RNA-Seq experiments. CD performed quantitative EMSA studies and cell-associated heme measurements. MK, CD, AF, and JF analyzed the data. AF and TP performed bioinformatics analysis of sequencing data. MK, CD and AF prepared the figures. MK and JF wrote the manuscript. MK, CD, AF, UV, EP, TP, MBa, MBo and JF edited the manuscript.
Overall contribution CD: 15%.

AF: Andrei Filipchyk, CD: Cedric-Farhad Davoudi, EP: Eugen Pfeifer, JF: Julia Frunzke, MBa: Meike Baumgart, MBo: Michael Bott, MBr: Melanie Brocker, MK: Marc Keppel, TP: Tino Polen, UV: Ulrike Viets, XM: Xenia Morosov

JBC ARTICLE

The copper-deprivation stimulon of *Corynebacterium glutamicum* comprises proteins for biogenesis of the actinobacterial cytochrome bc_1–aa_3 supercomplex

Received for publication, May 22, 2018, and in revised form, August 21, 2018 Published, Papers in Press, August 28, 2018, DOI 10.1074/jbc.RA118.004117

Xenia Morosov[1,2], **Cedric-Farhad Davoudi**[1], **Meike Baumgart, Melanie Brocker, and Michael Bott**[3]

From the Institute of Bio- and Geosciences, IBG-1: Biotechnology, Forschungszentrum Jülich, 52425 Jülich, Germany

Edited by Chris Whitfield

Aerobic respiration in *Corynebacterium glutamicum* involves a cytochrome bc_1–aa_3 supercomplex with a diheme cytochrome c_1, which is the only *c*-type cytochrome in this species. This organization is considered as typical for aerobic Actinobacteria. Whereas the biogenesis of heme–copper type oxidases like cytochrome aa_3 has been studied extensively in α-proteobacteria, yeast, and mammals, nothing is known about this process in Actinobacteria. Here, we searched for assembly proteins of the supercomplex by identifying the copper-deprivation stimulon, which might include proteins that insert copper into cytochrome aa_3. Using gene expression profiling, we found two copper starvation–induced proteins for supercomplex formation. The Cg2699 protein, named CtiP, contained 16 predicted transmembrane helices, and its sequence was similar to that of the copper importer CopD of *Pseudomonas syringae* in the N-terminal half and to the cytochrome oxidase maturation protein CtaG of *Bacillus subtilis* in its C-terminal half. CtiP deletion caused a growth defect similar to that produced by deletion of subunit I of cytochrome aa_3, increased copper tolerance, triggered expression of the copper-deprivation stimulon under copper sufficiency, and prevented co-purification of the supercomplex subunits. The secreted Cg1884 protein, named CopC, had a C-terminal transmembrane helix and contained a Cu(II)-binding motif. Its absence caused a conditional growth defect, increased copper tolerance, and also prevented co-purification of the supercomplex subunits. CtiP and CopC are conserved among aerobic Actinobacteria, and we propose a model of their functions in cytochrome aa_3 biogenesis. Furthermore, we found that the copper-deprivation response involves additional regulators besides the ECF sigma factor SigC.

Actinobacteria represents one of the largest phyla within bacteria, with currently 57 families (1, 2). It includes several important human pathogens like *Mycobacterium tuberculosis*, *Mycobacterium leprae*, and *Corynebacterium diphtheriae*, and biotechnologically important species such as antibiotic-producing representatives belonging to the *Streptomycetales* or *Corynebacterium glutamicum*, a major host for amino acid production in multimillion ton scale. Due to its industrial importance, *C. glutamicum* has become a model organism for studying metabolism and regulation (3–6). It is a facultative anaerobic bacterium with the capability for limited growth either by nitrate respiration to nitrite (7, 8) or by mixed acid fermentation with L-lactate, succinate, and acetate as major products (9). However, the preferred way of growth is by aerobic respiration, which is performed by a branched respiratory chain composed of several dehydrogenases transferring electrons to menaquinone and two pathways for transferring electrons from menaquinol to oxygen, one involving a cytochrome bc_1 complex and a cytochrome aa_3 oxidase and the second one composed of cytochrome *bd* oxidase (10).

A unique feature of this respiratory chain is the presence of a cytochrome bc_1–aa_3 supercomplex, which was identified by co-purification of all subunits of the bc_1 complex (QcrB, QcrA, and QcrC) and of cytochrome aa_3 oxidase (CtaD, CtaC, CtaE, and CtaF) by affinity chromatography with either Strep-tagged QcrB (cytochrome *b*) or Strep-tagged CtaD (subunit I) (11). The existence of such a supercomplex had previously been suggested by us based on the observation that *C. glutamicum* contains a diheme cytochrome c_1, which is the only *c*-type cytochrome encoded in the genome (12–15). Mutational analysis confirmed that both heme groups of cytochrome c_1 are essential for the activity of the bc_1–aa_3 supercomplex, and the second heme group probably takes over the function of a separate cytochrome *c*, usually shuttling electrons from the bc_1 complex to cytochrome aa_3 oxidase (11).

Recently, studies have led to a structural model of the bc_1–aa_3 supercomplex, the determination of the redox potentials of the cofactors, and a detailed kinetic characterization of the partial reactions catalyzed by the supercomplex (16, 17). With respect to bioenergetics, the bc_1–aa_3 supercomplex is predicted to transport 6 H^+ per 2 e^- from the cytoplasm to the outside, whereas the alternative cytochrome *bd* oxidase is assumed to have a stoichiometry of only 2 H^+/2 e^- (10). Analysis of defined mutants lacking either the genes of the bc_1 complex (*qcrCAB*) or the gene for subunit I of the aa_3 oxidase (*ctaD*) showed reduced growth rates and decreased biomass yields (12). A mutant lacking only the *qcrA* gene for the Rieske iron–sulfur protein, whose assembly was shown to be dependent on the TatABC translocase, showed the

The authors declare that they have no conflicts of interest with the contents of this article.

This article contains Table S1 and Figs. S1–S6.

The microarray data have been deposited to the GEO database and are accessible under accession numbers GSE117530 and GSE117566.

[1] Both authors contributed equally to this work.

[2] Supported by the Northrhine-Westfalia (NRW) Research School BioStruct.

[3] To whom correspondence should be addressed. Tel.: 49-2461-613294; Fax: 49-2461-612710; E-mail: m.bott@fz-juelich.de.

same phenotype (18). In contrast, a mutant lacking the *cydAB* genes for the cytochrome *bd* oxidase showed no growth defects in the exponential growth phase, but only thereafter, leading to reduced biomass formation (19). These results support the key role of the bc_1–aa_3 supercomplex in aerobic respiration of *C. glutamicum*.

A comprehensive genetic analysis revealed that the cytochrome bc_1–aa_3 supercomplex is not restricted to *Corynebacterium*, but is probably characteristic for the majority of Actinobacteria (except for the anaerobic orders Actinomycetales and Bifidobacteriales) due to the absence of genes for a monoheme cytochrome *c* and the universal presence of the gene for diheme cytochrome c_1 (17). This view is supported by studies in *Mycobacterium* (20–22), *Rhodococcus* (23), and *Streptomyces* (24).

The functionality of the cytochrome bc_1–aa_3 supercomplex depends on the correct assembly of the heme groups, of the iron–sulfur cluster, and of the copper centers. Currently, no studies have been reported on proteins involved in the biogenesis of the supercomplex. Here, we addressed this question with a focus on the proteins required for copper insertion. With respect to copper homeostasis in *C. glutamicum*, two regulatory systems involved in the response to copper excess stress have been identified, the two-component signal transduction system CopRS (25) and the one-component transcriptional regulator CsoR (26). The target genes of these regulators included genes presumably encoding copper exporters, but no obvious copper importers. As a starting point in our search for proteins involved in copper insertion into cytochrome aa_3 oxidase, we determined the copper-deprivation stimulon of *C. glutamicum* and analyzed genes with increased expression. Copper deprivation is known to influence the content of cytochrome aa_3 oxidase in various bacteria (27, 28). Using this approach, two candidate proteins were identified and characterized, CtiP (Cg2699) and CopC (Cg1884).

Results

Copper consumption by C. glutamicum and influence of copper deprivation on growth and cytochrome composition

The activity of the cytochrome bc_1–aa_3 supercomplex of Actinobacteria depends on the presence of the Cu_A and Cu_B centers in subunit II (CtaC) and subunit I (CtaD), respectively, of cytochrome aa_3 oxidase. To search for proteins involved in the formation of the copper centers, we analyzed the transcriptional response of *C. glutamicum* to copper deprivation. We assumed that genes for such assembly factors might show an increased expression under these conditions. In initial studies, we analyzed copper consumption by *C. glutamicum*, established copper-deprivation conditions, and tested their influence on growth and cytochrome composition.

In standard CGXII glucose minimal medium, copper is supplied as a trace element in a concentration of 1.25 μM $CuSO_4$. To analyze copper consumption in this medium, the concentration in freshly prepared medium just before inoculation and in the culture supernatant after 25 h of cultivation of *C. glutamicum* WT was determined via inductively coupled plasma MS. The copper concentration decreased from the

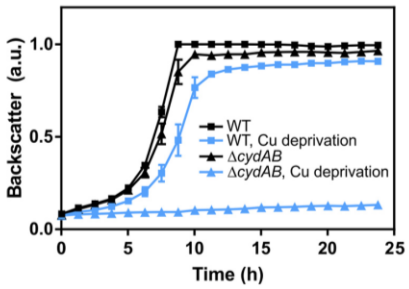

Figure 1. Influence of copper deprivation on growth of *C. glutamicum* WT and the Δ*cydAB* mutant. Strains were cultivated either in standard CGXII medium with 2% (w/v) glucose and 1.25 μM $CuSO_4$ or in copper-deprived CGXII medium with 2% (w/v) glucose without added $CuSO_4$ and supplemented with 150 μM BCS and 1 mM ascorbate. The growth experiment was performed in FlowerPlates™ with 800 μl of medium using a Biolector microcultivation system (30 °C, 1200 rpm). Mean and S.D. (*error bars*) from three biological replicates are shown. *a.u.*, arbitrary units.

measured 1.25 ± 0.26 μM copper before inoculation to 0.18 ± 0.02 μM copper after 25 h. Based on this difference and the cell density after 25 h (A_{600} = 60, corresponding to 1.68×10^{10} cells/ml), an average uptake of 3.8×10^4 copper ions/cell was calculated.

To study the growth behavior of *C. glutamicum* under copper-deprivation conditions, we omitted $CuSO_4$ from the CGXII medium and supplemented it with a 150 μM concentration of the copper-specific chelator bathocuproine disulfonate (BCS)[4] and 1 mM ascorbate for reduction of Cu(II) to Cu(I) (29). When cultivated in shake flasks rinsed with 0.1 N HCl before the addition of medium to remove residual trace metal ions, the WT showed a reduced growth rate of 0.36 ± 0.01 h^{-1} under copper deprivation compared with 0.40 ± 0.01 h^{-1} under standard copper conditions. In contrast, the growth rate of a *C. glutamicum* Δ*cydAB* mutant lacking the copper-independent cytochrome *bd* oxidase showed a strongly reduced growth rate of 0.15 ± 0.01 h^{-1} under copper deprivation compared with growth under standard copper conditions (μ = 0.40 ± 0.01 h^{-1}) (data not shown). As oxygen respiration of the *C. glutamicum* Δ*cydAB* mutant should be strictly dependent on the copper-dependent cytochrome aa_3 oxidase (30), the residual growth of the Δ*cydAB* mutant under copper deprivation indicated that, under the experimental conditions applied, copper is still available to some extent and allows synthesis of some functional cytochrome aa_3. To eliminate residual copper, the growth experiment was repeated in a Biolector microcultivation system using FlowerPlates™ made of high-purity polystyrene, and in this case, the Δ*cydAB* mutant showed no growth under copper deprivation (Fig. 1). After the addition of copper sulfate, growth could be recovered (data not shown). Thus, in the absence of copper aerobic respiration of *C. glutamicum* depends on cytochrome *bd* oxidase.

To obtain further insights into the consequences of copper deprivation on the composition of the respiratory chain, reduced spectra of *C. glutamicum* cells cultivated in shake flasks either under standard conditions or under copper

[4] The abbreviations used are: BCS, bathocuproine disulfonate; BHI, brain heart infusion; kb, kilobases; ECF, extracytoplasmic function.

Biogenesis of actinobacterial cytochrome c oxidase

limitation were recorded (Fig. S1). The spectra revealed that under copper deprivation, the peak at 630 nm was clearly increased, in line with an increased content of cytochrome *bd* oxidase. At the same time, the cytochrome *a* peak at 602 nm was reduced and slightly blue-shifted, and the cytochrome *c* peak at 552 nm was reduced. These changes are in agreement with previous data (28) and show that copper deprivation has a severe influence on the composition of the respiratory chain.

Determination of the copper-deprivation stimulon of *C. glutamicum*

To determine the copper-deprivation stimulon of *C. glutamicum*, we compared global gene expression of WT cells cultivated in shake flasks either under copper deprivation or under standard conditions using DNA microarrays. RNA was isolated from cells that had been harvested at an A_{600} of 20. 16 genes showed a ≥3-fold increased mRNA ratio under copper deprivation, and 10 genes showed a ≥3-fold lowered mRNA ratio (Table 1). The genes with the highest up-regulation under copper deprivation were those of the *cydABDC* operon encoding cytochrome *bd* oxidase and an ABC transporter required for functional synthesis of this terminal oxidase (19, 31). Other highly up-regulated genes encoded heme *o* synthase (*ctaB*), an ABC transporter with a binding protein for metal ions of the TroA_a family (cg1832 and cg1833), CopC, a secreted protein with a CopC domain and a C-terminal transmembrane helix (cg1884) (32), a secreted lipoprotein belonging to the PCu_AC family (cg1883) (33), a DyP-type heme peroxidase with a Tat signal peptide (cg1881), an integral membrane protein with a PepSY-associated TM region (cg2556), a large integral membrane protein (cg2699) with both a CopD (34) and a CtaG domain (35), and an integral membrane protein with a DUF3817 domain (cg2750). The gene displaying the strongest down-regulation under copper deprivation was cg2546, encoding an integral membrane protein of the DctM family of transporters. In addition, several other genes encoding transporter proteins and two genes of the *ctaE-qcrCAB* operon encoding subunit III of cytochrome aa_3 oxidase and the cytochrome bc_1 complex were found to be down-regulated. The up-regulation of the *cydABDC* operon and the concomitant down-regulation of the *ctaE-qcrCAB* operon are in agreement with the results of the cytochrome spectra reported above.

Several of the genes listed in Table 1 were also reported in a previous study to show altered expression in *C. glutamicum* strain R upon copper deficiency; *cydA*, *ctaA*, *ctaB*, cgR_0179 (homolog of cg1884), cgR_2208 (homolog of cg2556), and cgR_2412 (homolog of cg2750) were found to be up-regulated 1 h after the addition of 0.5 mM BCS, whereas expression of *ctaE* was found to be down-regulated. It was shown that these alterations in gene expression were due to the ECF sigma factor SigC (36).

The target genes of the Cu(I)-regulated repressor CsoR (26) did not show reduced expression under copper deprivation, indicating that the intracellular concentration of "free" copper was comparable with growth with 1.25 μM $CuSO_4$. Because members of the CsoR family have extremely high affinities for Cu(I) with K_d values in the range of 10^{-19} to 10^{-21} M (37, 38), we assume the "free" cytoplasmic Cu(I) concentration to be extremely low already under standard growth conditions with 1.25 μM $CuSO_4$. Studies in yeast calculated less than one free copper ion per cell (39), supporting this assumption.

In silico characterization of CtiP (Cg2699)

Bioinformatic analysis of the genes up-regulated under copper deprivation revealed that the protein encoded by Cg2699 was a promising candidate for being involved in the biogenesis of the cytochrome bc_1–aa_3 supercomplex. It comprises 717 amino acid residues (calculated mass 79.2 kDa) and is predicted to contain 16 transmembrane helices. PFAM analysis (40) revealed that a region in the N-terminal half (residues 269–364) shows sequence similarity to the CopD family (PF05425), whereas the C-terminal region (residues 418–661) displays similarity to the Caa3-CtaG family (PF09678). The CopD integral membrane protein of *Pseudomonas syringae* was proposed to function together with the CopC protein, a periplasmic copper-binding protein (homologous to Cg1884 of *C. glutamicum*), in copper import, as overexpression of *copCD* led to copper hypersensitivity (41). The function of the *ctaG* gene was characterized until now only in *Bacillus subtilis*, where the results indicate that it is required specifically for the synthesis of a functional cytochrome *c* oxidase, cytochrome caa_3 (35). Note that CtaG of *B. subtilis* is unrelated to CtaG/Cox11p of proteobacteria and eukaryotic cells. Cg2699 apparently represents a fusion protein that could combine the function of CopD in copper import and the function of CtaG in the biogenesis of cytochrome *c* oxidase. Based on results described below, we named the protein CtiP for "copper transport and insertion protein" and the gene accordingly *ctiP*. In Fig. 2, a topology model of CtiP is shown, which also highlights the regions assigned to the CopD family and the Caa3-CtaG family.

Impact of CtiP on growth, cytochrome content, copper resistance, and global gene expression

To test a possible involvement of CtiP in the maturation of the cytochrome bc_1–aa_3 supercomplex, the deletion mutant Δ*ctiP* was constructed and analyzed for its growth behavior. In standard CGXII glucose medium, strain Δ*ctiP* showed a lowered growth rate compared with the WT (Fig. 3*A*). This growth defect could be abolished by expression of *ctiP* with plasmid pEKEx2-*ctiP*, confirming that it is caused by the deletion of *ctiP* (Fig. S2). A growth defect of the Δ*ctiP* mutant was also clearly visible on brain heart infusion (BHI) agar plates, where the colonies were much smaller than those of the WT and similar in size to that of a Δ*ctaD* mutant lacking subunit I of cytochrome aa_3 oxidase (Fig. 3*D*). These results support the assumption that CtiP is a candidate for being involved in the biogenesis of the cytochrome aa_3 oxidase.

To study the influence of CtiP on the composition of the respiratory chain, cytochrome spectra of dithionite-reduced cells were recorded. As shown in Fig. 2, the spectra of the Δ*ctiP* strain grown either in standard CGXII glucose medium (1.25 μM $CuSO_4$) or under copper deprivation were similar to those

Table 1

Transcriptome comparisons of the indicated strains using DNA microarrays

Listed are all genes that showed a ≥3-fold altered mRNA ratio with a p value ≤ 0.1 in either the comparison of the WT cultivated under copper deprivation (−$CuSO_4$, +150 μM BCS, +1 mM ascorbate) with the WT cultivated with the standard copper concentration (1.25 μM initially) or the comparison of the Δ*ctiP* mutant and the WT, both cultivated with the standard copper concentration (1.25 μM initially). For each comparison, three independent biological replicates were performed, and only those values are listed for which at least two of the experiments could be evaluated. For each gene in the table, a ≥3-fold altered mRNA ratio in one comparison (WT *versus* WT or Δ*ctiP versus* WT) was sufficient to be listed, and the values of the other comparison were added, even if the ratio did not meet the cut-off. Genes shown in boldface type showed ≥3-fold altered mRNA ratio, with a p value ≤ 0.1 in both comparisons (12 up-regulated genes, 4 down-regulated genes). Genes whose locus tags are underlined were deleted in the course of this study, and the deletion mutants were analyzed with respect to their phenotype. ND, not determined.

Gene			WT, Cu deprivation/ WT, 1.25 μM Cu		Δ*ctiP*, 1.25 μM Cu/ WT, 1.25 μM Cu	
Locus tag	Name	Annotated function	mRNA ratio	p	mRNA ratio	p
cg0569[a]		Cation-transporting ATPase	4.74	0.04	4.19	0.06
cg1291		Putative membrane protein	2.15	0.00	3.06	0.04
cg1298[a]	*cydC*	ABC-type transport system required for functional synthesis of cytochrome *bd* oxidase, ATPase and permease component	27.79	0.01	8.79	0.00
cg1299[a]	*cydD*	ABC-type transport system required for functional synthesis of cytochrome *bd* oxidase, ATPase and permease component	10.54	0.02	16.09	0.00
cg1300[a]	*cydB*	Cytochrome *bd* oxidase, subunit II	14.55	0.03	12.55	0.00
cg1301[a]	*cydA*	Cytochrome *bd* oxidase, subunit I	14.99	0.01	14.03	0.00
cg1424	*lysE*	Secondary exporter for L-lysine and L-arginine	3.30	0.01	2.16	0.01
cg1744		Cation-transporting ATPase	4.01	0.09	3.27	0.01
cg1769[a]	*ctaA*	Heme *o* monoxygenase, heme *a* synthase	2.75	0.01	5.90	0.01
cg1773[a]	*ctaB*	Protoheme IX-farnesyltransferase, heme *o* synthase	8.49	0.07	5.83	0.00
cg1832		ABC-type Fe^{3+}-siderophore transporter, permease component	6.69	0.00	1.58	0.01
cg1833		ABC-type Fe^{3+}-siderophore transporter, secreted binding protein (lipoprotein)	8.56	0.00	2.51	0.03
cg1881[a]		Conserved protein of the DyP-type peroxidase family secreted via Tat pathway (PFAM PF04261)	12.84	0.02	15.37	0.00
cg1883[a]		Putative secreted lipoprotein, putative copper chaperone PCu_AC (PFAM PF04314)	12.01	0.02	16.49	0.00
cg1884[a]	*copC*	Putative secreted copper resistance protein with *copC* domain (PFAM PF04234)	12.94	0.01	16.99	0.00
cg2556[a]		Integral membrane protein of unknown function with a PepSY-associated TM region	10.04	0.03	6.49	0.00
cg2691	*ssb*	Single-stranded DNA-binding protein	ND		12.37	0.00
cg2699	*ctiP*	Putative copper resistance protein	4.94	0.01	0.05	0.01
cg2750[a]		Putative conserved membrane protein	6.88	0.01	6.28	0.00
cg2782	*ftn*	Ferritin	2.43	0.03	3.53	0.08
cg3138	*ppmA*	Putative membrane-bound protease modulator	1.20	0.21	4.83	0.00
cg3139		Hypothetical protein	1.33	0.09	3.57	0.01
cg3140	*tagA1*	DNA-3-methyladenine glycosylase	1.10	0.33	3.50	0.00
cg0133		Secondary transporter of the *p*-amino-benzoyl-glutamate transporter family TCDB 2.A.68	0.27	0.07	0.25	0.00
cg0759	*prpD2*	2-Methylcitrate dehydratase	ND		0.12	0.00
cg0760	*prpB2*	2-Methylisocitrate lyase	ND		0.15	0.00
cg0762	*prpC2*	2-Methylcitrate synthase	ND		0.15	0.00
cg0899		Glutamine amidotransferase involved in pyridoxine biosynthesis	0.45	0.02	0.33	0.01
cg0924		Putative secreted Fe^{3+}-siderophore-binding lipoprotein	0.27	0.02	0.18	0.08
cg0952	*mctB*	Putative integral membrane protein, probably functionally related to *mctT*	0.31	0.03	0.23	0.00
cg0953	*mctT*	Monocarboxylate transporter	0.31	0.05	0.23	0.00
cg1293		Putative secreted protein	0.32	0.01	0.43	0.00
cg1836		Putative terminase for peptidoglycan polymerization (YceG-like protein)	0.33	0.09	0.67	0.12
cg2403[a]	*qcrB*	Cytochrome bc_1 complex, cytochrome *b*	0.31	0.01	0.58	0.03
cg2406[a]	*ctaE*	Cytochrome aa_3 oxidase, subunit III	0.31	0.00	0.66	0.02
cg2546		Conserved secondary C_4-dicarboxylate transporter, tripartite ATP-independent transporter, TRAP-T-family	0.03	0.08	0.34	0.00
cg2557		Putative secondary Na^+/bile acid symporter, BASS-family	0.29	0.01	0.43	0.02
cg2836	*sucD*	Succinyl-CoA synthetase, α-subunit	ND		0.26	0.00
cg2837	*sucC*	Succinyl-CoA synthetase, β-subunit	1.03	0.48	0.22	0.01
cg3022		Acetyl-CoA acetyltransferase	ND		0.26	0.01
cg3195		Putative flavin-containing monooxygenase	0.58	0.13	0.23	0.00
cg3335	*mez*	Malic enzyme	0.35	0.02	0.11	0.00

[a] Homologs of these genes were shown to be regulated by the alternative sigma factor SigC in *C. glutamicum* strain R (36).

of the WT grown under copper deprivation; the cytochrome *d* peak at 630 nm was increased compared with the WT grown with standard copper levels, the cytochrome *a* peak at 602 nm was reduced and slightly blue-shifted, and the cytochrome *c* peak at 552 nm was reduced. This result provided evidence for a role of CtiP in respiration and in particular suggested that the Δ*ctiP* mutant behaves like the WT under copper deprivation. To support a role of CtiP in copper metabolism, we analyzed growth of the Δ*ctiP* mutant under copper deprivation and under copper excess stress and observed WT-like growth under copper limitation but an improved growth rate in the presence of 100 μM $CuSO_4$ (Fig. 3, *B* and *C*). An increased copper tolerance could be explained by assuming that CtiP functions as a copper importer, as implied by the sequence similarity to CopD (see above).

The growth behavior and the cytochrome spectra of the Δ*ctiP* mutant under regular copper concentrations (1.25 μM) were similar to those of the WT under copper deprivation. These observations prompted us to compare global gene expression of the Δ*ctiP* mutant and the WT under standard copper levels (1.25 μM initially) using DNA microarrays. RNA was isolated from cells that had been harvested at an A_{600} of 20. In total, 19 genes showed a ≥3-fold increased mRNA ratio in the Δ*ctiP* mutant, and 15 genes showed a ≥3-fold lowered mRNA ratio (Table 1). Remarkably, 12 of the 19 genes up-regulated in the Δ*ctiP* mutant were also ≥3-fold up-regulated in

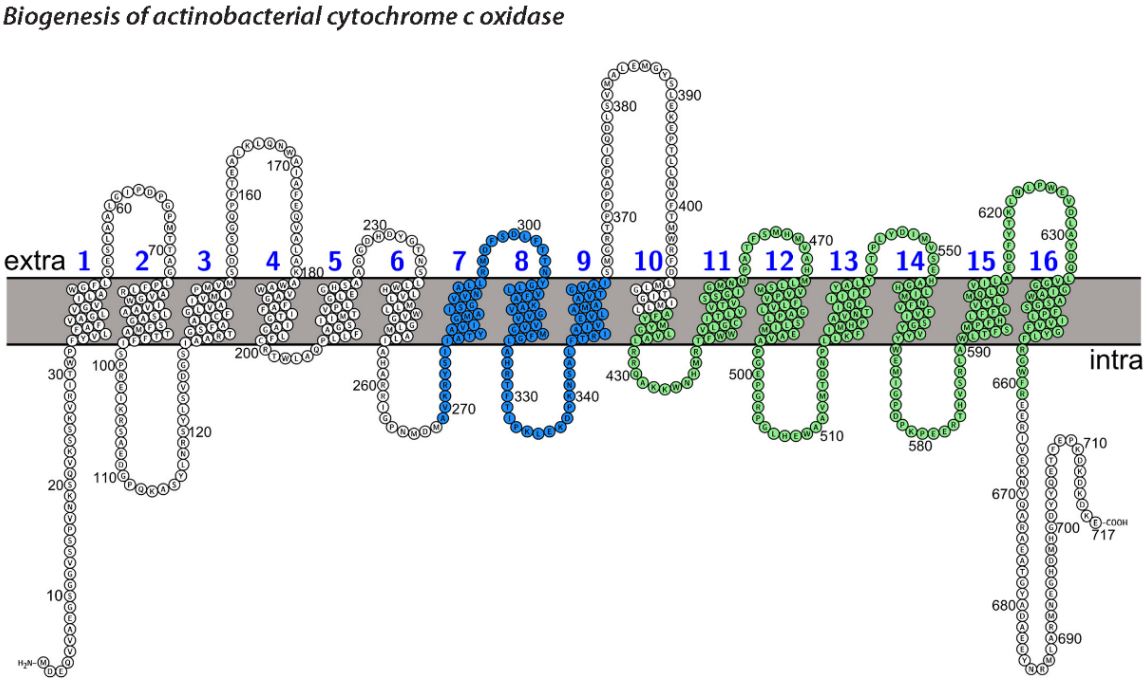

Figure 2. Topology model of the CtiP protein (Cg2699) created with the PROTTER software (72). The *regions labeled* in *blue* and *green* show sequence similarity to the CopD family (PFAM PF05425) and Caa3-CtaG family (PFAM PF09678), respectively.

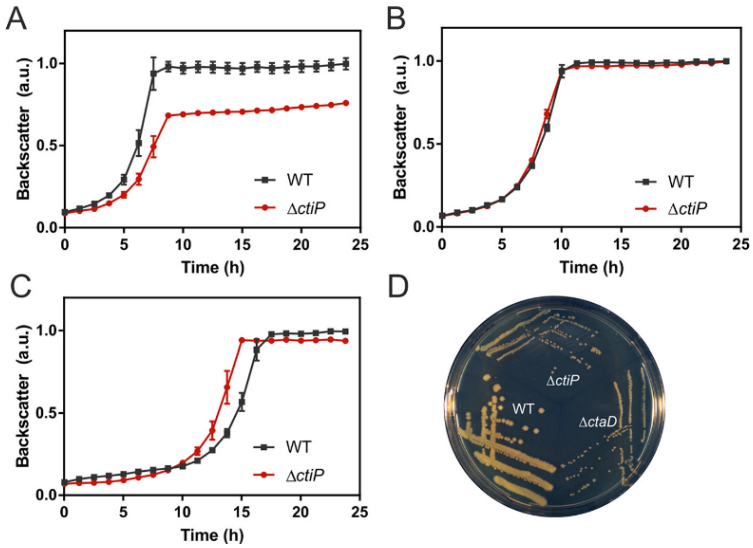

Figure 3. Growth properties of the *C. glutamicum* deletion mutant Δ*ctiP*. *C. glutamicum* WT and the deletion mutant Δ*ctiP* were cultivated at 30 °C and 1200 rpm in a BioLector microcultivation system using FlowerPlates™ containing 800 μl of CGXII medium with 2% (w/v) glucose. For *A*, standard medium with 1.25 μM $CuSO_4$ was used. In *B*, the medium was devoid of added $CuSO_4$ and supplemented with a 150 μM concentration of the copper chelator BCS and 1 mM ascorbate. In *C*, the standard medium was supplemented with 100 μM $CuSO_4$ to trigger copper excess stress. *A–C*, growth was followed online as backscatter at 620 nm every hour. All backscatter values were normalized by setting the maximal backscatter value of the WT cultures used for comparison as 1. Mean and S.D. (*error bars*) of three biological replicates are shown. *D*, *C. glutamicum* WT, the Δ*ctiP* mutant, and the Δ*ctaD* mutant were cultivated for 2 days on BHI agar.

the WT under copper deprivation, clearly supporting the idea that the absence of CtiP results in copper deficiency or at least in a situation that elicits the copper-deprivation response. This is in line with a copper import function of CtiP. Of the 15 genes with a ≥3-fold lowered mRNA level in the Δ*ctiP* mutant, only four also had ≥3-fold lowered mRNA levels in the WT under copper deprivation (*i.e.* the congruence was much lower than for the up-regulated genes).

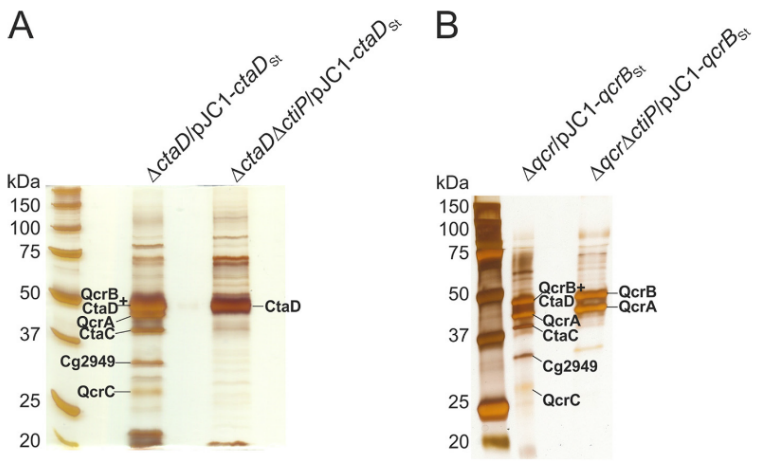

Figure 4. Purification of cytochrome bc_1–aa_3 supercomplex subunits either with Strep-tagged CtaD (*A*) or with Strep-tagged QcrB (*B*) in the presence and absence of CtiP. The indicated *C. glutamicum* strains were cultivated in BHI medium with 2% (w/v) glucose at 30 °C in shaking flasks and harvested in the early exponential phase at an A_{600} of 5. The purified membranes were used for Streptactin affinity chromatography. The protein fractions eluted with desthiobiotin were combined and separated by SDS-PAGE (12% separating gel). The gels were stained with silver. In parallel, Coomassie-stained gels were prepared and used for the identification of the proteins by peptide-mass fingerprinting.

Impact of CtiP on the assembly of the cytochrome bc_1–aa_3 supercomplex

The presence of a CtaG-like domain in the C-terminal part of CtiP pointed to an involvement of the protein in the assembly of cytochrome c oxidase. To address such a function, we tested whether the absence of CtiP has an influence on the ability to purify the cytochrome bc_1–aa_3 supercomplex. We constructed the double-deletion mutant Δ*ctaD*Δ*ctiP*, transformed it with the plasmid pJC1-*ctaD*$_{St}$ expressing C-terminally Strep-tagged CtaD from its native promoter, and purified CtaD$_{St}$ by Strep-Tactin affinity chromatography as described (11). As a reference, we used strain Δ*ctaD*/pJC1-*ctaD*$_{St}$. The proteins eluted with desthiobiotin were analyzed by SDS-PAGE and identified by peptide mass fingerprinting. As shown in Fig. 4*A*, the lack of CtiP had a severe impact on the purification result. Whereas in the eluate of the reference strain besides CtaD$_{St}$, also CtaC, QcrB, QcrA, QcrC, and Cg2949 were co-purified, the eluate of strain Δ*ctaD*Δ*ctiP*/pJC1-*ctaD*$_{St}$ contained CtaD$_{St}$, but other proteins were absent or present in such low amounts that identification was not possible.

In an analogous approach, we constructed the strain Δ*qcr*Δ*ctiP* in which, besides *ctiP*, the *qcrCAB* genes are deleted and transformed it with plasmid pJC1-*qcrB*$_{St}$ expressing the *ctaE-qcrCAB* operon from its native promoter, with QcrB containing a C-terminal StrepTag. Solubilized membrane proteins of strain Δ*qcr*Δ*ctiP*/pJC1-*qcrB*$_{St}$ and, for comparison, of strain Δ*qcr*/pJC1-*qcrB*$_{St}$ were subjected to StrepTactin affinity chromatography, and the eluates were analyzed as described above. Whereas the eluate of strain Δ*qcr*/pJC1-*qcrB*$_{St}$ contained not only QcrB$_{St}$, but also QcrA, QcrC, CtaD, and Cg2949, in the eluate of strain Δ*qcr*Δ*ctiP*/pJC1-*qcrB*$_{St}$, only QcrB$_{St}$ and QcrA were detectable (Fig. 4*B*).

These results indicate that the formation of the cytochrome bc_1–aa_3 supercomplex is disturbed in the absence of CtiP. The co-purification of QcrB$_{St}$ and QcrA from strain Δ*qcr*Δ*ctiP*/pJC1-*qcrB*$_{St}$ is comparable with the purification result obtained with a Δ*ctaD* mutant carrying pJC1-*qcrB*$_{St}$ (11), indicating that the lack of CtiP has no influence on the interaction of QcrB with QcrA. However, the absence of CtiP prevented co-purification of the other subunits of cytochrome aa_3 oxidase with CtaD$_{St}$, which was previously shown to be independent of the presence of the cytochrome bc_1 complex (11). This suggests that in the absence of CtiP, either CtaD itself or at least one of the subunits CtaC, CtaE, or CtaF is altered in a way that prevents formation of a stable oxidase complex that can be purified with CtaD$_{St}$. Possible reasons could be an insufficient metallation of either the Cu_B center in CtaD or the Cu_A center in CtaC, as delineated under "Discussion."

Growth behavior of deletion mutants lacking individual genes of the copper-deprivation stimulon

To search for additional genes of the copper-deprivation stimulon that might be involved in the biogenesis of the cytochrome bc_1–aa_3 supercomplex, nine *C. glutamicum* deletion mutants were constructed lacking cg0569, cg1744, cg1832, cg1833, cg1881, cg1883, *copC* (cg1884), cg2556, or cg2750. All of the genes could be deleted, showing that none of them is essential. The growth properties of the resulting mutant strains were analyzed in standard CGXII medium, in copper-deprived CGXII medium, and in CGXII medium supplemented with 100 μM $CuSO_4$ to elicit copper excess stress. In standard CGXII medium, none of the mutants except for strain Δ*ctiP* revealed a growth defect (Fig. S3), and in copper-deprived medium, all mutants, including Δ*ctiP*, grew like the WT (Fig. S4). In CGXII medium supplemented with 100 μM $CuSO_4$, besides the Δ*ctiP* strain, also the Δ*copC* mutant showed a growth advantage compared with the WT (Fig. S5). The CopC protein contains a Sec-type signal peptide (residues 1–34) and a C-terminal transmembrane helix (residues 176–198). The extracytoplasmic part (residues 35–175) shows similarity to the CopC domain

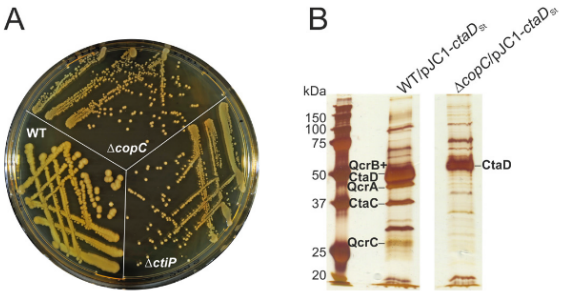

Figure 5. Properties of the Δ*copC* mutant. *A*, *C. glutamicum* WT, the Δ*copC* mutant, and the Δ*ctiP* mutant were grown on a BHI agar plate for 2 days. *B*, solubilized membranes of the indicated strains were subjected to Streptactin affinity chromatography, and the eluates (10 μg) were analyzed by SDS-PAGE and silver staining. The labeled proteins were identified by MS using protein bands from a Coomassie-stained gel performed in parallel.

(PF04234). In *P. syringae*, CopC has been described as a copper-binding protein that, in concert with CopD, mediates copper import (41). Accordingly, the CopC protein of *C. glutamicum* might also be a copper-binding protein involved in copper import, which could explain the enhanced copper resistance. A sequence alignment (Fig. S6) revealed that the Cu(II)-binding residues known from the structure of *P. syringae* CopC (His^{1}, Glu^{27}, Asp^{89}, and His^{91}) are highly conserved in *C. glutamicum* CopC except for a Glu^{27}–Asp exchange, whereas the majority of the Cu(I)-binding residues (Met^{40}, Met^{43}, Met^{46}, His^{48}, Met^{51}, and Tyr^{79}) of *P. syringae* CopC, except for His^{48} and Tyr^{79}, are not conserved in the *C. glutamicum* homolog (42). Therefore, *C. glutamicum* CopC probably contains a Cu(II)-binding site, but no Cu(I)-binding site.

Further studies on the phenotype of the ΔcopC mutant

Due to its likely function as copper-binding protein, we further studied the phenotype of the Δ*copC* mutant. Although the strain grew like WT in standard CGXII glucose medium (Fig. S3), a clear growth defect was observed on BHI agar plates (Fig. 5*A*) and in BHI liquid medium (data not shown). In view of the similarities between the Δ*ctiP* and the Δ*copC* mutants, we also tested the latter for the assembly of cytochrome aa_3 oxidase. Strain Δ*copC* and the WT were transformed with plasmid pJC1-*ctaD*$_{St}$, and Strep-tagged CtaD was purified by Strep-Tactin affinity chromatography of solubilized membrane proteins. As shown in Fig. 5*B*, CtaC, QcrB, QcrA, and QcrC were co-purified with CtaD$_{St}$ in the WT, whereas in the eluate of the Δ*copC* mutant, only CtaD was found. This result suggests that in the absence of CopC, the stability of the cytochrome aa_3 oxidase complex is impaired. In view of the likely function of CopC as a copper-binding protein, a role in the metallation of the copper centers appears to be a possible reason.

Discussion

Numerous studies have addressed the biogenesis of respiratory cytochromes in bacteria, yeast, and mammals and a multitude of proteins involved in this process have been identified (43, 44). In bacteria, the majority of experimental work was performed with α-proteobacteria, such as *Rhodobacter sphaeroides* and *Paracoccus denitrificans*. Knowledge on the assembly of respiratory oxidases in Gram-positive bacteria is sparse, and this is particularly true for the large phylum of the Actinobacteria. This study aimed at the identification of proteins involved in the insertion of copper ions into cytochrome *c* oxidase of *C. glutamicum*.

Our approach was based on the hypothesis that proteins involved in copper insertion into cytochrome aa_3 oxidase might show an elevated expression under copper deprivation. Therefore, we determined the copper-deprivation stimulon of *C. glutamicum* and identified 16 genes with an at least 3-fold elevated expression. Interestingly, all 12 genes previously shown to be transcriptionally activated by the ECF sigma factor SigC in *C. glutamicum* strain R were included in the copper-deprivation stimulon of strain ATCC13032, except for cgR_0144, which appears to be a paralog of cgR_1719 (cg1884) only present in strain R (36). Our results are in full agreement with those obtained previously in strain R by quantitative RT-PCR showing that *cydA*, *ctaA*, and *ctaB* were up-regulated under copper deprivation in a SigC-dependent manner (36).

Expression of the *sigC* gene itself, however, was not up-regulated by copper deprivation, neither in strain R nor in our studies with strain ATCC13032, indicating that increased expression of the genes of the SigC regulon is not due to increased *sigC* transcription. It was suggested that SigC is activated by an impaired electron transfer via cytochrome aa_3 oxidase (36), but the mechanism is still unknown. Based on these results, it can be assumed that SigC is responsible for up-regulation of its 11 target genes included in the copper-deprivation stimulon of *C. glutamicum* ATCC13032. The observation that the genes of the *cydABDC* operon exhibited the highest up-regulation under copper deprivation is in line with the fact that cytochrome *bd* oxidase is copper-independent and therefore can replace cytochrome aa_3 oxidase under these conditions.

Besides the known genes of the SigC regulon, however, six additional genes were found to be up-regulated at least 3-fold under copper deprivation in strain ATCC13032. Inspection of their promoter regions revealed no obvious SigC-binding motifs (data not shown). Four of these are likely involved in metal ion transport. The genes cg0569 and cg1744 were both annotated as cation-transporting ATPases, whereas cg1832 and cg1833 encode the permease and a secreted substrate-binding lipoprotein of an ABC transporter. The binding protein belongs to the TroA_a family of proteins that are predicted to function as initial receptors in ABC transport of metal ions in eubacteria. The up-regulation of these four genes under copper deprivation points to a role in copper uptake. The *lysE* gene (cg1424) encodes a secondary exporter for lysine and arginine (45, 46). Its expression is activated by the transcriptional regulator LysG, which senses elevated levels of lysine, arginine, and histidine (46–48). We assume that copper deprivation and the concomitantly reduced growth rate presumably results in increased intracellular concentrations of one or several of these amino acids and activation of *lysE* expression. The protein encoded by cg2699 has been intensively studied in this work and will be discussed below.

Except for *lysE*, the mechanisms responsible for increased expression of the genes not belonging to the SigC regulon under

copper deprivation are unclear at present. In the case of cg1832 and cg1833, the gene cg1831 located upstream and divergent to cg1832 encodes an ArsR-type transcriptional repressor, which could be responsible for derepression under copper starvation. Overall, the results of the transcriptome comparison suggest that expression control of the genes up-regulated under copper deprivation involves not only SigC, but also other transcriptional regulators and possibly different stimuli.

Our studies of the Δ*ctiP* mutant indicate that the CtiP protein is involved in the biogenesis of cytochrome aa_3 oxidase and the cytochrome bc_1–aa_3 supercomplex. The Δ*ctiP* mutant had a clear growth defect in BHI medium, on BHI agar plates, and in standard glucose minimal medium with 1.25 μM $CuSO_4$, but it grew like the WT under copper-deprived conditions and even better than the WT in medium containing 100 μM $CuSO_4$ (Fig. 3). The increased copper tolerance indicates an involvement of CtiP in copper import, which is supported by the fact that almost the entire copper-deprivation stimulon was induced in the Δ*ctiP* mutant during growth under standard conditions with 1.25 μM $CuSO_4$. Thus, in the absence of CtiP, the mechanisms signaling copper deprivation are activated although sufficient copper ions are present in the medium. The growth defect of the Δ*ctiP* mutant under standard copper concentrations is most likely due to an impaired cytochrome aa_3 biogenesis, which was indicated by the failure to purify the cytochrome bc_1–aa_3 supercomplex (Fig. 4). An impaired formation of the Cu_A or the Cu_B center is a possible explanation for this result, assuming that these copper centers are necessary for the formation of a stable supercomplex.

The Cu_A center is located in the extracytoplasmic domain of CtaC and involves two copper ions that are bridged by two sulfur ligands from cysteine residues (Cys^{285} and Cys^{289} in the case of *C. glutamicum* CtaC). It is formed after the translocation of the domain by the Sec machinery. In bacteria, three proteins have been described to be involved in the formation of the Cu_A center, the Sco protein (synthesis of cytochrome oxidase), the PCu_AC protein (protein Cu_A chaperone), and the TlpA protein (thioredoxin-like protein A). Sco proteins are membrane-bound copper chaperones belonging to the thioredoxin family. They are located in the periplasm and contain a C*XXX*C motif involved in copper binding. Sco proteins can function both as disulfide reductases that reduce the cysteines of apo-Cu_A and as copper donor to the Cu_A center (44). Whereas *B. subtilis* contains an Sco protein presumably involved in Cu_A formation of the cytochrome caa_3 oxidase (49), *C. glutamicum* does not possess an Sco homolog.

The TlpA protein was identified in *Bradyrhizobium japonicum* in a screen for tetramethyl-*p*-phenylenediamine oxidase-negative transposon mutants (50) and is a membrane-anchored periplasmic protein with the active site sequence WCVPC (51). It was recently shown that TlpA is a specific reductant for the copper chaperone ScoI and the apo-Cu_A center in CoxB of *B. japonicum* (52). In *C. glutamicum*, two TlpA candidates were found. Cg0354 has the motif WCEPC and may contain a signal peptide, but no transmembrane helix. Therefore, a function of this protein as a reductant for apo-Cu_A in CtaC seems questionable. Cg0520 is a secreted lipoprotein with the active site sequence WCAPC and is encoded in a gene cluster involved in cytochrome *c* biogenesis (10). A function of Cg0520 as CtaC reductant appears possible, but this requires further experimental studies.

Biogenesis of actinobacterial cytochrome c oxidase

PCu_AC proteins are copper chaperones that bind a single Cu(I) in a cupredoxin-like fold (33, 53, 54). In *Thermus thermophilus*, PCu_AC was shown to serve as copper donor to the Cu_A center (53). Also, *C. glutamicum* possesses a PCu_AC homolog encoded by cg1883. This gene is part of an operon including *copC* (cg1884) and cg1881, all of which were found to be up-regulated under copper deprivation and are part of the SigC regulon. Cg1883 contains a signal peptide with the lipobox VMAACS (55) and thus presumably is a lipoprotein. The copper-binding motif in the structurally and functionally analyzed PCu_AC homologs was found to be $(H/M)X_{10}MX_{21}HXM$. The Cg1883 protein and its homologs from other actinobacteria contain a slightly different motif with the sequence $HX_6MX_{22}HXM$. As the Δcg1883 mutant constructed in our study showed no growth phenotype under the conditions tested, the function of Cg1883 remains unclear. It might support Cu_A assembly of actinobacterial cytochrome aa_3 oxidase but apparently is not essential for this process.

The Cu_B center, which is an invariable characteristic of heme–copper oxidases, is located within the transmembrane region closer to the positive side of the membrane (56). In yeast, mammals, and several bacteria, the Cox11 protein was shown to be involved in formation of the Cu_B center. In *R. sphaeroides*, lack of Cox11 led to a cytochrome aa_3 oxidase containing all centers except Cu_B, even when copper was in excess, indicating that in this species, Cox11 is essential for Cu_B formation (57). Cox11 is a membrane-anchored protein with a periplasmic domain containing a CFCF motif that binds Cu(I) and donates it to the Cu_B center. As *C. glutamicum* does not contain a Cox11 homolog, other mechanisms and proteins must be involved in the formation of the Cu_B center.

Based on the presence of a CtaG domain and our data, the CtiP protein is a good candidate for Cu_B formation. However, for *B. subtilis* CtaG, a function in the assembly of the Cu_A center or another feature only present in the cytochrome *c* oxidase caa_3 was proposed based on the observation that a mutant lacking *ctaG* and *cydABCD* was still able to grow on agar plates (35). Respiratory growth of this mutant was assumed to be dependent on cytochrome aa_3, a heme–copper type menaquinol oxidase, which does not possess a Cu_A center, but the heme a_3-Cu_B center (35). If CtaG would be required for Cu_B formation, not only cytochrome caa_3, but also cytochrome aa_3 should be defective, and the mutant lacking *ctaG* and *cydABCD* should not be able to grow. This assumption, however, might be wrong, as *B. subtilis* possesses a second *bd*-type oxidase encoded by the *ythAB* genes (58), which could allow growth of the mutant even if cytochrome caa_3 and cytochrome aa_3 are inactive due to the lack of CtaG. Alternatively, a protein different from CtaG could be responsible for Cu_B formation in the cytochrome aa_3 menaquinol oxidase.

The data available for the *C. glutamicum* Δ*ctiP* mutant suggest that CtiP might couple copper import via its N-terminal part with copper insertion into the Cu_B center via its C-terminal part. This would imply that insertion of copper into Cu_B does not proceed from the extracytoplasmic side of the

Biogenesis of actinobacterial cytochrome c oxidase

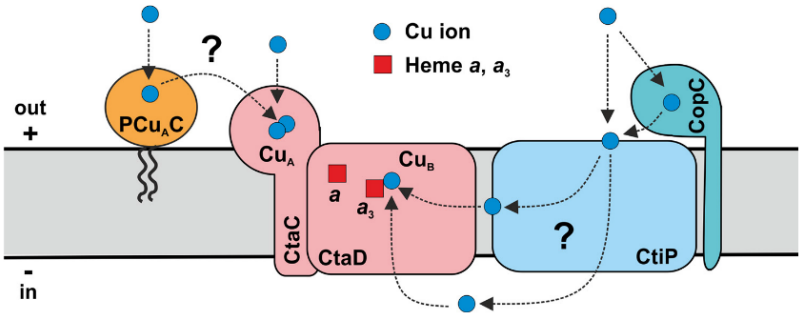

Figure 6. Model of the roles of CtiP (Cg2699), CopC (Cg1884), and PCu_AC (Cg1883) in the biogenesis of cytochrome aa_3 oxidase in *C. glutamicum*. The CtiP protein is assumed to have a dual function in copper transport and copper transfer to the Cu_B center of CtaD (subunit I). The absence of CtiP triggers the copper-deprivation response under copper excess. The CopC protein is a membrane-bound copper chaperone with a Cu(II)-binding motif that might donate copper to CtiP under copper deprivation. PCu_AC is a secreted lipoprotein with a Cu(I)-binding motif that might be involved in the formation of the Cu_A center. In contrast to the strains lacking CtiP or CopC, the mutant lacking PCu_AC showed no growth defects under the conditions tested. *Blue circles*, copper ions; *red squares*, heme groups.

membrane, as assumed for the Cox11-mediated process in *R. sphaeroides*, but from the cytoplasmic side or intramembranously. Alternatively, an additional copper chaperone might be involved, which is loaded by CtiP in the cytoplasm or intramembranously, and then transfers the copper to Cu_B on the extracytoplasmic side, as suggested in a recent study for the assembly of the Cu_B center of the cbb_3-type cytochrome *c* oxidase in *Rhodobacter* (59). In this example, the secondary copper importer CcoA is responsible for copper import and required for biogenesis of cytochrome cbb_3 oxidase (60).

As shown by the examples described above, different routes for the formation of the Cu_B center of heme–copper type terminal oxidases have been evolved. In the case of *C. glutamicum*, CtiP is likely to be involved in this process, which implies that the protein should be conserved in Actinobacteria, most of which harbor the genes for the cytochrome bc_1–aa_3 supercomplex (17). Bioinformatic analysis confirmed that CtiP homologs are encoded in all actinobacterial orders except for most species of the predominantly anaerobic members of the Actinomycetales and Bifidobacteriales (data not shown). This distribution supports the proposed function of CtiP.

A second protein that we identified in this study to be presumably involved in the biogenesis of cytochrome aa_3 oxidase of *C. glutamicum* was CopC. It contains a Sec-type signal peptide, a C-terminal transmembrane helix anchoring the protein in the cytoplasmic membrane, and a Cu(II)-binding site. In contrast to *ctiP*, the *copC* gene is part of the SigC regulon. A Δ*copC* mutant grew like WT in standard glucose minimal medium but showed a growth defect on BHI agar plates similar to the Δ*ctiP* mutant and a growth advantage under copper excess stress. The latter phenotype suggests a role of CopC in copper import. Furthermore, impaired purification of the cytochrome bc_1–aa_3 supercomplex from membranes of the Δ*copC* mutant suggested disturbed or at least weakened complex formation. CopC might serve as an extracytoplasmic copper chaperone supporting copper import under copper deprivation (*e.g.* by donating Cu(II) to CtiP). Like CtiP, CopC was also found to be highly conserved in Actinobacteria containing the genes for the cytochrome bc_1–aa_3 supercomplex (data not shown).

In summary, our study has provided the first data on the biogenesis of respiratory enzymes in Actinobacteria, a topic that has been neglected in the past. Based on the determination of the copper-deprivation stimulon of *C. glutamicum*, we identified two proteins involved in the maturation of cytochrome aa_3 oxidase. A model of this process based on our data is shown in Fig. 6. Obviously, further studies are required to validate this model and to identify additional proteins involved in the assembly process.

Experimental procedures

Bacterial strains, media, and growth conditions

Bacterial strains and plasmids used or constructed in this work are listed in the Table 2. *C. glutamicum* strains were cultivated aerobically at 30 °C either in CGXII minimal medium containing 2 or 4% (w/v) glucose as carbon and energy source and 30 mg/liter 3,4-dihydroxybenzoate as iron chelator (61) or in BHI medium supplemented with 2 or 4% (w/v) glucose or on BHI agar plates. Cultivations were performed either in 500-ml glass shake flasks containing 50 ml of medium that were incubated on a rotary shaker at 120 rpm or in a Biolector microcultivation system using FlowerPlates™ with 800 μl of medium that were shaken at 1200 rpm (m2p-labs, Baesweiler, Germany). For cultivation under copper deprivation, copper (regular concentration 1.25 μM) was excluded from the CGXII medium in the preculture and the main culture. The latter was supplemented with a 150 μM concentration of the copper-specific chelator BCS. Because BCS binds Cu(I), the medium was additionally supplemented with freshly prepared ascorbate (1 mM) for reduction of Cu(II) to Cu(I), as described (29). For cultivation under copper excess stress, CGXII medium was supplemented with 100 μM $CuSO_4$. Copper concentrations in the medium before and after cultivation were determined via inductively coupled plasma MS at ZEA, Forschungszentrum Jülich. *E. coli* DH5α was used as host for cloning purposes. The *E. coli* strains were cultivated aerobically in lysogeny broth medium (10 g/liter tryptone, 5 g/liter yeast extract, 10 g/liter NaCl) at 37 °C. When appropriate, kanamycin was

Table 2
Bacterial strains and plasmids used in this study

Strain or plasmid	Description	Source or reference
Strains		
C. glutamicum ATCC13032	Biotin-auxotrophic WT strain	Ref. 69
C. glutamicum Δ*cydAB*	Derivative of ATCC13032 with in-frame deletion of the *cydAB* genes (cg1301, cg1300)	Ref. 19
C. glutamicum Δ*ctaD*	Derivative of ATCC13032 with in-frame deletion of the *ctaD* gene (cg2780)	This work
C. glutamicum Δ*qcr*	Derivative of ATCC13032 with in-frame deletion of the *qcrCAB* genes	Ref. 12
C. glutamicum Δ*ctiP*	Derivative of ATCC13032 with in-frame deletion of the *ctiP* gene (cg2699)	This work
C. glutamicum Δ*ctaD*Δ*ctiP*	Derivative of ATCC13032 Δ*ctaD* with in-frame deletion of the *ctiP* gene	This work
C. glutamicum Δ*qcr*Δ*ctiP*	Derivative of ATCC13032 Δ*qcr* with in-frame deletion of the *ctiP* gene	This work
C. glutamicum Δcg0569	Derivative of ATCC13032 with in-frame deletion of the cg0569 gene	This work
C. glutamicum Δcg1744	Derivative of ATCC13032 with in-frame deletion of the cg1744 gene	This work
C. glutamicum Δcg1832	Derivative of ATCC13032 with in-frame deletion of the cg1832 gene	This work
C. glutamicum Δcg1833	Derivative of ATCC13032 with in-frame deletion of the cg1833 gene	This work
C. glutamicum Δcg1881	Derivative of ATCC13032 with in-frame deletion of the cg1881 gene	This work
C. glutamicum Δcg1883	Derivative of ATCC13032 with in-frame deletion of the cg1883 gene	This work
C. glutamicum Δ*copC*	Derivative of ATCC13032 with in-frame deletion of the *copC* gene (cg1884)	This work
C. glutamicum Δcg2566	Derivative of ATCC13032 with in-frame deletion of the cg2566 gene	This work
C. glutamicum Δcg2750	Derivative of ATCC13032 with in-frame deletion of the cg2750 gene	This work
E. coli DH5α	F^- φ80*dlac*Δ(*lacZ*)M15 Δ(*lacZYA-argF*) U169 *endA1 recA1 hsdR17* (r_K^-, m_K^+)*deoR thi-1 phoA supE44* λ^- *gyrA96 relA1*	Invitrogen
Plasmids		
pK19*mobsacB*	Kan^R, vector for allelic exchange in *C. glutamicum* (pK18 $oriV_{Ec}$ *sacB lacZ*α)	Ref. 70
pK19*mobsacB*-Δ*ctiP*	Kan^R, pK19*mobsacB* derivative containing a 1-kb overlap-extension PCR product (EcoRI/PstI) that covers the flanking regions of the *C. glutamicum ctiP* gene (cg2699)	This work
pK19*mobsacB*-Δcg0569	Kan^R, pK19*mobsacB* derivative containing a 1-kb PCR product (SalI/BamHI) that covers the flanking regions of the *C. glutamicum* cg0569 gene	This work
pK19*mobsacB*-Δcg1744	Kan^R, pK19*mobsacB* derivative containing a 1-kb PCR product (SalI/BamHI) that covers the flanking regions of the *C. glutamicum* cg1744 gene	This work
pK19*mobsacB*-Δcg1832	Kan^R, pK19*mobsacB* derivative containing a 1-kb PCR product (SalI/BamHI) that covers the flanking regions of the *C. glutamicum* cg1832 gene	This work
pK19*mobsacB*-Δcg1833	Kan^R, pK19*mobsacB* derivative containing a 1-kb PCR product (SalI/BamHI) that covers the flanking regions of the *C. glutamicum* cg1833 gene	This work
pK19*mobsacB*-Δcg1881	Kan^R, pK19*mobsacB* derivative containing a 1-kb PCR product (SalI/BamHI) that covers the flanking regions of the *C. glutamicum* cg1881 gene	This work
pK19*mobsacB*-Δcg1883	Kan^R, pK19*mobsacB* derivative containing a 1-kb overlap-extension PCR product (PstI/XmaI) that covers the flanking regions of the *C. glutamicum* cg1883 gene	This work
pK19*mobsacB*-ΔcopC	Kan^R, pK19*mobsacB* derivative containing a 1-kb overlap-extension PCR product (EcoRI/HindIII) that covers the flanking regions of the *C. glutamicum copC* gene (cg1884)	This work
pK19*mobsacB*-Δcg2566	Kan^R, pK19*mobsacB* derivative containing a 1-kb PCR product (SalI/BamHI) that covers the flanking regions of the *C. glutamicum* cg2566 gene	This work
pK19*mobsacB*-Δcg2750	Kan^R, pK19*mobsacB* derivative containing a 1-kb PCR product (SalI/BamHI) that covers the flanking regions of the *C. glutamicum* cg2750 gene	This work
pEKEx2	Kan^R, *C. glutamicum*/*E. coli* shuttle vector for regulated gene expression (P_{tac} *lacI*^{Q} pBL1 $oriV_{Cg}$ pUC18 $oriV_{Ec}$)	Ref. 71
pEKEx2-*ctiP*	Kan^R, pEKEx2 derivative containing the *ctiP* gene from *C. glutamicum* under control of the *tac* promoter	This work
pJC1-$ctaD_{St}$	Kan^R, expression plasmid for strep-tagged CtaD; *ctaD* expressed from its native promoter and with 10 additional codons at the 3′-end (AAWSHPQFEK)	Ref. 11
pJC1-$qcrB_{St}$	Kan^R; expression plasmid for Strep-tagged QcrB; *ctaE-qcrCAB* expressed from their native promoter; *qcrB* with 10 additional codons at the 3′-end (AAWSHPQFEK)	Ref. 11

added to a concentration of 50 μg/ml (*E. coli*) or 25 μg/ml (*C. glutamicum*).

Recombinant DNA work

The enzymes for recombinant DNA work were obtained from Roche Diagnostics (Mannheim Germany) or New England Biolabs (Frankfurt am Main, Germany). All oligonucleotides (Table S1) were synthesized by Eurofins (Ebersberg, Germany). Routine methods like PCR, restriction, or ligation were carried out according to standard protocols (62). The generation of all PCR products was performed with High Fidelity DNA polymerase (Roche Diagnostics). Plasmids were isolated from *E. coli* with the QIAprep Spin Miniprep kit (Qiagen, Hilden, Germany). *E. coli* was transformed by the RbCl method (63). Transformation of *C. glutamicum* was performed as described previously (64). All plasmid constructs described in this work were controlled by DNA sequencing (Eurofins MWG Operon, Ebersberg, Germany).

Construction of C. glutamicum deletion mutants

In-frame deletion mutants of *C. glutamicum* (Table 1) were constructed via a two-step homologous recombination procedure as described previously (12).

Global gene expression analysis

DNA microarray analysis was used to compare (i) the genome-wide mRNA levels of *C. glutamicum* WT cultivated under copper-deprived conditions (see above) with those of *C. glutamicum* WT cultivated in standard CGXII medium (1.25 μM $CuSO_4$) and (ii) the genome-wide mRNA levels of the *C. glutamicum* Δ*ctiP* mutant with those of *C. glutamicum* WT, both strains cultivated in standard CGXII medium (1.25 μM $CuSO_4$). RNA was prepared as described previously (65). For RNA isolation, the strains were cultured in CGXII medium with 4% (w/v) glucose and the indicated copper concentrations and harvested at an A_{600} of 20 in the late exponential growth phase. All DNA microarray analyses were performed with custom-made DNA microarrays based on 70-mer oligonucleotides

Biogenesis of actinobacterial cytochrome c oxidase

obtained from Operon Biotechnologies and later from Agilent Technologies. For each of the two comparisons, three independent biological replicates were performed, and p values were calculated using Student's t test (Excel, Microsoft). The experimental details and the data evaluation were performed as described previously (66). The microarray data have been deposited in the NCBI Gene Expression Omnibus (GEO) database and are accessible under accession numbers GSE117530 and GSE117566.

Purification of Strep-tagged CtaD and QcrB

The preparation of cell membranes, the solubilization of membrane proteins with n-dodecyl-β-D-maltoside, and the affinity chromatography with Strep-Tactin-Sepharose were performed as described (11). Isolated proteins were analyzed by SDS-PAGE and identified by peptide mass fingerprinting using MALDI-TOF MS (67).

Analysis of cytochromes

For recording dithionite-reduced spectra of intact cells, they were resuspended in 100 mM Tris-HCl buffer, pH 7.4, to an A_{600} of 100 and analyzed at room temperature using 5-mm light path cuvettes with a Jasco V560 spectrometer equipped with a silicon photodiode detector for turbid samples (68).

Author contributions—X. M., C. D., M. Brocker, M. Baumgart, and M. Bott designed the experiments and analyzed the data; X. M. and C. D. performed the experiments; X. M. and C. D. prepared the figures; and M. Bott wrote the manuscript.

Acknowledgment—We thank Dr. Tino Polen for help with the DNA microarray experiments, including upload of the data to the GEO database.

References

1. Gao, B., and Gupta, R. S. (2012) Phylogenetic framework and molecular signatures for the main clades of the phylum Actinobacteria. *Microbiol. Mol. Biol. Rev.* **76,** 66–112 CrossRef Medline
2. Lewin, G. R., Carlos, C., Chevrette, M. G., Horn, H. A., McDonald, B. R., Stankey, R. J., Fox, B. G., and Currie, C. R. (2016) Evolution and ecology of Actinobacteria and their bioenergy applications. *Annu. Rev. Microbiol.* **70,** 235–254 CrossRef Medline
3. Eggeling, L., and Bott, M. (eds) (2005) *Handbook of Corynebacterium glutamicum*, CRC Press, Boca Raton, FL
4. Burkovski, A. (ed) (2008) *Corynebacteria: Genomics and Molecular Biology*, Caister Academic Press, Norfolk, UK
5. Yukawa, H., and Inui, M. (eds) (2013) *Corynebacterium glutamicum: Biology and Biotechnology*, Springer, Heidelberg
6. Burkovski, A. (ed) (2015) *Corynebacterium glutamicum: From Systems Biology to Biotechnological Applications*, Caister Academic Press, Norfolk, UK
7. Nishimura, T., Vertès, A. A., Shinoda, Y., Inui, M., and Yukawa, H. (2007) Anaerobic growth of *Corynebacterium glutamicum* using nitrate as a terminal electron acceptor. *Appl. Microbiol. Biotechnol.* **75,** 889–897 CrossRef Medline
8. Takeno, S., Ohnishi, J., Komatsu, T., Masaki, T., Sen, K., and Ikeda, M. (2007) Anaerobic growth and potential for amino acid production by nitrate respiration in *Corynebacterium glutamicum*. *Appl. Microbiol. Biotechnol.* **75,** 1173–1182 CrossRef Medline
9. Michel, A., Koch-Koerfges, A., Krumbach, K., Brocker, M., and Bott, M. (2015) Anaerobic growth of *Corynebacterium glutamicum* via mixed-acid fermentation. *Appl. Environ. Microbiol.* **81,** 7496–7508 CrossRef Medline
10. Bott, M., and Niebisch, A. (2003) The respiratory chain of *Corynebacterium glutamicum*. *J. Biotechnol.* **104,** 129–153 CrossRef Medline
11. Niebisch, A., and Bott, M. (2003) Purification of a cytochrome bc_1–aa_3 supercomplex with quinol oxidase activity from *Corynebacterium glutamicum*: identification of a fourth subunit of cytochrome aa_3 oxidase and mutational analysis of diheme cytochrome c_1. *J. Biol. Chem.* **278,** 4339–4346 CrossRef Medline
12. Niebisch, A., and Bott, M. (2001) Molecular analysis of the cytochrome bc_1–aa_3 branch of the *Corynebacterium glutamicum* respiratory chain containing an unusual diheme cytochrome c_1. *Arch. Microbiol.* **175,** 282–294 CrossRef Medline
13. Kalinowski, J., Bathe, B., Bartels, D., Bischoff, N., Bott, M., Burkovski, A., Dusch, N., Eggeling, L., Eikmanns, B. J., Gaigalat, L., Goesmann, A., Hartmann, M., Huthmacher, K., Krämer, R., Linke, B., *et al.* (2003) The complete *Corynebacterium glutamicum* ATCC 13032 genome sequence and its impact on the production of L-aspartate-derived amino acids and vitamins. *J. Biotechnol.* **104,** 5–25 CrossRef Medline
14. Ikeda, M., and Nakagawa, S. (2003) The *Corynebacterium glutamicum* genome: features and impacts on biotechnological processes. *Appl. Microbiol. Biotechnol.* **62,** 99–109 CrossRef Medline
15. Sone, N., Nagata, K., Kojima, H., Tajima, J., Kodera, Y., Kanamaru, T., Noguchi, S., and Sakamoto, J. (2001) A novel hydrophobic diheme c-type cytochrome: purification from *Corynebacterium glutamicum* and analysis of the *qcrCBA* operon encoding three subunit proteins of a putative cytochrome reductase complex. *Biochim. Biophys. Acta* **1503,** 279–290 CrossRef Medline
16. Graf, S., Fedotovskaya, O., Kao, W. C., Hunte, C., Ädelroth, P., Bott, M., von Ballmoos, C., and Brzezinski, P. (2016) Rapid electron transfer within the III-IV supercomplex in *Corynebacterium glutamicum*. *Sci. Rep.* **6,** 34098 CrossRef Medline
17. Kao, W. C., Kleinschroth, T., Nitschke, W., Baymann, F., Neehaul, Y., Hellwig, P., Richers, S., Vonck, J., Bott, M., and Hunte, C. (2016) The obligate respiratory supercomplex from Actinobacteria. *Biochim. Biophys. Acta* **1857,** 1705–1714 CrossRef Medline
18. Oertel, D., Schmitz, S., and Freudl, R. (2015) A TatABC-type Tat translocase is required for unimpaired aerobic growth of *Corynebacterium glutamicum* ATCC13032. *PLoS One* **10,** e0123413 CrossRef Medline
19. Kabus, A., Niebisch, A., and Bott, M. (2007) Role of cytochrome *bd* oxidase from *Corynebacterium glutamicum* in growth and lysine production. *Appl. Environ. Microbiol.* **73,** 861–868 CrossRef Medline
20. Kim, M. S., Jang, J., Ab Rahman, N. B., Pethe, K., Berry, E. A., and Huang, L. S. (2015) Isolation and characterization of a hybrid respiratory supercomplex consisting of *Mycobacterium tuberculosis* cytochrome *bcc* and *Mycobacterium smegmatis* cytochrome aa_3. *J. Biol. Chem.* **290,** 14350–14360 CrossRef Medline
21. Megehee, J. A., Hosler, J. P., and Lundrigan, M. D. (2006) Evidence for a cytochrome *bcc-aa*$_3$ interaction in the respiratory chain of *Mycobacterium smegmatis*. *Microbiology* **152,** 823–829 CrossRef Medline
22. Matsoso, L. G., Kana, B. D., Crellin, P. K., Lea-Smith, D. J., Pelosi, A., Powell, D., Dawes, S. S., Rubin, H., Coppel, R. L., and Mizrahi, V. (2005) Function of the cytochrome bc_1–aa_3 branch of the respiratory network in mycobacteria and network adaptation occurring in response to its disruption. *J. Bacteriol.* **187,** 6300–6308 CrossRef Medline
23. Kishikawa, J., Kabashima, Y., Kurokawa, T., and Sakamoto, J. (2010) The cytochrome *bcc-aa*$_3$-type respiratory chain of *Rhodococcus rhodochrous*. *J. Biosci. Bioeng.* **110,** 42–47 CrossRef Medline
24. Sawers, R. G., Falke, D., and Fischer, M. (2016) Oxygen and nitrate respiration in *Streptomyces coelicolor* A3(2). *Adv. Microb. Physiol.* **68,** 1–40 CrossRef Medline
25. Schelder, S., Zaade, D., Litsanov, B., Bott, M., and Brocker, M. (2011) The two-component signal transduction system CopRS of *Corynebacterium glutamicum* is required for adaptation to copper-excess stress. *PLoS One* **6,** e22143 CrossRef Medline
26. Teramoto, H., Yukawa, H., and Inui, M. (2015) Copper homeostasis-related genes in three separate transcriptional units regulated by CsoR in *Corynebacterium glutamicum*. *Appl. Microbiol. Biotechnol.* **99,** 3505–3517 CrossRef Medline

27. Hubbard, J. A., Hughes, M. N., and Poole, R. K. (1989) Effects of copper concentration in continuous culture on the aa_3-type cytochrome oxidase and respiratory chains of *Paracoccus denitrificans*. *Arch. Microbiol.* **151,** 300–306 CrossRef
28. Sugiyama, Y., Kitano, K., and Kanzaki, T. (1973) Role of copper ions in regulation of L-glutamate biosynthesis. *Agric. Biol. Chem.* **37,** 1837–1847 CrossRef
29. Frangipani, E., Slaveykova, V. I., Reimmann, C., and Haas, D. (2008) Adaptation of aerobically growing *Pseudomonas aeruginosa* to copper starvation. *J. Bacteriol.* **190,** 6706–6717 CrossRef Medline
30. Koch-Koerfges, A., Pfelzer, N., Platzen, L., Oldiges, M., and Bott, M. (2013) Conversion of *Corynebacterium glutamicum* from an aerobic respiring to an aerobic fermenting bacterium by inactivation of the respiratory chain. *Biochim. Biophys. Acta* **1827,** 699–708 CrossRef Medline
31. Kusumoto, K., Sakiyama, M., Sakamoto, J., Noguchi, S., and Sone, N. (2000) Menaquinol oxidase activity and primary structure of cytochrome *bd* from the amino-acid fermenting bacterium *Corynebacterium glutamicum*. *Arch. Microbiol.* **173,** 390–397 CrossRef Medline
32. Cha, J. S., and Cooksey, D. A. (1991) Copper resistance in *Pseudomonas syringae* mediated by periplasmic and outer membrane proteins. *Proc. Natl. Acad. Sci. U.S.A.* **88,** 8915–8919 CrossRef Medline
33. Thompson, A. K., Gray, J., Liu, A., and Hosler, J. P. (2012) The roles of *Rhodobacter sphaeroides* copper chaperones PCu_AC and Sco (PrrC) in the assembly of the copper centers of the aa_3-type and the cbb_3-type cytochrome *c* oxidases. *Biochim. Biophys. Acta* **1817,** 955–964 CrossRef Medline
34. Cooksey, D. A. (1994) Molecular mechanisms of copper resistance and accumulation in bacteria. *FEMS Microbiol. Rev.* **14,** 381–386 CrossRef Medline
35. Bengtsson, J., von Wachenfeldt, C., Winstedt, L., Nygaard, P., and Hederstedt, L. (2004) CtaG is required for formation of active cytochrome *c* oxidase in *Bacillus subtilis*. *Microbiology* **150,** 415–425 CrossRef Medline
36. Toyoda, K., and Inui, M. (2016) The extracytoplasmic function σ factor σ^C regulates expression of a branched quinol oxidation pathway in *Corynebacterium glutamicum*. *Mol. Microbiol.* **100,** 486–509 CrossRef Medline
37. Liu, T., Ramesh, A., Ma, Z., Ward, S. K., Zhang, L., George, G. N., Talaat, A. M., Sacchettini, J. C., and Giedroc, D. P. (2007) CsoR is a novel *Mycobacterium tuberculosis* copper-sensing transcriptional regulator. *Nat. Chem. Biol.* **3,** 60–68 CrossRef Medline
38. Ma, Z., Cowart, D. M., Scott, R. A., and Giedroc, D. P. (2009) Molecular insights into the metal selectivity of the copper(I)-sensing repressor CsoR from *Bacillus subtilis*. *Biochemistry* **48,** 3325–3334 CrossRef Medline
39. Rae, T. D., Schmidt, P. J., Pufahl, R. A., Culotta, V. C., and O'Halloran, T. V. (1999) Undetectable intracellular free copper: the requirement of a copper chaperone for superoxide dismutase. *Science* **284,** 805–808 CrossRef Medline
40. Finn, R. D., Coggill, P., Eberhardt, R. Y., Eddy, S. R., Mistry, J., Mitchell, A. L., Potter, S. C., Punta, M., Qureshi, M., Sangrador-Vegas, A., Salazar, G. A., Tate, J., and Bateman, A. (2016) The Pfam protein families database: towards a more sustainable future. *Nucleic Acids Res.* **44,** D279–D285 CrossRef Medline
41. Cha, J. S., and Cooksey, D. A. (1993) Copper hypersensitivity and uptake in *Pseudomonas syringae* containing cloned components of the copper resistance operon. *Appl. Environ. Microbiol.* **59,** 1671–1674 Medline
42. Arnesano, F., Banci, L., Bertini, I., Mangani, S., and Thompsett, A. R. (2003) A redox switch in CopC: an intriguing copper trafficking protein that binds copper(I) and copper(II) at different sites. *Proc. Natl. Acad. Sci. U.S.A.* **100,** 3814–3819 CrossRef Medline
43. Thöny-Meyer, L. (1997) Biogenesis of respiratory cytochromes in bacteria. *Microbiol. Mol. Biol. Rev.* **61,** 337–376 Medline
44. Nyvltova, E., Barrientos, A., and Hosler, J. (2017) Assembly of heme a_3-Cu_B and Cu_A in cytochrome *c* oxidase. in *Encyclopedia of Inorganic and Bioinorganic Chemistry*, pp. 1–27, John Wiley & Sons, Ltd., Chichester, UK
45. Vrljic, M., Sahm, H., and Eggeling, L. (1996) A new type of transporter with a new type of cellular function: L-lysine export from *Corynebacterium glutamicum*. *Mol. Microbiol.* **22,** 815–826 CrossRef Medline
46. Bellmann, A., Vrljić, M., Pátek, M., Sahm, H., Krämer, R., and Eggeling, L. (2001) Expression control and specificity of the basic amino acid exporter LysE of *Corynebacterium glutamicum*. *Microbiology* **147,** 1765–1774 CrossRef Medline
47. Binder, S., Schendzielorz, G., Stäbler, N., Krumbach, K., Hoffmann, K., Bott, M., and Eggeling, L. (2012) A high-throughput approach to identify genomic variants of bacterial metabolite producers at the single-cell level. *Genome Biol.* **13,** R40 CrossRef Medline
48. Schendzielorz, G., Dippong, M., Grünberger, A., Kohlheyer, D., Yoshida, A., Binder, S., Nishiyama, C., Nishiyama, M., Bott, M., and Eggeling, L. (2014) Taking control over control: use of product sensing in single cells to remove flux control at key enzymes in biosynthesis pathways. *ACS Synth. Biol.* **3,** 21–29 CrossRef Medline
49. Hill, B. C., and Andrews, D. (2012) Differential affinity of BsSCO for Cu(II) and Cu(I) suggests a redox role in copper transfer to the Cu_A center of cytochrome *c* oxidase. *Biochim. Biophys. Acta* **1817,** 948–954 CrossRef Medline
50. Bott, M., Bolliger, M., and Hennecke, H. (1990) Genetic analysis of the cytochrome *c*-aa_3 branch of the *Bradyrhizobium japonicum* respiratory chain. *Mol. Microbiol.* **4,** 2147–2157 CrossRef Medline
51. Loferer, H., Bott, M., and Hennecke, H. (1993) *Bradyrhizobium japonicum* TlpA, a novel membrane-anchored thioredoxin-like protein involved in the biogenesis of cytochrome aa_3 and development of symbiosis. *EMBO J.* **12,** 3373–3383 Medline
52. Abicht, H. K., Schärer, M. A., Quade, N., Ledermann, R., Mohorko, E., Capitani, G., Hennecke, H., and Glockshuber, R. (2014) How periplasmic thioredoxin TlpA reduces bacterial copper chaperone ScoI and cytochrome oxidase subunit II (CoxB) prior to metallation. *J. Biol. Chem.* **289,** 32431–32444 CrossRef Medline
53. Abriata, L. A., Banci, L., Bertini, I., Ciofi-Baffoni, S., Gkazonis, P., Spyroulias, G. A., Vila, A. J., and Wang, S. (2008) Mechanism of Cu_A assembly. *Nat. Chem. Biol.* **4,** 599–601 CrossRef Medline
54. Banci, L., Bertini, I., Ciofi-Baffoni, S., Katsari, E., Katsaros, N., Kubicek, K., and Mangani, S. (2005) A copper(I) protein possibly involved in the assembly of Cu_A center of bacterial cytochrome *c* oxidase. *Proc. Natl. Acad. Sci. U.S.A.* **102,** 3994–3999 CrossRef Medline
55. Sutcliffe, I. C., and Harrington, D. J. (2002) Pattern searches for the identification of putative lipoprotein genes in Gram-positive bacterial genomes. *Microbiology* **148,** 2065–2077 CrossRef Medline
56. Iwata, S., Ostermeier, C., Ludwig, B., and Michel, H. (1995) Structure at 2.8 Å resolution of cytochrome *c* oxidase from *Paracoccus denitrificans*. *Nature* **376,** 660–669 CrossRef Medline
57. Hiser, L., Di Valentin, M., Hamer, A. G., and Hosler, J. P. (2000) Cox11p is required for stable formation of the Cu_B and magnesium centers of cytochrome *c* oxidase. *J. Biol. Chem.* **275,** 619–623 CrossRef Medline
58. von Wachenfeldt, C., and Hederstedt, L. (2001) Respiratory cytochromes, other heme proteins, and heme biosynthesis. in *Bacillus subtilis and Its Closest Relatives: From Genes to Cells* (Sonenshein, A. L., Hoch, J. A., and Losick, R., eds) pp. 163–179, ASM Press, Washington, D. C.
59. Khalfaoui-Hassani, B., Wu, H., Blaby-Haas, C. E., Zhang, Y., Sandri, F., Verissimo, A. F., Koch, H. G., and Daldal, F. (2018) Widespread distribution and functional specificity of the copper importer CcoA: distinct Cu uptake routes for bacterial cytochrome *c* oxidases. *MBio* **9,** e00065-18 CrossRef Medline
60. Ekici, S., Yang, H., Koch, H. G., and Daldal, F. (2012) Novel transporter required for biogenesis of cbb_3-type cytochrome *c* oxidase in *Rhodobacter capsulatus*. *MBio* **3,** e00293-11 CrossRef Medline
61. Keilhauer, C., Eggeling, L., and Sahm, H. (1993) Isoleucine synthesis in *Corynebacterium glutamicum*: molecular analysis of the *ilvB-ilvN-ilvC* operon. *J. Bacteriol.* **175,** 5595–5603 CrossRef Medline
62. Sambrook, J., and Russell, D. (2001) *Molecular Cloning: A Laboratory Manual*, 3rd Ed., Cold Spring Harbor Laboratory Press, Cold Spring Harbor, NY
63. Hanahan, D., Jessee, J., and Bloom, F. R. (1991) Plasmid transformation of *Escherichia coli* and other bacteria. *Methods Enzymol.* **204,** 63–113 CrossRef Medline
64. van der Rest, M. E., Lange, C., and Molenaar, D. (1999) A heat shock following electroporation induces highly efficient transformation of *Co-*

rynebacterium glutamicum with xenogeneic plasmid DNA. *Appl. Microbiol. Biotechnol.* **52,** 541–545 CrossRef Medline

65. Möker, N., Brocker, M., Schaffer, S., Krämer, R., Morbach, S., and Bott, M. (2004) Deletion of the genes encoding the MtrA-MtrB two-component system of *Corynebacterium glutamicum* has a strong influence on cell morphology, antibiotics susceptibility and expression of genes involved in osmoprotection. *Mol. Microbiol.* **54,** 420–438 CrossRef Medline
66. Frunzke, J., Engels, V., Hasenbein, S., Gätgens, C., and Bott, M. (2008) Co-ordinated regulation of gluconate catabolism and glucose uptake in *Corynebacterium glutamicum* by two functionally equivalent transcriptional regulators, GntR1 and GntR2. *Mol. Microbiol.* **67,** 305–322 Medline
67. Schaffer, S., Weil, B., Nguyen, V. D., Dongmann, G., Günther, K., Nickolaus, M., Hermann, T., and Bott, M. (2001) A high-resolution reference map for cytoplasmic and membrane-associated proteins of *Corynebacterium glutamicum*. *Electrophoresis* **22,** 4404–4422 CrossRef Medline
68. Castiglioni, E., Grilli, E., and Sanguinetti, S. (1997) A new simple and low cost scattered transmission accessory for commercial double beam ultraviolet-visible spectrophotometers. *Rev. Sci. Instrum.* **68,** 4288–4289 CrossRef
69. Abe, S., Takayama, K., and Kinoshita, S. (1967) Taxonomical studies on glutamic acid producing bacteria. *J. Gen. Appl. Microbiol.* **13,** 279–301 CrossRef
70. Schäfer, A., Tauch, A., Jäger, W., Kalinowski, J., Thierbach, G., and Pühler, A. (1994) Small mobilizable multipurpose cloning vectors derived from the *Escherichia coli* plasmids pK18 and pK19: selection of defined deletions in the chromosome of *Corynebacterium glutamicum*. *Gene* **145,** 69–73 CrossRef Medline
71. Eikmanns, B. J., Kleinertz, E., Liebl, W., and Sahm, H. (1991) A family of *Corynebacterium glutamicum*/*Escherichia coli* shuttle vectors for cloning, controlled gene expression, and promoter probing. *Gene* **102,** 93–98 CrossRef Medline
72. Omasits, U., Ahrens, C. H., Müller, S., and Wollscheid, B. (2014) Protter: interactive protein feature visualization and integration with experimental proteomic data. *Bioinformatics* **30,** 884–886 CrossRef Medline

Identification of Surf1 as an assembly factor of the cytochrome bc_1-aa_3 supercomplex of *Actinobacteria*

Cedric-Farhad Davoudi, Meike Baumgart and Michael Bott*

Institute of Bio- and Geosciences, IBG-1: Biotechnology, Forschungszentrum Jülich, Germany

*Corresponding author:

Email
m.bott@fz-juelich.de
Phone +49 2461 61 3294
Fax +49 2461 61 2710

Keywords:
Corynebacterium glutamicum, Actinobacteria, respiratory chain, cytochrome bc_1-aa_3 supercomplex, biogenesis/assembly of respiratory enzyme complexes, Surf1

Abstract

Respiration in aerobic *Actinobacteria* involves a cytochrome bc_1-aa_3 supercomplex with a diheme cytochrome c_1, first identified in *Corynebacterium glutamicum*. Synthesis of a functional cytochrome *c* oxidase requires incorporation of Cu_A, Cu_B, heme *a*, and heme a_3. In contrast to eukaryotes and α-proteobacteria, this process is poorly understood in Actinobacteria. Here, we analyzed the role of a Surf1 homolog of *C. glutamicum* in the formation of a functional bc_1-aa_3 supercomplex. Deletion of the *surf1* gene (cg2460) in *C. glutamicum* caused a strong growth defect and an increased copper sensitivity. Cytochrome spectra revealed reduced levels of cytochrome *c* and *a* and an increased level of cytochrome *d*. Membranes of the Δ*surf1* strain had completely lost the ability to oxidize the artificial electron donor *N*,*N*,*N*',*N*'-tetramethyl-*p*-phenylendiamine, indicating that Surf1 is essential for the formation of functional cytochrome aa_3 oxidase. In contrast to the wild type, a bc_1-aa_3 supercomplex could not be purified from solubilized membranes of the Δ*surf1* mutant. A transcriptome comparison revealed that the genes of the SigC regulon including those for cytochrome *bd* oxidase were upregulated in the Δ*surf1* strain as well as the copper deprivation-inducible gene *ctiP*. Complementation studies showed that the Surf1 homologs of *Corynebacterium diphtheriae*, *Mycobacterium tuberculosis*, and *Mycobacterium smegmatis* could abolish the growth defect of the *C. glutamicum* Δ*surf1* mutant, indicating that Surf1 is a conserved assembly factor for actinobacterial cytochrome aa_3 oxidase.

Introduction

Aerobic bacterial respiratory chains are characterized by a large diversity including various types of terminal oxidases acting either as quinol oxidases or as cytochrome *c* oxidases [1, 2]. Bacteria typically contain two or more terminal oxidases allowing adaptation to changing environmental conditions with respect to oxygen partial pressure, copper availability, or varying demands for respiratory activity. Actinobacteria form a large phylum within the Gram-positive bacteria and include a variety of species of high medical and biotechnological relevance, such as *Mycobacterium tuberculosis* or *Corynebacterium glutamicum*. Strains of *C. glutamicum* are used in the biotech industry for production of about five million tons of amino acids per year, mainly L-glutamate and L-lysine. These processes are performed under aerobic conditions and depend on respiration.

The respiratory chain of *C. glutamicum* is branched and contains two terminal oxidases, a cytochrome *c* oxidase of the aa_3-type and the menaquinol oxidase cytochrome *bd* [3]. A unique feature of the respiratory chain of *C. glutamicum* is the presence of a cytochrome bc_1-aa_3 supercomplex with a diheme

cytochrome c_1 that represents the only *c*-type cytochrome of this species [4, 5]. The supercomplex was purified in active form by affinity chromatography with either Strep-tagged cytochrome *b* (QcrB) or with Strep-tagged subunit I (CtaD) of cytochrome aa_3 and included besides the subunits of the bc_1 complex and the aa_3 oxidase three additional proteins, a secreted lipoprotein (Cg2949), an integral membrane protein (Cg2211) and a cytosolic protein (Cg2444) [5]. Deletion of the corresponding genes had no growth phenotype, indicating that these proteins are not essential for activity [5]. The complex was characterized with respect to the redox potential of the prosthetic groups and a structural model was build [6]. Moreover, the complex was characterized kinetically [7].

Complexes similar to the one of *C. glutamicum* were later also described for *Mycobacterium* species [8, 9]. With the availability of a large set of genome sequences it became clear that a bc_1-aa_3 supercomplex is presumably characteristic for all aerobic *Actinobacteria* [6]. Most recently, the structure of the bc_1-aa_3 supercomplex was solved by cryo-electron microscopy in two parallel studies [10, 11]. These studies confirmed key features of the model proposed for *C. glutamicum* and revealed new and interesting aspects, such as the presence of a periplasmic superoxide dismutase associated with cytochrome *b* or the presence of cytochrome c_1 in two different confirmations [10, 11]. Moreover, the cryo-EM structures revealed the presence of accessory proteins, including homologs of Cg2211 (PRSAF1) and Cg2949 (LpqE) previously found to be associated with supercomplex of *C. glutamicum*.

The formation of a catalytically active bc_1-aa_3 supercomplex requires an assembly process for insertion of the cofactors, which are Cu_A, Cu_B, heme *a*, and heme a_3 in the case of the aa_3 oxidase. Many proteins involved in these maturation events have been identified and characterized in mammals, *Saccharomyes cerevisiae*, and α-proteobacteria [12], but knowledge for *Actinobacteria* is scarce. By analyzing the transcriptional response of *C. glutamicum* to copper deprivation we recently identified two proteins involved in copper insertion into the aa_3 oxidase, the membrane-integral copper transport and insertion protein CtiP and the secreted Cu(II)-binding protein CopC, which were found to be conserved in aerobic *Actinobacteria* [13].

In the present study, we analyzed another protein, Cg2460, presumed to be a potential assembly factor for the aa_3 oxidase in *C. glutamicum*. The protein showed weak sequence similarity to Surf1 proteins from other organisms. Surf1 was identified as a protein that was able to complement cytochrome oxidase defects causing the Leigh syndrome in humans, a severe human neurodegenerative disease, and therefore proposed to be involved in cytochrome oxidase biogenesis [14]. The homolog from *S. cerevisiae* is Shy1p and deletion of the corresponding gene also led to reduced oxidase activity [15]. The role of Surf1 in mitochondrial cytochrome oxidase biogenesis is still unknown and the functions proposed include stabilization of subunit I and involvement in copper homeostasis [16, 17]. A much better picture is available for the role of Surf1 homologs in α-proteobacteria (reviewed by [18]). Biochemical analysis of cytochrome aa_3 oxidase in *Rhodobacter sphaeroides* indicated that Surf1 plays a role in facilitating the insertion of heme a_3 into the active site the oxidase [19]. In *Paracoccus denitrificans*, two Surf1 homologs are present and shown to be involved in oxidase assembly, Surf1q acting on the *ba*-type quinol oxidase and Surf1c acting on the aa_3-type cytochrome *c* oxidase [20]. Further studies revealed that the *P. denitrificans* Surf1 proteins bind heme *a* in a 1:1 stoichiometry with K_d values of 0.3 – 0.7 µM, indicating that the Surf1 protein are involved in the transfer of heme *a* from the heme *a* synthase CtaA to subunit I and its insertion [20, 21].

In Gram-positive bacteria, the role of Surf1 proteins has not been studied until now. We therefore investigated the impact of the putative Surf1 homolog Cg2460 of *C. glutamicum* on the assembly and activity of the cytochrome bc_1-aa_3 supercomplex. Furthermore, to gain information about regulatory mechanisms, we compared global gene expression of a *surf1* mutant and the wild type. Lastly, the conservation of Surf1 within actinobacterial species was examined.

Materials and Methods

Bacterial strains, plasmids, and growth conditions

All bacterial strains and plasmids used in this work are listed in Table 1. The *C. glutamicum* type strain ATCC 13032 was used as wild type (WT). To start cultivation, 5 ml brain heart infusion broth (BHI, Difco Laboratories, Detrot, MI) was inoculated with a single colony from an agar plate and incubated for 9 h at 30 °C and 170 rpm. When appropriate, 25 µg/ml kanamycin was added. The cells of this first preculture were used to inoculate a second preculture in 750 µl CGXII minimal medium [22] containing 30 mg l^{-1} 3,4-dihydroxybenzoate as iron chelator and 2% (w/v) glucose. The cultivation was performed overnight at 30 °C and 1200 rpm using a BioLector microcultivation system and a 48-well FlowerPlate (m2p-labs, Baesweiler, Germany). For larger cultivation volumes, 50 ml BHI medium was inoculated with 500 µl preculture in 500 ml-Erlenmeyer flasks that were incubated overnight at 140 rpm and 30 °C. The main cultures were performed in the same medium as the second preculture with the addition of 2% (w/v) glucose. For Biolector and shake flask cultivations, the initial optical density at 600 nm (OD_{600}) was set to 1 and 0.5, respectively. For complementation experiments, in which the cells carried expression plasmids with a *tac* promoter, 100 µM isopropyl-β-D-thiogalactoside (IPTG) was added to the medium immediately after inoculation. All cloning steps were performed with *Escherichia coli* DH5α as host, which was cultivated at 37 °C on LB agar plates or in liquid LB medium [23] with 50 µg/ml kanamycin [24].

Recombinant DNA work and construction of deletion mutants

All plasmids and oligonucleotides used in this study are listed in Tables 1 and 2. Routine methods such as PCR and DNA restriction were performed using established protocols [24]. Gibson assembly was used for plasmid construction [25]. DNA sequencing and oligonucleotide synthesis were performed by Eurofins Genomics (Ebersberg, Germany). In-frame gene deletion strains of *C. glutamicum* were constructed *via* a two-step homologous recombination protocol using 500 bp flanks [4]. Colony PCR using oligonucleotides annealing outside the deleted regions was performed to confirm the chromosomal deletions.

For construction of the reporter plasmids pJC1-P*cydA*-*venus* and pJC1-P*ctaD*-*venus*, approximately 500 bp upstream of the start codon and 30 bp of the coding region followed by an introduced stop codon were amplified from chromosomal DNA by PCR using the oligonucleotide pairs ctaD_venus_fwd/ctaD_venus_rev and cydA_venus_fwd/ cydA_venus_rev, resulting in PCR products of 589 bp and 611 bp. Amplification of the *venus* gene including a ribosome binding site was performed with the oligonucleotide pair venus_3_fwd/venus_4_rev and pJC1-*venus*-term as template, resulting in a PCR product of 755 bp. The individual promotor and *venus* fragments were ligated into a BamHI/SpeI-linearized pJC1 vector using Gibson assembly [26]. After sequencing of the plasmids, they were transferred into *C. glutamicum* wt, the Δ*surf1* mutant and the Δ*ctiP* mutant.

Global gene expression analysis

For a comparative transcriptome analysis of the *C. glutamicum* Δ*surf1* mutant and the parent WT, the cells were cultivated in shake flasks using CGXII medium with 2% (w/v) glucose as described above until they reached the early exponential phase (OD_{600} of about 5). Then RNA was isolated and used for DNA microarray analysis using custom-made 60mer DNA microarrays for genome-wide gene expression analysis from Agilent Technologies (Waldbronn, Germany). Four independent biological replicates were performed for comparison of the Δ*surf1* mutant and the WT and *p* values were calculated using Student's t test (Excel, Microsoft). The experimental details and the data evaluation were performed as described previously [27]. The microarray data have been deposited in the NCBI Gene Expression Omnibus (GEO) database and are accessible under the accession number GSE123974.

Tables

Table 1

Bacterial strains and plasmids used in this study.

Strain or plasmid	Relevant characteristics	Source or reference
E. coli		
DH5α	F⁻ Φ80*dlac*Δ(*lacZ*)M15 Δ(*lacZYA-argF*) U169 *endA1 recA1 hsdR17* (r_K^-, m_K^+) *deoR thi-1 phoA supE44* λ⁻ *gyrA96 relA1*; strain used for cloning procedures	[35]
C. glutamicum		
ATCC13032	Biotin-auxotrophic wild type	[36]
C. glutamicum Δ*ctiP*	Derivative of ATCC13032 with in-frame deletion of the *ctiP* (cg2699) gene	[13]
C. glutamicum Δ*ctaD*	Derivative of ATCC13032 with in-frame deletion of the *ctaD* (cg2780) gene	[4]
C. glutamicum Δ*surf1*	Derivative of ATCC13032 with in-frame deletion of the *surf1* (cg2460) gene	This work
C. glutamicum Δ*qcr*	Derivative of ATCC13032 with in-frame deletion of the *ctaE-qcrCAB* operon (cg2406-2404)	[4]
C. glutamicum Δ*qcr*Δ*ctiP*	Derivative of ATCC13032 with in-frame deletion of the *ctaE-qcrCAB* operon and *ctiP* genes	[13]
C. glutamicum Δ*qcr*Δ*surf1*	Derivative of ATCC13032 with in-frame deletion of the *ctaE-qcrCAB* operon and *surf1*	This work
C. glutamicum Δ*ctaD*Δ*ctiP*	Derivative of ATCC13032 with in-frame deletion of *ctaD* and *ctiP*	[13]
C. glutamicum Δ*ctaD*Δ*surf1*	Derivative of ATCC13032 with in-frame deletion of *ctaD* and *surf1*	This work
C. diphtheriae DSM44123	Wild type, genomic DNA was used as a PCR template	DSM 44123
M. smegmatis MC² 155	Wild type, genomic DNA was used as a PCR template	ATCC 700084
M. tuberculosis H37Rv	Wild type, genomic DNA was used as a PCR template	ATCC 25618
Plasmids		
pK19*mobsacB*	Kan^R; plasmid for allelic exchange in *C. glutamicum* (pK18 *ori*V$_{E.c.}$, *sacB*, *lacZ*α)	[37]
pK19*mobsacB*-Δ*surf1*	Kan^R; pK19*mobsacB* derivative containing a 1 kb PCR-product (EcoRI/PstI) which covers the flanking regions of the *C. glutamicum surf1* gene	This work
pAN6	Kan^R; *C. glutamicum*/*E. coli* shuttle vector for regulated gene expression using the P_{tac} promoter; derivative of pEKEx2	[38]
pAN6-*surf1*	Kan^R; pAN6 derivative containing *surf1* gene (cg2460) of *C. glutamicum* under control of P_{tac}	This work
pAN6-CDC7B1688	Kan^R; pAN6 derivative containing the CDC7B_1688 gene (*surf1* homolog) of *C. diphtheriae* DSM44123 under control of the *tac* promoter	This work
pAN6-MSMEG4311	Kan^R; pAN6 derivative containing the MSMEG4311 gene (*surf1* homolog) of	This work

pAN6-Rv2235	Kan^R; pAN6 derivative containing the Rv2235 gene (*surf1* homolog) of *M. tuberculosis* H37Rv under control of the *tac* promoter	This work
pJC1	Kan^R; *E. coli*/*C. glutamicum* shuttle vector (pHM1519 ori_{Cg}, pACYC177 ori_{Ec})	[39]
pJC1-*venus*-term	Kan^R; pJC1 derivative harboring the *venus* gene and additional terminators	[40]
pJC1-$qcrB_{St}$	Kan^R; expression plasmid for purification of Strep-tagged QcrB; contains the *ctaE-qcrCAB* operon expressed from its native promotor; *qcrB* with 10 additional codons at the 3'-end (AAWSHPQFEK)	[5]
pJC1-$ctaD_{St}$	Kan^R; expression plasmid for purification of Strep-tagged CtaD; *ctaD* expressed from its native promotor with 10 additional codons at the 3'-end (AAWSHPQFEK)	[5]

Table 2
Oligonucleotides used in this study.

Oligonucleotide	Sequence (5' → 3') and properties[a]
Construction of deletion plasmid pK19mobsacB-Δ*surf1* and PCR analysis of the resulting mutants	
cg2460-D1	**CAAGCTTGCATGCCTGCAGGTCGAC**CTGGCTTGGAAGACAACGTC
cg2460-D2	**TGTTTAAGTTTAGTGGATGGG**CGGAATAGCGGGAGCTCACG
cg2460-D3	**CCCATCCACTAAACTTAAACA**GCGATCAACACCGCAATCAC
cg2460-D4	**TTGTAAAACGACGGCCAGTGAATTC**GGGTGGTGGAGCGTACTAAC
cg2460_seq_fwd	AGTCATCGCGAAGGCAAAAGC
cg2460_seq_rev	CTGGGTGATCAGCACTAAAGG
Construction of expression plasmids pAN6-*surf1*, pAN6-CDC7B1668, pAN6-MSMEG4311, pAN6-Rv2235 and PCR analysis of the resulting plasmids	
*surf1*_pAN6_fwd	**GCCTGCAGAAGGAGATATACATATG**GACAGCAAGGTAAATAGCCC
*surf1*_pAN6_rev	**CTGTAAAACGACGGCCAGTGAATTC**TTAGAAGCGCTCTTGGTCTC
CDC7B_pAN6_fwd	**GCCTGCAGAAGGAGATATACATATG**CCTAGGACGCACACAACTGTCAC
CDC7B_pAN6_rev	**CTGTAAAACGACGGCCAGTGAATTC**TTACTGATTATGCCGTGAGCTACCG
MSMEG4311_pAN6_fwd	**GCCTGCAGAAGGAGATATACATATG**CGCCGGCTCGGCTTTCTC
MSMEG4311_pAN6_rev	**CTGTAAAACGACGGCCAGTGAATTC**TCAGCGGCGCTTGCCGTAG
Rv2235_pAN6_fwd	**GCCTGCAGAAGGAGATATACATATG**CCCCGCCTAGCGTTCCTGCTG
Rv2235_pAN6_rev	**CTGTAAAACGACGGCCAGTGAATTC**TTACCGCCGGCGGCCGTAG
pAN6_seq_fwd	ATGACCATGATTACGCCAAGC
pAN6_seq_rev	CGGCGTTTCACTTCTGAGTTC

[a]) Overlaps for Gibson assembly are written in bold letters.

Purification of the cytochrome bc_1-aa_3 supercomplex

C. glutamicum strains carrying expression plasmids were cultivated in 5 l shake flasks with 500 ml BHI medium supplemented with 2% (w/v) glucose at 30°C and 90 rpm and harvested at an OD_{600} of 8. Membrane isolation, solubilization of membrane proteins with *n*-dodecyl-β-D-maltoside and subsequent purification of Strep-tagged CtaD or Strep-tagged QcrB was performed as described previously [5]. Aliquots of the purified proteins were separated by SDS-PAGE using 12% polyacrylamide gels (BioRad, Munich, Germany) which were subsequently stained with Coomassie dye-based RAPIDStain solution (G-Biosciences, St. Louis, MO, USA). Protein bands were identified after in-gel trypsin digestion [28] by peptide mass fingerprinting using an Ultraflex III TOF/TOF mass spectrometer (Bruker Daltonics, Bremen, Germany) as described previously [29].

Redox difference spectroscopy

Spectra were recorded at room temperature using 5-mm-light-path cuvettes with a Jasco V560 spectrophotometer. For recording the dithionite-reduced spectrum of intact cells (oxidation of cytochromes in intact cells proved to be difficult), a suspension of *C. glutamicum* cells in 100 mM Tris-HCl, pH 7.5 with an OD_{600} of 100 and a silicon photodiode detector for turbid samples [30] was used. Dithionite-reduced minus ferricyanide-oxidized difference spectra of isolated membranes (30 mg/ml) resuspended in 100 mM Tris-HCl, pH 7.5 were also recorded with the silicon photodiode detector. Dithionite-reduced minus ferricyanide-oxidized difference spectra of protein samples (0.5 mg/ml) obtained after affinity chromatography of $CtaD_{St}$ were recorded using the standard photomultiplier detector of the Jasco V560 spectrophotometer. A few grains of sodium dithionite or potassium ferricyanide were added to the samples to reduce and oxidize the cytochromes, respectively.

TMPD oxidase assay

N,N,N',N'-Tetramethyl-*p*-phenylenediamine (TMPD) oxidase activity of isolated membranes was measured spectrophotometrically at 562 nm in air-saturated 100 mM Tris-HCl buffer, pH 7.5, containing 200 µM TMPD, at 30 °C. For the calculation, an extinction coefficient of 10.5 mM^{-1} cm^{-1} was used [31]. One unit of activity is defined as 1 µmol of TMPD oxidized per min. Autooxidation rates of TMPD was recorded using samples containing only buffer and TMPD and subtracted from the rates of the membranes.

Results and discussion

In silico characterization of a Surf1 homolog in C. glutamicum

Studies in the α-proteobacteria *Paracoccus denitrificans* and *Rhodobacter sphaeroides* indicated that Surf1 proteins are involved in transferring the heme *a* group from heme *a* synthase, CtaA, to subunit I of cytochrome *c* oxidase and transiently bind heme *a* [18, 19]. In aerobic Actinobacteria like *C. glutamicum*, which are characterized by a cytochrome bc_1-aa_3 supercomplex, nothing is currently known about assembly factors involved in heme incorporation. In the genome of *C. glutamicum*, the gene with the locus tag cg2460 encodes a protein of 333 amino acid residues (predicted molecular mass 37.24 kDa) with 24% amino acid sequence identity to Surf1c of *P. denitrificans* [20] and 18% amino acid sequence identity to Surf1 of *R. sphaeroides* [19]. Bioinformatic analysis indicated that Cg2460, similar to previously characterized Surf1 proteins, possesses two transmembrane helices (residues 35-56 and 245-264) enclosing an extracytoplasmic SURF1 domain (Prosite PS50895) of 189 residues [32] (Fig. 1). An amino acid sequence alignment (Fig. S1) revealed the presence of the motifs $W^{62}Q^{63}$ and $Y^{244}xxxW^{248}$ in Cg2460, which were shown to be crucial not only for heme binding, but also for differentiation between heme types [21]. Furthermore, the histidine residue H^{241} reported to serve as axial ligand of the heme iron in *P. denitrificans* Surf1 was conserved in *C. glutamicum* Surf1 (Fig. 1, Fig. S1). Unlike in other bacteria, such as *P. denitrificans*, the *surf1* gene of *C. glutamicum* is not located in the immediate neighborhood of genes coding for components of the respiratory chain or heme biosynthesis [33].

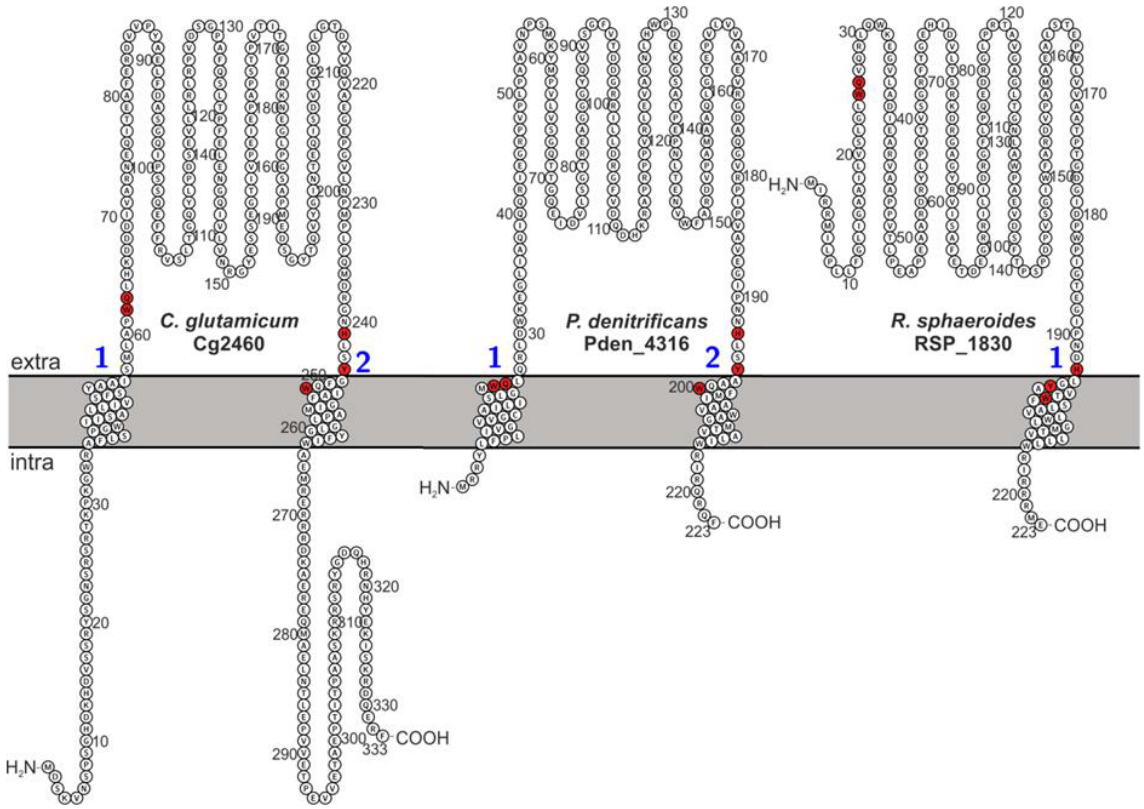

Fig. 1. Topology models of Surf1 proteins from *C. glutamicum* (Cg2460), *P. denitrificans* (Pden_4316) and *R. sphaeroides* (RSP_1830). Predictions of protein architectures were done using the PROTTER software [32]. Red shaded amino acid residues were shown to be involved in heme a binding in *P. denitrificans* Surf1 [18].

Phenotype of a surf1 deletion mutant of C. glutamicum

To analyze the role of Surf1 in *C. glutamicum,* a *surf1* deletion strain was constructed and analyzed regarding growth. The loss of Surf1 caused to a strong growth defect on BHI agar plates (data not shown) and in CGXII minimal medium (Fig. 2A), which was similar to the growth defect of a Δ*ctaD* strain lacking subunit I of cytochrome aa_3 oxidase and of a Δ*ctiP* strain lacking the copper transport and insertion protein CtiP [13]. Thus, Surf1 is important for optimal growth of *C. glutamicum*. Under copper excess stress, the *surf1* mutant of *C. glutamicum* showed a growth defect comparable to the one observed under standard copper levels (Fig. 2C). In contrast, the Δ*surf1* mutant grew like the wt under copper deprivation (Fig. 2D), which is a clear evidence for the involvement of Surf1 in cytochrome aa_3 assembly. Under copper deprivation, cytochrome aa_3 oxidase is inactive due to the lack of copper and cytochrome *bd* oxidase serves as terminal oxidase. Therefore, if Surf1 is an assembly factor of cytochrome aa_3 oxidase, its absence should have no consequences under copper deprivation, as observed before for the assembly factor CtiP [13]. Complementation experiments with the native *surf1* gene restored wild-type like growth (Fig. 2B), confirming that the growth phenotype is due to the lack of *surf1* gene rather than to secondary mutations. Plasmid-based expression of *cta4*, coding for heme *a* synthase, did not complement the growth defect of *C. glutamicum* Δ*surf1* (data not shown).

To study the impact of the *surf1* deletion on the cytochrome content of the cell, an absorbance spectrum of a dithionite-reduced cell suspension was recorded and compared with the corresponding spectrum of the wt (Fig. 3A). The Δ*surf1* mutant differed from the wt by a decreased cytochrome *c* peak, a shift of the cytochrome *b* peak from 564 nm to 559 nm, a shift of the cytochrome *a* peak from 600 nm to 596 nm and the appearance of a cytochrome *d* peak at about 623 nm. These results were confirmed by reduced-minus-oxidized difference spectra of isolated membranes (Fig.

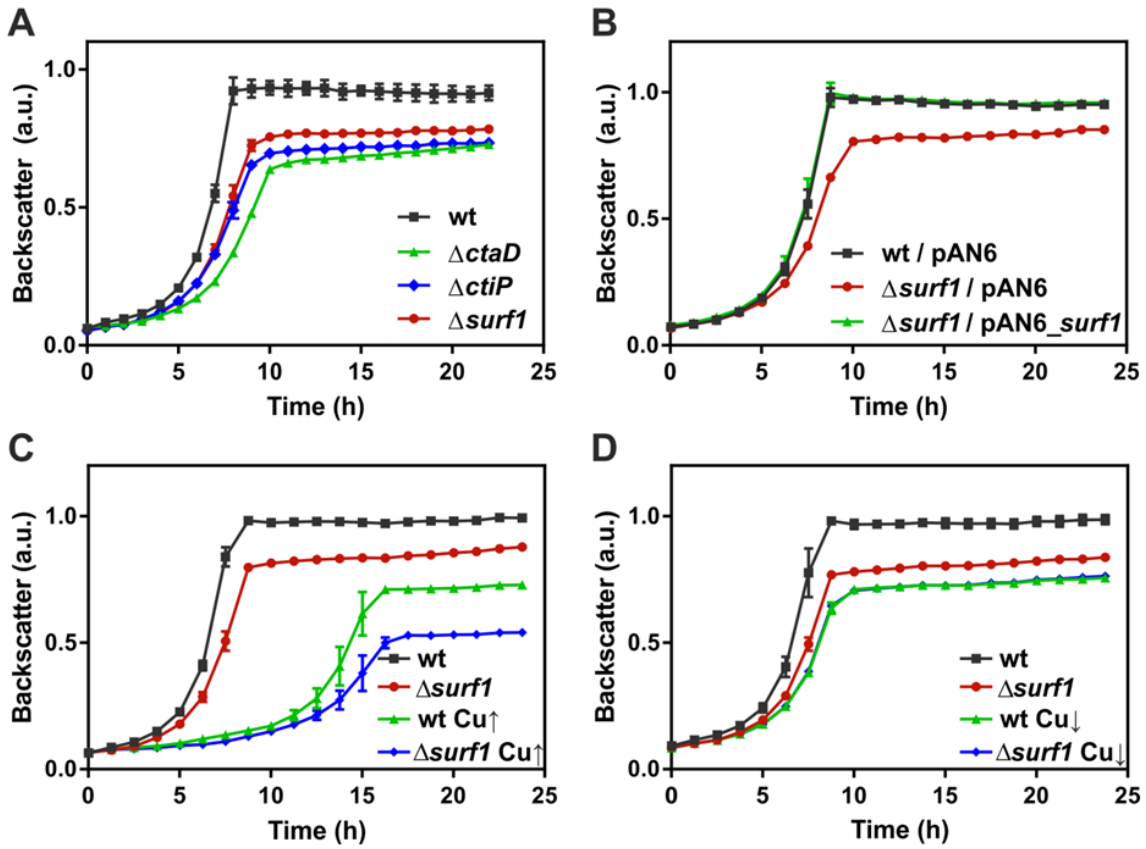

Fig. 2. Growth studies of the indicated *C. glutamicum* strains under different cultivation conditions. (A, B) Growth in standard CGXII medium supplemented with 2% (w/v) glucose and 1.25 µM $CuSO_4$. (C) Growth in CGXII medium with 2% (w/v) glucose supplemented with 100 µM $CuSO_4$ (Cu↑) and for comparison growth with 1.25 µM $CuSO_4$. (D) Growth in copper-deprived CGXII medium with 2% (w/v) glucose supplemented with 150 µM BCS and 1 mM ascorbate (Cu↓). For comparison, growth with 1.25 µM CuSO4 is shown. Cells were cultivated in a FlowerPlate using a Biolector microcultivation system (30 °C, 1200 rpm). Growth was measured online as backscatter at 620 nm every hour. All backscatter values were normalized by setting the maximal backscatter value of the wt used for comparison as 1. Depicted are mean values and standard deviation (bars) from three biological replicates. *a.u.*. arbitrary units.

3B) and showed that the lack of Surf1 has a strong effect on the cytochrome composition of the cell.

To test for the influence of Surf1 on cytochrome aa_3 oxidase activity, the oxidation of *N,N,N',N'*-tetramethyl-*p*-phenylendiamine (TMPD) was measured with isolated membranes. Whereas a specific activity of 52.3 nmol TMPD oxidized per min and mg protein (mean value of three biological replicates) was detected with membranes of the wt, no activity above the autooxidation rate of TMPD (1.1 nmol per min) was found for the Δ*surf1* mutant and for the Δ*ctiP* mutant. This indicates that both Surf1 and CtiP are required for the formation of an active cytochrome aa_3 oxidase.

Impact of the absence of Surf1 on the purification of the cytochrome bc_1-aa_3 supercomplex

To gain further insights into the possible function of Surf1 in the assembly of the cytochrome bc_1-aa_3 supercomplex, purification experiments by StrepTactin affinity chromatography were performed. In one series, C-terminally Strep-tagged QcrB was purified from dodecylmaltoside-solubilized membranes of strains Δ*qcr*/pJC1-$qcrB_{St}$, Δ*qcr*Δ*surf1*/pJC1-$qcrB_{St}$, and Δ*qcr*Δ*ctiP*/pJC1-$qcrB_{St}$. In a second series, C-terminally Strep-tagged CtaD was purified from the dodecylmaltoside-solubilized membranes of strains Δ*ctaD*/pJC1-$ctaD_{St}$, Δ*ctaD*Δ*surf1*/pJC1-$ctaD_{St}$, and Δ*ctaD*Δ*ctiP*/pJC1-$ctaD_{St}$. Strains Δ*qcr*Δ*ctiP*

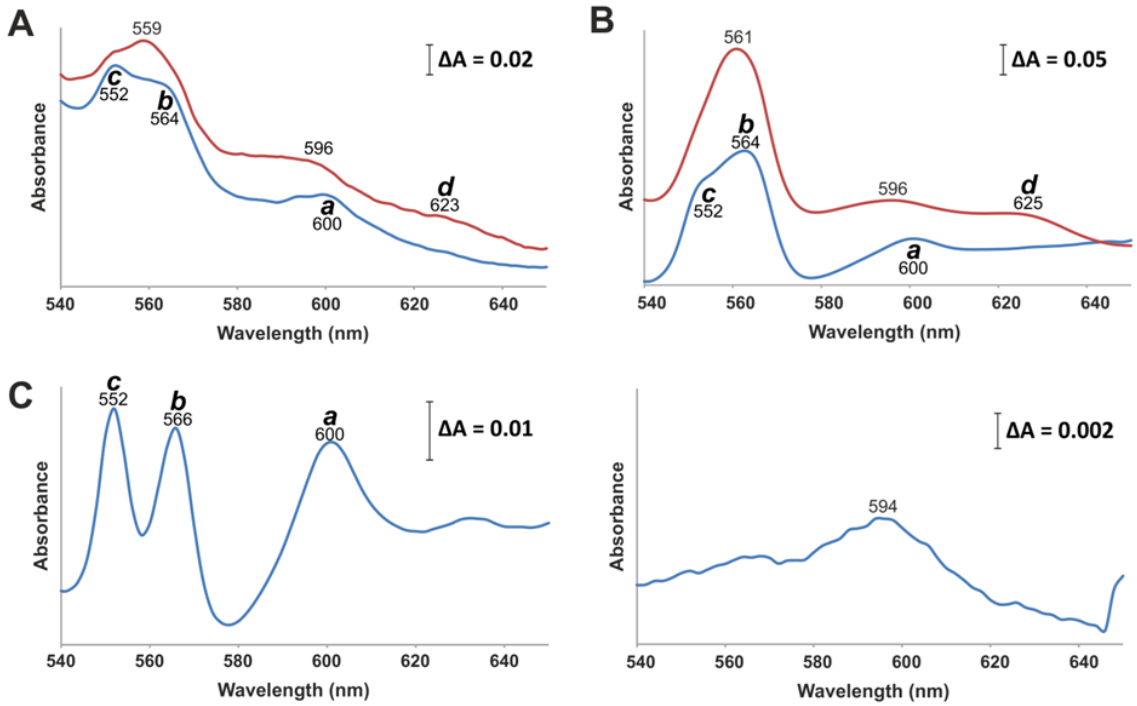

Fig. 3. Cytochrome spectra of the *C. glutamicum* wt and its Δ*surf1* mutant. (A) Dithionite-reduced spectra of intact cells. (B) Dithionite-reduced-*minus*-ferricyanide-oxidized difference spectra of membranes isolated from the *C. glutamicum* Δ*surf1* mutant (red) and the wt (blue). (C) Dithionite-reduced-*minus*-ferricyanide-oxidized difference spectra of the proteins purified by StrepTactin-affnity chromatography of $CtaD_{St}$ from strain Δ*ctaD*/pJC1-*ctaD*$_{St}$ (left) and from strain Δ*ctaD*Δ*surf1*//pJC1-*ctaD*$_{St}$ (right). The absorption maxima of cytochrome *c*, cytochrome *b*, cytochrome *a*, and cytochrome *d* are depicted. Altered cytochrome peak maxima are indicated in the graphs. Cells were grown aerobically in BHI medium with 2% (w/v) glucose. All measurements were performed in 100 mM Tris/HCl (pH 7.5).

and Δ*ctaD*Δ*ctiP* were included as we recently had shown that the absence of CtiP also impaired the assembly of the bc_1-aa_3 supercomplex [13] and thus could follow differences in the effects of CtiP and Surf1.

Purification of $QcrB_{St}$ from strain Δ*qcr*/pJC1-*qcrB*$_{St}$ resulted in the purification of a complex composed of the subunits of the cytochrome bc_1 complex, $QcrB_{St}$, QcrA, and QcrC, of the cytochrome aa_3 oxidase subunits CtaD (subunit I) and CtaC (subunit II), and of the lipoprotein Cg2949 (Fig. 4A). The complex purified from strain Δ*qcr*Δ*surf1*/pJC1-*qcrB*$_{St}$ contained only QcrA besides $QcrB_{St}$, but neither QcrC nor subunits of the cytochrome aa_3 oxidase nor Cg2949 (Fig. 4A). The same pattern was observed for $QcrB_{St}$ purification from strain Δ*qcr*Δ*ctiP*/pJC1-*qcrB*$_{St}$, confirming the previous data [13]. It should be noted that the amount of proteins purified from the strains lacking Surf1 or CtiP was much lower (approx. 25%) than the amount purified from the strain containing these proteins, which might be due to an impaired stability of an incompletely assembled supercomplex.

Cytochrome spectra of the complexes purified with $CtaD_{St}$ from different strain backgrounds revealed strong differences. Whereas the spectrum of the complex purified from Δ*ctaD*/pJC1-*ctaD*$_{St}$ revealed peaks for *a*-, *b*-, *c*-type cytochromes with maxima at 600 nm, 566 nm, and 552 nm, the spectrum of the complex obtained from Δ*ctaD*Δ*surf1*/pJC1-*ctaD*$_{St}$ contained only a small peak at 594 nm (Fig. 4C). In the case of the complex purified from Δ*ctaD*Δ*ctiP*/pJC1-*ctaD*$_{St}$, no cytochromes at all were observed (data not shown).

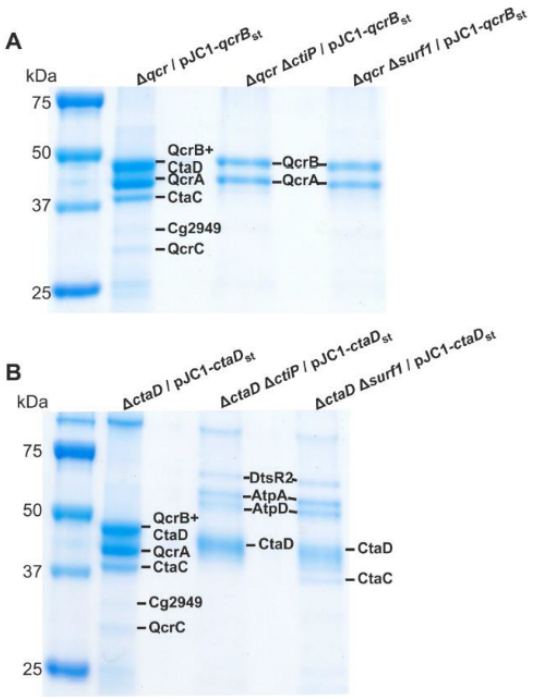

Fig. 4. Purification of cytochrome bc_1–aa_3 supercomplex subunits either with Strep-tagged QcrB (A) or with Strep-tagged CtaD (B) in the presence and absence of Surf1 or CtiP. The indicated *C. glutamicum* strains were cultivated in BHI medium with 2% (w/v) glucose at 30 °C in shaking flasks and harvested in the exponential phase at an OD_{600} of 8. The purified membranes were used for Streptactin affinity chromatography. The protein fractions eluted with desthiobiotin were combined and separated by SDS-PAGE (12% separating gel). The gels were stained with Coomassie Blue. Identification of the protein bands was done by peptide mass fingerprinting after in-gel tryptic digestion and MALDI-ToF-MS analysis of the peptides.

Impact of the surf1 deletion on global gene expression

To gain insight into the consequences of *surf1* deletion at the transcriptional level, global gene expression of the Δ*surf1* mutant and the wt were compared using DNA microarray experiments. The two strains were cultivated in CGXII glucose medium and cells were harvested in the exponential growth phase and used for RNA isolation. The comparison revealed 13 genes upregulated ≥2.5-fold and 11 genes downregulated ≥2.5-fold (Table 3). Seven of the genes upregulated in the Δ*surf1* strain belong to the SigC regulon, which are the *cydABDC* operon and the cg1881-cg1883-*copC* cluster. Four further members of the SigC regulon also showed increased mRNA levels, but are not listed in Table 3 because the cut-off was set at a ratio of 2.5, namely *ctaA* (cg1769, 1.71-fold increased), *ctaB* (cg1773, 2.23-fold increased), cg2556 (2.39-fold increased) and cg2750 (2.07-fold increased). The *ctiP* gene, which is not belonging to the SigC regulon, also showed a 2.66-fold increased mRNA level. The other genes with an increased mRNA level encode metabolic enzymes (*mtlD*, *sucCD*), a transporter (*pacL*), and a transcriptional regulator (*fruR*). The genes found to have a ≥2.5-fold decreased mRNA level in the Δ*surf1* strain encode for proteins with diverse cellular functions and an obvious relationship to the absence of Surf1 could not be deduced. The transcriptome data are in line with the presence of a defective bc_1-aa_3 supercomplex in the Δ*surf1* mutant, which was previously shown to activate the alternative sigma factor SigC [13, 34]. Upregulaton of the *ctiP* gene, which is not part part of the SigC regulon, suggests the existence of another regulatory system sensing a defective cytochrome aa_3 oxidase.

To confirm the results of the DNA microarray data, the expression of the *cydABDC* operon and for comparison of *ctaD* was measured using the reporter plasmids pJC1-P*cydA-venus* and pJC1-P*ctaD-venus* in *C. glutamicum* wt, the Δ*surf1* mutant and the Δ*ctiP* mutant. The strains were grown in CGXII glucose medium either under standard copper conditions or under copper deprivation and the specific fluorescence corresponding to the expression level of *cydA* and *ctaD* was measured after 24 h. As expected from the DNA microrarray data, the *cydA* promoter activity was 2-fold higher in the Δ*surf1* mutant and also in the Δ*ctiP* mutant (Table 4). Under copper deprivation, *cydA* promoter activity was two-fold increased in the wt and the activity in the Δ*surf1* mutant and in the Δ*ctiP* mutant was comparable under these conditions, i.e. no further increase was observed. In the case of *ctaD*, the promoter activity in the Δ*surf1* mutant and also in Δ*ctiP* mutant was slightly increased compared to the wt (factor 1.5) under standard copper conditions. Copper deprivation caused a small increase in *ctaD* promoter activity in the wt, which was not further increased in the two assembly mutants (Table 4).

Table 3
Transcriptome analysis of the *surf1* deletion strain compared to the wt under standard CGXII conditions in four biological replicates during the early exponential phase. Depicted are upregulated genes with an at least 2.5-fold regulation (p-value ≤ 0.05). The locus tags of genes belonging to the SigC regulon are underlined.

Locus tag	Gene name	Annotated function	mRNA ratio	*p*
cg0143	***mtlD***	Mannitol-1-phosphate 5-dehydrogenase	9.74	0.00
cg1298	***cydC***	ABC-type transport system required for functional synthesis of cytochrome *bd* oxidase, ATPase and permease componen	2.80	0.00
cg1299	***cydD***	ABC-type transport system required for functional synthesis of cytochrome *bd* oxidase, ATPase and permease component	5.76	0.00
cg1300	***cydB***	Cytochrome *bd* oxidase, subunit II	6.26	0.00
cg1301	***cydA***	Cytochrome *bd* oxidase, subunit I	6.62	0.00
cg1744	***pacL***	Cation-transporting ATPase	2.61	0.00
cg1881		Conserved protein of the DyP-type peroxidase family (PFAM PF04261) secreted via the Tat pathway	3.95	0.00
cg1883		Secreted copper(I)-binding lipoprotein, PCu_AC homolog	3.74	0.00
cg1884	***copC***	Membrane-bound copper(II)-binding protein C	4.12	0.00
cg2118	***fruR***	Transcriptional regulator of sugar metabolism	3.12	0.00
cg2699	***ctiP***	Copper transport and insertion protein	2.66	0.00
cg2836	***sucD***	Succinyl-CoA synthetase α subunit, ADP-forming	2.50	0.00
cg2837	***sucC***	Succinyl-CoA synthetase subunit β, ADP-forming	3.04	0.00
cg0693	***groEL***	60 kDa Chaperonin	0.38	0.00
cg0759	***prpD2***	2-Methycitrate dehydratase	0.31	0.00
cg0760	***prpB2***	2-Methylisocitrate lyase	0.31	0.00
cg0762	***prpC2***	2-Methylcitrate synthase	0.28	0.00
cg1290	***metE***	5-Methyltetrahydropteroyltriglutamate--homocysteine methyltransferase	0.29	0.00
cg2184	***oppD***	ABC-type peptide transport systems, ATPase component	0.25	0.00
cg2460	***surf1***	Assembly factor for cytochrome oxidase	0.06	0.00
cg2940	***siaI***	ABC-transporter for sialic acid	0.38	0.00
cg3141	***hmp***	Flavohemoprotein	0.33	0.00
cg3226		L-lactate permease	0.38	0.00
cg3395	***proP***	Proline/ectoine carrier	0.25	0.00

Table 4
Influence of the *surf1* deletion on the expression of the terminal oxidase genes *cydAB* and *ctaD*.*

Strain/reporter	pJC1-P*cydA-venus*		pJC1-P*ctaD-venus*	
	1.25 µM Cu	Cu deprivation	1.25 µM Cu	Cu deprviation
wt	1.00 ± 0.00	2.04 ± 0.08	1.00 ± 0.01	1.36 ± 0.06
Δ*surf1*	2.23 ± 0.01	2.08 ± 0.00	1.38 ± 0.02	1.36 ± 0.15

*The *C. glutamicum* strains with the reporter plasmids were grown in CGXII glucose medium either under standard copper conditions (1.25 µM $CuSO_4$) or under copper deprivation without added copper and supplemented with 150 µM BCS and 1 mM ascorbate. Expression of *cydA* was followed with the reporter plasmid pJC1-P*cydA-venus* (P_{cyd}) and expression of *ctaD* with the reporter plasmid pJC1-P*ctaD-venus* (P_{ctaD}). The strains were cultivated in FlowerPlates at 30°C and 1200 rpm using the BioLector microcultivation system. Growth was followed by measuring the backscatter at 620 nm and Venus fluorescence was measured by excitation at 510 nm and emission at 532 nm. The specific fluorescence (ratio of absolute fluorescence and backscatter) was determined after 24 h of cultivation. Mean values and standard deviations of biological triplicates were normalized by setting the wt values cultivated under standard copper conditions for each promoter as 1.

Conservation of Surf1 in Actinobacteria

As almost all aerobic Actinobacteria are expected to possess a cytochrome bc_1-aa_3 supercomplex with a diheme cytochrome c_1 [6], the assembly factors should also be conserved. In fact, Surf1 homologs were found to be present in all actinobacteria with a diheme cytochrome c_1 (data not shown). In order to confirm the equivalent function of the Surf1 homologs of other Actinobacteria, the corresponding proteins of *Corynebacterium diphtheriae* DSM44123 (CDC7B_1688), of *Mycobacterium tuberculosis* H37Rv (Rv2235), and of *M. smegmatis* MC^2 155 (MSMEG_4311) were chosen, which show 53%, 44%, and 43% amino acid sequence identity to *C. glutamicum* Surf1 (Fig. S1). The corresponding genes were cloned into the expression plasmid pAN6 and then transferred into the *C. glutamicum* Δ*surf1* strain in order to test whether they can abolish the growth defect of this mutant. *C. glutamicum* Δ*surf1* with pAN6 served as negative control and the wt with pAN6 as positive control. Basal expression of the *C. diphtheriae surf1* gene in the absence of the inducer isopropyl-β-D-thiogalactoside (IPTG) allowed full complementation of the growth defect of the *C. glutamicum* Δ*surf1* mutant (Fig. 5A). In the case of the *surf1* homologs of *M. tuberculosis* and *M. smegmatis*, IPTG-induced expression allowed partial or full complementation, respectively (Fig. 5B). These results support an identical function of the Surf1 homologs in Actinobacteria in the assembly of the cytochrome bc_1-aa_3 supercomplex.

Conclusions

The results obtained in this study provide strong evidence for an involvement of Surf1 (Cg2460) in the assembly of cytochrome aa_3 oxidase in *C. glutamium* and presumably all other actinobacterial species possessing the cytochrome bc_1-aa_3 supercomplex. According to the TMPD oxidase measurements, Surf1 appears to be essential for the formation of an active aa_3 oxidase in *C. glutamicum*.

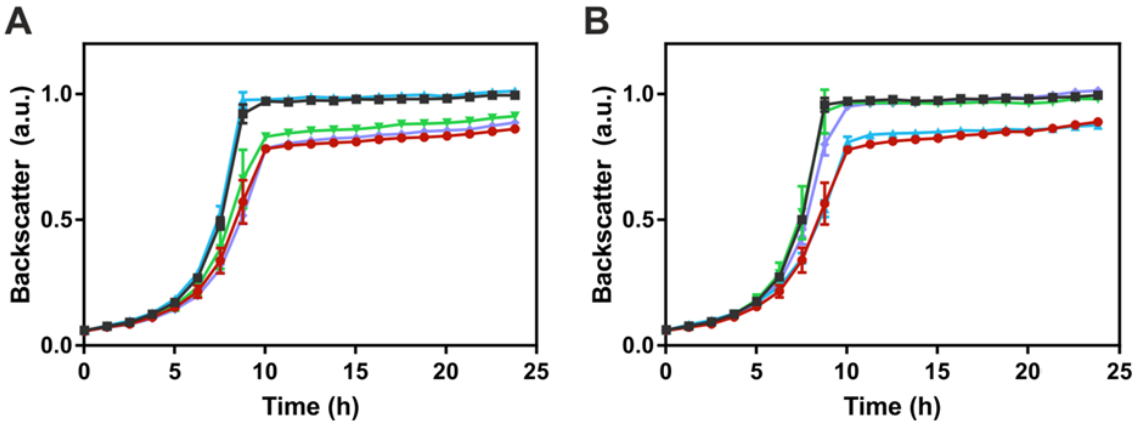

Fig. 5. Complementation of the growth defect of the *C. glutamicum* Δ*surf1* mutant with expression plasmids for genes encoding the Surf1 homologs of *Corynebacterium diphtheriae* (pAN6_CDC7B1688, blue triangles), *Mycobacterium smegmatis* (pAN6_MSMEG4311, green triangles), and *Mycobacterium tuberculosis* (pAN6_Rv2235, purple diamonds). The strains were cultivated in CGXII medium with 2% (w/v) glucose either in the absence of (A) or in the presence of 100 µM IPTG (B) at 30°C and 1200 rpm using a BioLector microcultivation system (m2p-labs, Aachen). As reference, *C. glutamicum* wt (black squares) and Δ*surf1* mutant (red circles), both carrying the pAN6 plasmid vector, were used. Growth was followed as backscatter at 620 nm and the maximal value obtained for the wt was set as 1. Mean values and standard deviation from three biological replicates are shown. *a.u.*. arbitrary units.

Acknowledgements

The authors thank Dr. Tino Polen for help with the DNA microarray experiments, including upload of the data to the GEO database. Further, we thank Sarah Nachtigall for construction of the reporter plasmids pJC1-P*cydA-venus* and pJC1-P*ctaD-venus*.

References

[1] J.A. García-Horsman, B. Barquera, J. Rumbley, J. Ma, R.B. Gennis, The superfamily of heme-copper respiratory oxidases, J Bacteriol, 176 (1994) 5587-5600.

[2] R.K. Poole, G.M. Cook, Redundancy of aerobic respiratory chains in bacteria? Routes, reasons and regulation, Adv Microb Physiol., 43 (2000) 165-224.

[3] M. Bott, A. Niebisch, The respiratory chain of *Corynebacterium glutamicum*, J Biotechnol, 104 (2003) 129-153.

[4] A. Niebisch, M. Bott, Molecular analysis of the cytochrome bc_1-aa_3 branch of the *Corynebacterium glutamicum* respiratory chain containing an unusual diheme cytochrome c_1, Arch Microbiol 175 (2001) 282-294.

[5] A. Niebisch, M. Bott, Purification of a cytochrome bc_1-aa_3 supercomplex with quinol oxidase activity from *Corynebacterium glutamicum*., J Biol Chem, 278 (2003) 4339-4346.

[6] W.C. Kao, T. Kleinschroth, W. Nitschke, F. Baymann, Y. Neehaul, P. Hellwig, S. Richers, J. Vonck, M. Bott, C. Hunte, The obligate respiratory supercomplex from *Actinobacteria*, Biochim. Biophys. Acta, 1857 (2016) 1705-1714.

[7] S. Graf, O. Fedotovskaya, W.C. Kao, C. Hunte, P. Adelroth, M. Bott, C. von Ballmoos, P. Brzezinski, Rapid Electron Transfer within the III-IV Supercomplex in *Corynebacterium glutamicum*, Sci Rep, 6 (2016) 34098.

[8] J.A. Megehee, J.P. Hosler, M.D. Lundrigan, Evidence for a cytochrome *bcc*-aa_3 interaction in the respiratory chain of *Mycobacterium smegmatis*, Microbiology, 152 (2006) 823-829.

[9] M.S. Kim, J. Jang, N.B. Ab Rahman, K. Pethe, E.A. Berry, L.S. Huang, Isolation and Characterization of a Hybrid Respiratory Supercomplex Consisting of *Mycobacterium tuberculosis* Cytochrome *bcc* and *Mycobacterium smegmatis* Cytochrome aa_3, J Biol Chem, 290 (2015) 14350-14360.

[10] B. Wiseman, R.G. Nitharwal, O. Fedotovskaya, J. Schafer, H. Guo, Q. Kuang, S. Benlekbir, D. Sjostrand, P. Adelroth, J.L. Rubinstein, P. Brzezinski,

M. Hogbom, Structure of a functional obligate complex III_2IV_2 respiratory supercomplex from *Mycobacterium smegmatis*, Nature structural & molecular biology, 25 (2018) 1128-1136.

[11] H. Gong, J. Li, A. Xu, Y. Tang, W. Ji, R. Gao, S. Wang, L. Yu, C. Tian, J. Li, H.Y. Yen, S. Man Lam, G. Shui, X. Yang, Y. Sun, X. Li, M. Jia, C. Yang, B. Jiang, Z. Lou, C.V. Robinson, L.L. Wong, L.W. Guddat, F. Sun, Q. Wang, Z. Rao, An electron transfer path connects subunits of a mycobacterial respiratory supercomplex, Science, 362 (2018).

[12] E. Nyvltova, A. Barrientos, J. Hosler, Assembly of Heme a_3-Cu_B and Cu_A in Cytochrome *c* Oxidase, in: Encyclopedia of Inorganic and Bioinorganic Chemistry, John Wiley & Sons, Ltd., Chichester, UK, (2017), pp. 1–27.

[13] X. Morosov, C.F. Davoudi, M. Baumgart, M. Brocker, M. Bott, The copper-deprivation stimulon of *Corynebacterium glutamicum* comprises proteins for biogenesis of the actinobacterial cytochrome bc_1-aa_3 supercomplex, J Biol Chem, (2018).

[14] Z. Zhu, J. Yao, T. Johns, K. Fu, I. De Bie, C. Macmillan, A.P. Cuthbert, R.F. Newbold, J. Wang, M. Chevrette, G.K. Brown, R.M. Brown, E.A. Shoubridge, *SURF1*, encoding a factor involved in the biogenesis of cytochrome *c* oxidase, is mutated in Leigh syndrome, Nat. Genet., 20 (1998) 337-343.

[15] G. Mashkevich, B. Repetto, D.M. Glerum, C. Jin, A. Tzagoloff, *SHY1*, the yeast homolog of the mammalian *SURF-1* gene, encodes a mitochondrial protein required for respiration, J Biol Chem, 272 (1997) 14356-14364.

[16] A. Barrientos, K. Gouget, D. Horn, I.C. Soto, F. Fontanesi, Suppression mechanisms of COX assembly defects in yeast and human: insights into the COX assembly process, Biochim. Biophys. Acta, 1793 (2009) 97-107.

[17] L. Stiburek, K. Vesela, H. Hansikova, H. Hulkova, J. Zeman, Loss of function of Sco1 and its interaction with cytochrome *c* oxidase, American journal of physiology. Cell physiology, 296 (2009) C1218-1226.

[18] A. Hannappel, F.A. Bundschuh, B. Ludwig, Role of Surf1 in heme recruitment for bacterial COX biogenesis, Biochim. Biophys. Acta, Bioenerg., 1817 (2012) 928-937.

[19] D. Smith, J. Gray, L. Mitchell, W.E. Antholine, J.P. Hosler, Assembly of cytochrome-*c* oxidase in the absence of assembly protein Surf1p leads to loss of the active site heme, J Biol Chem, 280 (2005) 17652-17656.

[20] F.A. Bundschuh, K. Hoffmeier, B. Ludwig, Two variants of the assembly factor Surf1 target specific terminal oxidases in *Paracoccus denitrificans*, Biochim. Biophys. Acta, Bioenerg., 1777 (2008) 1336-1343.

[21] A. Hannappel, F.A. Bundschuh, B. Ludwig, Characterization of heme-binding properties of *Paracoccus denitrificans* Surf1 proteins, FEBS J., 278 (2011) 1769-1778.

[22] C. Keilhauer, L. Eggeling, H. Sahm, Isoleucine synthesis in *Corynebacterium glutamicum*: molecular analysis of the *ilvB-ilvN-ilvC* operon, J Bacteriol, 175 (1993) 5595-5603.

[23] G. Bertani, Studies on lysogenesis. I. The mode of phage liberation by lysogenic *Escherichia coli*, J Bacteriol, 62 (1951) 293-300.

[24] J. Sambrook, Molecular cloning: A laboratory manual, Cold Spring Harbor Laboratory Press, Cold Spring Harbor, (2001).

[25] D.G. Gibson, L. Young, R.Y. Chuang, J.C. Venter, C.A. Hutchison, 3rd, H.O. Smith, Enzymatic assembly of DNA molecules up to several hundred kilobases, Nature methods, 6 (2009) 343-345.

[26] D.G. Gibson, L. Young, R.Y. Chuang, J.C. Venter, C.A. Hutchison, H.O. Smith, Enzymatic assembly of DNA molecules up to several hundred kilobases, Nat. Methods, 6 (2009).

[27] M. Vogt, S. Haas, S. Klaffl, T. Polen, L. Eggeling, J. van Ooyen, M. Bott, Pushing product formation to its limit: metabolic engineering of *Corynebacterium glutamicum* for L-leucine overproduction, Metab. Eng., 22 (2014) 40-52.

[28] S. Schaffer, B. Weil, V.D. Nguyen, G. Dongmann, K. Gunther, M. Nickolaus, T. Hermann, M. Bott, A high-resolution reference map for cytoplasmic and

membrane-associated proteins of *Corynebacterium glutamicum*, Electrophoresis, 22 (2001) 4404-4422.

[29] M. Bussmann, M. Baumgart, M. Bott, RosR (Cg1324), a hydrogen peroxide-sensitive MarR-type transcriptional regulator of *Corynebacterium glutamicum*, J Biol Chem, 285 (2010) 29305-29318.

[30] E. Castiglioni, E. Grilli, S. Sanguinetti, A new simple and low cost scattered transmission accessory for commercial double beam ultraviolet-visible spectrophotometers, Rev. Sci. Instrum., 68 (1997) 4288-4289.

[31] J. Sakamoto, T. Shibata, T. Mine, R. Miyahara, T. Torigoe, S. Noguchi, K. Matsushita, N. Sone, Cytochrome *c* oxidase contains an extra charged amino acid cluster in a new type of respiratory chain in the amino-acid-producing Gram-positive bacterium *Corynebacterium glutamicum*, Microbiology, 147 (2001) 2865-2871.

[32] U. Omasits, C.H. Ahrens, S. Muller, B. Wollscheid, Protter: interactive protein feature visualization and integration with experimental proteomic data, Bioinformatics (Oxford, England), 30 (2014) 884-886.

[33] J. Kalinowski, B. Bathe, D. Bartels, N. Bischoff, M. Bott, A. Burkovski, The complete *Corynebacterium glutamicum* ATCC 13032 genome sequence and its impact on the production of L-aspartate-derived amino acids and vitamins, J Biotechnol, 104 (2003).

[34] K. Toyoda, M. Inui, The extracytoplasmic function s factor s^C regulates expression of a branched quinol oxidation pathway in *Corynebacterium glutamicum*, Mol Microbiol, 100 (2016) 486-509.

[35] D. Hanahan, Studies on transformation of *Escherichia coli* with plasmids, J. Mol. Biol., 166 (1983) 557-580.

[36] S. Kinoshita, S. Udaka, M. Shimono, Studies of amino acid fermentation. I. Production of L-glutamic acid by various microorganisms, J. Gen. Appl. Microbiol., 3 (1957) 193-205.

[37] A. Schäfer, A. Tauch, W. Jager, J. Kalinowski, G. Thierbach, A. Puhler, Small mobilizable multi-purpose cloning vectors derived from the *Escherichia coli* plasmids pK18 and pK19: selection of defined deletions in the chromosome of *Corynebacterium glutamicum*, Gene, 145 (1994) 69-73.

[38] J. Frunzke, V. Engels, S. Hasenbein, C. Gatgens, M. Bott, Co-ordinated regulation of gluconate catabolism and glucose uptake in *Corynebacterium glutamicum* by two functionally equivalent transcriptional regulators, GntR1 and GntR2, Mol. Microbiol., 67 (2008) 305-322.

[39] J. Cremer, L. Eggeling, H. Sahm, Cloning the *dapA dapB* cluster of the lysine-secreting bacterium *Corynebacterium glutamicum*, Mol Gen Genet, 220 (1990) 478-480.

[40] M. Baumgart, K. Luder, S. Grover, C. Gätgens, G.S. Besra, J. Frunzke, IpsA, a novel LacI-type regulator, is required for inositol-derived lipid formation in *Corynebacteria* and *Mycobacteria*, BMC Biol, 11 (2013) 122-122.

HrrSA orchestrates a systemic response to heme and determines prioritisation of terminal cytochrome oxidase expression

Marc Keppel[#], Cedric-Farhad Davoudi[#], Andrei Filipchyk[#], Ulrike Viets, Eugen Pfeifer, Tino Polen, Meike Baumgart, Michael Bott, and Julia Frunzke*

Institute of Bio- and Geosciences, IBG-1: Biotechnology, Forschungszentrum Jülich, Germany

*Corresponding author:

Email
j.frunzke@fz-juelich.de
Phone +49 2461 61 5430
Fax +49 2461 61 2710

Keywords: Heme signaling, *Corynebacterium glutamicum*, *Corynebacterium diphtheriae*, two-component systems, bacterial transcription, regulatory networks, HrrSA

[#]These authors contributed equally to this work.

Abstract

Heme is a multifaceted molecule. While serving as a prosthetic group for many important proteins, elevated levels are toxic to cells. The complexity of this stimulus has shaped bacterial network evolution. However, only a small number of targets controlled by heme-responsive regulators have been described to date. Here, we used a genome-wide approach to monitor the *in vivo* promoter occupancy of HrrA, the response regulator of the heme-regulated two-component system HrrSA of *Corynebacterium glutamicum*. Time-resolved profiling revealed dynamic binding of HrrA to more than 250 different genomic targets encoding proteins associated with heme biosynthesis, the respiratory chain, oxidative stress response and cell envelope remodeling. By repression of *sigC*, which encodes an activator of the *cydABCD* operon, HrrA prioritizes the expression of genes encoding the cytochrome bc_1-aa_3 supercomplex. These data describe for the first time the systemic response strategy that bacteria have evolved to respond to the versatile signaling molecule heme.

Introduction

Heme (iron bound protoporphyrin IX) is a versatile molecule that is synthesized and used by virtually all aerobic eukaryotic and prokaryotic cells[1] because it serves as the prosthetic group of hemoglobins, hydroxylases, catalases, peroxidases, and cytochromes[2] and is thereby essential for many cellular processes, such as electron transfer, respiration and oxygen metabolism[3]. Furthermore, salvaged heme represents the most important iron source for a variety of pathogenic bacteria[4,5], and also non-pathogenic bacteria can meet their iron demand by degradation of environmental heme. This becomes evident from the diverse set of heme uptake systems and heme oxygenases that catalyze the degradation of the protoporphyrin ring to biliverdin and the concomitant release of carbon monoxide and iron[6].

While heme represents an essential cofactor for a variety of proteins, this molecule also exhibits severe toxicity at high concentrations. Therefore, organisms have evolved sophisticated regulatory networks to tightly control heme uptake, detoxification, synthesis and degradation [4]. Several heme-regulated transcription factors have been described, including *the heme activator protein (Hap) 1, which is an activator of genes required for aerobic growth of the yeast Saccharomyces cerevisiae*[7]; the transcription factor BACH1 (BTB and CNC homology 1), which is conserved in mammalian cells[8,9]; and the rhizobial Irr protein, which is a heme-regulated member of the Fur family of transcriptional regulators[10-12].

In Gram-positive bacteria, two-component systems (TCSs) appear to play a prevalent role in heme-responsive signaling[13,14], as exemplified by the heme sensor system HssRS of *Staphylococcus aureus* and *Bacillus anthracis, which controls the expression of the hrtBA operon, encoding a heme efflux system in both species*[15,16].

Remarkably, several members of the *Corynebacteriaceae* family, including the human pathogen *Corynebacterium diphtheriae* and the biotechnological platform strain *Corynebacterium glutamicum,* have two paralogous TCSs, namely, HrrSA and ChrSA, dedicated to heme-responsive control of gene expression[17-20]. The kinases HrrS and ChrS were recently shown to perceive transient changes in heme availability by direct intramembrane interactions with heme[21,22]. Heme binding triggers autophosphorylation of the sensor kinase, followed by transfer of the phosphoryl group to the cognate response regulators HrrA and ChrA. In *C. glutamicum*, significant cross-phosphorylation was observed between the closely related systems; however, this crosstalk is proofread by a highly specific phosphatase activity of the kinases toward the cognate response regulators under non-inducing conditions[23]. While the ChrSA system appears to be mainly involved in rapid activation of the HrtBA detoxification system[19], previous data suggest that HrrSA coordinates a homeostatic response to heme[18]. In recent studies, six direct targets have been described for HrrA, including genes encoding enzymes involved in heme synthesis (*hemE*, *hemA* and *hemH*) and heme utilization (*hmuO*, encoding a heme oxygenase) and the *ctaE-qcrCAB* operon, encoding the heme-containing cytochrome bc_1-aa_3 supercomplex of the respiratory chain[18].

C. glutamicum possesses a branched electron transport chain comprising the cytochrome bc_1-aa_3 supercomplex (encoded by *ctaD*, the *ctaCF* operon, and *ctaE-qcrCAB*) and the cytochrome *bd* oxidase, encoded by the first two genes of the *cydABDC* operon[24]. Although both the cytochrome aa_3 oxidase and *bd* oxidase are involved in the establishment of a proton-motive force (PMF), the aa_3 oxidase is an active proton pump that is responsible for the increased proton translocation number ($6\ H^+/2\ e^-$) of the cytochrome bc_1-aa_3 supercomplex compared to that of the *bd* oxidase ($2\ H^+/2\ e^-$)[24]. The presence of the cytochrome bc_1-aa_3 supercomplex was previously shown to be a characteristic feature of almost all Actinobacteria because members of this phylum lack a soluble cytochrome *c*, instead harboring a diheme cytochrome c_1 that directly shuttles electrons from the bc_1 complex to the aa_3 oxidase[25-29]. Furthermore, both terminal oxidases differ in heme content, as the bc_1-aa_3 supercomplex harbors six heme molecules, while the *bd* oxidase harbors only three. Surprisingly, not much is known about the regulation of terminal oxidases in *C. glutamicum*. In addition to the described activation of the *ctaE-qcr* operon by HrrA, the hydrogen peroxide-sensitive regulator OxyR was described as a repressor of the *cydABCD* operon[30,31]. Furthermore, the extracytoplasmic function (ECF) sigma factor SigC (σ^C) was shown to activate expression of the *cydABCD* operon[30,32]. For σ^C, a speculated stimulus is the defect electron transfer in the aa_3 oxidase[32] and such a defect was observed under copper-deprivation, which resulted in activation of the σ^C regulon[33].

Interestingly, the regulons of prokaryotic heme regulators described thus far comprise only a low number of direct target genes, most of which are involved in heme export (e.g., *hrtBA*) or degradation (*hmuO*). This picture of prokaryotic heme signaling, however, does not match the complexity of the stimulus. In this study, we performed a time-resolved and genome-wide binding profiling (ChAP-Seq) of HrrA in *C. glutamicum* describing the transient HrrA promoter occupancy of more than 250 genomic targets in response to heme. The obtained results emphasize that HrrSA is a truly global regulator of heme homeostasis, which also integrates the response to oxidative stress and cell envelope remodeling. Transcriptome analysis (RNA-Seq) at different time points after heme induction revealed HrrA to be an important regulator of the respiratory chain, which coordinates the expression of components of both quinol oxidation branches as well as menaquinol synthesis and reduction. Remarkably, HrrA was found to prioritize the expression of operons encoding the

cytochrome bc_1-aa_3 supercomplex by repressing *sigC* expression.

Materials and Methods

Bacterial strains and growth conditions

Bacterial strains used in this study are listed in Table S1. The *Corynebacterium glutamicum* strain ATCC 13032 was used as wild type[27] and cultivations were performed in liquid BHI (brain heart infusion, Difco BHI, BD, Heidelberg, Germany), as complex medium or CGXII[59] containing 2 % (w/v) glucose as minimal medium. The cells were cultivated at 30°C; if appropriate, 25 µg/ml kanamycin was added. *E. coli* (DH5α and BL21 (DE3)) was cultivated in Lysogeny Broth (Difco LB, BD, Heidelberg, Germany) medium at 37°C in a rotary shaker and for selection, 50 µg/ml kanamycin was added to the medium.

Recombinant DNA work and cloning techniques

Cloning and other molecular methods were performed according to standard protocols[60]. As template, chromosomal DNA of *C. glutamicum* ATCC 13032 was used for PCR amplification of DNA fragments and was prepared as described previously[61]. All sequencing and synthesis of oligonucleotides was performed by Eurofins Genomics (Ebersberg, Germany). For ChAP sequencing, the plasmid pJC1_P_{hrrSA}-*hrrSA-twin-strep*_P_{chrSA}-*chrSA-his* was constructed after amplification of *hrrS-hrrA-twin-strep* and *chrS-chrA-his*, including promoter (500 bp upstream of the first gene) from stock plasmids, using the primers indicated in Table S2. The fragments were cloned into pJC1 using the created overhangs and Gibson assembly[62].

ChAP Sequencing – Sample preparation

The preparation of DNA for ChAP sequencing was adapted from [63]. The *C. glutamicum* strain Δ*hrrSA*Δ*chrSA* was transformed with a plasmid carrying genes for both TCSs encoding tagged RRs (pJC1_P_{hrrSA}-*hrrSA-twin-strep*_P_{chrSA}-*chrSA-his*). A preculture was inoculated in liquid BHI medium (25 µg/ml kanamycin) from a fresh BHI agar plate and incubated for 8-10 h at 30°C in a rotary shaker. After that, cells were transferred into a second preculture in CGXII medium containing 2 % (w/v) glucose and 0 µM $FeSO_4$ to starve the cells from iron. Protocatechuic acid (PCA), which was added to the medium, allowed the uptake of trace amounts of iron. From an overnight culture, six main cultures were inoculated to an OD_{600} of 3.0 in 1 L CGXII medium containing 4 µM hemin as sole iron source. For the time point t=0, the cells were added to 1 L fresh CGXII containing no additional iron source. After 0 h, 0.5 h, 4 h, 9 h and 24 h, cells corresponding to an OD_{600} of 3.5 in 1 L were harvested by centrifugation at 4 °C, 5000 *x g* and washed once in 20 ml CGXII. Subsequently, the cell pellet was resuspended in 20 ml CGXII containing 1 % (v/v) formaldehyde to crosslink the regulator protein to the DNA. After incubation for 20 min at RT, the cross linking was stopped by addition of glycine (125 mM), followed by an additional 5 minutes of incubation. After that, the cells were washed three times in buffer A (100 mM Tris-HCl, 1 mM EDTA, pH=8.0) and the pellets stored overnight at -80 °C. For cell disruption, the pellet was resuspended buffer A containing "complete" protease inhibitor cocktail (Roche, Germany) and passed through a French pressure cell (SLM Ainco, Spectronic Instruments, Rochester, NY) five times at 207 MPa. The DNA was fragmented to ~500 bp by sonication (Branson Sonifier 250, Branson Ultrasonics Corporation, Connecticut, USA) and the supernatant was collected after ultra-centrifugation (150.000 x *g*, 4 °C, 1 h). The DNA-bound by the twin-Strep tagged HrrA protein was purified using Strep-Tactin XT Superflow column material (IBA Lifesciences, Göttingen, Germany) according to the supplier's manual (applying the gravity flow protocol, 1.5 ml column volume). Washing of the column was performed with buffer W (100 mM Tris-HCl, 1 mM EDTA, 150 mM NaCl, pH 8,0) and the tagged protein was eluted with buffer E (100 mM Tris-HCl, 1 mM EDTA, 150 mM NaCl, pH 8.0, added 50 mM D-Biotin). After purification, 1 % (w/v) SDS was added to the elution fractions and the samples were incubated overnight at 65°C. For the digestion of protein, 400 µg/ml Proteinase K (AppliChem GmbH, Darmstadt, Germany) was added and incubated for 3 h at 55 °C. Subsequently, the DNA was purified as following: Roti-Phenol/Chloroform/Isoamyl alcohol (Carl Roth GmbH, Karlsruhe, Germany) was added to the samples in a 1:1 ratio and the organic phase

was separated using Phase Lock Gel (PLG) tubes (VWR International GmbH, Darmstadt, Germany) according to the supplier's manual. Afterwards, the DNA was precipitated by adding ice cold ethanol (to a conc. of 70 %) and centrifugation at 16.000x*g*, 4 °C for 10 min. The DNA was washed with ice cold 70 % ethanol, then dried for 3 h at 50 °C and eluted in dH_2O. The resulting DNA was used for library preparation and indexing using the TruSeq DNA PCR-free sample preparation kit (Illumina, California, USA) according to the manufacturer's instructions, only skipping fragmentation of the DNA. The resulting libraries were quantified using the KAPA library quant kit (Peqlab, Bonn, Germany) and normalized for pooling.

RNA Sequencing – Sample preparation

For RNA sequencing, *C. glutamicum* wild type and the Δ*hrrA* mutant strain were cultivated under the same conditions as described for ChAP Sequencing. Both strains did not contain any plasmids and, hence, were cultivated without addition of antibiotics in biological duplicates. After 0 h (no heme), 0.5 h and 4 h, cells corresponding to an OD_{600} of 3 in 0.1 L were harvested in falcon tubes filled with ice by centrifugation at 4 °C and 5000 *x g* for 10 minutes and the pellets were stored at -80 °C. For the preparation of the RNA, the pellets were resuspended in 800 µl RTL buffer (QIAGEN GmbH, Hilden, Germany) and the cells disrupted by 3 x 30 s silica bead beating, 6000 rt/min (Precellys 24, VWR International GmbH, Darmstadt, Germany). After ultra-centrifugation (150.000 x *g*, 4 °C, 1 h), the RNA was purified using the RNeasy Mini Kit (QIAGEN GmbH, Hilden, Germany) according to the supplier's manual. Subsequently, the ribosomal RNA was removed by running twice the workflow of the Ribo-Zero rRNA Removal Kit [Bacteria] (Illumina, California, USA) in succession. Between steps, the depletion of rRNA as well as the mRNA quality was analysed using the TapeStation 4200 (Agilent Technologies Inc, Santa Clara, USA). After removal of rRNA, the fragmentation of RNA, cDNA strand synthesis and indexing was carried out using the TruSeq Stranded mRNA Library Prep Kit (Illumina, California, USA) according to the supplier's manual. Afterwards, the cDNA was purified using Agencourt AMPure XP magnetic beads (Beckman Coulter, Indianapolis, USA). The resulting libraries were quantified using the KAPA library quant kit (Peqlab, Bonn, Germany) and normalized for pooling.

Sequencing and sequence analysis

Pooled libraries were sequenced on a MiSeq (Illumina, California, USA) generating paired-end reads with a length of 2 × 75 bases. Data analysis and base calling were performed with the Illumina instrument software and stored as fastq output files. We then proceeded as follows:

ChAP-Seq analysis

The obtained DNA fragments of each sample (up to 2 µg) were used for library preparation and indexing using the TruSeq DNA PCR-free sample preparation kit according to the manufacturer's instruction, yet omitting the DNA size selection steps (Illumina, Chesterford, UK). The resulting libraries were quantified using the KAPA library quant kit (Peqlab, Bonn, Germany) and normalized for pooling. Sequencing of pooled libraries was performed on a MiSeq (Illumina) using paired-end sequencing with a read-length of 2 x 150 bases. Data analysis and base calling were accomplished with the Illumina instrument software and stored as fastq output files. The sequencing data obtained for each sample were imported into CLC Genomics Workbench (Version 9, Qiagen Aarhus A/S) for trimming and base quality filtering. The output was mapped to accession BX927147 as *C. glutamicum* reference genome (www.ncbi.nlm.nih.gov/pubmed/12948626). Genomic coverage was convoluted with second order Gaussian kernel. The kernel was truncated at 4 sigmas (that is all kernel values positioned further then 4 sigmas from the center were set to zero) and expanded to the "expected peak width". The expected peak width was estimated *via* the following procedure: 1) all the peaks higher than 3 mean coverage were detected 2) Points at which their coverage dropped below ½ of the maximal peak height were found and the distance between them was considered as a peak width 3) The "estimated peak width" was

set equal to the median peak width. The convolution profile was scanned in order to find points were first derivative changes its sign from positive to negative (Figure S12). Each such point was considered as a potential peak and was assigned with a convolution score (that is convolution with second order Gaussian kernel centered at the peak position). Further we explored the distribution of the convolution scores. It appeared to resemble normal distribution, but with a heavy right tail. We assumed that this distribution is indeed bimodal of normal distribution (relatively low scores) representing 'noise' and a distribution of 'signal' (relatively high scores). We fit the Gaussian curve to the whole distribution (via optimize.fit function from SciPy package[64]) and set a score thresholds equal mean + 4 sigmas of the fitted distribution. Further filtering with this threshold provided estimated FDR (false discovery rate) of 0.004-0.013 depending on a sample. Filtered peaks were normalized to allow inter-sample comparisons. Sum of coverages of the detected peaks was negated from the total genomic coverage. The resulting difference was used as normalization coefficient; that is peak intensities were divided by this coefficient.

RNA-seq analysis

Sequencing reads quality was explored with the FastQC [65] tool. Since reads appeared to be of a good quality and didn't harbor significant fraction of adapters or overrepresented sequences, no preprocessing was undertaken. Identical reads were collapsed with a custom script in order to prevent gene levels' misquantification caused by PCR overamplification. Reads were mapped to the *Corynebacterium glutamicum* genome (BX927147) with Bowtie2[66]. Bowtie2 was run with the following parameters: bowtie2 -1 [path to the reads, 1st mate] -2 [path to the reads, 2nd mate] -S [path to the mappings] –phred33 –sensitive-local –local –score-min C,90 –rdg 9,5 –rfg 9,5 -a –no-unal -I 40 -X 400 –no-mixed –ignore-quals.

The reads mapped to multiple locations were split proportionally between parental genes. That is if 3 reads are mapped to gene A and gene B, expression of gene A is 10 and expression of gene B is 5, then 2 reads will go to gene A and 1 read to gene B. For each *C. glutamicum* gene[67] we assign an expression value equal to the average read coverage over the gene region. These expression values were then normalized to TPM (transcripts per million) values[68].

Furthermore, we analyzed which genes are significantly differentially expressed between conditions. We set combinatorial thresholds on normalized GEC (gene expression change) [|expr1-expr2|/(expr1+expr2)] and MGE (mean gene expression) [log2((expr1+expr2)/2)] where "expr1" is gene expression for the first condition and "expr2" for the second. Thresholds were set in a way to achieve maximal sensitivity while keeping FDR (false discovery rate) less than 0.05. FDR was estimated as GECintra/(GECintra + GECinter); where GECintra is a number of genes passed the thresholds based on intrasample GEC (that is gene expression change between the replicates for the same condition), GECinter is a number of genes passed the thresholds based on intersample GEC (that is gene expression change between two different conditions). Threshold function for GEC was defined as: 1 | if MGE < C; 2**(-A*MGE) + B | if MGE >= C; where A, B, C are parameters to be adjusted. Parameters A, B, C were adjusted with genetic algorithm optimization approach to achieve maximal sensitivity in discovery of differentially expressed genes while keeping FDR below 0.05.

Accession numbers

All ChAP-Seq and RNA-Seq datasets were deposited in the GEO database under the accession number GSE120924.

Measurement of cell-associated hemin

The *C. glutamicum* strain Δ*hrrSA*Δ*chrSA* (carrying the pJC1_P_{hrrSA}-*hrrSA-twin-strep*_P_{chrSA}-*chrSA-his* plasmid) was cultivated in 4 µM hemin as described above (see ChAP Sequencing). To measure the cell-associated heme pool, CGXII minimal medium supplemented with 2 % (w/v) glucose and 4 µM heme was inoculated to an OD_{600} of 3.5. Samples were taken 0.5, 2, 4, 9 and 24 hours after addition of heme. Cells were harvested, resuspended in 100 mM Tris-HCl (pH 8) and adjusted to an OD_{600} of 100. Cells cultivated in 4 µM $FeSO_4$ supplemented medium were taken

as a control and harvested at the same time points. Absolute spectra of cells reduced with a spatula tip of sodium dithionite were measured at room temperature using the Jasco V560 with a silicon photodiode detector in combination with 5 mm light path cuvettes. Absorption values at 406 nm were normalized by subtracting the measured absorption values of Fe-cultivated cells.

Electrophoretic mobility shift assays (EMSA)

The promotor regions of HrrA target genes were chosen based on the ChAP-Seq analyses and comprised 50 bp up- and downstream of the maximal peak height (for primers see Table S2) . For quantitative measurements, the DNA fragments were increased to 250 bp up- and downstream of the peak maximum. Before addition of DNA, HrrA was phosphorylated by incubation for 60 min with MBP-HrrSΔ1-248 in a ratio of 2:1 and 5 mM ATP. Binding assays were performed in a total volume of 20 µl using 15 nM DNA and increasing HrrA concentrations from 25 to 100 nM or 75 to 1500 nM, respectively. The binding buffer contained 20 mM Tris-HCl (pH 7.5), 50 mM KCl, 10 mM MgCl2, 5% (v/v) glycerol, 0.5 mM EDTA and 0.005% (w/v) Triton X-100. After incubation for 20 min at room temperature, the reaction mixtures were loaded onto a 10 % native polyacrylamide gel and subsequently stained using Sybr green I (Sigma Aldrich). The band intensities of unbound DNA were quantified using AIDA v.4.15 (Raytest GmbH, Germany) and K*d* values calculated using GraphPad Prism 7.

Results

Genome-wide profiling of HrrA promoter occupancy

In previous studies, a number of direct target operons were described in *C. glutamicum* and *C. diphtheriae,* emphasizing the important role of the HrrSA TCS in the control of heme homeostasis[17-20]. In this study, we investigated the genome-wide binding profile of HrrA by chromatin affinity purification of twin-Strep-tagged HrrA combined with DNA sequencing (ChAP-Seq). A series of preceding experiments revealed that plasmid-based expression of *hrrA* is required for the envisaged analysis, as, for instance, several known HrrA targets were obscured when *hrrA* was expressed only from one genomic copy. For this purpose, *C. glutamicum* ATCC 13032 lacking both heme-dependent TCSs (Δ*hrrSA*Δ*chrSA*) was transformed with a plasmid encoding the particular systems under the control of their native promoters (pJC1_P_{hrrSA}-*hrrSA-twin-strep*_P_{chrSA}-*chrSA-his*). To obtain insights into the stimulus-dependent DNA association and dissociation, *C. glutamicum* cells starved of iron (see Material and Methods) were grown in iron-depleted glucose minimal medium, and samples were obtained before (T_0) and 0.5, 2, 4, 9 and 24 h after the addition of 4 µM hemin. HrrA was purified, and the bound DNA fragments were sequenced (Figure 1A). We obtained substantial enrichment of known HrrA targets in response to heme (e.g., 10-fold *hmuO*, 33-fold *hemE*, 52-fold *ctaE*; Figure 1B, C, D, respectively) and identified more than 250 previously unknown HrrA-binding sites in the *C. glutamicum* genome (Table S3).

As expected, the highest number of peaks was identified at the first time point after the heme pulse (0.5 h), with 272 peaks meeting our applied threshold (peak maximal coverage >3-fold average genomic coverage and a distance of <700 bp to the next translational start site). In comparison, 79 peaks were identified before hemin addition (T_0). These data illustrate the fast and transient DNA binding by HrrA in response to heme. It has to be noted, that the membrane embedded HrrS sensor kinase is also activated by endogenously synthesized heme (Figure S1 and Reference[21]) and that the addition of external heme led to a boost of the HrrSA response. In general, the majority of the discovered HrrA binding sites were close to gene start sites (Figure S2). The binding of HrrA to 11 selected targets was confirmed by electrophoretic mobility shift assays (Figure S3), and a weak palindromic binding motif was deduced from the tested DNA fragments (Figure S4).

The HrrA binding patterns depicted in Figure 1B-D are representative of many bound regions. Thirty minutes after the heme pulse, the average peak intensities increased approximately 4.5-fold in comparison to those at T_0 (Figure 2A). After 2 h of cultivation in hemin, the average peak intensity dropped 2.6-

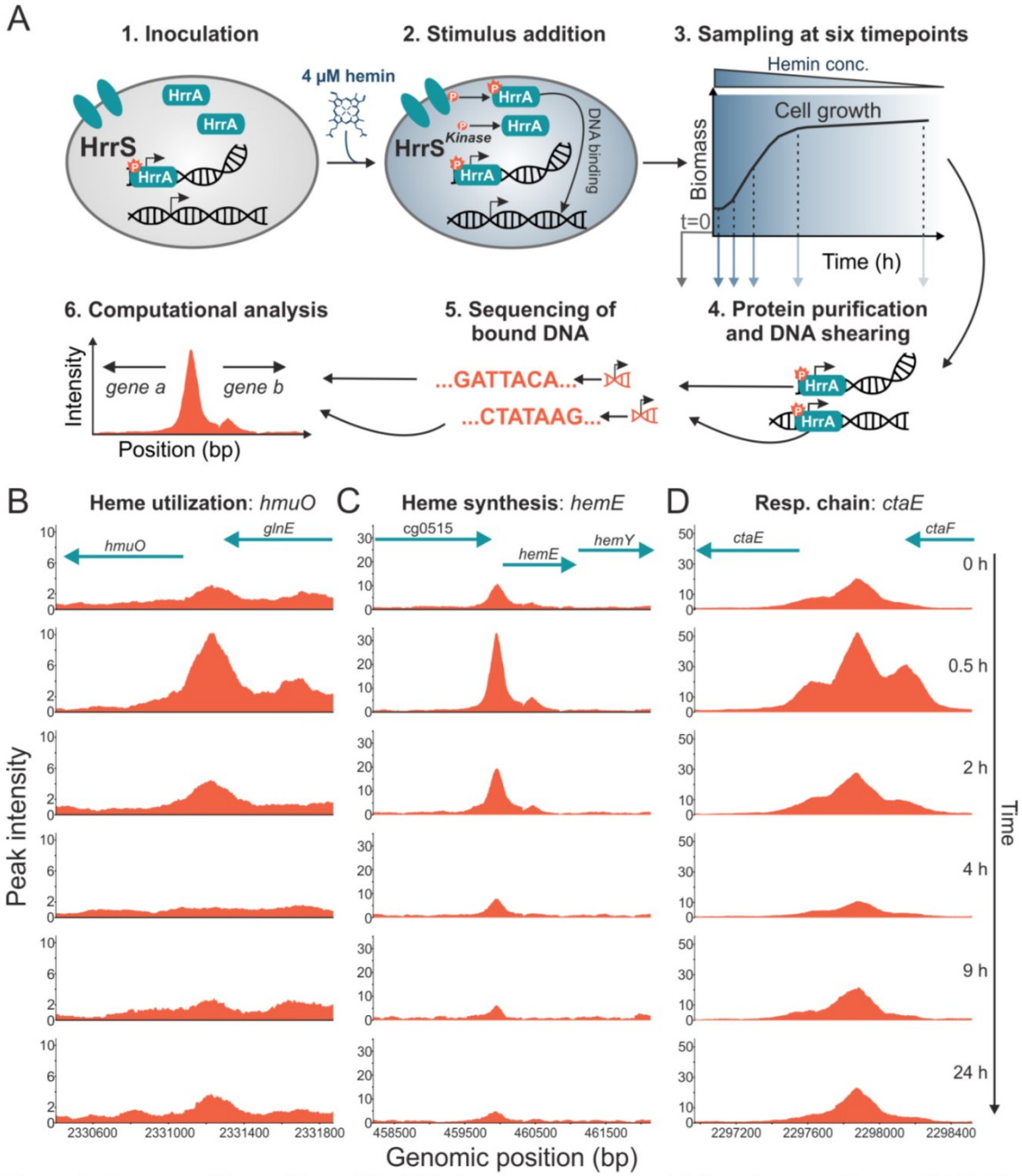

Figure 1: Genome-wide profiling of HrrA binding in response to addition of external heme. (A) ChAP-Seq analysis on the *C. glutamicum* strain Δ*hrrSA*Δ*chrSA* (pJC1_P_{hrrSA}-*hrrSA-twin-strep*_P_{chrSA}-*chrSA-his*) grown in iron-depleted glucose minimal medium before and after addition of 4 µM hemin. The experimental approach is briefly depicted: Cells were harvested at different time points, twin-Strep tagged HrrA was purified and co-purified DNA was sequenced to identify HrrA genomic targets. This approach resulted in the identification of more than 250 genomic regions bound by HrrA upon addition of hemin after 30 minutes. Exemplarily shown is the HrrA binding to regions upstream of operons involved in (B) heme degradation (*hmuO*), (C) heme biosynthesis (*hemE*) and (D) the respiratory chain (*ctaE*).

fold in comparison to that of the sample taken after 30 minutes, further decreasing for the sample taken after 4 h (7.1-fold decrease). In our approach, the HrrA peaks reached a minimum after 9 h of cultivation (Figure 2). This dissociation of HrrA from its target promoters

is caused by rapid depletion of heme, which was confirmed by spectroscopy of *C. glutamicum* cells (Figure 2A, dashed line) and was also obvious upon visual inspection (Figure S5). However, a slight increase in HrrA DNA binding was noted for cells in the stationary phase, which was likely triggered by the intrinsic heme pool and DtxR derepression of the *hrrA* gene when iron sources become limiting[34] (Figure 2A and D). Of all peaks, that passed our threshold, 128 were upstream of uncharacterized genes, while 144 could be assigned to genes with known or predicted function (Figure 2B).

A relatively high correlation between peak intensities for the time points 0, 0.5, 2 and 4 h (Figure 2C) showed that, while the strength of HrrA binding changed in response to heme availability, the system reacted proportionally for a majority of the binding sites. As expected, the binding at 9 h exhibited the lowest correlation to other time points (Figure 2C). This sample was obtained during the early stationary phase and the low correlation of HrrA peak intensities demonstrated overrelaxation and rewiring of the regulatory network. Here, interference with other regulators likely contributed to the significant changes in the HrrA binding pattern.

The HrrSA TCS shapes heme homeostasis by integrating the response to oxidative stress and cell envelope remodeling

Our dataset confirmed the binding of HrrA to all the targets identified thus far. HrrA was found to bind to the upstream promoter region of genes encoding components of heme biosynthesis (*hemE*, *hemH* and *hemA*), degradation (*hmuO*), and export (*hrtBA*) pathways and heme-containing complexes of the respiratory chain (*ctaE-qcrCAB* operon and *ctaD*). A comprehensive overview of all identified HrrA targets is presented in a separate, supplementary file (Table S3); selected target genes are listed in Table 1. Among the more than 250 novel targets identified in this study, we observed HrrA binding upstream of *ctaB*, which encodes a protoheme IX farnesyltransferase that catalyzes the conversion of heme *b* to heme *o*[24] and upstream of *ctaC*, which encodes subunit 2 of the cytochrome aa_3 oxidase. Remarkably, HrrA binding was also observed upstream of the *cydABDC* operon, which encodes the cytochrome *bd* oxidase of the respiratory chain. Altogether, this set of target genes highlights the global role of the HrrSA system in heme-dependent coordination of both branches of the respiratory chain. The HrrA regulon appeared to cover also the aspect of cofactor supply for the respiratory chain, as several HrrA targets encode enzymes involved in menaquinone biosynthesis (*menA*, *menD*, and *menG*) and reduction (*sdhCD*, *lldD* and *dld*). Remarkably, HrrA binding was also observed upstream of *gapA* (glyceraldehyde-3-phosphate dehydrogenase) and *tkt* (transketolase), encoding enzymes involved in the central metabolism and previously described as important hubs in the cellular response to oxidative stress[35]. However, due to the binding of HrrA in the intergenic region of *tkt* and the divergently encoded *ctaB*, as described earlier, no further regulatory function could be ascertained (Figure S6). Additional genes involved in the oxidative stress response were identified, including *trxB* (thioredoxin reductase[36]), *mpx* (mycothiol peroxidase), *tusG* (trehalose uptake system[37]) and *msrB* (methionine sulfoxide reductase[38]). These findings suggest that the HrrSA system not only controls heme biosynthesis and degradation but also integrates the response to heme-induced oxidative stress.

A further important class of HrrA targets is represented by genes associated with the regulation or maintenance of the *C. glutamicum* cell envelope. The gene products of these previously unknown HrrA targets are, for instance, involved in the synthesis of peptidoglycan (*murA*, *murB*, *murF*), lysine (*lysI*, *lysA*, *lysC*), the peptidoglycan precursor meso-2,6-diaminopimelate (mDAP), inositol-derived lipids (*ino1*) and arabinogalactan (*aftC*). HrrA also exhibited binding to the promoter region of *malR*, which encodes a global regulator involved in stress-responsive cell envelope remodeling (Hünnefeld & Frunzke, manuscript submitted). In addition to *malR*, other genes encoding global transcriptional regulators (e.g., *ramA*, *ramB*, *amtR* and *dtxR*) were identified as direct HrrA targets, adding a further level of complexity to this systemic response to heme.

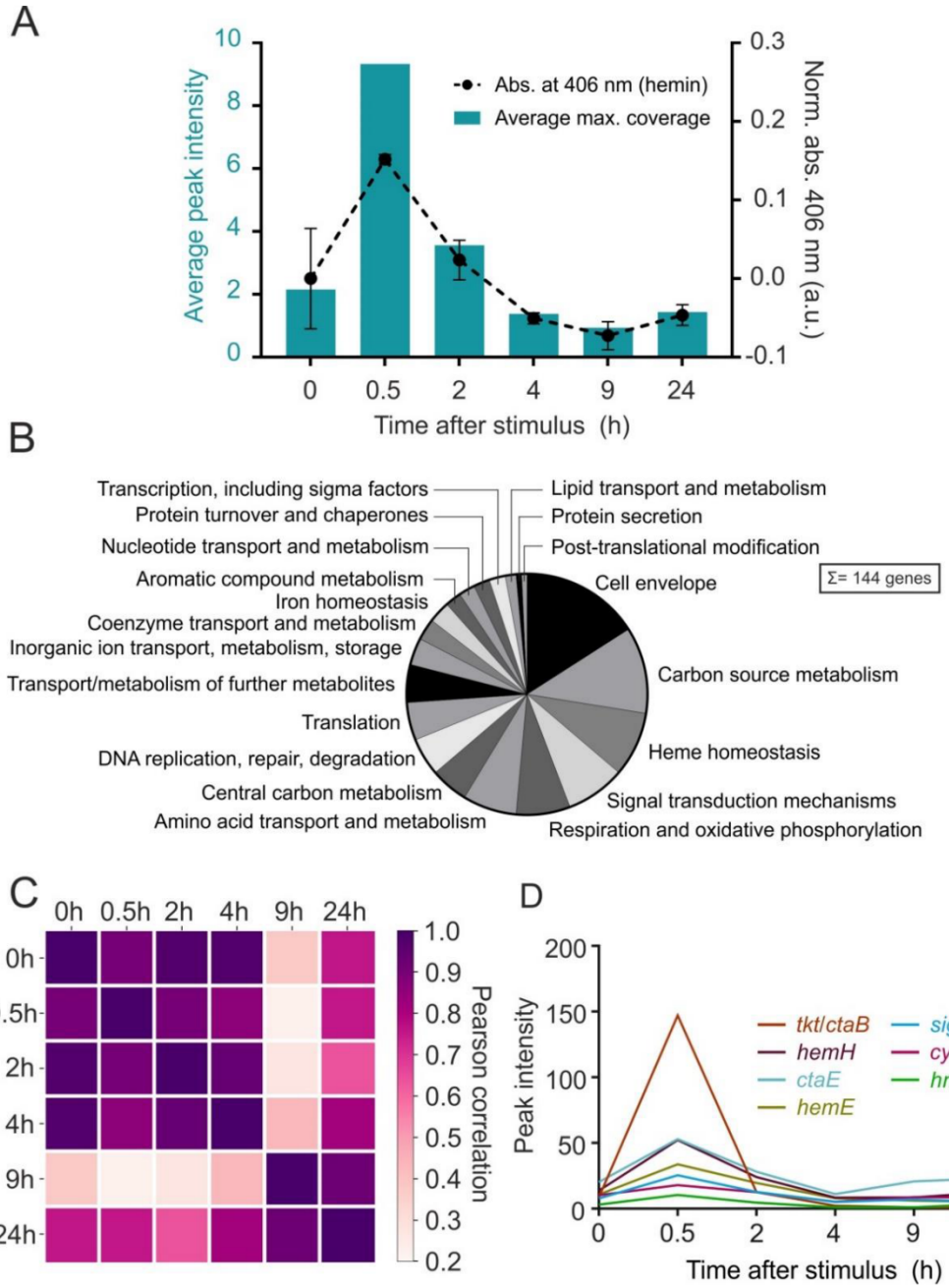

Figure 2: ChAP-Seq analysis revealed HrrA to be a global regulator of heme homeostasis in *C. glutamicum*. (A) HrrA binding in response to the addition of hemin. The bar plot reflects the average peak intensities among detected peaks in ChAP-Seq experiments (peak maximal coverage > 3-fold average genomic coverage and a distance of < 700 bp to the next gene start site). The binding was correlated with the amount of cell-associated hemin (dashed line), measured at corresponding time points by spectroscopy as described in *Material and Methods*. (B) Pie chart presenting the functional categories of HrrA targets (total of 272 genes, among which, 128 encode proteins of unknown function, e.g., several genes of the CGP3 prophage). For a complete overview of HrrA targets, see Table S3. (C) For each peak that passed the threshold (peak maximal coverage > 3-fold average genomic coverage and a distance of < 700 bp to the next ORF start site (TLS)) at time point A, the highest peak in the same region (± 50 nucleotides from the center of the peak) was selected for time point B and *vice versa*. Thus 'paired' peaks for these two time points were obtained, and the Pearson correlation of the intensities of all paired peaks was calculated for all six time points. (D) Peak intensities of selected HrrA targets over time, as identified by ChAP-Seq.

Table 1: Selected target genes of HrrA. Shown are the locus tag (cg number), the gene name and annotation together with a) the distance of the HrrA binding peak, identified via ChAP-Seq, to the start codon (translational start site, TLS) and b) the corresponding peak intensity (*indicate regions on the pJC1_P_{hrrSA}-*hrrSA-twin-strep*_P_{chrSA}-*chrSA-his* plasmid), c) relative ratios of the transcript levels in the Δ*hrrA* deletion mutant compared to wild type (log_2 fold change). The values are derived from a comparison between the two strains 0.5 h after hemin addition (in brackets are fold change values after 4 h for Δ*hrrA*/wt). The log_2(Δ*hrrA*/wt) value for was not determined for the *hrrA* gene (n.d.).

Locus tag	Gene name	Annotation	Dist. TLS[a]	Peak intensity[b]	log_2 (Δ*hrrA*/wt)[c] RNA-Seq
Heme homeostasis/metabolism					
cg2445	***hmuO***	heme oxygenase	150	10.4	-3.1
cg0516	***hemE***	uroporphyrinogen decarboxylase	60	33.7	3.1
cg0497	***hemA***	glutamyl-tRNA reductase	26	25.8	0.6 (1.0)
cg0517	***hemY***	protoporphyrinogen oxidase	642	6.4	2.8
cg3156	***htaD***	secreted heme transport-associated protein	151	17.3	-0.3
cg3118	***cysI***	sulfite reductase hemoprotein	498	3.7	-0.7 (3.1)
cg1734	***hemH***	ferrochelatase	16	52.9	4.0
cg3247	***hrrA***	Heme-dependent response regulator	108	*	n.d.
cg2201	***chrS***	heme-dependent histidine kinase (*chrSA* operon)	32	*	-0.4
cg2202	***hrtB***	heme exporter (*hrtBA* operon)	78	*	-1.0
Respiratory chain					
cg2406	***ctaE***	cytochrome aa_3 oxidase, subunit 3	324	52.9	-1.7
cg2780	***ctaD***	cytochrome aa_3 oxidase, subunit 1	314	21.8	-1.1
cg1301	***cydA***	cytochrome *bd* oxidase	177	17.9	-0.7 (-2.6)
cg2409	***ctaC***	cytochrome *aa*3 oxidase, subunit 2	259	16.1	-1.4
cg0645	***creJ***	part of a putative cytochrome P450 system	678	5.1	-0.1 (-1.3)
cg1773	***ctaB(/tkt)***	protoheme IX farnesyltransferase	204	147.0	0.4 (-1.4)

cg2403	***qcrB***	cytochrome bc1 complex, cytochrome b subunit	221	4.8	-1.8
cg3226		L-lactate permease, operon with *lldD*	622	5.5	-1.7
cg0309	***sigC*(*/katA*)**	RNA polymerase σ factor	38	25.4	2.1
Signal transduction					
cg3315	***malR***	transcriptional regulator, MarR-family	91	5.2	1.1
cg0444	***ramB***	transcriptional regulator, involved in acetate metabolism	224	26.7	-0.7
cg2831	***ramA***	transcriptional regulator, acetate metabolism, LuxR-family	42	5.0	-0.5
cg2103	***dtxR***	master regulator of iron-dependent gene expression	579	3.3	-0.4
Oxidative stress					
cg3422	***trxB***	thioredoxin reductase	5	5.8	-0.8
cg2078	***msrB***	peptide methionine sulfoxide reductase-related protein	282	3.0	-0.7
cg2867	***mpx***	mycothiol peroxidase, GSH peroxidase-family	56	5.6	-1.5
cg0310	***katA*(*/sigC*)**	catalase	???	25.4	-0.7 (-1.2)
cg1774	***tkt*(*/ctaB*)**	transketolase	16	147.0	0.0
cg1791	***gapA***	glyceraldehyde-3-phos. dehydrogenase, glycolysis	287	4.4	-0.3
cg1069	***gapB***	glyceraldehyde-3-phos. dehydrogenase, gluconeogenesis	284	3.5	1.6
Cell envelope					
cg3323	***ino1***	D-myo-inositol-1-phosphate synthase	156	7.6	1.7
cg0337	***whcA***	negative role in SigH-mediated oxidative stress response	125	6.4	-0.5
cg2747	***mepA***	putative cell wall peptidase	69	4.1	-0.2 (-1.4)
cg0061	***rodA***	putative FTSW/RODA/SPOVE-family cell cycle protein	389	8.7	-1.1
cg0306	***lysC***	aspartate kinase	40	12.2	0.7
cg2373	***murF***	D-alanine:D-alanine-adding enzyme	133	23.1	-0.2
cg0423	***murB***	UDP-N-acetylenolpyruvoylglucosamine reductase	2	18.7	-0.3

Temporal dynamics of promoter occupancy reveal hierarchy in the HrrA regulon

With this time-resolved and genome-wide analysis of HrrA binding, we were also able to visualize distinct binding patterns of HrrA in response to addition and depletion of stimulus. Consequently, we asked whether the binding patterns (ChAP-Seq coverage) could provide information regarding the dissociation constant (K_d) of HrrA to specific genomic targets. We compared the *in vivo* binding patterns of *ctaE*, *cydAB* and *hmuO* (Figure 1). While a constitutively high peak was observed upstream of the *ctaE* promoter, the relative

increase upon the addition of exogenous heme was smaller than that observed for other targets (Figure 1D). In contrast, binding to the promoter of *hmuO* occurred with apparently high stimulus dependency and appeared to be very transient, as HrrA was fully dissociated from this promoter 4 h after the addition of hemin (Figure 1B). The addition of heme also resulted in the appearance of secondary binding sites in the *ctaE*, *cydAB* and *hmuO* upstream promoter regions, providing evidence for cooperative binding and/or DNA loop formation in response to high heme levels. In general, we found that genes that were not bound or only moderately bound before the addition of a stimulus generally exhibited higher fold increases in coverage than constitutively bound targets (Figure S7).

Subsequently, we determined the *in vitro* affinity of phosphorylated HrrA to the promoter regions of *ctaE*, *cydAB* and *hmuO* (Table 2, Figure S8). Consistent with the ChAP-Seq data, we measured the highest affinity of HrrA to P_{ctaE} with an apparent K_d of 0.10 µM (± 0.003). We therefore hypothesize that the *ctaE* promoter is a prime target that is constitutively activated by HrrA to maintain high gene expression of the operon encoding the bc_1-aa_3 supercomplex. In contrast, we measured an almost 3-fold lower apparent K_d for P_{cydAB}, which was consistent with the relatively transient binding pattern observed for this target. With an apparent K_d of 0.19 µM, the *in vitro* binding affinity of HrrA to the *hmuO* promoter was rather high considering the genomic coverage measured in the ChAP-Seq analysis. However, *in vitro* analysis does not account for the widespread interference among regulatory networks *in vivo*. In the particular example of *hmuO*, the pattern of HrrA binding was likely the result of interference with the global regulator of iron homeostasis, DtxR, which has been previously described to repress *hmuO* expression by binding to adjacent sites[34]. Taken together, these results show that *in vivo* promoter occupancy is not only influenced by the binding affinity of the regulator to the particular target, but also significantly shaped by internetwork interference. Consequently, high *in vivo* promoter occupancy indicates high binding affinity, but conclusions based on weakly bound regions may be confounded by competition with other binding factors.

HrrA activates the expression of genes encoding components of both branches of the quinol oxidation pathway

To evaluate how HrrA binding impacts the expression of individual target genes, we analyzed the transcriptome (RNA-Seq) of the *C. glutamicum* wild type strain (ATCC 13032) as well as a Δ*hrrA* mutant. Analogous to the ChAP-Seq experiments, RNA-Seq analysis was performed prior to the addition of heme (T_0) and 0.5 and 4 h after the heme pulse (in medium containing no other iron source).

At T_0, before the addition of heme, already 158 genes showed a more that 2-fold altered expression level in wild type cells compared to Δ*hrrA* cells (Δ*hrrA*/wt). In contrast, directly after the addition of stimulus, the expression of 274 of the significantly affected genes (Figure 3A, orange dots) changed more than 2-fold. Of these genes, 120 were upregulated and 154 were downregulated in the *hrrA* deletion strain. 4 h after addition of heme, only 118 genes exhibited a greater than 2-fold increase or decrease (scatter plots for additional time points are presented in Figure S9).

The *hrrA* expression decreased after 0.5 h upon the addition of heme, which was likely caused by DtxR repression in response to increased intracellular iron levels (Figure 3B). In contrast, after 4 h of cultivation, *hrrA* levels significantly increased, reflecting the depletion of heme as an alternative iron source and dissociation of DtxR. Furthermore, differential gene expression analysis revealed HrrA to be an activator of all genes encoding components of

Table 2: Apparent K_d values of HrrA to the promoters of *hmuO*, *ctaE*, *sigC* and *cydA*. The affinity of phosphorylated HrrA to the indicated regions was measured using purified protein in increasing concentrations and its ability to shift 15 nM DNA fragments covering 250 bp up- and downstream of the maximal ChAP-Seq peak height (for detailed information, see Figure S8).

Promoter	Function	Apparent K_d value (µM)	Peak intensity after hemin addition (ChAP-Seq)
P_{hmuO}	Heme oxygenase	0.19 ± 0.013	10.4
P_{ctaE}	Cytochrome aa_3 oxidase	0.10 ± 0.003	52.9
P_{sigC}	ECF sigma factor σ^C	0.27 ± 0.012	25.4
P_{cydA}	Cytochrome *bd* oxidase	0.26 ± 0.007	17.9

the respiratory chain (*ctaE*, *ctaD*, *ctaF* and *cydA*) and as a repressor of heme biosynthesis (*hemA*, *hemE* and *hemH)* (Figure 3C). Additionally, *lldD*, encoding a lactate dehydrogenase contributing to the reduced menaquinone pool, was downregulated more than three-fold upon deletion of *hrrA*. Remarkably, we identified HrrA as a repressor of *sigC*, encoding an ECF involved in the control of the branched respiratory chain in response to cytochrome aa_3 deficiency[32].

In addition to the considerable differences between the wild type and the Δ*hrrA* mutant, we also observed slightly decreased mRNA levels of genes involved in the oxidative stress response (e.g., *mpx*, mycothiol peroxidase) or cell envelope remodeling (e.g., *malR*, *murB*) in the Δ*hrrA* mutant, suggesting HrrA to be an activator of these targets. In many cases, promoter occupancy by HrrA did not result in altered expression levels of the particular target gene (e.g., genes involved in peptidoglycan biosynthesis or the transketolase *tkt*) in a Δ*hrrA* mutant under the tested conditions (Table 1). This finding is, however, not surprising considering the multiplicity of signals and regulators affecting gene expression under changing environmental conditions.

Correlation between promoter occupancy and differential gene expression is higher for repressed targets

In nature, all relevant stimuli for a specific gene act as inputs, and therefore, the output and adaptation of gene expression is affected by a multitude of parameters. We examined how HrrA binding (ChAP-Seq) translates to changes in expression of target genes (RNA-Seq) and found that binding and differential gene expression exhibit significantly higher correlation for repressed targets than for genes activated by HrrA (Figure 3B). This phenomenon can be attributed to a generally high hierarchical position of repressors and can be demonstrated for the transcriptional control of the heme oxygenase HmuO. While HrrA binds to P_{hmuO} directly after addition of the stimulus, the iron-dependent regulator DtxR also binds to this promoter and represses *hmuO*. As a result, HrrA binding does not instantly translate to increased expression but is delayed until DtxR dissociates (see Figure S10 for mRNA levels of *hmuO* in wild type and Δ*hrrA* cells). In cases where HrrA represses expression, such as of *hemE/hemY*, binding is apparently enough for heme-dependent inhibition, just as DtxR-mediated repression of *hmuO* overwrites the activation of this gene by HrrA.

HrrA determines the prioritization of terminal cytochrome oxidases by repression of *sigC*

The results from ChAP-Seq and RNA-Seq experiments highlight the important role of HrrA in the control of the respiratory chain, including cofactor supply. Our data revealed that HrrA activates the expression of genes encoding the cytochrome bc_1-aa_3 supercomplex (*ctaE-qcrCAB*, *ctaD*, *ctaFC*, Figure 4) and of *cydAB*, encoding the cytochrome *bd* branch of the respiratory chain. In both cases, multiple HrrA peaks were identified in ChAP-Seq experiments; however, the association of these multiple peaks with the control of particular target operons remains to be studied. Remarkably, the mRNA profiles of the corresponding operons exhibited significantly delayed activation of *cydAB* in response to heme, which was

abolished in the Δ*hrrA* mutant (Figure 4). In contrast, *ctaE* expression was significantly higher in wild type cells, even before hemin addition (T_0), and reaches a plateau 30 minutes after stimulus addition. In this context, notably, we also observed binding of HrrA upstream of

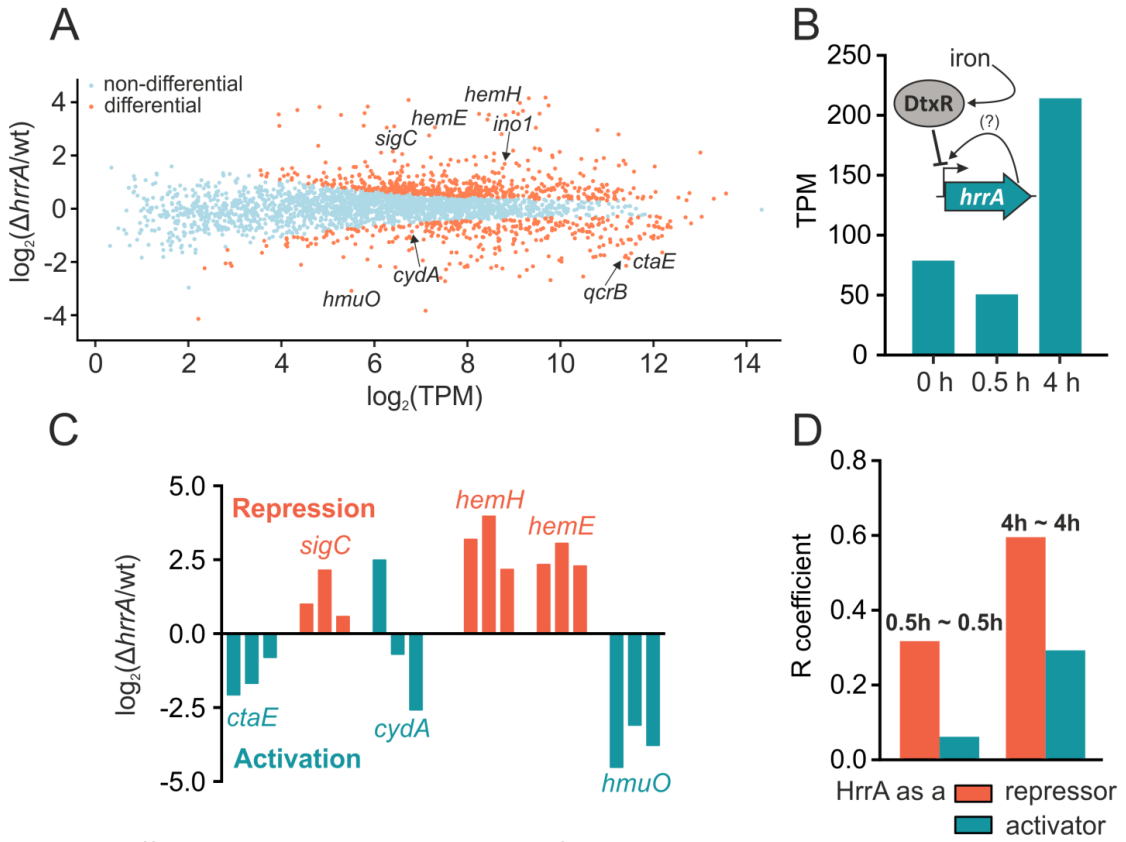

Figure 3: Differential gene expression analysis of wild type *C. glutamicum* and a Δ*hrrA* mutant. (A) Differential gene expression analysis (RNA-Seq) revealed 120 upregulated and 154 downregulated genes in the *hrrA* deletion strain compared to the wild type (in transcripts per million, TPM) after 30 minutes of cultivation in iron-depleted glucose minimal medium containing 4 µM heme. (B) Expression levels of *hrrA* (TPM) 0, 0.5 and 4 h after the addition of hemin. A scheme depicts HrrA autoregulation and iron-dependent DtxR repression. (C) Impact of *hrrA* deletion on the transcript levels of six selected target genes at three different time points (0 h, 0.5 h, 4 h; orange: HrrA acts as a repressor, turquoise: HrrA acts as an activator). (D) ChAP-Seq and RNA-Seq experiments demonstrate higher correlation of ChAP-Seq peak intensities and impact on gene expression (RNA-Seq, Δ*hrrA*/wt) for targets where HrrA functions as a repressor instead of an activator

sigC, which encodes an extracytoplasmic sigma factor that was shown to be involved in the activation of the *cydAB* operon[32]. The mRNA level of *sigC* increased more than two-fold in the Δ*hrrA* mutant, indicating HrrA to be a repressor of this gene (Figure 4). Consistent with this hypothesis, *sigC* expression was slightly decreased in response to the addition of heme, which correlated with increased HrrA peak intensity (Figure 4E). Additionally, the higher *cydAB* expression, observed in the Δ*hrrA* strain before addition of stimulus (Figure 4C) is likely a byproduct of increased *sigC* expression (Figure 4B) and the subsequent σ^C activation of the *cydAB* operon in the same strain. Dissociation of HrrA from P_{sigC} at a later time point (4 h after heme pulse) led to derepression of *sigC* and concomitantly increased expression of *cydAB* in the wild type. Because *cydAB* levels were constitutively low in the Δ*hrrA* mutant in response to heme, we hypothesized that activation by HrrA together with an additional boost by SigC (Figure 5) leads to delayed activation of *cydAB* after the heme

pulse. Thus, the cells were able to channel most of the available heme pool into the more efficient cytochrome bc_1-aa_3 supercomplex. The lower apparent K_d of HrrA for the *ctaE* promoter (0.1 µM) than for P*cydAB* (0.26 µM) or P*sigC* (0.27 µM) also reflects this prioritization of HrrA targets. Consequently, this almost 3-fold decrease in affinity (apparent K_d) increases the threshold for HrrSA activity to control these targets.

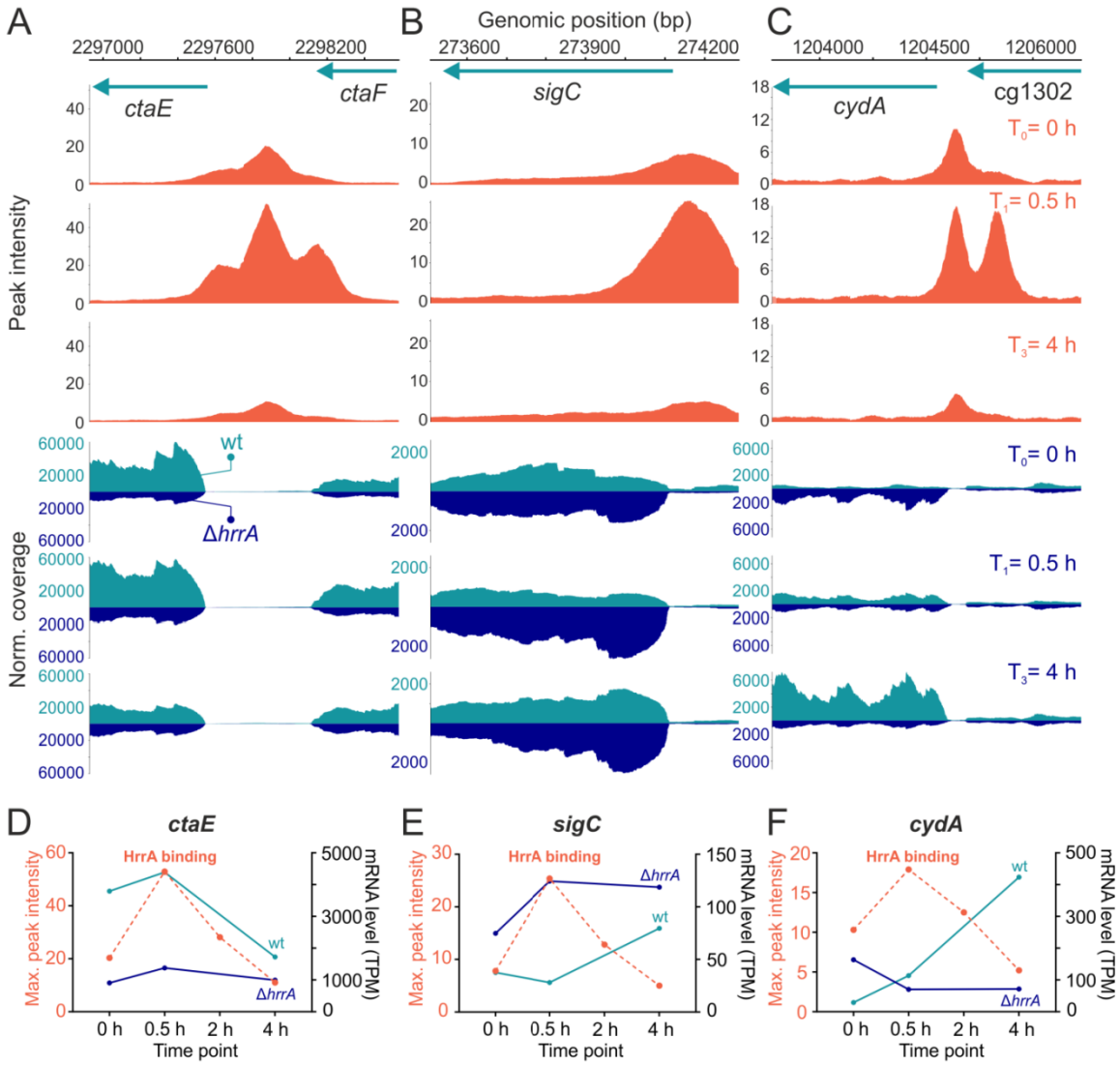

Figure 4: HrrA prioritizes the expression of genes encoding components of the bc_1-aa_3 supercomplex. Depicted are HrrA binding peaks as identified by ChAP-Seq analysis (Figure 1 and 2) in comparison to the normalized coverage of RNA-Seq results (wild type and the Δ*hrrA* mutant) for the genomic loci of *ctaE* (A, D), *sigC* (B, E) and *cydA* (C, F). D-F: HrrA binding (max. peak intensities measured by ChAP-Seq experiments) and the mRNA levels (in transcripts per million, TPM) of the respective genes in the Δ*hrrA* strain as well as in wild type *C. glutamicum* cells 0, 0.5 and 4 h after the addition of hemin.

Discussion

In this study, we used a genome-wide approach to identify more than 250 genomic target regions of the "heme-responsive regulator" HrrA in *C. glutamicum*. This intriguingly diverse set of target genes, encoding enzymes involved in heme biosynthesis, heme-containing proteins, components of the respiratory chain, oxidative stress response proteins and proteins involved in cell envelope remodeling, provided unprecedented insight into the systemic

response to heme coordinated by the TCS HrrSA.

In Gram-positive bacteria, TCSs appear to play a central role in transient heme sensing, and heme-responsive systems have been described in several prominent pathogens, including *C. diphtheriae*, *S. aureus* and *B. anthracis*[15-18]. For all prokaryotic heme regulatory systems, however, only a small number of target genes have been described to date, focusing on targets involved in degradation (*hmuO*[18,39]), heme export (*hrtBA*[19,40]) or heme biosynthesis (*hemA*[18,20]). Systems orthologous to HrrSA are found in almost all corynebacterial species, and the high amino acid sequence identity shared by response regulators (87 %, between *C. glutamicum* and *C. diphtheriae* HrrA, Figure S11) suggests that the important role of HrrSA in the control of heme homeostasis is conserved.

Coping with heme stress

While being an essential cofactor for many proteins, heme causes severe toxicity to cells at high levels[4]. In mammalian cells, the BACH1 regulator is inactivated by heme binding and plays a key role in maintaining the balance of the cellular heme pool[8,41]. Heme oxygenases are targets of various heme-dependent regulators[18,42,43], and consistent with this principle, the mammalian *HMOX1* gene, encoding an NADPH-dependent oxygenase, is regulated by BACH1[41]. Other identified BACH1 targets are involved in redox regulation, the cell cycle, and apoptosis as well as subcellular transport processes[9], and the regulon includes genes encoding thioredoxin reductase 1, the iron storage protein ferritin[44] and NAD(P)H menadione oxidoreductase 1[45].

Although neither the regulator nor the constitution of the regulon is conserved, the responses of BACH1 and HrrSA share a similar logic. Analogous to eukaryotic BACH1, we observed HrrA-mediated activation of *trxB* (thioredoxin reductase), *mpx* (mycothiol peroxidase), and *katA* (catalase), which appear to be required to counteract oxidative stress caused by elevated heme levels. Additionally, HrrA binds to the intergenic region between the divergent genes *ctaB* and *tkt*, the latter encoding a transketolase. While BACH1 has previously exhibited regulation of a transketolase (*TKT*)[9], the effect of HrrA on the expression of *tkt* could not be conclusively determined in this study (see Table 2). Notably, however, transketolase, an important enzyme of the nonoxidative part of the pentose phosphate pathway (PPP), was recently shown to be required for cancer cell growth, helping the cells meet the high demand for NAPDH[35].

Remarkably, HrrA binding was also observed upstream of both *gapA* and *gapB*, which encode glyceraldehyde-3-phosphate dehydrogenases (GapDHs) and are involved in glycolysis and gluconeogenesis, respectively. Previous studies have revealed that oxidative stress may block glycolysis by inhibiting glyceraldehyde-3-phosphate dehydrogenase (GapDH) in baker's yeast and mammalian cells[46,47]. Furthermore, GapDH of *C. diphtheriae* was recently shown to be redox-controlled by S-mycothiolation[48]. Slight activation of *gapA* by HrrA may thus counteract an impaired glycolytic flux under conditions of heme stress. Furthermore, several HrrA targets play a role in the biosynthesis and remodeling of the corynebacterial cell envelope, including *mepA* (a putative cell wall peptidase[49]); *ino1*, which is required for the synthesis of inositol-derived lipids[50]; and *malR*, encoding a MarR-type regulator that is possibly involved in stress-responsive cell envelope remodeling (Hünnefeld & Frunzke, manuscript submitted). Taken together, these insights emphasize the important role of the HrrSA system in the control of heme stress responses.

Coordinated control of the respiratory chain

Among the most significantly affected targets in the Δ*hrrA* mutant were many genes encoding components of the respiratory chain[24], including all the genes constituting the cytochrome bc_1-aa_3 branch of the respiratory chain (*ctaE-qcrCAB*, *ctaCF* and *ctaD*)[51]; genes encoding the cytochrome *bd* branch (*cydAB*[24]); *ctaA*[52] and *ctaB*[53], encoding enzymes responsible for heme *a* synthesis; and *lldD* and *dld*, encoding lactate dehydrogenases that contribute to the reduced menaquinone pool[24].

In a recent study, Toyoda and Inui described the ECF sigma factor σ^C to be an important regulator of both branches of the

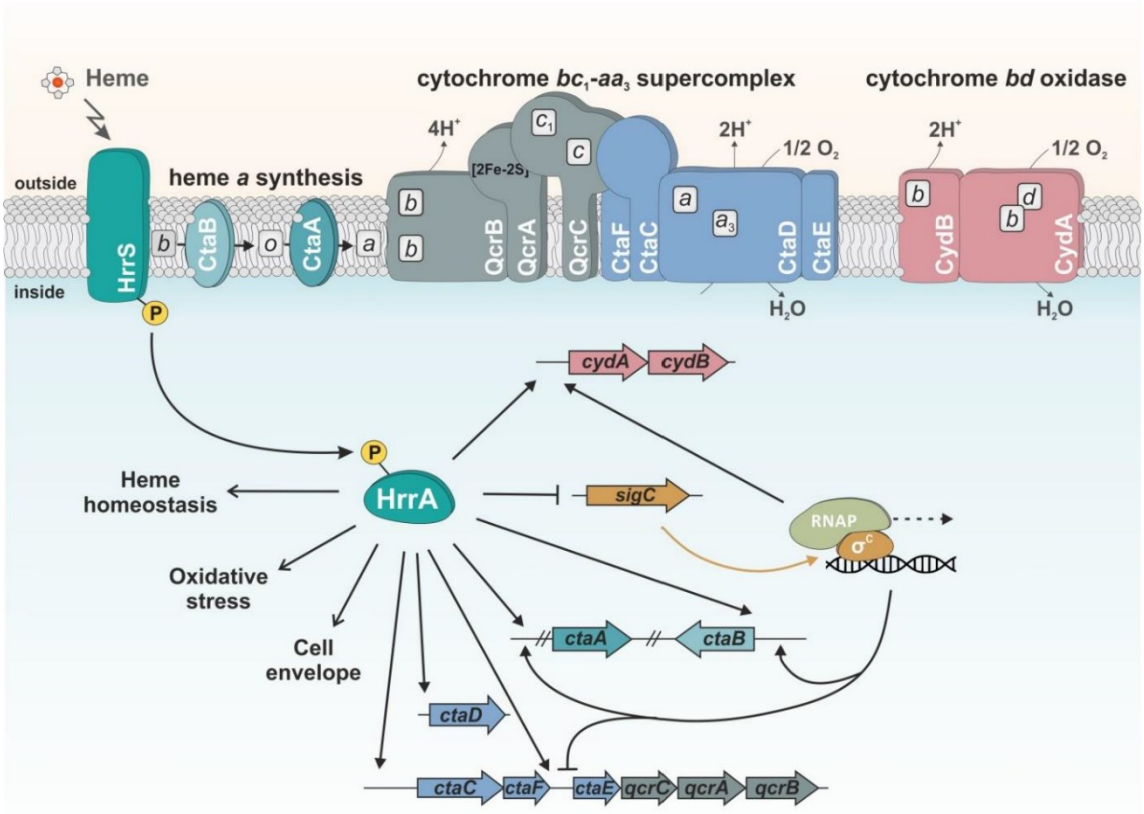

Figure 5: Model of heme-responsive control of components of the respiratory chain by HrrSA. The results of this study reveal HrrSA as a global regulator of heme homeostasis coordinating the expression of genes involved in heme biosynthesis, oxidative stress responses and cell envelope remodeling. An important part of the HrrA regulon is comprised by genes encoding the components of the branched respiratory chain of *C. glutamicum*. While HrrA acts as an activator of all components (*ctaE-qcrCAB*, *ctaA*, *ctaB*, *cydAB*), it represses transcription of the *sigC* gene encoding an important sigma factor required for *cydAB* expression. This regulatory network architecture consequently confers prioritization to the synthesis of the more efficient proton pump, the cytochrome bc_1-aa_3 supercomplex. Bordered boxes, b, c, a, d: heme *b*, heme *c*, heme *a*, heme *d*.

C. glutamicum respiratory chain. The *ctaE-qcrCAB* operon was shown to be significantly downregulated after σ^C overexpression due to binding of the sigma factor to the antisense strand of the promoter[32]. Here, we demonstrated that this repression is counteracted by HrrA, which not only represses *sigC* but also activates *ctaE-qcrCAB* expression. While the two proteins have antagonistic effects on the expression of the supercomplex, both σ^C and HrrA positively regulate the *cyd* operon, encoding the cytochrome *bd* branch of the respiratory chain (Figure 5).

Interestingly, a hierarchy in the regulon was reflected by the differences in the apparent K_d values of HrrA with P_{cydA} and P_{sigC}, which were two-fold lower than those with the promoter of *ctaE.* These findings were also consistent with the ChAP-Seq experiments, where the peaks upstream of *ctaE* and *ctaB* were among the highest peaks at T_0 and after 0.5 h (Figure 4A). These data suggest that under conditions of sufficient heme supply, production of the cytochrome bc_1-aa_3 supercomplex is preferred, which is highly effective but requires the incorporation of six heme cofactors. Repression of *sigC* by HrrA and the relatively low affinity to the *cydAB* promoter results in delayed production of the *bd* branch. At high cell densities (mid-exponential phase), available heme is thus first channeled to the cytochrome bc_1-aa_3 supercomplex before the cytochrome *bd* oxidase is used, which is less efficient but has a higher oxygen affinity.

There is further overlap between the HrrA and σ^C regulons in the case of *ctaB*, which encodes a farnesyltransferase, catalyzing the conversion of heme *b* to heme *o*. Because both HrrA and σ^C positively regulate *ctaB*, the expression of this gene parallels that of the *cyd* operon, exhibiting delayed induction (Figure S6) in response to heme. This phenomenon is counterintuitive because the conversion of heme *b* to heme *a* is needed to fulfill the heme *a* requirement of the bc_1-aa_3 supercomplex. In general, only a few studies have examined the transcriptional regulation of heme *a* synthesis in prokaryotes. In *B. subtilis, ctaA* and *ctaB* are regulated by the ResDE TCS in an oxygen-dependent but heme-independent manner[54]. Furthermore, upon production of CtaA and CtaB of *B. subtilis* in *Escherichia coli*, the *in vivo* formation of a physiologically relevant complex was suggested that efficiently catalyzed the heme *b* to heme *a* conversion with heme *o* as intermediate[55]. In *C. glutamicum*, further studies are needed to unravel the stoichiometry of this complex. For now, one can only speculate that cellular heme *a* stock is used to meet the initial cofactor demand of the bc_1-aa_3 supercomplex. Subsequently, upregulation of the *ctaB-ctaA* synthesis pathway is needed to replenish these stores. This concept would foster a rapid response to potentially available external heme sources and may represent an important adaptive trait of pathogenic species.

Interference with other regulatory networks

Deletion of the *hrrA* gene led to more than 2-fold upregulation of 120 genes, while 154 genes were downregulated after the addition of heme. Several other genes were significantly affected but to a lesser extent. Remarkably, among the direct target genes controlled by HrrA, we identified several prominent global regulators, including the regulators of acetate metabolism *ramA* and *ramB*[56,57]; *malR*, which is involved in cell envelope remodeling (Hünnefeld & Frunzke, manuscript submitted); and *dtxR*, encoding the global iron-dependent regulator in corynebacterial species[34,58]. This finding is intriguing because it reveals the close association and reciprocal control between HrrA and DtxR. While DtxR represses *hrrA* transcription under conditions of sufficient iron supply[34], HrrA slightly upregulates *dtxR* expression (~1.5-fold) in response to heme.

Conclusion

Genome-wide analyses of targets controlled by prokaryotic transcription factors will change our view on many systems we believe to know. In this study, we provide an unprecedented insight into the systemic response to heme coordinated by the HrrSA TCS. Given the many properties of this molecule, the complexity of this response is actually not surprising but paves the way for further functional analysis of HrrA targets with so far unknown functions.

Acknowledgements

We thank Eva Davoudi for fruitful discussions and critical reading of the manuscript. We thank Helga Etterich for her practical help with the sequencing experiments.

REFERENCES

1. Ponka P. 1999. Cell biology of heme. Am J Med Sci 318:241-56.
2. Layer G, Reichelt J, Jahn D, Heinz DW. 2010. Structure and function of enzymes in heme biosynthesis. Protein Science : A Publication of the Protein Society 19:1137-1161.
3. Ajioka RS, Phillips JD, Kushner JP. 2006. Biosynthesis of heme in mammals. Biochim Biophys Acta 1763:723-36.
4. Anzaldi LL, Skaar EP. 2010. Overcoming the heme paradox: heme toxicity and tolerance in bacterial pathogens. Infect Immun 78:4977-89.
5. Huang W, Wilks A. 2017. Extracellular Heme Uptake and the Challenge of Bacterial Cell Membranes. Annu Rev Biochem 86:799-823.
6. Wilks A. 2002. Heme oxygenase: evolution, structure, and mechanism. Antioxid Redox Signal 4:603-14.
7. Hickman MJ, Winston F. 2007. Heme levels switch the function of Hap1 of *Saccharomyces cerevisiae* between transcriptional activator and transcriptional repressor. Molecular and Cellular Biology 27:7414-24.
8. Ogawa K, Sun J, Taketani S, Nakajima O, Nishitani C, Sassa S, Hayashi N, Yamamoto M, Shibahara S, Fujita H, Igarashi K. 2001. Heme mediates derepression of Maf recognition element through direct binding to transcription repressor Bach1. The EMBO journal 20.
9. Warnatz HJ, Schmidt D, Manke T, Piccini I, Sultan M, Borodina T, Balzereit D, Wruck W, Soldatov A, Vingron M, Lehrach H, Yaspo ML. 2011. The BTB and CNC homology 1 (BACH1) target genes are involved in the oxidative stress response and in control of the cell cycle. J Biol Chem 286:23521-32.
10. Qi Z, Hamza I, O'Brian MR. 1999. Heme is an effector molecule for iron-dependent degradation of the bacterial iron response regulator (Irr) protein. Proc Natl Acad Sci U S A 96:13056-61.
11. Qi Z, O'Brian MR. 2002. Interaction between the bacterial iron response regulator and ferrochelatase mediates genetic control of heme biosynthesis. Mol Cell 9:155-62.
12. O'Brian MR. 2015. Perception and Homeostatic Control of Iron in the *Rhizobia* and Related Bacteria. Annu Rev Microbiol 69:229-45.
13. Torres VJ, Stauff DL, Pishchany G, Bezbradica JS, Gordy LE, Iturregui J, Anderson KL, Dunman PM, Joyce S, Skaar EP. 2007. A *Staphylococcus aureus* regulatory system that responds to host heme and modulates virulence. Cell Host Microbe 1:109-19.
14. Mike LA, Choby JE, Brinkman PR, Olive LQ, Dutter BF, Ivan SJ, Gibbs CM, Sulikowski GA, Stauff DL, Skaar EP. 2014. Two-component system cross-regulation integrates *Bacillus anthracis* response to heme and cell envelope stress. PLoS Pathog 10:e1004044.
15. Stauff DL, Skaar EP. 2009. The heme sensor system of *Staphylococcus aureus*. Contrib Microbiol 16:120-35.
16. Stauff DL, Skaar EP. 2009. *Bacillus anthracis* HssRS signalling to HrtAB regulates haem resistance during infection. Mol Microbiol 72:763-78.
17. Bibb LA, Kunkle CA, Schmitt MP. 2007. The ChrA-ChrS and HrrA-HrrS signal transduction systems are required for activation of the *hmuO* promoter and repression of the *hemA* promoter in *Corynebacterium diphtheriae*. Infect Immun 75:2421-31.
18. Frunzke J, Gatgens C, Brocker M, Bott M. 2011. Control of heme homeostasis in *Corynebacterium glutamicum* by the two-component system HrrSA. J Bacteriol 193:1212-21.
19. Heyer A, Gatgens C, Hentschel E, Kalinowski J, Bott M, Frunzke J. 2012. The two-component system ChrSA is crucial for haem tolerance and interferes with HrrSA in haem-dependent gene regulation in *Corynebacterium glutamicum*. Microbiology 158:3020-31.
20. Burgos JM, Schmitt MP. 2016. The ChrSA and HrrSA Two-Component Systems Are Required for Transcriptional Regulation of the *hemA* Promoter in *Corynebacterium diphtheriae*. J Bacteriol 198:2419-30.
21. Keppel M, Davoudi E, Gätgens C, Frunzke J. 2018. Membrane Topology and Heme Binding of the Histidine Kinases HrrS and ChrS in *Corynebacterium glutamicum*. Frontiers in Microbiology 9.
22. Ito Y, Nakagawa S, Komagata A, Ikeda-Saito M, Shiro Y, Nakamura H. 2009. Heme-dependent autophosphorylation of a heme sensor kinase, ChrS, from *Corynebacterium diphtheriae* reconstituted in proteoliposomes. FEBS Lett 583:2244-8.
23. Hentschel E, Mack C, Gatgens C, Bott M, Brocker M, Frunzke J. 2014. Phosphatase activity of the histidine kinases ensures pathway specificity of the ChrSA and HrrSA two-component systems in *Corynebacterium glutamicum*. Mol Microbiol 92:1326-42.
24. Bott M, Niebisch A. 2003. The respiratory chain of *Corynebacterium glutamicum*. J Biotechnol 104:129-53.
25. Kao WC, Kleinschroth T, Nitschke W, Baymann F, Neehaul Y, Hellwig P, Richers S, Vonck J, Bott M, Hunte C. 2016. The obligate respiratory supercomplex from Actinobacteria. Biochim Biophys Acta 1857:1705-14.
26. Niebisch A, Bott M. 2001. Molecular analysis of the cytochrome bc_1-aa_3 branch of the *Corynebacterium glutamicum* respiratory chain containing an unusual diheme cytochrome c_1. Arch Microbiol 175:282-94.
27. Kalinowski J, Bathe B, Bartels D, Bischoff N, Bott M, Burkovski A, Dusch N, Eggeling L, Eikmanns BJ, Gaigalat L, Goesmann A, Hartmann M, Huthmacher K, Kramer R, Linke B, McHardy AC, Meyer F, Mockel B, Pfefferle W, Puhler A, Rey DA, Ruckert C, Rupp O, Sahm H, Wendisch VF, Wiegrabe I, Tauch A. 2003. The complete *Corynebacterium glutamicum* ATCC 13032 genome sequence and its impact on the production of L-aspartate-derived amino acids and vitamins. J Biotechnol 104:5-25.
28. Ikeda M, Nakagawa S. 2003. The *Corynebacterium glutamicum* genome: features and impacts on biotechnological processes. Appl Microbiol Biotechnol 62:99-109.
29. Sone N, Nagata K, Kojima H, Tajima J, Kodera Y, Kanamaru T, Noguchi S, Sakamoto J. 2001. A novel hydrophobic diheme c-type cytochrome. Purification from *Corynebacterium glutamicum* and analysis of the QcrCBA operon encoding three subunit proteins of a putative cytochrome reductase complex. Biochim Biophys Acta 1503:279-90.
30. Teramoto H, Inui M, Yukawa H. 2013. OxyR acts as a transcriptional repressor of hydrogen peroxide-inducible antioxidant genes in *Corynebacterium glutamicum* R. FEBS J 280:3298-312.
31. Milse J, Petri K, Ruckert C, Kalinowski J. 2014. Transcriptional response of *Corynebacterium glutamicum* ATCC 13032 to hydrogen peroxide stress and characterization of the OxyR regulon. J Biotechnol 190:40-54.
32. Toyoda K, Inui M. 2016. The extracytoplasmic function sigma factor sigma(C) regulates expression of a branched quinol oxidation pathway in *Corynebacterium glutamicum*. Molecular Microbiology 100:486-509.
33. Morosov X, Davoudi CF, Baumgart M, Brocker M, Bott M. 2018. The copper-deprivation stimulon of *Corynebacterium glutamicum* comprises proteins for biogenesis of the actinobacterial cytochrome bc_1-aa_3 supercomplex. J Biol Chem doi:10.1074/jbc.RA118.004117.
34. Wennerhold J, Bott M. 2006. The DtxR regulon of *Corynebacterium glutamicum*. J Bacteriol 188:2907-18.
35. Xu IM, Lai RK, Lin SH, Tse AP, Chiu DK, Koh HY, Law CT, Wong CM, Cai Z, Wong CC, Ng IO. 2016. Transketolase counteracts oxidative stress to drive cancer development. Proc Natl Acad Sci U S A 113:E725-34.

36. Arner ES, Holmgren A. 2000. Physiological functions of thioredoxin and thioredoxin reductase. Eur J Biochem 267:6102-9.
37. Alvarez-Peral FJ, Zaragoza O, Pedreno Y, Arguelles JC. 2002. Protective role of trehalose during severe oxidative stress caused by hydrogen peroxide and the adaptive oxidative stress response in *Candida albicans*. Microbiology 148:2599-606.
38. Pang YY, Schwartz J, Bloomberg S, Boyd JM, Horswill AR, Nauseef WM. 2014. Methionine sulfoxide reductases protect against oxidative stress in *Staphylococcus aureus* encountering exogenous oxidants and human neutrophils. J Innate Immun 6:353-64.
39. Bibb LA, King ND, Kunkle CA, Schmitt MP. 2005. Analysis of a heme-dependent signal transduction system in *Corynebacterium diphtheriae*: deletion of the *chrAS* genes results in heme sensitivity and diminished heme-dependent activation of the *hmuO* promoter. Infect Immun 73:7406-12.
40. Bibb LA, Schmitt MP. 2010. The ABC transporter HrtAB confers resistance to hemin toxicity and is regulated in a hemin-dependent manner by the ChrAS two-component system in *Corynebacterium diphtheriae*. J Bacteriol 192:4606-17.
41. Sun J, Hoshino H, Takaku K, Nakajima O, Muto A, Suzuki H, Tashiro S, Takahashi S, Shibahara S, Alam J, Taketo MM, Yamamoto M, Igarashi K. 2002. Hemoprotein Bach1 regulates enhancer availability of heme oxygenase-1 gene. The EMBO journal 21.
42. Ratliff M, Zhu W, Deshmukh R, Wilks A, Stojiljkovic I. 2001. Homologues of neisserial heme oxygenase in gram-negative bacteria: degradation of heme by the product of the *pigA* gene of *Pseudomonas aeruginosa*. J Bacteriol 183:6394-403.
43. Schmitt MP. 1997. Transcription of the *Corynebacterium diphtheriae hmuO* gene is regulated by iron and heme. Infect Immun 65:4634-41.
44. Hintze KJ, Katoh Y, Igarashi K, Theil EC. 2007. Bach1 repression of ferritin and thioredoxin reductase1 is heme-sensitive in cells and in vitro and coordinates expression with heme oxygenase1, beta-globin, and NADP(H) quinone (oxido) reductase1. J Biol Chem 282:34365-71.
45. Dhakshinamoorthy S, Jain AK, Bloom DA, Jaiswal AK. 2005. Bach1 competes with Nrf2 leading to negative regulation of the antioxidant response element (ARE)-mediated NAD(P)H:quinone oxidoreductase 1 gene expression and induction in response to antioxidants. J Biol Chem 280:16891-900.
46. Kuehne A, Emmert H, Soehle J, Winnefeld M, Fischer F, Wenck H, Gallinat S, Terstegen L, Lucius R, Hildebrand J, Zamboni N. 2015. Acute Activation of Oxidative Pentose Phosphate Pathway as First-Line Response to Oxidative Stress in Human Skin Cells. Molecular Cell 59:359-71.
47. Ralser M, Wamelink MM, Latkolik S, Jansen EE, Lehrach H, Jakobs C. 2009. Metabolic reconfiguration precedes transcriptional regulation in the antioxidant response. Nat Biotechnol 27:604-5.
48. Hillion M, Imber M, Pedre B, Bernhardt J, Saleh M, Loi VV, Maaß S, Becher D, Astolfi Rosado L, Adrian L, Weise C, Hell R, Wirtz M, Messens J, Antelmann H. 2017. The glyceraldehyde-3-phosphate dehydrogenase GapDH of *Corynebacterium diphtheriae* is redox-controlled by protein S-mycothiolation under oxidative stress. Scientific Reports 7:5020.
49. Möker N, Brocker M, Schaffer S, Kramer R, Morbach S, Bott M. 2004. Deletion of the genes encoding the MtrA-MtrB two-component system of *Corynebacterium glutamicum* has a strong influence on cell morphology, antibiotics susceptibility and expression of genes involved in osmoprotection. Molecular Microbiology 54:420-38.
50. Baumgart M, Luder K, Grover S, Gatgens C, Besra GS, Frunzke J. 2013. IpsA, a novel LacI-type regulator, is required for inositol-derived lipid formation in *Corynebacteria* and *Mycobacteria*. BMC Biol 11:122.
51. Niebisch A, Bott M. 2003. Purification of a cytochrome *bc-aa*3 supercomplex with quinol oxidase activity from *Corynebacterium glutamicum*. Identification of a fourth subunity of cytochrome aa3 oxidase and mutational analysis of diheme cytochrome c1. J Biol Chem 278:4339-46.
52. Mueller JP, Taber HW. 1989. Isolation and sequence of *ctaA*, a gene required for cytochrome aa_3 biosynthesis and sporulation in *Bacillus subtilis*. J Bacteriol 171:4967-78.
53. Svensson B, Lubben M, Hederstedt L. 1993. *Bacillus subtilis* CtaA and CtaB function in haem *A* biosynthesis. Mol Microbiol 10:193-201.
54. Paul S, Zhang X, Hulett FM. 2001. Two ResD-controlled promoters regulate *ctaA* expression in *Bacillus subtilis*. J Bacteriol 183:3237-46.
55. Brown BM, Wang Z, Brown KR, Cricco JA, Hegg EL. 2004. Heme *O* synthase and heme *A* synthase from *Bacillus subtilis* and *Rhodobacter sphaeroides* interact in *Escherichia coli*. Biochemistry 43:13541-8.
56. Auchter M, Cramer A, Huser A, Ruckert C, Emer D, Schwarz P, Arndt A, Lange C, Kalinowski J, Wendisch VF, Eikmanns BJ. 2011. RamA and RamB are global transcriptional regulators in *Corynebacterium glutamicum* and control genes for enzymes of the central metabolism. J Biotechnol 154:126-39.
57. Shah A, Blombach B, Gauttam R, Eikmanns BJ. 2018. The RamA regulon: complex regulatory interactions in relation to central metabolism in Corynebacterium glutamicum. Appl Microbiol Biotechnol 102:5901-5910.
58. Schiering N, Tao X, Zeng H, Murphy JR, Petsko GA, Ringe D. 1995. Structures of the apo- and the metal ion-activated forms of the diphtheria tox repressor from *Corynebacterium diphtheriae*. Proc Natl Acad Sci U S A 92:9843-50.
59. Keilhauer C, Eggeling L, Sahm H. 1993. Isoleucine synthesis in *Corynebacterium glutamicum*: molecular analysis of the *ilvB-ilvN-ilvC* operon. Journal of Bacteriology 175:5595-5603.
60. Sambrook J. RD. 2001. Molecular Cloning: A Laboratory Manual, 3rd edn. . NY: Cold Spring Harbor Laboratory Press.
61. Eikmanns BJ, Thum-Schmitz N, Eggeling L, Ludtke KU, Sahm H. 1994. Nucleotide sequence, expression and transcriptional analysis of the *Corynebacterium glutamicum gltA* gene encoding citrate synthase. Microbiology 140 (Pt 8):1817-28.
62. Gibson DG, Young L, Chuang RY, Venter JC, Hutchison CA, 3rd, Smith HO. 2009. Enzymatic assembly of DNA molecules up to several hundred kilobases. Nat Methods 6:343-5.
63. Pfeifer E, Hünnefeld M, Popa O, Polen T, Kohlheyer D, Baumgart M, Frunzke J. 2016. Silencing of cryptic prophages in *Corynebacterium glutamicum*. Nucleic Acids Research 44:10117-10131.
64. Jones E, Oliphant T, Peterson P. 2001. SciPy: Open source scientific tools for Python http://wwwscipyorg/.
65. Andrews S. 2010. FASTQC. A quality control tool for high throughput sequence data.
66. Langmead B, Salzberg SL. 2012. Fast gapped-read alignment with Bowtie 2. Nat Methods 9:357-9.
67. Baumgart M, Unthan S, Kloss R, Radek A, Polen T, Tenhaef N, Muller MF, Kuberl A, Siebert D, Bruhl N, Marin K, Hans S, Kramer R, Bott M, Kalinowski J, Wiechert W, Seibold G, Frunzke J, Ruckert C, Wendisch VF, Noack S. 2018. *Corynebacterium glutamicum* Chassis C1*: Building and Testing a Novel Platform Host for Synthetic Biology and Industrial Biotechnology. ACS Synth Biol 7:132-144.
68. Pachter L. 2011. Models for transcript quantification from RNA-Seq. Conference Proceedings.

4 Discussion

4.1 Biogenesis of cytochrome oxidases

Energy transduction is crucial for survival and reproduction of living organisms. Utilization of PMF generated by a terminal oxidase to drive the ATP synthesis *via* the F_1F_0-ATP synthase is ubiquitous in all aerobic kingdoms of life (Boyer, 1997; Börsch and Duncan, 2013; Grüber *et al.*, 2014). Albeit being such a common process and using similar enzymes, differences especially in regards of biogenesis of terminal oxidases make transfer of knowledge across species difficult.

In this thesis, a major aim was the identification of proteins involved in the assembly of the cytochrome bc_1-aa_3 supercomplex of *C. glutamicum*, the main branch for aerobic respiration in this organism. The cytochrome aa_3 oxidase of the supercomplex is a typical member of the heme-copper oxidases and requires a Cu_A center in subunit II (CtaC) and heme *a* and the heme a_3-Cu_B center in subunit I (CtaD) for activity. We addressed two aspects in the biogenesis of the oxidase, which were the search for proteins involved in formation of the copper centers and the characterization of a Surf1 homologue as a candidate protein for insertion of heme *a* into cytochrome aa_3 oxidase.

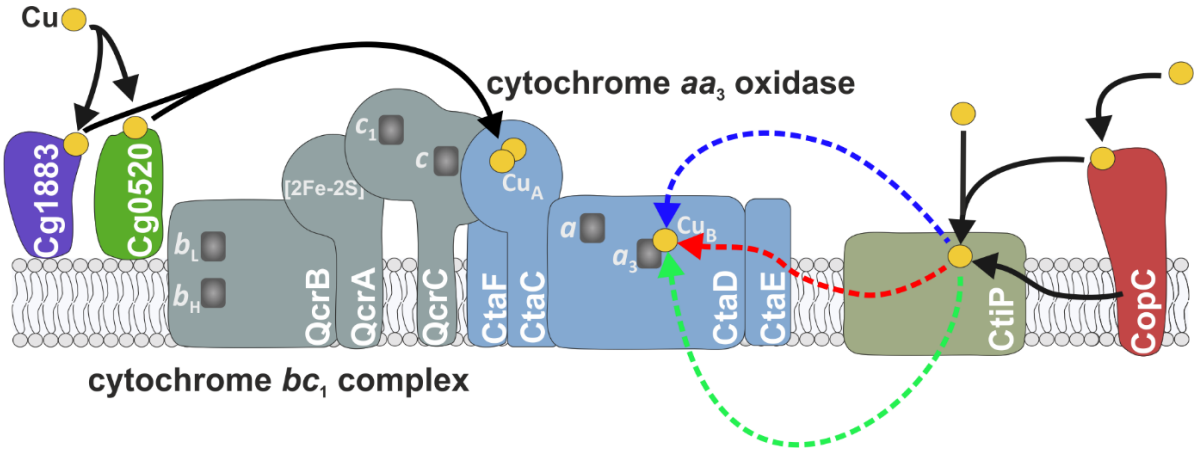

Figure 6: Predicted copper-delivery routes to Cu_A and Cu_B of the cytochrome aa_3 oxidase in *C. glutamicum*. Cg1883 and Cg0520 are secreted lipoproteins presumed to be involved in biogenesis of Cu_A, which due to its localization in CtaC (subunit II) of the cytochrome aa_3 oxidase is likely formed in the periplasm. Regarding the Cu_B formation, different modes for copper-insertion are conceivable: Either copper ions are transferred from CopC towards CtiP in a yet unresolved manner or CtiP directly binds copper in the periplasm. Subsequent CtiP-dependent Cu_B-loading can either occur *via* the periplasm (blue arrow), inner membrane (red arrow) or succeeding cytoplasmic transfer (green arrow).

4.1.1 Essential function of CtiP as a cytochrome *bc*$_1$-*aa*3 supercomplex assembly factor

As an approach to discover proteins involved in copper insertion and therefore biogenesis of the *bc*$_1$-*aa*$_3$ supercomplex, investigation of the copper-deprivation stimulon of *C. glutamicum* was performed, leading to the discovery of CtiP (Morosov *et al.*, 2018). Loss of CtiP resulted in a strong growth defect on BHI agar plates, in BHI complex medium and in standard glucose medium conditions containing 1.25 µM $CuSO_4$, resembling the *aa*$_3$ oxidase-deficient Δ*ctaD* strain (Morosov *et al.*, 2018). In copper-deprivation medium growth of the Δ*ctiP* strain was comparable to that of the wt, whereas in copper excess medium the deletion strain grew better than the wt, indicating a putative copper-importing function of CtiP (Morosov *et al.*, 2018). This observation coincides with transcriptome analyses of the Δ*ctiP* mutant revealing the upregulation of genes of the copper-deprivation stimulon (Morosov *et al.*, 2018). Moreover, loss of CtiP led to the failure of purification of the *bc*$_1$-*aa*$_3$ supercomplex, suggesting an important copper-related function of CtiP in the assembly of the supercomplex. Bioinformatic analyses revealed the occurrence of CtiP in all actinobacterial species with the exception of the mostly anaerobic Actinomycetales and Bifidobacteriales, further implying an important supercomplex-associated function (Morosov *et al.*, 2018). As a result of the described data, a CtiP-mediated copper-insertion into either the Cu_A center or the Cu_B center is conceivable. However, due to the localization of Cu_B in the membrane rather than peeking into the periplasm as in the case of Cu_A, the necessity for an integral membrane protein such as CtiP in the biogenesis of Cu_B is more likely. Nevertheless, the route of copper delivery and insertion into subunit I of the cytochrome *aa*$_3$ oxidase of *C. glutamicum* is still unclear; however, three possibilities can be envisaged: (i) direct copper insertion *via* the periplasm, (ii) transfer of copper through the membrane or (iii) copper-import into the cytoplasm followed by insertion into apo-CtaD (Figure 6). While an initial copper import into the cytoplasm pre-insertion into subunit I cannot be ruled out, several arguments oppose this possibility. Firstly, although CtiP shares sequence similarity with the copper-transporter CopD, this domain within the sequence of CtiP only covers a small portion of the CopD protein of *P. syringae*, thus questioning identical function of CtiP and CopD (Morosov *et al.*, 2018). Besides, in *C. glutamicum* unbound copper in the cytoplasm is sensed by the repressor CsoR with a very high affinity to copper ions which causes de-repression of its target genes (Schelder, 2011; Teramoto *et al.*, 2015). Analysis of transcriptome data of a Δ*ctaD* mutant did not exhibit a decreased repression of CsoR target

genes, indicating no unbound copper in the cytoplasm (Koch-Koerfges, 2011). This suggests that a putative copper-importing function of CtiP either has to be coupled with insertion into subunit I of the *aa*$_3$ oxidase or copper-transport *via* CtiP follows subsequent binding to further copper-chaperones. Latter is highly speculative and there is no evidence for additional chaperones involved.

The copper-insertion into subunit I of the *aa*$_3$ oxidase is presumably achieved by the CtaG domain of CtiP. Initial analyses of CtaG concerning copper center biogenesis were performed in *B. subtilis* where CtaG was reported to be involved in delivering copper to Cu_A (Bengtsson *et al.*, 2004). Loss of CtaG led to a decrease in protein level and enzyme activity of the cytochrome *caa*$_3$ oxidase, possessing Cu_A and Cu_B. Growth analyses of a strain additionally lacking cytochrome *bd* oxidase genes resulted in a comparable growth to the parental *bd* oxidase deficient strain. As growth of this strain was believed to be dependent on the cytochrome *aa*$_3$ quinol oxidase, lacking Cu_A but harboring a heme-Cu_B center, CtaG was postulated to function as a Cu_A biogenesis chaperone (Bengtsson *et al.*, 2004). However, DNA sequence analysis of *B. subtilis* predicted a forth terminal (quinol) oxidase encoded by the *ythAB* genes, which could be responsible for the unaffected growth of the double deletion (Winstedt and von Wachenfeldt, 2000), questioning the conclusion that CtaG affects Cu_A assembly.

Although the characterization of CtiP in *C. glutamicum* points towards an involvement in Cu_B formation rather than in formation of Cu_A, latter cannot be excluded completely. As copper insertion requires direct interaction of apo-protein and insertion-chaperone, protein-protein studies have to be performed to demonstrate interaction of CtiP to either CtaD (subunit I) for Cu_B formation or to CtaC (subunit II) for biogenesis of Cu_A.

4.1.2 Role of CopC in the assembly of the cytochrome *bc*$_1$-*aa*$_3$ supercomplex

The analysis of the copper-deprivation stimulon led to the discovery of the copper-resistance protein CopC, encoded by cg1884 (Morosov *et al.*, 2018). Analysis of the Δ*copC* strain resulted in no observable growth defect in glucose minimal medium with 1.25 µM $CuSO_4$ or under copper-starvation conditions. However, a similar growth defect to Δ*ctiP* strain was exhibited in BHI liquid medium and on agar plates which indicates an important function of CopC solely under these conditions (Morosov *et al.*, 2018). The increased copper-tolerance of the Δ*copC* strain compared to the wt additionally suggests the involvement of CopC in

copper import. Moreover, the inhibited co-purification of cytochrome bc_1-aa_3 supercomplex subunits after loss of CopC suggests a copper-insertion function either into Cu_A or Cu_B of the cytochrome aa_3 oxidase (Morosov *et al.*, 2018). Structural evidence and bioinformatic analyses of CopC family members have been shown to harbor predominantly Cu(II) binding sites (Lawton *et al.*, 2016), which are also conserved in *C. glutamicum* (Morosov *et al.*, 2018).

In *P. syringae* CopC was first described as a copper-importer due to phenotypic characterization revealing a hypersensitivity towards copper upon overexpression of *copD* together with *copC* (Cha and Cooksey, 1993). Furthermore, the copper content increased by 40% in these hypersensitive cells expressing the *copCD* genes compared to cells harboring the empty vector. Overexpression of either *copC* or *copD* alone did not lead to observable differences in copper tolerance, therefore suggesting an interaction between CopD and CopC and an involvement in cellular copper uptake (Cha and Cooksey, 1993). An interaction between these proteins is supported by the corresponding genes being located together in one operon, which in *P. syringae* further includes *copA*, encoding a periplasmic multicopper oxidase, and *copB*, encoding an outer membrane protein (Argüello *et al.*, 2013). Gene clustering analyses revealed that *copC* most commonly occurs in a genomic neighborhood related to copper homeostasis and almost exclusively preceding *copD*, not seldomly even as a *copCD* gene fusion (Lawton *et al.*, 2016). In *C. glutamicum* an interaction between CopC and the CopD domain of CtiP is also conceivable. Based on the above-mentioned growth analyses in *C. glutamicum* it could be hypothesized that CtiP sufficiently binds copper directly in CGXII minimal medium but is dependent on CopC-mediated copper-loading in BHI medium (Figure 6). The necessity for different modes of copper-acquisition could be explained by the differences in copper content of the media, which although measured approximately the same copper concentration (CGXII: 1.25 µM Cu, BHI: ~1 µM Cu; unpublished data) likely differ in their bioavailability of copper ions. To test this hypothesis, affinity measurements of CtiP and CopC towards copper have to be performed to assess putative differences which would suggest the need for a more sensitive copper-binding protein under copper-limited conditions. Furthermore, protein-protein interaction studies could clarify a mechanistic cooperation of CtiP and CopC.

4.1.3 Cg1883 and Cg0520 are putative Cu_A biogenesis chaperones

The copper-deprivation stimulon of *C. glutamicum* further includes a gene of significance concerning biogenesis of the supercomplex, namely cg1883, which is also part of the σ^C regulon (Toyoda and Inui, 2016; Morosov *et al.*, 2018). This gene encodes a PCu_AC homologue shown to be involved in Cu_A biogenesis in other bacteria (Figure 6) (Abriata *et al.*, 2008; Thompson *et al.*, 2012). In *C. glutamicum* cg1883 is part of the *copC* operon, further including cg1881, which codes for a secreted Dyp-type heme peroxidase. Deletion of cg1883 exhibited no growth defect under copper-sufficiency, copper-limitation or copper-deprivation and is therefore not crucial for the formation of the supercomplex, or more specifically the aa_3 oxidase (Morosov *et al.*, 2018). PCu_AC proteins only occur in bacteria and bind Cu(I) in a 1:1 stoichiometry which is then transferred to subunit II of the heme-Cu oxidase to form the Cu_A center (Banci *et al.*, 2005; Abriata *et al.*, 2008; Thompson *et al.*, 2012). A common copper-binding motif for PCu_AC is (H/M)X_{10}MX_{21}HXM, although in actinobacterial homologues this sequence varies with the motif being HX_6MX_{22}HXM (Banci *et al.*, 2005; Morosov *et al.*, 2018).

Formation of the Cu_A center presumably underlies a different mechanism of copper-insertion than Cu_B formation, as Cu_A in subunit II is located towards the periplasm and is not embedded in the membrane as Cu_B in subunit I (Gong *et al.*, 2018; Wiseman *et al.*, 2018). Therefore, biogenesis of Cu_A is likely to take place in the periplasm and thus requires periplasmic proteins or membrane proteins with a copper-binding periplasmic region.

The most intensively characterized chaperones involved in Cu_A formation are the Sco proteins. First described in yeast, these membrane-bound chaperones are able to transfer one Cu(I) or Cu(II) ion to subunit II (Schulze and Rodel, 1988; Nyvltova *et al.*, 2017). Additionally, Sco proteins are members of the thioredoxin superfamily and were predicted to have a disulfide reductase activity for reduction of the cysteine residues involved in complexing the copper ions in the Cu_A center. However, this function was also attributed to TlpA of *Bradyrhizobium japonicum*, suggesting an involvement in direct metalation of Cu_A (Abicht *et al.*, 2014). Moreover, this membrane-anchored protein was shown to specifically reduce ScoI (Mohorko *et al.*, 2012). In *C. glutamicum* a homologue for ScoI is missing, but two homologue candidates for TlpA were found, namely Cg0354 and Cg0520. Cg0354 may contain a signal peptide but lacks a predicted transmembrane domain and its involvement in Cu_A reduction appears unlikely but cannot be excluded. Cg0520 is a more likely functional

TlpA homologue as it is a secreted lipoprotein harboring a domain of the AhpC/TSA family shown to be related to alkyl hydroperoxide reductases (AhpC) and thiol-specific antioxidants (TSA) (Chae *et al.*, 1994). Furthermore, its corresponding gene is located in a cluster involved in cytochrome *c* biogenesis (Bott and Niebisch, 2003). To characterize the function of Cg0520, analysis of supercomplex formation in a cg0520 deletion strain has to be performed coupled with further biochemical analyses.

4.1.4 Surf1 is crucial for cytochrome *bc*$_1$-*aa*$_3$ supercomplex assembly

Besides copper, heme is an important prosthetic group of the cytochrome *bc*$_1$-*aa*$_3$ supercomplex and is essential for functionality of the enzyme. Within this thesis, further investigations were performed to find chaperones involved in biogenesis of the supercomplex, which resulted in the discovery of Cg2460, a homologue of the putative heme *a* insertion chaperone Surf1 (Davoudi *et al.*, 2018). Loss of *C. glutamicum* Surf1 led to a strong growth defect both under copper-sufficiency and under excess copper stress. The former was comparable to that of a cytochrome *aa*$_3$ oxidase-deficient strain. Cytochrome measurements of $CtaD_{St}$ purified from the Δ*surf1* strain showed the loss of wild-type cytochrome peaks and exhibited only a small peak at 594 nm suggesting a disturbed heme environment (Davoudi *et al.*, 2018). Similar to CtiP and CopC, loss of Surf1 prevented co-purification of supercomplex subunits, which indicates a crucial function in supercomplex assembly. Interestingly, CtaC was co-purified with $CtaD_{St}$ in the Δ*surf1* background, which is in contrast to the Δ*ctiP* strain, where co-purification of further *aa*$_3$ oxidase subunits was not observed (Davoudi *et al.*, 2018). This proposes the prevention of supercomplex formation rather than of *aa*$_3$ oxidase assembly upon loss of Surf1 in *C. glutamicum*, whereas impairment of copper-insertion also causes failure to form a stable *aa*$_3$ oxidase.

The role of Surf1 has been analyzed in eukaryotic and prokaryotic homologues and it has been described to be involved in cytochrome biogenesis (Poyau *et al.*, 1999; Mick *et al.*, 2007). Functional characterization of *Rhodobacter sphaeroides* Surf1 demonstrated the inability of a corresponding gene deletion strain to form a heme *a*$_3$-Cu_B center without affecting heme *a* or Cu_A. It was therefore postulated that Surf1 is involved in heme *a*$_3$ insertion into the active site of the terminal oxidase (Smith *et al.*, 2005). For *Paracoccus denitrificans*, which possesses two Surf1 variants, the proteins were shown to bind heme with K_D values of 0.3 – 0.6 µM (Bundschuh *et al.*, 2009). These variants

additionally exhibited specificity towards a particular terminal oxidase (Bundschuh *et al.*, 2008; Bundschuh *et al.*, 2009). In *P. denitrificans*, analysis of the architecture of Surf1 revealed a periplasmic loop harboring two heme-binding motifs (WQ and Y*XXX*W) shown to differentiate between heme types and are located at either side of the transmembrane helices (Hannappel *et al.*, 2011). These characteristic features of the Surf1 architecture are also conserved in *C. glutamicum* (Davoudi *et al.*, 2018). The specificity of Surf1 towards heme *a* was described to serve as a heme filter discriminating between heme types and directly transferring heme *a* from the heme *a* synthase CtaA to the active site of the terminal oxidase (Bundschuh *et al.*, 2008; Hannappel *et al.*, 2011; Hannappel *et al.*, 2012). In agreement with previous data, direct interaction of subunit I of the cytochrome *c* oxidase and Surf1 was detected in *Saccharomycces cerevisiae* and *P. denitrificans* (Khalimonchuk *et al.*, 2010; Hannappel *et al.*, 2012). Albeit the size of the heme *a* molecule which could be assumed to be structure-defining and therefore promoting oxidase stability, studies in *R. sphaeroides* deficient in heme *a* synthesis demonstrated accumulation of the apo-form of the oxidase (Hiser *et al.*, 2000). Nevertheless, it is possible that Surf1 interaction with subunit I of cytochrome oxidase could not only lead to the insertion of heme a_3 but also to the stabilization of the subunit until a complex with subunit II is formed (Hannappel *et al.*, 2012). Whether Surf1 is involved only in heme a_3 insertion or also in heme *a* insertion is still unresolved.

In humans, yeast and bacteria Surf1 deficiency results in a drastically decreased cytochrome *c* oxidase activity but, in contrast to *C. glutamicum* (Davoudi *et al.*, 2018), was never shown to eliminate it (Mashkevich *et al.*, 1997; Zhu *et al.*, 1998). It is conceivable that the remaining oxidase activity could be due to CtaA directly inserting synthesized heme *a* into subunit I which would have to occur in a less efficient manner than with Surf1. This is supported by the observation that in *P. denitrificans* overexpression of *ctaA* restored the cytochrome *c* oxidase activity after loss of both Surf1 variants (Hannappel *et al.*, 2012). In *C. glutamicum* a similar approach by overexpressing native *ctaA* failed to restore aa_3 oxidase activity, deduced by the unaltered growth defect of a Δ*surf1* strain harboring the *ctaA* expression plasmid or the empty vector (Figure S6.4.1).

While only heme-associated properties were described for Surf1 homologues, an effect of Surf1 on the copper homeostasis could be observed in *C. glutamicum*. The Δ*surf1* strain not only exhibited a strong growth defect under copper-excess conditions but transcriptome

analyses also revealed the induction of the copper-starvation stimulon after loss of Surf1 (Davoudi *et al.*, 2018). Although also human Surf1 was described to potentially be involved in copper homeostasis (Stiburek *et al.*, 2009), a direct involvement of Surf1 in copper regulation is unlikely and presumably is a result of secondary effects. However, Surf1 potentially interacts with other copper-dependent chaperones involved in cytochrome *c* oxidase maturation. Co-purification experiments in yeast showed that Surf1 transiently interacts with the Cu_B biogenesis chaperone Cox11 (Khalimonchuk *et al.*, 2010). As CtiP harbors a CtaG domain postulated to be involved in Cu_B formation an interaction with Surf1 could be possible. In an attempt to find Surf1 interaction partners, plasmid-based expression of a *surf1* variant encoding a Strep-tagged Surf1 protein in the *C. glutamicum* Δ*surf1* strain background and subsequent StrepTactin affinity purification among others resulted in the identification of bc_1-aa_3 supercomplex subunits CtaC, CtaD, CtaE, QcrA and QcrB (Table S6.4). However, in this approach the complete elution fraction was used for LC-MS analysis, leading to the identification of more than 200 proteins, making the interpretation of the data difficult. To further investigate a potential interaction of Surf1 with CtiP and/or supercomplex subunits, a genomically encoded Surf1 variant has to be constructed and analyzed in more detail. Several attempts to construct a strain genomically encoding a C-terminally twin-Strep tagged Surf1 variant were unsuccessful.

4.2 Regulation of terminal oxidases

As heme is an important prosthetic group in various proteins including respiratory complexes, another aim of this work was the investigation of a global response towards a heme stimulus. For this purpose, the major focus was a kinetic target gene profiling of the heme-sensing TCS HrrSA.

4.2.1 HrrSA-dependent heme distribution to terminal oxidases

Conclusions about regulatory mechanisms are typically based on single time point studies, which allow only a glimpse on the dynamic nature of gene regulation and adaptation. In this work, time-resolved ChAP-Seq analyses using a plasmid-encoded HrrA variant coupled with time-resolved RNA-Seq analyses of an *hrrA* mutant compared to the wt aided in the

broadening of the HrrSA regulon (Keppel *et al.*, 2019). Crucial conditions for this study were the absence of iron, as the regulator DtxR represses *hrrA* expression upon binding of iron, as well as the presence of heme to ensure HrrA activation (Wennerhold and Bott, 2006; Frunzke *et al.*, 2011). Under these conditions it was found that upon stimulus HrrSA regulates more than 250 genes involved in heme biosynthesis, oxidative stress, cell envelope remodeling and the respiratory chain (Keppel *et al.*, 2019). HrrSA is highly conserved in Actinobacteria and the ability to sense heme is not only crucial for iron acquisition but is also vital for pathogenic organisms (Bibb *et al.*, 2007; Stauff and Skaar, 2009; Stauff and Skaar, 2009; Frunzke *et al.*, 2011). The closely related *C. diphtheriae* HrrSA not only shares high sequence identity with *C. glutamicum* HrrSA but was also shown to activate similar targets (Bibb *et al.*, 2007; Frunzke *et al.*, 2011). The current knowledge about heme homeostasis and heme-dependent regulation includes genes involved in heme degradation, biosynthesis and export (Bibb *et al.*, 2007; Bibb and Schmitt, 2010; Frunzke *et al.*, 2011; Heyer *et al.*, 2012; Burgos and Schmitt, 2016). Interestingly, heme import is still poorly understood but was attributed to an HrrA-regulated ABC-transporter, encoded by the *hmuTUV* operon (Drazek *et al.*, 2000; Schmitt and Drazek, 2001; Frunzke *et al.*, 2011). However, reporter analyses in a Δ*hmuTUV* strain cultivated under iron-limitation and supplemented with 2.5 µM heme did not result in an altered HrrA signal output, suggesting either the existence of a yet uncharacterized importer or a passive transport through the membrane due to its lipophilic characteristics (Hentschel, 2015).

Besides regulation of heme homeostasis, an intriguing finding was the extended involvement of HrrSA in the activation of respiratory chain genes (Keppel *et al.*, 2019). Coinciding with previous data, HrrA-mediated activation of cytochrome bc_1-aa_3 supercomplex genes comprises *ctaD* and the *ctaE-qcrCAB* operon (Frunzke *et al.*, 2011) and was now shown to further include the *ctaCF* operon (Figure 7) (Keppel *et al.*, 2019). Moreover, HrrA additionally activates the *cyd* genes of the cytochrome *bd* branch (Keppel *et al.*, 2019). This activation is retarded towards the mid-exponential growth phase with decreasing heme concentrations and coupled with depression of *sigC,* encoding the activator of the *cyd* operon σ^C (Toyoda and Inui, 2016; Keppel *et al*., 2019). As σ^C was described to simultaneously be a repressor of the *ctaE-qcrCAB* operon (Toyoda and Inui, 2016) HrrA not only functions as a direct activator for respiratory chain genes under iron limitation and simultaneous presence of heme, but is responsible for altering between respiratory chain

complexes depending on heme availability (Figure 7) (Keppel *et al.*, 2019). In contrast to heme-sufficiency, under heme-limitation conditions the less heme-demanding cytochrome *bd* branch is favored (Figure 7). Therefore, this work seems to have unraveled a complex mechanism of HrrSA-mediated heme distribution prioritising the more efficient bc_1-aa_3 branch emphasizing the pivotal function of the TCS on the respiratory chain when iron is limiting (Keppel *et al.*, 2019).

Selectivity between respiratory branches has been extensively researched and can have various causes. On the one hand, limited copper-availability can be a reason to switch to a copper-independent respiratory branch (Morosov *et al.*, 2018), but also oxygen-limitation demands a shift from aerobic to anaerobic growth. Besides the TCS ArcAB, shown to sense the redox state of the quinone pool and regulate terminal oxidases in response to oxygen levels (Gunsalus and Park, 1994; Georgellis *et al.*, 2001), the key regulator mediating these shifts was shown to be FNR first described in *E. coli* (Spiro and Guest, 1991; Spiro, 1994). This global transcriptional regulator contains a $[2Fe\text{-}2S]^{2+}$ cluster and was described to function as an intracellular redox sensor targeting a vast number of genes in an oxygen-dependent manner (Spiro, 1994; Unden *et al.*, 1995; Kiley and Beinert, 1998). However, transcript profiling in *Herbaspirillum seropedicae* revealed that FNR in presence of oxygen controls the composition of the aerobic respiratory chain to optimize energy transduction *via* terminal oxidases (Batista *et al.*, 2013).

A heme-dependent regulation of respiratory complexes was previously described for the translational activator Mss51 of *S. cerevisiae* (Perez-Martinez *et al.*, 2003; Soto *et al.*, 2012). Besides the essential function of specifically promoting COX1 mRNA translation and further aiding in the biogenesis of the cytochrome *c* oxidase, Mss51 was shown to harbor two CPX motifs and exhibited *in-vitro* heme-binding which was required for correct Mss51 functionality (Soto *et al.*, 2012). It was therefore postulated that biogenesis of the cytochrome *c* oxidase is severely dependent on heme-sensing by Mss51.

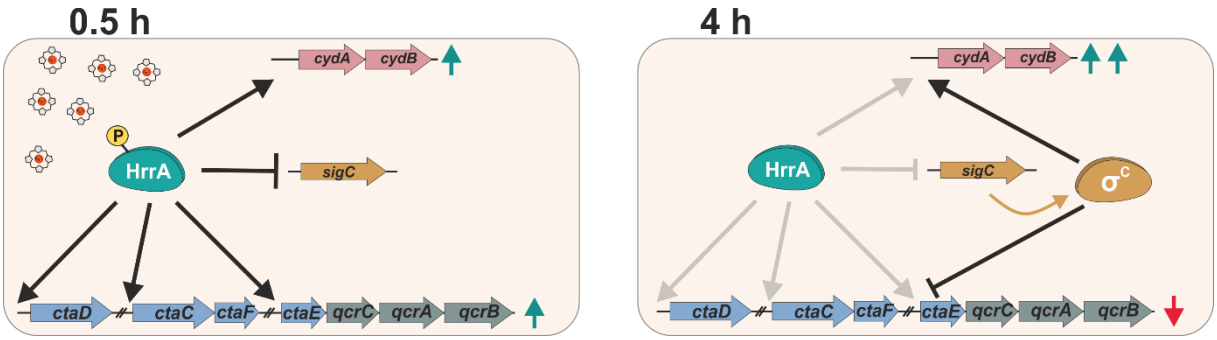

Figure 7: Working model of HrrSA-mediated respiratory chain gene regulation in response to heme under iron-limiting growth conditions. During the early growth phase (0.5 h after addition of 4 µM hemin) with an abundance of heme HrrA activates all genes encoding subunits of the cytochrome bc_1-aa_3 branch (*ctaD*, *ctaCF*, *ctaE-qcrCAB*) and the cytochrome *bd* branch (*cydAB*) while repressing *sigC* expression. Decreasing heme concentrations (4 h after hemin addition) lead to derepression of *sigC* resulting in a further upregulation of the *cyd* genes and simultaneous repression of the *ctaE-qcrCAB* operon (modified from (Keppel *et al.*, 2019)).

Although the findings in this work shed light on the complex regulation of respiratory chain branches *via* HrrSA in *C. glutamicum* and presumably many other *Actinobacteria*, there is still a lot of investigation needed to completely understand the different layers of control. As our approach only focused on heme-dependent regulation through HrrSA, interference by the orthologous TCS ChrSA was not analyzed. Due to the overlap of HrrSA and ChrSA target genes (Heyer *et al.*, 2012), analysis of the complete ChrSA regulon could broaden the understanding of heme homeostasis. Further, this work had to be performed under iron-limitation, thereby neglecting regulatory influences of DtxR, which under iron-sufficiency represses *hrrA* (Wennerhold and Bott, 2006). Moreover, to enable assertions about physiological target binding without overproduction of plasmid-based *hrrA*, ChAP-Seq analyses have to be performed with a strain harboring genomically encoded tagged HrrA.

4.2.2 How is the activity of the ECF σ factor σ^C controlled?

As mentioned above, σ^C is an important regulator of respiratory chain genes and as it is well conserved in all species of Corynebacteria (Pátek and Nesvera, 2011), understanding of the regulatory processes controlled by σ^C should be of high value for the genus. Regulation of σ^C is still unknown, however the discovery of genes regulated by σ^C allows deduction of potential mechanisms (Toyoda and Inui, 2016). Of the 16 upregulated genes (threshold ≥3) within the copper-deprivation stimulon found in this work (Morosov *et al.*, 2018), 12 genes are part of the σ^C regulon described in *C. glutamicum* R (Toyoda and Inui, 2016). The only gene missing from the regulon is cgR_0144, seemingly a paralogue of cgR_1719, which is a

homologue of cg1884 (*copC*). Coinciding with previous data (Toyoda and Inui, 2016), the *bd* oxidase genes as well as *ctaA*, encoding heme *o* monooxygenease (heme *a* synthase), and *ctaB*, encoding protoheme IX farnesyltransferase (heme *o* synthase), were found to be upregulated under copper-deprivation in *C. glutamicum* (Morosov *et al.*, 2018). Interestingly, the copper-deprivation stimulon comprises a number of upregulated genes which are not part of the σ^C regulon and therefore have to be regulated in a different manner. These genes encode cation-transporting ATPases, an amino acid exporter, siderophore transporters, as well as *ctiP* (Morosov *et al.*, 2018). However, an overlap of different ECF σ factor regulons is not uncommon and was already described for σ^D and σ^H in *C. glutamicum* (Dostálová *et al.*, 2019). A similar mechanism between σ^C and another σ factor is therefore not unlikely.

It was suggested, that the σ^C reponse is induced by oxidative stress, due to an inefficient aa_3 oxidase under low oxygen conditions and the presumable formation of superoxide anions (Toyoda and Inui, 2016). This hypothesis coincides with previous studies, showing catalase activity of the *bd* oxidase of *E. coli* as well as H_2O_2 sensitivity of *bd* oxidase-deficient strains of *E. coli* and *M. smegmatis* (Wall *et al.*, 1992; Lindqvist *et al.*, 2000; Borisov *et al.*, 2013; Lu *et al.*, 2015). Furthermore, the genomic location of *C. glutamicum sigC* is directly divergent to *katA* encoding a catalase, suggesting a potential link (Kalinowski *et al.*, 2003). Interestingly, in contrast to an aa_3 oxidase-deficient strain, in which the σ^C response can be observed, analysis of σ^C targets in a bc_1 complex-deficient strain did not show upregulated mRNA levels (Toyoda and Inui, 2016).

Conversely to the hypothesis of an oxidative stress-dependent stimulus, examination of transcriptome studies stored in our in-house *C. glutamicum* microarray database suggests an induction of the σ^C stimulon occurring at any time the bc_1-aa_3 supercomplex is affected. As seen in Table 1, upregulation of σ^C targets can be observed if the supercomplex is disturbed directly (e.g. copper-deprivation) or indirectly (e.g. anaerobic conditions) (Michel, 2014; Morosov *et al.*, 2018) (Table 1). Intriguingly, the lacking upregulation of *ctaA* and *ctaB* under anaerobic conditions suggests competition with another regulator (Table 1). It is important to point out that also a *C. glutamicum* strain expressing the supercomplex genes *ctaE-qcrCAB*, *ctaCF*, and *ctaD* under control of the *tac* promoter rather than under their native promoters (*C. glutamicum* SC^{plus}) (Platzen, 2012) leads to the σ^C response (Table 1). The most common regulation of ECF σ factors is the inhibition through a cognate anti-σ factor. Therefore, the σ^C response in *C. glutamicum* SC^{plus} could hint towards an inhibitory

mechanism of σ^C by supercomplex-associated proteins (Cg2211, Cg2444, Cg2949) potentially acting as putative anti-σ factors. In the absence of a σ^C inhibitor the σ^C targets, including the *cyd* genes, would be induced (Toyoda and Inui, 2016). Overexpression of the *cydABDC* genes was shown to lead to a growth defect in *C. glutamicum* (Kabus et al., 2007). Deletions of the genes cg2211, cg2444, and cg2949 encoding the supercomplex-associated proteins in *C. glutamicum* did not result in an observable growth defect (Niebisch and Bott, 2003), although σ^C-mediated *cyd* activation is not expected to be as high as plasmid-based *cyd*-overexpression. However, a plasmid-based *cyd* promoter fusion to a *venus* reporter gene to measure *cyd* promoter activity revealed a comparable fluorescence output in the deletion strains as in the wt, thus a σ^C-specific anti-σ function of these proteins is unlikely (Figure S6.5.1). As positive control the Δ*ctaF* strain was used.

This promoter fusion construct was further tested in single gene deletion strains of the copper-deprivation stimulon, which resulted in wild-type fluorescence output in all deletions with the exception of the Δcg2750 strain where the specific fluorescence was 30% higher than in the wt (Figure S6.5.2). The cg2750 gene codes for an integral membrane protein with a molecular mass of 13 kDa, which harbors a DUF3187 domain and three predicted transmembrane helices with a putative cytoplasmic N-terminus and a periplasmic C-terminus. Loss of Cg2750 resulted in wild-type growth in CGXII liquid medium but in a growth defect on CGXII and BHI agar plates (Figure S6.5.3), in BHI liquid medium and under copper-excess (Figure S6.5.4). Plasmid-based expression of cg2750 in the Δcg2750 strain successfully complemented the growth defect (Figure S6.5.5). Further investigation of the Δcg2750 strain using reporter fusions of other known σ^C target promotors (*copC*, cg2556) resulted in the same observation of an increased promotor activity compared to the wt, suggesting an induction of the σ^C regulon (Figure S6.5.6). Purification of plasmid-encoded twin-Strep tagged Cg2750 among others revealed the co-purification of QcrB of the bc_1 complex as well as supercomplex-associated proteins (Cg2211, Cg2444), indicating a direct interaction with the supercomplex (Table S6.5). It could therefore be hypothesized that Cg2750 binds σ^C and simultaneously interacts with the bc_1 complex functioning as a sensor for correct supercomplex assembly. Under conditions where supercomplex assembly is impaired Cg2750 might be degraded, thereby releasing σ^C to activate target genes. Therefore, interaction of Cg2750 with σ^C has to be further investigated. Moreover, to ensure

an induction of the σ^C response in the Δcg2750 strain, microarray or RNA-seq analysis have to be performed.

A deletion of *sigC* was previously described for *C. glutamicum* R, but resulted in inconclusive growth effects, presumably due to spontaneous mutations (Toyoda and Inui, 2016). Characterization of the ATCC 13032 *sigC* deletion strain exhibited wild-type growth in standard CGXII glucose medium but showed no growth under copper-deprivation, indicating that σ^C is the only activator of the *cyd* operon under this condition (Figure S6.5.7). Furthermore, to initiate the investigation of σ^C interaction partners, a strain harboring a genomically C-terminally twin-strep-tagged *sigC* was constructed to perform co-purification experiments. Besides this direct approach the constructed strain could also be used for σ^C localization. Harvesting of cells under copper-starvation conditions as well as under copper-sufficiency and subsequent Western Blot analysis of cell fractionations could give insights into a potential membrane-association of σ^C, which would suggest a membrane-bound anti-σ factor responsible for σ^C regulation.

Table 1: Transcriptome levels of upregulated σ^C target genes induced under different conditions. Values depicted originate from the in-house *C. glutamicum* microarray database. The median of three individual experiments (p value ≤ 0.05) is shown or otherwise labeled with the number of available experiments in the database. If not stated otherwise, strains were cultivated under aerobic conditions in standard CGXII glucose medium (1.25 µM $CuSO_4$). Not identified transcripts are listed as n.a.

Locus tag	Gene	Function	wt, Cu-deprivation/ wt	Δ*ctiP*/ wt	Δ*surf1*/ wt	SC^{plus}/ wt[a]	Δ*ctaD*/ wt[b]	wt, anaerob, 120 min/ wt[c]
cg1298	*cydC*	ABC-type transport system, ATPase component	27.79	8.79	2.80	3.34	n.a.	1.53[2]
cg1299	*cydD*	ABC-type transport system, ATPase component	10.54	16.09	5.76	6.00	n.a.	3.04[2]
cg1300	*cydB*	Cytochrome *d* terminal oxidase polypeptide subunit	14.55	12.55	6.26	6.29	2.08	2.09[2]
cg1301	*cydA*	Cytochrome *d* ubiquinol oxidase subunit I	14.99	14.03	6.62	6.44	2.36	2.16[2]
cg1769	*ctaA*	Heme *a* synthase (heme *o* monooxygenase)	2.75	5.90	1.71	1.52	n.a.	0.78
cg1773	*ctaB*	Heme *o* synthase (protoheme IX farnesyltransferase)	8.49	5.83	2.23	5.30	3.15	0.63
cg1881		Putative iron-dependent peroxidase	12.84	15.37	3.95	10.26	n.a.	3.97[2]
cg1883		Hypothetical protein	12.01	16.49	3.74	9.02	2.63	3.26[2]
cg1884	*copC*	Putative secreted copper resistance protein	12.94	16.99	4.12	9.07	2.99	2.85[2]
cg2556		Uncharacterized iron-regulated membrane protein	10.04	6.49	2.39	8.40	3.53	1.94[2]
cg2750		Putative membrane protein	6.88	6.28	2.07	3.43	3.19	2.35[2]

a, performed by Laura Platzen; *b*, performed by Abigail Koch-Körfges; *c*, performed by Andrea Michel

The cytochrome bc_1-aa_3 supercomplex of *C. glutamicum* is a model for homologous complexes in *Actinobacteria*. In this work, the complex biogenesis of this supercomplex was investigated which requires multiple chaperones involved in copper and heme *a* insertion. Moreover, this work revealed an intricate regulation of respiratory branches upon environmental cues which is essential for optimal cellular growth.

5 Literature

Abicht, H.K., Schärer, M.A., Quade, N., Ledermann, R., Mohorko, E., Capitani, G., Hennecke, H. and Glockshuber, R., (2014). How periplasmic thioredoxin TlpA reduces bacterial copper chaperone ScoI and cytochrome oxidase subunit II (CoxB) prior to metallation. *J. Biol. Chem.*, **289**: 32431-32444

Abriata, L.A., Banci, L., Bertini, I., Ciofi-Baffoni, S., Gkazonis, P., Spyroulias, G.A., Vila, A.J. and Wang, S., (2008). Mechanism of Cu_A assembly. *Nat. Chem. Biol.*, **4**: 599

Andrews, S.C., Robinson, A.K. and Rodríguez-Quiñones, F., (2003). Bacterial iron homeostasis. *FEMS Microbiol. Rev.*, **27**: 215-237

Andries, K., Verhasselt, P., Guillemont, J., Göhlmann, H.W.H., Neefs, J.-M., Winkler, H., Van Gestel, J., Timmerman, P., Zhu, M., Lee, E., Williams, P., de Chaffoy, D., Huitric, E., Hoffner, S., Cambau, E., Truffot-Pernot, C., Lounis, N. and Jarlier, V., (2005). A diarylquinoline drug active on the ATP synthase of *Mycobacterium tuberculosis*. *Science*, **307**: 223

Argüello, J.M., Raimunda, D. and Padilla-Benavides, T., (2013). Mechanisms of copper homeostasis in bacteria. *Front. Cell Infect. Microbiol.*, **3**: 73

Bald, D., Villellas, C., Lu, P. and Koul, A., (2017). Targeting energy metabolism in *Mycobacterium tuberculosis* a new paradigm in antimycobacterial drug discovery. *mBio*, **8**: e00272-00217

Balemans, W., Vranckx, L., Lounis, N., Pop, O., Guillemont, J., Vergauwen, K., Mol, S., Gilissen, R., Motte, M., Lançois, D., De Bolle, M., Bonroy, K., Lill, H., Andries, K., Bald, D. and Koul, A., (2012). Novel antibiotics targeting respiratory ATP synthesis in Gram-positive pathogenic bacteria. *Antimicrob. Agents Chemother.*, **56**: 4131

Banci, L., Bertini, I., Ciofi-Baffoni, S., Katsari, E., Katsaros, N., Kubicek, K. and Mangani, S., (2005). A copper(I) protein possibly involved in the assembly of Cu_A center of bacterial cytochrome *c* oxidase. *Proc. Natl. Acad. Sci. U.S.A.*, **102**: 3994

Baron, S. (ed.) (1996). *Medical Microbiology*. 4th Edn., University of Texas Medical Branch at Galveston, Texas, USA

Batista, M.B., Sfeir, M.Z.T., Faoro, H., Wassem, R., Steffens, M.B.R., Pedrosa, F.O., Souza, E.M., Dixon, R. and Monteiro, R.A., (2013). The *Herbaspirillum seropedicae* SmR1 Fnr orthologs controls the cytochrome composition of the electron transport chain. *Sci. Rep.*, **3**: 2544

Becker, J., Zelder, O., Hafner, S., Schroder, H. and Wittmann, C., (2011). From zero to hero - design-based systems metabolic engineering of *Corynebacterium glutamicum* for L-lysine production. *Metab. Eng.*, **13**: 159-168

Bellmann, A., Vrljic, M., Patek, M., Sahm, H., Kramer, R. and Eggeling, L., (2001). Expression control and specificity of the basic amino acid exporter LysE of *Corynebacterium glutamicum*. *Microbiology*, **147**: 1765-1774

Bengtsson, J., von Wachenfeldt, C., Winstedt, L., Nygaard, P. and Hederstedt, L., (2004). CtaG is required for formation of active cytochrome *c* oxidase in *Bacillus subtilis*. *Microbiology*, **150**: 415-425

Berube, B.J. and Parish, T., (2017). Combinations of respiratory chain inhibitors have enhanced bactericidal activity against *Mycobacterium tuberculosis*. *Antimicrob. Agents Chemother.*, **62**: e01677-01617

Bibb, L.A., Kunkle, C.A. and Schmitt, M.P., (2007). The ChrA-ChrS and HrrA-HrrS signal transduction systems are required for activation of the *hmuO* promoter and repression of the *hemA* promoter in *Corynebacterium diphtheriae*. *Infect. Immun.*, **75**: 2421-2431

Bibb, L.A. and Schmitt, M.P., (2010). The ABC transporter HrtAB confers resistance to hemin toxicity and is regulated in a hemin-dependent manner by the ChrAS two-component system in *Corynebacterium diphtheriae*. *J. Bacteriol.*, **192**: 4606-4617

Borisov, V.B., Forte, E., Davletshin, A., Mastronicola, D., Sarti, P. and Giuffrè, A., (2013). Cytochrome *bd* oxidase from *Escherichia coli* displays high catalase activity: An additional defense against oxidative stress. *FEBS Lett.*, **587**: 2214-2218

Borisov, V.B., Gennis, R.B., Hemp, J. and Verkhovsky, M.I., (2011). The cytochrome *bd* respiratory oxygen reductases. *Biochim. Biophys. Acta, Bioenerg.*, **1807**: 1398-1413

Börsch, M. and Duncan, Thomas M., (2013). Spotlighting motors and controls of single F_1F_0-ATP synthase. *Biochem. Soc. Trans.*, **41**: 1219

Bott, M. and Brocker, M., (2012). Two-component signal transduction in *Corynebacterium glutamicum* and other corynebacteria: on the way towards stimuli and targets. *Appl. Microbiol. Biotechnol.*, **94**: 1131-1150

Bott, M. and Niebisch, A., (2003). The respiratory chain of *Corynebacterium glutamicum*. *J. Biotechnol.*, **104**: 129-153

Boyer, P.D., (1997). The ATP synthase—a splendid molecular machine. *Annu. Rev. Biochem.*, **66**: 717-749

Brinkrolf, K., Brune, I. and Tauch, A., (2007). The transcriptional regulatory network of the amino acid producer *Corynebacterium glutamicum*. *J. Bacteriol.*, **129**: 191-211

Brinkrolf, K., Schröder, J., Pühler, A. and Tauch, A., (2010). The transcriptional regulatory repertoire of *Corynebacterium glutamicum*: Reconstruction of the network controlling pathways involved in lysine and glutamate production. *J. Bacteriol.*, **149**: 173-182

Brocker, M., Mack, C. and Bott, M., (2011). Target genes, consensus binding site, and role of phosphorylation for the response regulator MtrA of *Corynebacterium glutamicum*. *J. Bacteriol.*, **193**: 1237

Brocker, M., Schaffer, S., Mack, C. and Bott, M., (2009). Citrate utilization by *Corynebacterium glutamicum* is controlled by the CitAB two-component system through positive regulation of the citrate transport genes *citH* and *tctCBA*. *J. Bacteriol.*, **191**: 3869

Brune, I., Werner, H., Hüser, A.T., Kalinowski, J., Pühler, A. and Tauch, A.J.B.G., (2006). The DtxR protein acting as dual transcriptional regulator directs a global regulatory network involved in iron metabolism of *Corynebacterium glutamicum*. *BMC Genom.*, **7**: 21

Bundschuh, F.A., Hannappel, A., Anderka, O. and Ludwig, B., (2009). Surf1, associated with Leigh syndrome in humans, is a heme-binding protein in bacterial oxidase biogenesis. *J. Biol. Chem.*, **284**: 25735-25741

Bundschuh, F.A., Hoffmeier, K. and Ludwig, B., (2008). Two variants of the assembly factor Surf1 target specific terminal oxidases in *Paracoccus denitrificans*. *Biochim. Biophys. Acta, Bioenerg.*, **1777**: 1336-1343

Burgos, J.M. and Schmitt, M.P., (2016). The ChrSA and HrrSA two-component systems are required for transcriptional regulation of the *hemA* promoter in *Corynebacterium diphtheriae*. *J. Bacteriol.*, **198**: 2419-2430

Burkovski, A. (ed.) (2008). *Corynebacteria: Genomics and Molecular Biology*. Caister Academic Press, Norfolk, UK

Burkovski, A. (ed.) (2015). *Corynebacterium glutamicum: From Systems Biology to Biotechnological Applications*. Caister Academic Press, Norfolk, UK

Busche, T., Silar, R., Pičmanová, M., Pátek, M. and Kalinowski, J., (2012). Transcriptional regulation of the operon encoding stress-responsive ECF sigma factor SigH and its anti-sigma factor RshA, and control of its regulatory network in *Corynebacterium glutamicum*. *BMC Genom.*, **13**

Capaldi, R.A., (1990). Structure and function of cytochrome *c* oxidase. *Annu. Rev. Biochem.*, **59**: 569-596

Capra, E.J. and Laub, M.T., (2012). Evolution of two-component signal transduction systems. *Annu. Rev. Microbiol.*, **66**: 325-347

Cha, J.-S. and Cooksey, D.A., (1993). Copper hypersensitivity and uptake in *Pseudomonas syringae* containing cloned components of the copper resistance operon. *Appl. Environ. Microbiol.*, **59**: 1671-1674

Chae, H.Z., Robison, K., Poole, L.B., Church, G., Storz, G. and Rhee, S.G., (1994). Cloning and sequencing of thiol-specific antioxidant from mammalian brain: alkyl hydroperoxide reductase and thiol-specific antioxidant define a large family of antioxidant enzymes. *Proc. Natl. Acad. Sci. U.S.A.*, **91**: 7017-7021

Collins, M.D., Pirouz, T., Goodfellow, M. and Minnikin, D.E., (1977). Distribution of menaquinones in Actinomycetes and Corynebacteria. *J. Gen. Microbiol.*, **100**: 221-230

Davoudi, C.F., Baumgart, M. and Bott, M., (2018). Identification of Surf1 as an assembly factor of the cytochrome bc_1-aa_3 supercomplex of *Actinobacteria*. *Submitted*

de Lima Procópio, R.E., da Silva, I.R., Martins, M.K., de Azevedo, J.L. and de Araújo, J.M., (2012). Antibiotics produced by *Streptomyces*. *Braz. J. Infect. Dis.*, **16**: 466-471

Dostálová, H., Busche, T., Holátko, J., Rucká, L., Štěpánek, V., Barvík, I., Nešvera, J., Kalinowski, J. and Pátek, M., (2019). Overlap of promoter recognition specificity of stress response sigma factors SigD and SigH in *Corynebacterium glutamicum* ATCC 13032. *Front. Microbiol.*, **9**

Drazek, E.S., Hammack, C.A., Sr and Schmitt, M.P., (2000). *Corynebacterium diphtheriae* genes required for acquisition of iron from haemin and haemoglobin are homologous to ABC haemin transporters. *Mol. Microbiol.*, **36**: 68-84

Eggeling, L. and Bott, M., (2005). *Handbook of Corynebacterium glutamicum*. CRC Press, FL, USA

Ehira, S., Teramoto, H., Inui, M. and Yukawa, H., (2009). Regulation of *Corynebacterium glutamicum* heat shock response by the extracytoplasmic-function sigma factor SigH and transcriptional regulators HspR and HrcA. *J. Bacteriol.*, **191**: 2964

Finn, R.D., Bateman, A., Clements, J., Coggill, P., Eberhardt, R.Y., Eddy, S.R., Heger, A., Hetherington, K., Holm, L., Mistry, J., Sonnhammer, E.L., Tate, J. and Punta, M., (2014). Pfam: the protein families database. *Nucleic Acids Res.*, **42**: D222-230

Frunzke, J., Gatgens, C., Brocker, M. and Bott, M., (2011). Control of heme homeostasis in *Corynebacterium glutamicum* by the two-component system HrrSA. *J. Bacteriol.*, **193**: 1212-1221

Galperin, M.Y., Nikolskaya, A.N. and Koonin, E.V., (2001). Novel domains of the prokaryotic two-component signal transduction systems. *FEMS Microbiol. Lett.*, **203**: 11-21

Gao, B. and Gupta, R.S., (2012). Phylogenetic framework and molecular signatures for the main clades of the phylum *Actinobacteria*. *Microbiol. Mol. Biol. Rev.*, **76**: 66-112

Georgellis, D., Kwon, O. and Lin, E.C.C., (2001). Quinones as the redox signal for the Arc two-component system of bacteria. *Science*, **292**: 2314

Gong, H., Li, J., Xu, A., Tang, Y., Ji, W., Gao, R., Wang, S., Yu, L., Tian, C., Li, J., Yen, H.Y., Man Lam, S., Shui, G., Yang, X., Sun, Y., Li, X., Jia, M., Yang, C., Jiang, B., Lou, Z., Robinson, C.V., Wong, L.L., Guddat, L.W., Sun, F., Wang, Q. and Rao, Z., (2018). An electron transfer path connects subunits of a mycobacterial respiratory supercomplex. *Science*, **362**

Graf, S., Fedotovskaya, O., Kao, W.C., Hunte, C., Adelroth, P., Bott, M., von Ballmoos, C. and Brzezinski, P., (2016). Rapid electron transfer within the III-IV supercomplex in *Corynebacterium glutamicum*. *Sci. Rep.*, **6**: 34098

Groban, E.S., Clarke, E.J., Salis, H.M., Miller, S.M. and Voigt, C.A., (2009). Kinetic buffering of cross talk between bacterial two-component sensors. *J. Mol. Biol.*, **390**: 380-393

Grüber, G., Manimekalai, M.S.S., Mayer, F. and Müller, V., (2014). ATP synthases from archaea: The beauty of a molecular motor. *Biochim. Biophys. Acta*, **1837**: 940-952

Gunsalus, R.P. and Park, S.J., (1994). Aerobic-anaerobic gene regulation in *Escherichia coli*: control by the ArcAB and Fnr regulons. *Res. Microbiol.*, **145**: 437-450

Hannappel, A., Bundschuh, F.A. and Ludwig, B., (2011). Characterization of heme-binding properties of *Paracoccus denitrificans* Surf1 proteins. *FEBS J.*, **278**: 1769-1778

Hannappel, A., Bundschuh, F.A. and Ludwig, B., (2012). Role of Surf1 in heme recruitment for bacterial COX biogenesis. *Biochim. Biophys. Acta, Bioenerg.*, **1817**: 928-937

Helmann, J.D., (1999). Anti-sigma factors. *Curr. Opin. Microbiol.*, **2**: 135-141

Helmann, J.D., (2002). The extracytoplasmic function (ECF) sigma factors. In: *Adv. Microb. Physiol.* Academic Press, pp: 47-110

Hentschel, E., (2015). Interaction of the two-component systems HrrSA and ChrSA in *Corynebacterium glutamicum*. ISBN 978-3-95806-053-1

Hentschel, E., Mack, C., Gatgens, C., Bott, M., Brocker, M. and Frunzke, J., (2014). Phosphatase activity of the histidine kinases ensures pathway specificity of the ChrSA and HrrSA two-component systems in *Corynebacterium glutamicum*. *Mol. Microbiol.*, **92**: 1326-1342

Heyer, A., Gatgens, C., Hentschel, E., Kalinowski, J., Bott, M. and Frunzke, J., (2012). The two-component system ChrSA is crucial for haem tolerance and interferes with HrrSA in haem-dependent gene regulation in *Corynebacterium glutamicum*. *Microbiology*, **158**: 3020-3031

Hiser, L., Di Valentin, M., Hamer, A.G. and Hosler, J.P., (2000). Cox11p is required for stable formation of the Cu_B and magnesium centers of cytochrome *c* oxidase. *J. Biol. Chem.*, **275**: 619-623

Hoch, J.A. and Silhavy, T.J., (1995). *Two-component signal transduction*. ASM Press, Washington D. C.

Huynh, T.N. and Stewart, V., (2011). Negative control in two-component signal transduction by transmitter phosphatase activity. *Mol. Microbiol.*, **82**: 275-286

Ikeda, M., Baba, M., Tsukumoto, N., Komatsu, T., Mitsuhashi, S. and Takeno, S., (2009). Elucidation of genes relevant to the microaerobic growth of *Corynebacterium glutamicum*. *Biosci. Biotechnol. Biochem.*, **73**

Inouye, M. and Dutta, R., (2003). *Histidine kinases in signal transduction*. Academic press, San Diego, California

Jensen, R.B., Wang, S.C. and Shapiro, L., (2002). Dynamic localization of proteins and DNA during a bacterial cell cycle. *Nat. Rev. Mol. Cell Biol.*, **3**: 167

Kabashima, Y., Kishikawa, J.-i., Kurokawa, T. and Sakamoto, J., (2009). Correlation between proton translocation and growth: Genetic analysis of the respiratory chain of *Corynebacterium glutamicum*. *J. Biochem.*, **146**: 845-855

Kabus, A., Niebisch, A. and Bott, M., (2007). Role of cytochrome *bd* oxidase from *Corynebacterium glutamicum* in growth and lysine production. *Appl. Environ. Microbiol.*, **73**: 861

Kalinowski, J., Bathe, B., Bartels, D., Bischoff, N., Bott, M. and Burkovski, A., (2003). The complete *Corynebacterium glutamicum* ATCC 13032 genome sequence and its impact on the production of L-aspartate-derived amino acids and vitamins. *J. Biotechnol.*, **104**

Kao, W.C., Kleinschroth, T., Nitschke, W., Baymann, F., Neehaul, Y., Hellwig, P., Richers, S., Vonck, J., Bott, M. and Hunte, C., (2016). The obligate respiratory supercomplex from *Actinobacteria*. *Biochim. Biophys. Acta, Bioenerg.*, **1857**: 1705-1714

Keppel, M., Davoudi, C.F., Filipchyk, A., Viets, U., Pfeifer, E., Baumgart, M., Bott, M. and Frunzke, J., (2019). HrrSA orchestrates a systemic response to heme and determines prioritisation of terminal cytochrome oxidase expression. *To be submitted*

Khalimonchuk, O., Bestwick, M., Meunier, B., Watts, T.C. and Winge, D.R., (2010). Formation of the redox cofactor centers during Cox1 maturation in yeast cytochrome oxidase. *Mol. Cell. Biol.*, **30**: 1004

Kiley, P.J. and Beinert, H., (1998). Oxygen sensing by the global regulator, FNR: the role of the iron-sulfur cluster. *FEMS Microbiol. Rev.*, **22**: 341-352

Kim, T.-H., Kim, H.-J., Park, J.-S., Kim, Y., Kim, P. and Lee, H.-S., (2005). Functional analysis of *sigH* expression in *Corynebacterium glutamicum*. *Biochem. Biophys. Res. Commun.*, **331**: 1542-1547

Kinoshita, S., Udaka, S. and Shimono, M., (1957). Studies on the amino acid fermentation. *J. Gen. Appl. Microbiol.*, **1**: 331-343

Koch-Koerfges, A., (2011). Novel insights into the energy metabolism of *Corynebacterium glutamicum* by comprehensive analysis of mutants defective in respiration or oxidative phosphorylation. ISBN 978-3-89336-826-6

Koch-Koerfges, A., Pfelzer, N., Platzen, L., Oldiges, M. and Bott, M., (2013). Conversion of *Corynebacterium glutamicum* from an aerobic respiring to an aerobic fermenting bacterium by inactivation of the respiratory chain. *Biochim. Biophys. Acta, Bioenerg.*, **1827**: 699-708

Lawton, T.J., Kenney, G.E., Hurley, J.D. and Rosenzweig, A.C., (2016). The CopC family: Structural and bioinformatic insights into a diverse group of periplasmic copper binding proteins. *Biochemistry*, **55**: 2278-2290

Lewin, G.R., Carlos, C., Chevrette, M.G., Horn, H.A., McDonald, B.R., Stankey, R.J., Fox, B.G. and Currie, C.R., (2016). Evolution and ecology of *Actinobacteria* and their bioenergy applications. *Annu. Rev. Microbiol.*, **70**: 235-254

Lindqvist, A., Membrillo-Hernández, J., Poole, R.K. and Cook, G.M.J.A.v.L., (2000). Roles of respiratory oxidases in protecting *Escherichia coli* K12 from oxidative stress. *Antonie Van Leeuwenhoek*, **78**: 23-31

Lu, P., Heineke, M.H., Koul, A., Andries, K., Cook, G.M., Lill, H., van Spanning, R. and Bald, D., (2015). The cytochrome *bd*-type quinol oxidase is important for survival of *Mycobacterium smegmatis* under peroxide and antibiotic-induced stress. *Sci. Rep.*, **5**: 10333

Macomber, L. and Imlay, J.A., (2009). The iron-sulfur clusters of dehydratases are primary intracellular targets of copper toxicity. *Proc. Natl. Acad. Sci. U.S.A.*, **106**: 8344

Magnani, D. and Solioz, M., (2007). How Bacteria Handle Copper. In: *Molecular Microbiology of Heavy Metals*, D. H. Nies and S. Silver, (eds.). Springer Berlin Heidelberg, Berlin, Heidelberg pp: 259-285

Mascher, T., (2013). Signaling diversity and evolution of extracytoplasmic function (ECF) σ factors. *Curr. Opin. Microbiol.*, **16**: 148-155

Mascher, T., Helmann, J.D. and Unden, G., (2006). Stimulus perception in bacterial signal-transducing histidine kinases. *Microbiol. Mol. Biol. Rev.*, **70**: 910

Mashkevich, G., Repetto, B., Glerum, D.M., Jin, C. and Tzagoloff, A., (1997). *SHY1*, the yeast homolog of the mammalian *SURF-1* gene, encodes a mitochondrial protein required for respiration. *J. Biol. Chem.*, **272**: 14356-14364

Matsoso, L.G., Kana, B.D., Crellin, P.K., Lea-Smith, D.J., Pelosi, A., Powell, D., Dawes, S.S., Rubin, H., Coppel, R.L. and Mizrahi, V., (2005). Function of the cytochrome bc_1-aa_3 branch of the respiratory network in mycobacteria and network adaptation occurring in response to its disruption. *J. Bacteriol.*, **187**: 6300-6308

Merchant, S.S. and Helmann, J.D., (2012). Elemental economy: microbial strategies for optimizing growth in the face of nutrient limitation. *Adv. Microb. Physiol.*, **60**: 91-210

Michel, A., (2014). Anaerobes Wachstum von *Corynebacterium glutamicum* durch gemischte Säurefermentation. ISBN 978-3-95806-010-4

Michel, A., Koch-Koerfges, A., Krumbach, K., Brocker, M. and Bott, M., (2015). Anaerobic growth of *Corynebacterium glutamicum* via mixed-acid fermentation. *Appl. Environ. Microbiol.*, **81**: 7496

Mick, D.U., Wagner, K., van der Laan, M., Frazier, A.E., Perschil, I., Pawlas, M., Meyer, H.E., Warscheid, B. and Rehling, P., (2007). Shy1 couples Cox1 translational regulation to cytochrome *c* oxidase assembly. *EMBO J.*, **26**: 4347-4358

Milse, J., Petri, K., Rückert, C. and Kalinowski, J., (2014). Transcriptional response of *Corynebacterium glutamicum* ATCC 13032 to hydrogen peroxide stress and characterization of the OxyR regulon. *J. Bacteriol.*, **190**: 40-54

Mitchell, P., (1961). Coupling of phosphorylation to electron and hydrogen transfer by a chemi-osmotic type of mechanism. *Nature*, **191**: 144

Mohorko, E., Abicht, H.K., Bühler, D., Glockshuber, R., Hennecke, H. and Fischer, H.-M., (2012). Thioredoxin-like protein TlpA from *Bradyrhizobium japonicum* is a reductant for the copper metallochaperone ScoI. *FEBS Lett.*, **586**: 4094-4099

Morosov, X., Davoudi, C.F., Baumgart, M., Brocker, M. and Bott, M., (2018). The copper-deprivation stimulon of *Corynebacterium glutamicum* comprises proteins for biogenesis of the actinobacterial cytochrome bc_1-aa_3 supercomplex. *J. Biol. Chem.*

Nakunst, D., Larisch, C., Hüser, A.T., Tauch, A., Pühler, A. and Kalinowski, J., (2007). The extracytoplasmic function-type sigma factor SigM of *Corynebacterium glutamicum* ATCC 13032 is involved in transcription of disulfide stress-related genes. *J. Bacteriol.*, **189**: 4696-4707

Niebisch, A. and Bott, M., (2001). Molecular analysis of the cytochrome bc_1-aa_3 branch of the *Corynebacterium glutamicum* respiratory chain containing an unusual diheme cytochrome c_1. *Arch. Microbiol.*, **175**: 282-294

Niebisch, A. and Bott, M., (2003). Purification of a cytochrome bc_1-aa_3 supercomplex with quinol oxidase activity from *Corynebacterium glutamicum*. *J. Biol. Chem.*, **278**: 4339-4346

Nishimura, T., Vertès, A.A., Shinoda, Y., Inui, M. and Yukawa, H., (2007). Anaerobic growth of *Corynebacterium glutamicum* using nitrate as a terminal electron acceptor. *Appl. Microbiol. Biotechnol.*, **75**: 889-897

Nyvltova, E., Barrientos, A. and Hosler, J., (2017). Assembly of heme a_3-Cu_B and Cu_A in cytochrome *c* oxidase. In: *Encyclopedia of Inorganic and Bioinorganic Chemistry*. John Wiley & Sons, Ltd., Chichester, UK, pp: 1–27

Österberg, S., del Peso-Santos, T. and Shingler, V., (2011). Regulation of alternative sigma factor use. *Annu. Rev. Microbiol.*, **65**: 37-55

Paget, M.S., (2015). Bacterial sigma factors and anti-sigma factors: Structure, function and distribution. *Biomolecules*, **5**: 1245-1265

Park, S.-D., Youn, J.-W., Kim, Y.-J., Lee, S.-M., Kim, Y. and Lee, H.-S., (2008). *Corynebacterium glutamicum* σ^E is involved in responses to cell surface stresses and its activity is controlled by the anti-σ factor CseE. *Microbiology*, **154**: 915-923

Pátek, M. and Nesvera, J., (2011). Sigma factors and promoters in *Corynebacterium glutamicum*. *J. Biotechnol.*, **154**: 101-113

Perez-Martinez, X., Broadley, S.A. and Fox, T.D., (2003). Mss51p promotes mitochondrial Cox1p synthesis and interacts with newly synthesized Cox1p. *EMBO J.*, **22**: 5951-5961

Pierre, J.L. and Fontecave, M., (1999). Iron and activated oxygen species in biology: The basic chemistry. *BioMetals*, **12**: 195-199

Platzen, L., (2012). Modifikationen der Atmungskette in *Corynebacterium glutamicum* und Rolle des Flavohämoproteins Hmp. ISBN 978-3-89336-931-7

Podgornaia, A.I. and Laub, M.T., (2013). Determinants of specificity in two-component signal transduction. *Curr. Opin. Microbiol.*, **16**: 156-162

Poole, R.K., (2000). Aerobic respiration: oxidases and globins. In: *Encyclopaedia of Microbiology*. Academic Press, San Diego, USA

Poyau, A., Buchet, K. and Godinot, C., (1999). Sequence conservation from human to prokaryotes of Surf1, a protein involved in cytochrome *c* oxidase assembly, deficient in Leigh syndrome. *FEBS Lett.*, **462**: 416-420

Punta, M., Coggill, P.C., Eberhardt, R.Y., Mistry, J., Tate, J., Boursnell, C., Pang, N., Forslund, K., Ceric, G., Clements, J., Heger, A., Holm, L., Sonnhammer, E.L., Eddy, S.R., Bateman, A. and Finn, R.D., (2012). The Pfam protein families database. *Nucleic Acids Res.*, **40**: D290-301

Richardson, D.J., (2000). Bacterial respiration: A flexible process for a changing environment. *Microbiology*, **146**: 551-571

Ridge, P.G., Zhang, Y. and Gladyshev, V.N., (2008). Comparative genomic analyses of copper transporters and cuproproteomes reveal evolutionary dynamics of copper utilization and its link to oxygen. *PLoS One*, **3**: e1378

Schaaf, S. and Bott, M., (2007). Target genes and DNA-binding sites of the response regulator PhoR from *Corynebacterium glutamicum*. *J. Bacteriol.*, **189**: 5002

Schelder, S., (2011). CopRS and CsoR: two regulatory systems involved in copper homeostasis of *Corynebacterium glutamicum*. ISBN 978-3-89336-761-0

Schelder, S., Zaade, D., Litsanov, B., Bott, M. and Brocker, M., (2011). The two-component signal transduction system CopRS of *Corynebacterium glutamicum* is required for adaptation to copper-excess stress. *PLoS One*, **6**: e22143

Schmitt, M.P. and Drazek, E.S., (2001). Construction and consequences of directed mutations affecting the hemin receptor in pathogenic *Corynebacterium* species. *J. Bacteriol.*, **183**: 1476

Schulze, M. and Rodel, G., (1988). SCO1, a yeast nuclear gene essential for accumulation of mitochondrial cytochrome *c* oxidase subunit II. *Mol. Gen. Genet.*, **211**: 492-498

Simon, J., van Spanning, R.J.M. and Richardson, D.J., (2008). The organisation of proton motive and non-proton motive redox loops in prokaryotic respiratory systems. *Biochim. Biophys. Acta, Bioenerg.*, **1777**: 1480-1490

Siryaporn, A. and Goulian, M., (2008). Cross-talk suppression between the CpxA–CpxR and EnvZ–OmpR two-component systems in *E. coli*. *Mol. Microbiol.*, **70**: 494-506

Skerker, J.M., Perchuk, B.S., Siryaporn, A., Lubin, E.A., Ashenberg, O., Goulian, M. and Laub, M.T., (2008). Rewiring the specificity of two-component signal transduction systems. *Cell*, **133**: 1043-1054

Smith, D., Gray, J., Mitchell, L., Antholine, W.E. and Hosler, J.P., (2005). Assembly of cytochrome-*c* oxidase in the absence of assembly protein Surf1p leads to loss of the active site heme. *J. Biol. Chem.*, **280**: 17652-17656

Soto, Iliana C., Fontanesi, F., Myers, Richard S., Hamel, P. and Barrientos, A., (2012). A heme-sensing mechanism in the translational regulation of mitochondrial cytochrome *c* oxidase biogenesis. *Cell Metab.*, **16**: 801-813

Spiro, S., (1994). The FNR family of transcriptional regulators. *Antonie Van Leeuwenhoek*, **66**: 23-36

Spiro, S. and Guest, J.R., (1991). Adaptive responses to oxygen limitation in *Escherichia coli*. *Trends Biochem. Sci.*, **16**: 310-314

Stackebrandt, E., Rainey, F.A. and Ward-Rainey, N.L., (1997). Proposal for a new hierarchic classification system, *Actinobacteria* classis nov. *Int. J. Syst. Bacteriol.*, **47**: 479-491

Staron, A., Sofia, H.J., Dietrich, S., Ulrich, L.E., Liesegang, H. and Mascher, T., (2009). The third pillar of bacterial signal transduction: Classification of the extracytoplasmic function (ECF) sigma factor protein family. *Mol. Microbiol.*, **74**: 557-581

Stauff, D.L. and Skaar, E.P., (2009). *Bacillus anthracis* HssRS signalling to HrtAB regulates haem resistance during infection. *Mol. Microbiol.*, **72**: 763-778

Stauff, D.L. and Skaar, E.P., (2009). The heme sensor system of *Staphylococcus aureus*. *Contrib. Microbiol.*, **16**: 120-135

Stiburek, L., Vesela, K., Hansikova, H., Hulkova, H. and Zeman, J., (2009). Loss of function of Sco1 and its interaction with cytochrome *c* oxidase. *Am. J. Physiol. Cell Physiol.*, **296**: C1218-1226

Stock, A.M., Robinson, V.L. and Goudreau, P.N., (2000). Two-component signal transduction. *Annu. Rev. Biochem.*, **69**: 183-215

Takeno, S., Ohnishi, J., Komatsu, T., Masaki, T., Sen, K. and Ikeda, M., (2007). Anaerobic growth and potential for amino acid production by nitrate respiration in *Corynebacterium glutamicum*. *Appl. Microbiol. Biotechnol.*, **75**: 1173-1182

Taniguchi, H., Busche, T., Patschkowski, T., Niehaus, K., Pátek, M., Kalinowski, J. and Wendisch, V.F.J.B.M., (2017). Physiological roles of sigma factor SigD in *Corynebacterium glutamicum*. *BMC Microbiol.*, **17**: 158

Teramoto, H., Inui, M. and Yukawa, H., (2012). *Corynebacterium glutamicum* CsoR acts as a transcriptional repressor of two copper/zinc-inducible P_{1B}-type ATPase operons. *Biosci. Biotechnol. Biochem.*, **76**: 1952-1958

Teramoto, H., Inui, M. and Yukawa, H., (2013). OxyR acts as a transcriptional repressor of hydrogen peroxide-inducible antioxidant genes in *Corynebacterium glutamicum* R. *FEBS J.*, **280**: 3298-3312

Teramoto, H., Yukawa, H. and Inui, M., (2015). Copper homeostasis-related genes in three separate transcriptional units regulated by CsoR in *Corynebacterium glutamicum*. *Appl. Microbiol. Biotechnol.*, **99**: 3505–3517

Thompson, A.K., Gray, J., Liu, A. and Hosler, J.P., (2012). The roles of *Rhodobacter sphaeroides* copper chaperones PCu_AC and Sco (PrrC) in the assembly of the copper centers of the aa_3-type and the cbb_3-type cytochrome *c* oxidases. *Biochim. Biophys. Acta, Bioenerg.*, **1817**: 955-964

Toyoda, K. and Inui, M., (2016). The extracytoplasmic function σ factor σ^C regulates expression of a branched quinol oxidation pathway in *Corynebacterium glutamicum*. *Mol. Microbiol.*, **100**: 486-509

Toyoda, K. and Inui, M., (2018). Extracytoplasmic function sigma factor σ^D confers resistance to environmental stress by enhancing mycolate synthesis and modifying peptidoglycan structures in *Corynebacterium glutamicum*. *Mol. Microbiol.*, **107**: 312-329

Toyoda, K., Teramoto, H., Inui, M. and Yukawa, H., (2011). Genome-wide identification of *in vivo* binding sites of GlxR, a cyclic AMP receptor protein-type regulator in *Corynebacterium glutamicum*. *J. Bacteriol.*, **193**: 4123-4133

Trumpower, B.L., (1990). Cytochrome bc_1 complexes of microorganisms. *Microbiol. Rev.*, **54**: 101-129

Trumpower, B.L. and Gennis, R.B., (1994). Energy transduction by cytochrome complexes in mitochondrial and bacterial respiration: The enzymology of coupling electron transfer reactions to transmembrane proton translocation. *Annu. Rev. Biochem.*, **63**: 675-716

Ulrich, L.E., Koonin, E.V. and Zhulin, I.B., (2005). One-component systems dominate signal transduction in prokaryotes. *Trends Microbiol.*, **13**: 52-56

Unden, G., Becker, S., Bongaerts, J., Holighaus, G., Schirawski, J. and Six, S., (1995). O_2-sensing and O_2-dependent gene regulation in facultatively anaerobic bacteria. *Arch. Microbiol.*, **164**: 81-90

Wall, D., Delaney, J.M., Fayet, O., Lipinska, B., Yamamoto, T. and Georgopoulos, C., (1992). *arc*-dependent thermal regulation and extragenic suppression of the *Escherichia coli* cytochrome *d* operon. *J. Bacteriol.*, **174**: 6554

Wendisch, V., Eberhardt, D., Herbst, M. and Jensen, J., (2014). Biotechnological production of amino acids and nucleotides. In: *Biotechnological production of natural ingredients for food industry*. Bentham Science eBooks, pp: pp. 60-163

Wennerhold, J. and Bott, M., (2006). The DtxR regulon of *Corynebacterium glutamicum*. *J. Bacteriol.*, **188**: 2907

Wennerhold, J., Krug, A. and Bott, M., (2005). The AraC-type regulator RipA represses aconitase and other iron proteins from *Corynebacterium* under iron limitation and is itself repressed by DtxR. *J. Biol. Chem.*, **280**: 40500-40508

Winstedt, L. and von Wachenfeldt, C., (2000). Terminal oxidases of *Bacillus subtilis* strain 168: One quinol oxidase, cytochrome aa_3 or cytochrome *bd*, is required for aerobic growth. *J. Bacteriol.*, **182**: 6557

Wiseman, B., Nitharwal, R.G., Fedotovskaya, O., Schafer, J., Guo, H., Kuang, Q., Benlekbir, S., Sjostrand, D., Adelroth, P., Rubinstein, J.L., Brzezinski, P. and Hogbom, M., (2018). Structure of a functional obligate complex III_2IV_2 respiratory supercomplex from *Mycobacterium smegmatis*. *Nat. Struct. Mol. Biol.*, **25**: 1128-1136

Yap, L.L., Lin, M.T., Ouyang, H., Samoilova, R.I., Dikanov, S.A. and Gennis, R.B., (2010). The quinone-binding sites of the cytochrome bo_3 ubiquinol oxidase from *Escherichia coli*. *Biochim. Biophys. Acta, Bioenerg.*, **1797**: 1924-1932

Yoshida, Y., Furuta, S. and Niki, E., (1993). Effects of metal chelating agents on the oxidation of lipids induced by copper and iron. *Biochim. Biophys. Acta*, **1210**: 81-88

Yukawa, H. and Inui, M. (eds.), (2013). *Corynebacterium glutamicum: Biology and Biotechnology*. Springer, Heidelberg

Zhang, Y. and Gladyshev, V.N., (2010). General trends in trace element utilization revealed by comparative genomic analyses of Co, Cu, Mo, Ni, and Se. *J. Biol. Chem.*, **285**: 3393-3405

Zhu, Z., Yao, J., Johns, T., Fu, K., De Bie, I., Macmillan, C., Cuthbert, A.P., Newbold, R.F., Wang, J., Chevrette, M., Brown, G.K., Brown, R.M. and Shoubridge, E.A., (1998). *SURF1*, encoding a factor involved in the biogenesis of cytochrome *c* oxidase, is mutated in Leigh syndrome. *Nat. Genet.*, **20**: 337-343

6 Appendix

6.1 Supplement "The copper-deprivation stimulon of *Corynebacterium glutamicum* comprises proteins for biogenesis of the actinobacterial cytochrome bc_1-aa_3 supercomplex"

TABLE S1. Oligonucleotides used in this study.

Oligonucleotide	Sequence (5' → 3') and properties[a]
Construction of deletion plasmids and PCR analysis of the resulting *C. glutamicum* deletion mutants	
cg2699-1-for	TATACTGCAGCAATCCATAAGGTAGAGGCTATATG
cg2699-2-rev	**CCCATCCACTAAACTTAAGTA**GAGAAGAAACTCCACCAGAACCC
cg2699-3-for	**TACTTAAGTTTAGTGGATGGG**CTACCAGGAAACCTTCGAGCCC
cg2699-4-rev	TATAGAATTCTGTAGTGGTTCATGTCAATGCCGA
cg2699-out-for	ATGTGCTCGCAGCATGTTTATG
cg2699-out-rev	CTTGTAGGAGCGGGAGCTGG
cg1884-1-for	**CCCATCCACTAAACTTAAGTA**TTTTAGATTCTTCTCTGAAGCCACAT
cg1884-2-rev	TATAAAGCTTGATCCACCACAAACCAGGCTGG
cg1884-3-for	**TACTTAAGTTTAGTGGATGGG**GCAAAGAATCGTAACCAGAAATAAG
cg1884-4-rev	TATAGAATTCCTCGATTGGGTTCGCAAGCCC
cg1884-out-for	AGGTCATTCAGGCGGCTGG
cg1884-out-rev	ATGTCGCTCCTTATATATAGTGG
cg0569-1-for	**CAAGCTTGCATGCCTGCAGGTCGAC**TTCACTTCATTCATCGCCATTG
cg0569-2-rev	**TGTTTAAGTTTAGTGGATGGG**GTACAGGCTTCCCTTGGCAAGG
cg0569-3-for	**CCCATCCACTAAACTTAAACA**CAGGGTAACCTAAATGTCGTG
cg0569-4-rev	**ATTCGAGCTCGGTACCCGGGGATCC**AACTTTGCCATCCGAATCGG
cg0569-out-for	CATGGCCAATGCCTTCGCAC
cg0569-out-rev	GGGATCGGGCTTCTTCTGTTTC
cg1744-1-for	**CAAGCTTGCATGCCTGCAGGTCGAC**GGATATGATTGCGATCCCTGGCGAC
cg1744-2-rev	**TGTTTAAGTTTAGTGGATGGG**GACGACACCTAAAACAGACCTTTC
cg1744-3-for	**CCCATCCACTAAACTTAAACA**CTTTGCGGTCGTTGAAACCG
cg1744-4-rev	**ATTCGAGCTCGGTACCCGGGGATCC**CACCCTTGAAAAGTGAAAACATC
cg1744-out-for	GGTTCGCACAGGAGCAATTTC
cg1744-out-rev	TTGCCTCTAAAACCATCGCC
cg1832-1-for	**CAAGCTTGCATGCCTGCAGGTCGAC**TAACAGTGCACCAGGAAGGG
cg1832-2-rev	**TGTTTAAGTTTAGTGGATGGG**GAGAAAACACTAACACTCAAATGATC
cg1832-3-for	**CCCATCCACTAAACTTAAACA**GGAGCACCCTTCCTCCTG
cg1832-4-rev	**ATTCGAGCTCGGTACCCGGGGATCC**TGGAGATTTGTGACCAGACATC
cg1832-out-for	GAAATAAATCCCCGCCCACAC
cg1832-out-rev	ACGTTCCTTCAACGTTGCAATG
cg1833-1-for	**CAAGCTTGCATGCCTGCAGGTCGAC**GTTGTTCTGGCTGCTTGGATC
cg1833-2-rev	**TGTTTAAGTTTAGTGGATGGG**CCAGGGGAAGGGCTAATTTACG
cg1833-3-for	**CCCATCCACTAAACTTAAACA**CCGTCGATGGCCTAGAAAAAATC
cg1833-4-rev	**ATTCGAGCTCGGTACCCGGGGATCC**GTACGAGTGCTCGTGCGATG
cg1833-out-for	CTTGTTGATGTCCGGCGTAG
cg1833-out-rev	CGTGGAGGACGATGATGGAAC
cg1881-1-for	**CAAGCTTGCATGCCTGCAGGTCGAC**AGTGATTCCACCTCCACGAG
cg1881-2-rev	**TGTTTAAGTTTAGTGGATGGG**GTCGCTCCTTATATATAGTGGCCG
cg1881-3-for	**CCCATCCACTAAACTTAAACA**CCCGCCACGCGGTAGGATG
cg1881-4-rev	**ATTCGAGCTCGGTACCCGGGGATCC**CGGATTACTGCGCGGCCG
cg1881-out-for	GTCGCAGGTGCTGTACTGAG
cg1881-out-rev	GATGCCCAACTTGGTTCCTG
cg1883-1-for	TATACTGCAGAGCAATGCGGATTCCGGAGAGG
cg1883-2-rev	**CCCATCCACTAAACTTAAGTA**TGCGACAAAAAACTTCTTCATGGTG
cg1883-3-for	**TACTTAAGTTTAGTGGATGGG**ACTGAAGGCCACGAGGGCCAC
cg1883-4-rev	TATACCCGGGTCACGTCGAAAAGCGAAGCACC
cg1883-out-for	AGGTCATTCAGGCGGCTGG
cg1883-out-rev	CTGCTGCACCCACCGCGT
cg2556-3-for	**CCCATCCACTAAACTTAAACA**GAACACCAAACCACACCGC

cg2556-4-rev	**ATTCGAGCTCGGTACCCGGGGATCC**CGTGTATTCAAATTCCCAGAAGCAG
cg2556-out-for	TCATCGCCAATGAGCACGAG
cg2556-out-rev	TGTCGGACTCATCGTGTTCG
cg2750-1-for	**CAAGCTTGCATGCCTGCAGGTCGAC**AAGGCAAGTCACATTGTCTTTCTTC
cg2750-2-rev	**TGTTTAAGTTTAGTGGATGGG**GCAACTCTTCCTTCAAAAATAAAATAG
cg2750-3-for	**CCCATCCACTAAACTTAAACA**TTAAATACACAAAAACCTCCCCGTC
cg2750-4-rev	**ATTCGAGCTCGGTACCCGGGGATCC**ATCGCCACGATCGCCGATG
cg2750-out-for	CGCTTATCGTAAATCAGCAGGTAG
cg2750-out-rev	ATACGACGAGCCGATCGAAG
Construction of pEKEx2-citP	
pEKEx2-cg2699-for	TATACTGCAGAAGGAGGGGCATGGATGAGCAGGTCG
pEKEx2-cg2699-rev	TATAGAATTCTTATTCTTTGTCTTTGTCTTTGTCTTTG

[a]) Overlaps for overlap-extension PCR or Gibson assembly are written in bold letters. Restriction sites are underlined.

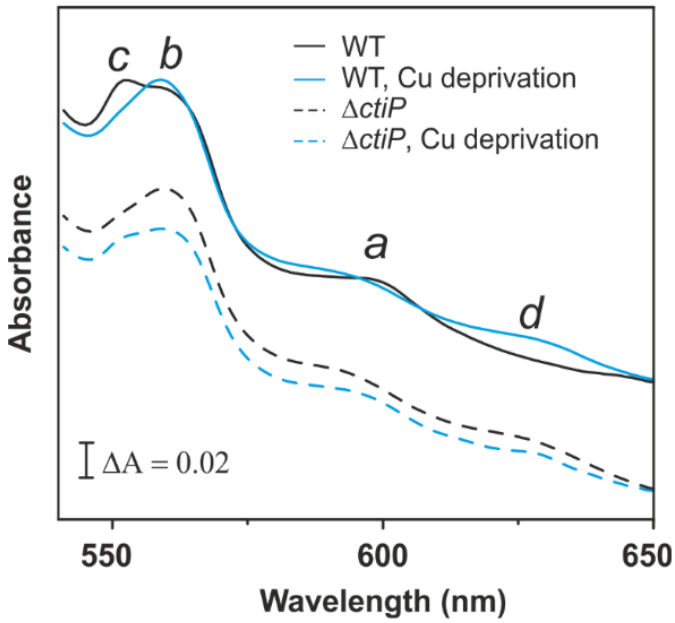

Figure S1. Dithionite-reduced spectra of *C. glutamicum* WT cells and Δcg2699 mutant cells cultivated either in standard CGXII medium or in copper-deprived CGXII medium. Cytochromes *c*, *b*, *a* and *d* are indicated at the wavelengths 552 nm, 562 nm, 600 nm and 630 nm, respectively.

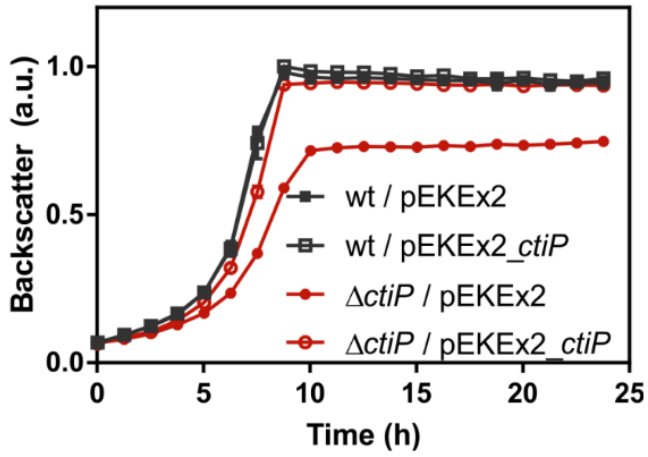

Figure S2. Complementation of the growth defect of the Δ*ctiP* mutant by plasmid-based expression of *ctiP* using plasmid pEKEx2_ctiP carrying *ctiP* under control of the P_{tac} promoter. The strains were cultivated in CGXII medium with 4% (w/v) glucose supplemented with 25 µg ml^{-1} kanamycin in a Biolector microcultivation system. Growth was followed online as backscatter at 620 nm. All backscatter values were normalized by setting the maximal backscatter value of the WT/pEKEx2 culture as 1. Mean values and standard deviations of three biological replicates are shown.

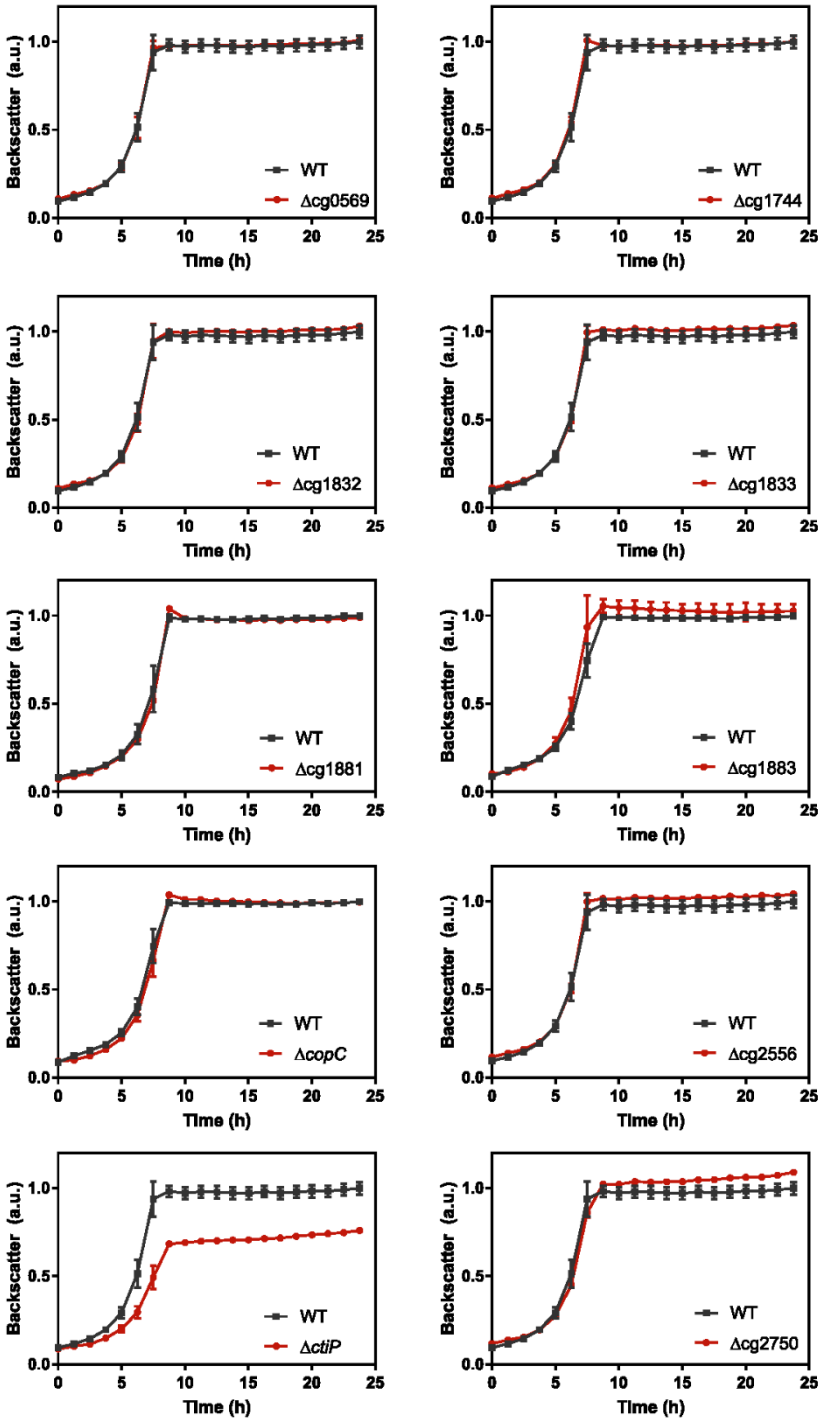

Figure S3. Growth of the wild type (black squares) and the indicated *C. glutamicum* mutants lacking individual genes of the copper deprivation stimulon (red circles) under standard copper conditions (1.25 µM $CuSO_4$). Precultures were first prepared in BHI medium and subsequently in standard CGXII minimal medium with 2% (w/v) glucose. The main cultures inoculated to an initial OD_{600} of 1 were performed in FlowerPlates™ with 800 µl standard CGXII minimal medium with 2% (w/v) glucose using the BioLector® microcultivation system. Growth was followed online as backscatter at 620 nm every hour. All backscatter values were normalized by setting the maximal backscatter value of the wild-type cultures used for comparison as 1. Mean values and standard deviations of three biological replicates are shown. The growth data for the Δ*ctiP* mutant and the WT are identical to those shown in Fig. 3A and are repeated here for comparison with the other mutants.

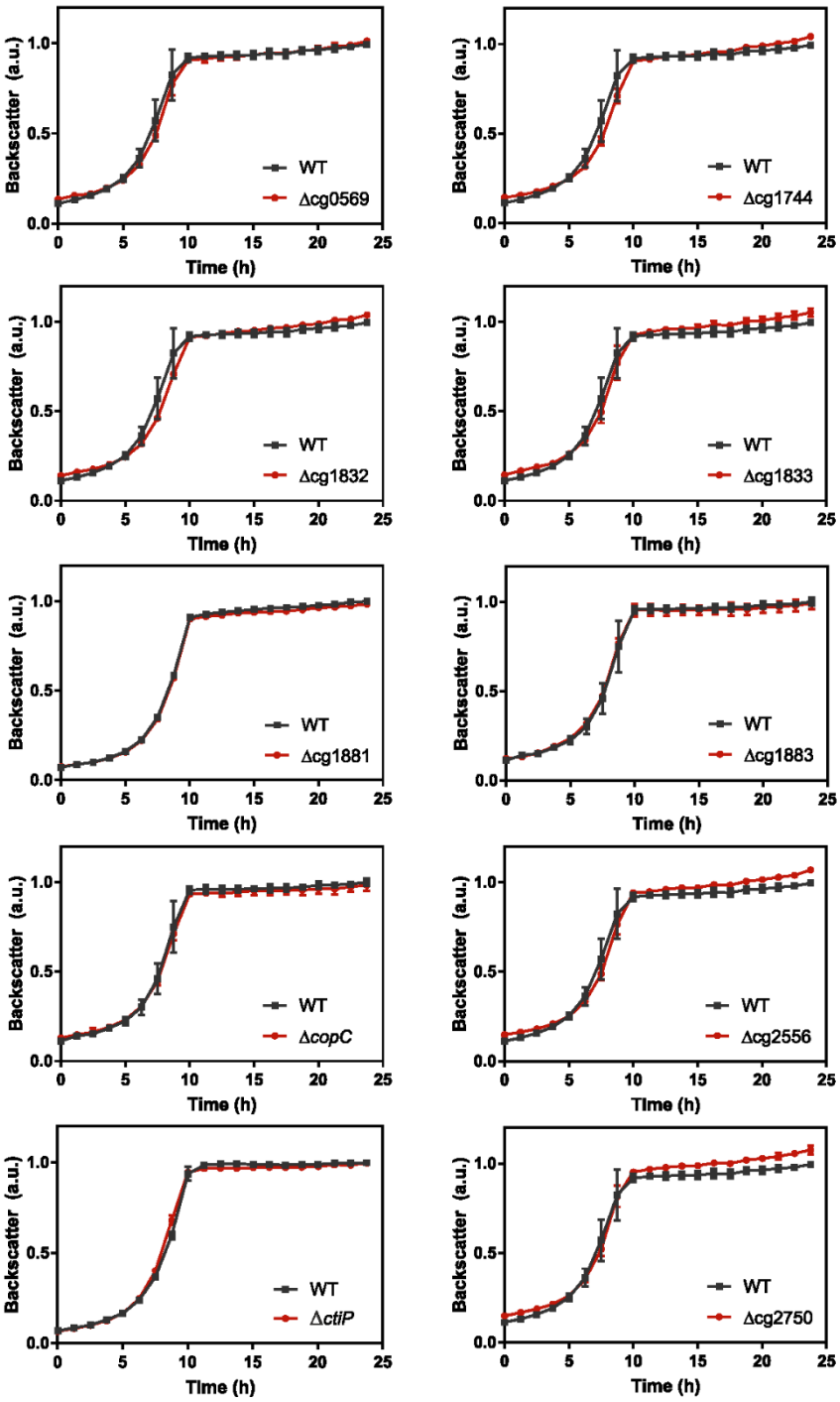

Figure S4. Growth of the wild type (black squares) and the indicated *C. glutamicum* mutants lacking individual genes of the copper deprivation stimulon (red circles) under copper deprivation conditions. Precultures were first prepared in BHI medium and subsequently in CGXII minimal medium with 2% (w/v) glucose to which no $CuSO_4$ had been added. The main cultures inoculated to an OD_{600} of 1 were performed in FlowerPlates™ with 800 µl CGXII minimal medium with 2% (w/v) glucose supplemented with 150 µM BCS and 1 mM ascorbate using the BioLector® microcultivation system. Growth was followed online as backscatter at 620 nm every hour. All backscatter values were normalized by setting the maximal backscatter value of the wild-type cultures used for comparison as 1. Mean values and standard deviations of three biological replicates are shown. The growth data for the Δ*ctiP* mutant and the WT are identical to those shown in Fig. 3B and are repeated here for comparison with the other mutants.

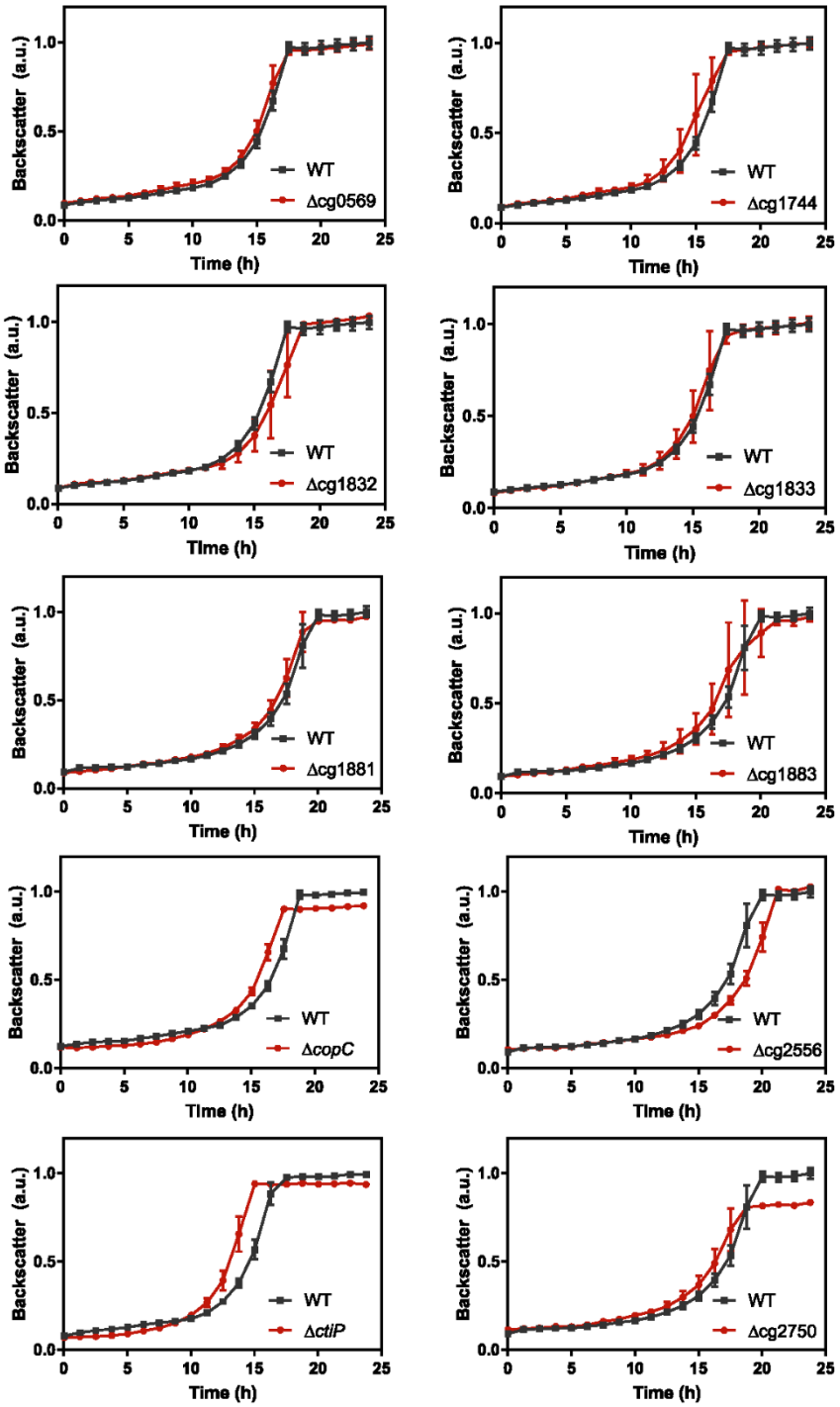

Figure S5. Growth of the wild type (black squares) and the indicated *C. glutamicum* mutants lacking individual genes of the copper deprivation stimulon (red circles) under copper excess stress. Precultures were first prepared in BHI medium and subsequently in standard CGXII minimal medium with 2% (w/v) glucose and 1.25 µM $CuSO_4$. The main cultures inoculated to an OD_{600} of 1 were performed in FlowerPlates™ with 800 µl CGXII minimal medium with 2% (w/v) glucose supplemented with 100 µM $CuSO_4$ using the BioLector® microcultivation system. Growth was followed online as backscatter at 620 nm every hour. All backscatter values were normalized by setting the maximal backscatter value of the wild-type cultures used for comparison as 1. Mean values and standard deviations of three biological replicates are shown. The growth data for the Δ*ctiP* mutant and the WT are identical to those shown in Fig. 3C and are repeated here for comparison with the other mutants.

```
Ps-CopC      1 HPKLLSSTPAEGSTV-QAPEKIELNFS----EKLTT----QFSGAKLIMT 41
               |      | |  || |   || ||| ||       ||
Cg-CopC      1 HDVVVDSNPENGSVVDEFPETIELEFSGIPQDLFTTVALSNADSGEVLTS 50

Ps-CopC     42 EMPGM-STHSPMGVKASVSGGADPKMMVISPTTSLTPGTYKVEWRAVSSD 90
                 |     |    |   |  ||                | |       |||
Cg-CopC     51 GTPQLEGQHLSYEVPSDVQTGA---------------GNYILGFQITSSD 85

Ps-CopC     91 THPITGSVTFKVK 103
                |   ||  | |
Cg-CopC     86 GHATKGSISFEVT 98
```

Figure S6. Sequence alignment of CopC of *P. syringae* and CopC (Cg1884) of *C. glutamicum*. The residues involved in Cu(II)- and Cu(I)-binding the *P. syringae* CopC protein are indicated in red and green, respectively. Identical amino acids are indicated by dashes.

6.2 Supplement "Identification of Surf1 as an assembly factor of the cytochrome bc_1-aa_3 supercomplex of *Actinobacteria*"

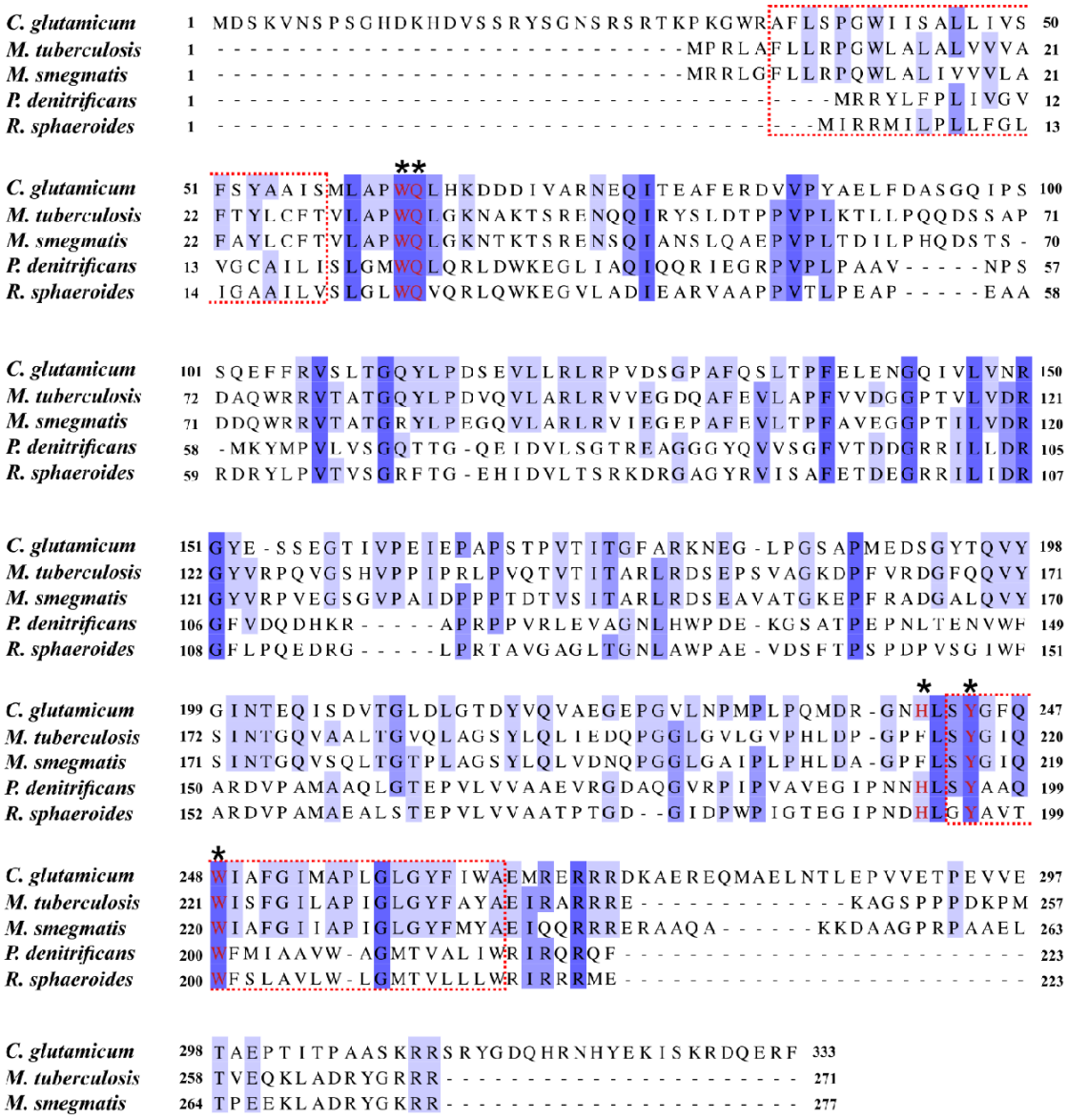

Fig. S1. Amino acid sequence alignment of Surf1 homologues. Depicted are variants of *C. glutamicum* (Cg2460), *M. tuberculosis* (Rv2235), *M. smegmatis* (MSMEG_4311), *P. denitrificans* (Pden_4316) and *R. sphaeroides* (RSP_1830). For the analysis Clustal Omega (https://www.ebi.ac.uk/Tools/msa/clustalo/) was used and visualized using Jalview (http://www.jalview.org/). Purple shade indicates identical amino acids in at least three sequences with a darkening of the color following the degree of conservation among the alignment. Conserved residues shown to be involved in heme *a* binding are indicated in red font and an asterisk. Red dotted boxes specify the two anticipated transmembrane helices.

6.3 Supplement "HrrSA orchestrates a systemic response to heme and determines prioritisation of terminal cytochrome oxidase expression"

Strains, plasmids and oligonucleotides used in this study.

Table S1: Bacterial strains and plasmids used in this study. Oligonucleotides used for the construction of the plasmids are listed in Table S2.

Strain	Relevant characteristics	Reference
Escherichia coli		
DH5α	*fhuA2 lac(del)U169 phoA glnV44 Φ80' lacZ(del)M15 gyrA96 recA1 relA1 endA1 thi-1 hsdR17*; for general cloning purposes	Invitrogen
BL21(DE3)	B F^- *ompT gal dcm lon* $hsdS_B(r_B^-m_B^-)$ λ(DE3 [*lacI lacUV5-T7p07 ind1 sam7 nin5*]) $[malB^+]_{K\text{-}12}(\lambda^S)$; overexpression of proteins.	[1]
Corynebacterium glutamicum		
C. glutamicum ATCC13032	Biotin-auxotrophic wild type strain	[2]
C. glutamicum Δ*hrrA*	Derivative of ATCC13032 with in-frame deletion of the *hrrA* gene	[3]
C. glutamicum Δ*hrrSA* Δ*chrSA*	Derivative of ATCC13032 with in-frame deletions of the *hrrS* (cg3248) and *hrrA* (cg3247) genes and the *chrSA* (cg2201-cg2200) operon.	[4]

Plasmid

Name	Resistance	Source
pJC1	Kanamycin	[5]
pJC1_P_{hrrSA}-*hrrSA-twin-strep*_P_{chrSA}-*chrSA-his*	Kanamycin	This study

Table S2: Oligonucleotides used in this study.

#	Name	Sequence
1	*hrrSA-twin-strep*-fw	TTTTGCGTTTCTACAAACTCTTTTGTTAGAGACCAAGATTCTGG
2	*hrrSA-twin-strep*-rv	CTGTAAAACGACGGCCAGTACTAGTCTATTTTTCGAACTGCGGGTG
3	*chrSA-his*-fw	CAGCGACGCCGCAGGGGGATCCCTACTACACTACATCATGCGCAGTAG
4	*chrSA-his*-rv	AGTAATCCAGAATCTTGGTCTCTAACAAAAGAGTTTGTAGAAACG
5	P_{hmuO} (EMSA) fw	GAGAAATCCTCACGCTCAC
6	P_{hmuO} (EMSA) rv	GGTGGGAGCCCCAAAGTTG
7	P_{ctaE} (EMSA) fw	CCCAAAGTGGTTTCCGCAGG
8	P_{ctaE} (EMSA) rv	ACGCCTTTTATTCGGGTTC
9	P_{pck} (EMSA) fw	CTTTCTATGGAGATGATCG
10	P_{pck} (EMSA) rv	CGATTTAAATGGACCCTAAAC
11	P_{ramB} (EMSA) fw	CCTGCGCAAAGTTGCTCCCTG
12	P_{ramB} (EMSA) rv	CTCACAGGATACCGATCCGAAC
13	P_{cg1080} (EMSA) fw	CGCTCCTCTGTGGGATTTGTC
14	P_{cg1080} (EMSA) rv	GCCTTCACTCCCTCAAAC
15	P_{xerC} (EMSA) fw	CTTAGGCTTGCCTCACACAC
16	P_{xerC} (EMSA) rv	AATGCGGAAATGCCATAAAACC
17	P_{cg3402}(EMSA) fw	CATAGGGGTATAGCCTTGAG
18	P_{cg3402}(EMSA) rv	CAGTGTGCGCAGGTCATGCC
19	P_{ctaC}(EMSA) fw	GGAATACCTAAAGTCTAGGC
20	P_{ctaC}(EMSA) rv	GTAGGAACGTAGGGGGTAAG
21	$P_{sigC/katA}$(EMSA) fw	GGTCACCATAAAGGTGTGTAG
22	$P_{sigC/katA}$(EMSA) rv	GCCACCAAATAATCAGCCC
23	P_{cyd} (EMSA) fw	GTTCCCGCTCACAGCTTAAC
24	P_{cyd} (EMSA) rv	GGTGACTTGTCAACAAGGGG
25	P_{trpS} (EMSA) fw	GACTTGTTTACCCAAGCAATAC
26	P_{trpS} (EMSA) rv	CCGGTGAGGCAACATTTACC
27	P_{htoA} (EMSA) fw	GTCATGATGGCGTCTCGGGC
28	P_{htoA} (EMSA) rv	GTAATCAACGCACAAATG

Table S3: Partial Dataset of genome wide HrrA binding (CHAP-Seq) and time resolved transcriptome analysis of C. glutamicum wild type and ΔhrrA (RNA-Seq). For CHAP-Seq analysis, the strain *C. glutamicum* Δ*hrrSA*Δ*chrSA* harboring the plasmid pJC1_P*hrrSA-hrrSA-twin-strep*_P*chrSA-chrSA-his* was cultivated in CGXII minimal medium supplemented with 2% (w/v) glucose and 4 µM hemin and was harvested at different time points as described in Figure 1. For RNA-Seq, wild type cells and a Δ*hrrA* were cultivated accordingly and harvested 0 h, 0.5 h and 4 h after hemin addition. For RNA-Seq analysis strains contained no plasmids and consequently no antibiotics were added to the medium. Column 1 and 2 show the locus and gene name and column 3 indicates the distance of the peak maximum to the translational start site of the gene in column 1/2. For all known transcriptional start sites, the distance to the TSS is indicated in column 4. In grey (5-10),ChAP-Seq peak intensities are indicated at 0 h, 0.5 h, 2 h, 4 h, 9 h and 24 h after hemin addition. In green (11-13) and red (14-16), the measured mRNA levels of the corresponding genes in the wild type strain (green) and a Δ*hrrA* strain are shown (in transcripts per million, mean of two biological replicates). All further information can be found in the full Table in Keppel *et al.* (2019).

cg number	Gene name	Distance ATG	Distance to TSS	ChAP-SeqT=0	T=0.5	T=2	T=4	T=9	T=24	mRNA wt t=0	mRNA wt t=0.5	mRNA wt t=4	mRNA Δ*hrrA* t=0	mRNA Δ*hrrA* t=0.5	mRNA Δ*hrrA* t=4
cg0019		24	24	1.4	4.7	2.1	1.3	1.0	1.0	21.0	20.8	23.5	28.5	21.6	15.2
cg0046		129	unknown	1.3	3.1	1.0	1.0	1.0	1.0	273.3	179.3	181.8	171.5	177.1	256.8
cg0061	*rodA*	389	unknown	1.7	8.7	2.6	1.0	1.0	1.0	141.2	331.2	212.2	159.7	157.7	148.7
cg0074		203	unknown	2.6	12.1	4.1	2.9	1.0	1.0	7.0	1.5	9.2	4.9	2.2	6.3
cg0076		245	unknown	3.2	18.9	8.2	3.1	1.0	1.5	21.7	5.7	15.2	11.3	3.6	11.8
cg0104	*codA*	72	41	1.0	3.4	2.1	1.0	1.0	1.0	196.4	30.3	35.4	57.2	64.4	21.5
cg0109	*lip1*	199	199	1.0	6.1	1.0	1.6	1.0	1.0	135.2	108.0	66.7	145.0	157.0	41.0
cg0113	*ureA*	585	561	3.2	21.4	5.5	1.9	1.0	1.0	391.8	157.5	111.5	155.0	204.3	89.3
cg0134	*abgB*	76	0	1.0	3.8	1.3	1.0	1.0	1.2	96.7	63.7	207.1	52.6	45.1	108.9
cg0142	*sixA*	253	253	1.0	4.4	1.0	1.7	1.0	1.0	32.9	29.5	42.2	36.2	40.2	32.2
cg0152		30	20	1.0	3.3	1.0	1.0	1.0	1.0	20.1	13.0	16.3	17.9	11.8	15.1
cg0153	*hde*	313	unknown	2.5	4.4	2.3	1.6	1.0	1.9	19.2	16.7	28.6	19.7	19.7	15.0
cg0163		438	unknown	2.4	12.0	4.2	2.2	1.6	1.0	160.3	290.8	172.4	53.3	48.0	84.1
cg0204	*iolG*	246	unknown	3.5	16.8	5.9	3.0	2.2	1.9	20.4	38.2	55.9	24.3	25.2	35.8
cg0219		251	unknown	1.1	3.9	2.0	1.0	1.7	1.0	40.8	40.5	35.4	49.1	66.8	22.9
cg0222		413	unknown	4.1	11.0	5.9	3.0	1.0	1.0	41.6	27.1	35.8	20.8	23.7	20.9
cg0222		30	unknown	1.0	3.8	2.0	1.0	1.0	1.0	41.6	27.1	35.8	20.8	23.7	20.9
cg0247		202	202	1.0	17.2	4.6	1.0	1.0	1.0	38.8	20.2	27.0	35.1	32.9	22.3
cg0296	*dnaZX*	56	56	1.0	5.1	2.2	1.0	1.0	1.0	183.7	140.0	225.0	131.2	137.8	181.2
cg0306	*lysC*	40	4	3.5	12.2	7.7	4.1	4.3	6.3	578.7	576.4	655.1	680.0	919.0	730.8
cg0309	*sigC*	38	unknown	7.8	25.4	12.8	5.0	7.1	4.8	37.5	28.1	79.5	74.8	124.4	118.7
cg0319	*arsC2 (arsX)*	70	unknown	1.0	6.8	2.9	1.0	1.0	1.0	83.0	112.1	32.8	72.4	47.4	24.2
cg0335		447	447	1.0	3.1	1.0	1.6	1.0	1.0	99.0	95.2	143.5	121.9	125.0	113.9
cg0337	*whcA (whiB4)*	125	21	1.0	6.4	4.6	1.6	1.0	1.0	1149.5	986.9	1054.7	709.3	702.9	648.4
cg0359		468	327	1.0	3.1	1.9	1.0	1.0	1.6	573.5	562.7	658.7	483.6	663.5	542.4
cg0382		259	unknown	0.9	7.8	2.5	1.0	1.0	1.0	23.7	44.3	21.9	21.0	27.2	11.7
cg0389		31	unknown	2.4	15.2	4.7	1.7	1.0	1.0	368.0	157.6	247.8	275.8	213.8	157.0
cg0390		387	unknown	3.5	6.6	3.5	2.1	1.0	3.0	92.6	92.5	52.4	55.5	85.7	41.9
cg0411		238	unknown	1.1	4.4	1.0	1.1	1.0	1.0	150.3	72.0	32.7	59.9	80.3	34.1
cg0415	*ptpA2*	696	1023	1.3	8.0	3.2	1.0	1.0	1.0	311.2	176.8	498.8	272.4	229.8	476.3
cg0420		354	272	4.8	25.6	12.2	4.7	1.0	1.0	178.4	88.3	136.7	61.4	78.0	45.7
cg0422	*murA*	701	651	3.0	14.1	6.2	2.4	1.0	2.8	221.0	151.3	206.6	223.7	136.7	196.5
cg0423	*murB*	2	unknown	2.1	18.7	5.4	1.9	1.0	2.1	219.5	148.5	240.5	205.2	122.3	210.4
cg0431		76	unknown	2.0	6.9	2.2	1.0	1.0	1.0	93.6	58.7	64.3	65.7	46.4	52.3
cg0432		49	594	3.8	29.3	6.0	1.9	1.0	1.2	238.1	186.5	242.2	194.1	156.2	214.2
cg0437	*wzy*	303	unknown	3.5	30.3	10.1	3.7	2.1	1.3	149.3	115.5	201.3	83.3	117.4	153.8

cg0438		65	15	2.1	8.5	4.8	1.5	1.0	3.0	399.7	345.9	433.0	364.2	378.1	251.8
cg0444	*ramB*	224	224	9.7	26.7	18.0	7.1	12.7	13.5	641.0	690.2	441.8	329.1	413.1	301.9
cg0453		45	unknown	2.1	5.4	3.8	1.0	1.0	1.6	212.1	301.0	475.9	411.8	531.9	398.6
cg0465		95	unknown	2.4	10.4	4.0	1.9	1.0	1.7	5.5	1.1	8.3	3.8	1.0	10.8
cg0475		386	386	13.8	34.4	16.7	7.2	8.3	12.0	588.0	681.2	1518.0	1042.4	1302.8	1540.3
cg0497	*hemA*	26	17	6.4	25.8	14.6	5.5	3.1	5.2	111.1	469.9	129.2	599.2	727.3	263.6
cg0500	*qsuR*	19	unknown	4.3	22.3	8.8	3.6	2.4	2.0	37.3	24.6	19.4	21.1	19.4	13.4
cg0505		462	462	2.1	6.2	1.0	1.3	1.0	1.0	76.6	57.8	77.2	119.3	88.5	40.0
cg0505		7	7	1.3	4.8	3.3	1.3	1.0	1.0	76.6	57.8	77.2	119.3	88.5	40.0
cg0516	*hemE*	60	60	10.8	33.7	19.6	7.9	6.1	5.0	54.6	32.9	51.2	275.3	273.6	249.9
cg0517	*hemY*	642	447	3.0	6.4	3.9	1.0	1.0	1.0	63.5	36.3	91.7	202.5	244.4	284.7
cg0556	*menG (ubiE)*	61	61	2.5	6.8	1.0	1.3	1.0	1.0	132.0	77.8	176.0	155.6	132.8	173.2
cg0557		33	unknown	2.5	7.0	4.0	2.4	2.9	2.1	23.4	24.1	27.0	32.0	52.8	41.1
cg0566	*gabT*	227	unknown	1.8	4.2	2.2	1.0	1.0	1.1	3.1	3.9	3.1	2.8	3.3	3.1
cg0612	*dkg*	120	120	1.5	4.8	1.0	1.0	1.0	1.0	76.4	60.2	137.1	95.1	107.3	68.7
cg0614		145	unknown	1.0	4.5	1.0	1.0	1.0	1.0	75.8	189.2	50.7	69.2	136.1	32.3
cg0617		629	unknown	3.7	15.3	5.5	1.9	1.0	1.0	219.6	670.2	82.7	145.8	343.0	51.8
cg0636	*creB*	33	unknown	4.4	28.5	9.0	3.0	1.0	1.0	48.8	48.0	17.9	39.6	29.4	12.5
cg0636	*creB*	453	unknown	3.5	12.2	4.7	1.9	1.7	1.7	48.8	48.0	17.9	39.6	29.4	12.5
cg0645	*creJ (cytP)*	678	unknown	1.3	5.1	1.8	1.0	1.0	1.0	4.5	1.8	16.0	2.1	1.7	6.4
cg0656	*rplQ*	1	unknown	2.2	6.1	3.4	1.6	1.0	1.0	1323.1	721.0	2899.2	1339.1	1385.0	3899.9
cg0671		696	unknown	3.8	12.3	4.6	1.8	1.0	1.0	7.6	2.1	8.3	3.2	3.9	3.0
cg0673	*rplM*	13	104	1.6	5.7	2.9	1.0	1.0	2.4	1686.2	1495.2	3974.2	2555.6	2381.4	5428.0
cg0688		38	38	5.1	16.1	8.6	4.0	5.5	6.1	47.7	39.8	108.3	61.8	71.3	86.2
cg0752		511	388	1.6	3.5	1.0	1.0	1.0	1.0	107.4	130.8	271.1	148.5	177.2	371.0
cg0753		106	106	7.7	29.0	16.4	5.7	3.3	5.0	278.2	365.7	329.4	476.8	563.7	199.4
cg0778		42	6	4.9	15.2	8.5	2.9	1.0	2.1	126.0	77.7	108.5	141.4	115.5	149.1
cg0831	*tusG*	25	unknown	2.6	23.4	6.6	2.1	0.9	1.0	140.9	125.0	428.3	122.7	122.0	385.2
cg0842		35	unknown	1.0	3.3	1.0	1.0	1.0	1.4	21.0	21.3	114.6	33.7	40.2	87.0
cg0844		3	unknown	1.7	9.2	3.8	1.9	1.0	1.5	55.2	67.4	209.5	73.8	83.2	166.0
cg0875		56	unknown	2.6	6.3	3.1	1.9	1.0	2.6	3.6	3.8	3.4	2.0	3.0	1.6
cg0879		60	unknown	1.0	7.0	1.0	1.0	1.8	1.0	25.5	13.1	20.5	6.7	16.6	31.7
cg0880		49	unknown	5.8	13.2	5.2	3.0	1.0	4.7	64.3	43.1	59.8	72.4	67.2	49.3
cg0908		157	unknown	1.8	33.8	5.5	1.0	1.0	1.0	18.3	21.6	24.9	29.4	24.9	17.3
cg0928		277	unknown	1.0	5.6	1.0	1.2	1.0	1.7	819.4	41.5	224.7	119.2	21.7	752.8
cg0931		369	369	3.5	7.6	4.8	1.0	3.8	3.1	26.2	16.8	7.5	16.3	12.0	5.4
cg0931		34	34	2.1	4.8	2.4	1.5	1.0	1.0	26.2	16.8	7.5	16.3	12.0	5.4
cg0950	*fkpA*	684	621	5.0	12.4	4.4	2.8	1.0	4.8	662.5	526.2	1121.2	677.8	902.8	1376.1
cg0951	*accD3*	84	43	4.9	25.9	10.3	2.7	1.9	1.0	488.6	701.6	375.5	126.5	148.0	114.8
cg0986	*amtR*	414	unknown	2.4	13.5	3.3	2.3	1.0	1.0	263.8	233.6	221.3	196.1	279.4	231.8
cg0996	*cgtR2*	120	116	1.5	6.4	2.5	1.3	1.0	1.0	221.1	218.7	193.3	207.2	204.4	125.1
cg1017	*metS*	1	unknown	1.0	3.5	1.0	1.0	1.0	1.0	612.9	545.6	419.0	551.7	132.2	383.1
cg1044		445	445	1.5	3.6	1.7	1.0	1.0	1.0	261.9	181.7	641.7	440.0	412.9	444.4
cg1050		60	unknown	8.6	24.6	13.3	5.0	3.0	1.0	48.1	25.8	87.0	97.4	111.1	161.1
cg1052	*cmt3*	249	205	2.2	6.2	2.3	1.9	1.0	2.1	86.1	64.8	72.2	70.3	84.9	41.4
cg1069	*gapB (gapX)*	284	204	3.4	3.5	1.0	1.0	1.0	2.8	72.8	92.4	509.6	84.1	288.5	481.9
cg1076	*glmU*	118	76	1.0	3.8	1.0	1.0	1.0	1.0	285.1	226.7	718.8	249.7	330.3	665.7

cg1077		17	unknown	14.7	41.8	18.9	10.5	15.4	13.6	4.3	2.8	6.8	21.7	24.3	20.4
cg1077		424	unknown	1.0	7.7	1.0	1.0	1.0	1.0	4.3	2.8	6.8	21.7	24.3	20.4
cg1086		257	unknown	1.0	4.8	1.0	1.0	1.0	1.0	78.6	39.8	53.3	58.3	59.0	40.7
cg1087		59	33	3.6	16.9	8.3	2.2	2.1	2.6	182.7	263.3	656.8	439.7	333.2	367.6
cg1105	*lysI*	517	517	2.2	4.2	2.3	1.6	1.6	2.6	22.5	13.8	12.9	19.0	16.9	10.7
cg1145	*fumC (fum)*	109	72	2.2	4.0	3.0	1.9	1.0	1.5	639.1	692.5	1421.6	634.5	1145.9	1466.3
cg1233		494	494	1.5	3.9	1.7	1.0	1.0	1.0	55.3	70.7	64.7	69.6	75.9	37.3
cg1233		33	33	1.0	3.8	1.0	1.0	1.1	1.0	55.3	70.7	64.7	69.6	75.9	37.3
cg1272	*cseE*	132	67	1.0	4.2	1.0	1.0	1.0	1.0	978.8	1099.2	464.4	1055.0	1012.8	280.6
cg1289		546	unknown	1.6	4.7	1.6	1.0	1.0	1.0	12.7	30.2	12.8	7.8	23.1	13.1
cg1292		105	unknown	4.1	10.7	4.3	1.9	4.3	2.8	80.2	28.5	331.7	72.8	38.8	312.0
cg1301	*cydA*	177	72	10.3	17.9	12.5	5.2	8.8	8.3	29.1	113.5	423.4	163.6	70.3	71.4
cg1301	*cydA*	571	466	1.0	17.0	3.8	1.0	1.0	1.0	29.1	113.5	423.4	163.6	70.3	71.4
cg1328		98	41	1.0	3.1	1.0	1.2	1.0	1.0	70.2	121.9	89.7	92.5	122.2	76.5
cg1334	*lysA*	116	unknown	5.8	12.8	5.2	2.4	1.0	5.1	315.7	318.8	501.9	257.1	319.3	563.0
cg1346	*mog*	528	495	1.0	7.7	3.0	1.3	1.0	1.0	94.4	84.8	200.7	100.5	97.1	143.2
cg1346	*mog*	476	443	2.7	7.7	1.0	1.0	1.0	2.2	94.4	84.8	200.7	100.5	97.1	143.2
cg1355	*prfA*	606	unknown	1.9	4.3	1.9	1.4	1.0	1.0	484.3	214.2	377.0	415.6	242.7	452.8
cg1449		608	unknown	1.1	3.3	1.0	1.2	1.0	1.0	265.5	114.3	138.4	124.3	119.3	119.8
cg1449		139	unknown	2.0	3.1	2.0	1.0	1.0	1.3	265.5	114.3	138.4	124.3	119.3	119.8
cg1454		303	unknown	1.7	7.6	2.0	1.0	1.0	1.0	81.0	122.6	94.2	115.0	134.9	63.7
cg1459		696	unknown	2.6	9.2	4.1	1.5	1.8	1.0	258.7	135.2	327.4	200.4	231.9	399.4
cg1464		125	unknown	1.9	3.1	1.0	1.0	1.1	1.0	12.9	21.7	20.7	7.1	11.6	21.3
cg1474		552	unknown	1.3	3.0	1.6	1.1	1.0	1.0	46.3	52.8	67.2	41.4	38.1	45.5
cg1484		23	4	1.0	7.2	1.0	1.6	1.0	1.0	96.8	183.1	95.5	132.8	176.8	102.7
cg1516		32	unknown	1.0	6.9	3.3	1.6	1.6	1.0	11.8	19.2	19.9	11.4	12.6	13.8
cg1526		29	unknown	1.5	4.5	2.3	1.4	1.0	1.0	3.0	1.2	2.0	3.1	2.0	1.4
cg1531	*rpsA*	391	241	2.6	6.5	4.1	1.0	2.1	2.1	1712.6	1757.9	3842.6	1882.6	2389.0	4889.1
cg1538	*coaE*	150	150	3.5	22.3	4.6	1.4	1.0	1.0	797.2	513.3	474.7	654.2	468.2	340.2
cg1568	*ugpA*	253	unknown	1.0	4.3	1.0	1.0	1.5	1.0	28.7	18.2	16.9	22.6	14.8	9.1
cg1603		42	unknown	1.0	5.6	2.0	1.0	1.0	1.0	263.2	359.7	316.8	200.9	336.3	295.4
cg1607		49	unknown	1.5	5.8	1.0	1.0	1.0	1.2	177.8	108.9	110.2	165.7	144.2	90.1
cg1628		18	2	1.9	3.9	2.3	1.0	1.0	2.3	56.9	186.8	18.1	38.0	333.2	29.4
cg1668		177	unknown	1.0	5.5	2.6	1.0	1.0	1.0	148.4	119.0	154.7	187.3	200.7	225.6
cg1691	*arc (mpa)*	50	unknown	1.6	5.1	2.1	1.6	1.0	1.0	434.6	346.3	190.7	340.0	291.0	155.1
cg1695		188	unknown	9.3	22.6	9.9	5.5	9.0	11.2	289.4	414.5	162.4	159.1	198.5	58.6
cg1702		345	345	1.0	3.0	1.0	1.3	1.6	1.0	10.9	7.1	15.7	15.3	11.7	7.3
cg1728		91	21	1.0	3.2	1.6	1.0	1.0	1.1	120.9	93.2	129.4	126.7	133.3	103.9
cg1731		140	140	4.6	21.0	7.8	2.9	5.3	5.0	453.9	312.9	715.7	378.1	468.8	503.5
cg1734	*hemH*	16	16	14.4	52.9	24.7	9.0	9.3	13.3	75.5	65.5	147.7	688.9	1029.3	663.1
cg1736		95	2	4.7	12.2	6.1	2.3	1.0	1.0	46.3	29.2	35.1	35.9	34.0	25.2
cg1767		19	19	9.2	31.9	16.1	5.7	4.3	7.9	40.0	15.9	45.8	123.5	131.7	123.8
cg1773	*ctaB*	204	43	1.8	5.0	1.0	1.2	1.0	1.0	92.2	70.9	298.0	69.7	95.8	110.1
cg1774	*tkt*	16	1	8.5	147.0	12.6	2.2	1.0	1.0	964.4	724.7	1241.6	954.6	721.5	1156.9
cg1791	*gapA (gap)*	287	104	3.6	4.4	3.7	1.0	1.0	4.8	6163.6	3596.8	6243.6	8801.8	2867.2	4950.7
cg1796	*ribX*	63	unknown	1.0	11.0	1.0	1.0	1.3	1.0	284.1	404.0	286.2	283.0	424.2	324.7
cg1801	*rpe*	38	38	2.6	15.6	6.0	1.0	1.0	1.0	337.8	365.3	421.5	335.8	363.9	397.7

cg1811	*ihf*	74	19	1.6	4.1	2.1	1.0	1.0	1.2	1586.5	1798.5	2336.7	1840.0	2223.8	2148.1
cg1867	*secD*	321	172	1.3	4.1	1.8	1.4	1.0	1.0	102.9	88.2	287.3	73.9	88.1	292.7
cg1893	*act4*	445	unknown	1.0	4.3	1.0	1.0	1.0	1.9	134.2	85.4	97.6	115.9	96.6	72.3
cg1904		7	unknown	1.0	3.9	1.0	1.0	1.0	1.0	248.4	180.2	284.3	193.7	195.1	222.4
cg1924		137	unknown	2.0	10.7	1.0	1.5	1.0	1.3	1.9	3.3	#NV	3.3	2.9	#NV
cg1926		30	unknown	1.7	4.9	2.5	1.5	1.0	2.0	73.2	42.8	37.2	37.5	67.6	30.0
cg1942		402	unknown	1.3	4.3	1.0	1.0	1.7	1.0	9.4	21.0	17.9	7.3	8.6	17.1
cg1944		43	14	3.3	35.1	9.4	1.0	1.0	1.0	16.1	15.8	13.6	35.7	22.5	13.0
cg1945		577	116	1.0	8.3	2.7	1.0	1.0	1.0	34.4	17.4	23.8	28.3	19.8	17.4
cg1946		99	unknown	1.0	3.1	1.0	1.0	1.0	1.0	53.8	57.3	30.5	40.3	48.2	27.4
cg1956	*recJ*	1	unknown	1.3	3.6	2.2	0.9	1.0	1.0	14.8	12.7	16.1	20.4	21.7	17.8
cg1959	*priP*	26	unknown	4.3	21.3	6.8	2.6	1.0	1.0	4.6	2.5	2.5	3.5	2.5	2.0
cg1981		598	unknown	1.0	6.2	1.0	1.0	1.0	1.0	12.4	6.7	5.8	8.9	5.4	4.2
cg1981		433	unknown	1.0	6.2	1.0	1.5	1.2	1.0	12.4	6.7	5.8	8.9	5.4	4.2
cg1981		12	unknown	1.0	3.5	1.0	1.0	1.0	1.0	12.4	6.7	5.8	8.9	5.4	4.2
cg2003		170	unknown	1.3	4.2	1.0	1.0	1.0	1.0	45.2	60.5	34.8	71.5	44.6	24.4
cg2005		246	unknown	7.2	24.2	7.4	1.6	1.0	1.0	15.4	14.2	11.5	16.0	13.9	9.0
cg2005		531	unknown	1.0	12.5	4.3	1.0	1.0	1.0	15.4	14.2	11.5	16.0	13.9	9.0
cg2007		177	unknown	1.7	3.3	1.0	1.0	1.0	1.0	10.3	6.9	10.4	8.0	6.0	6.8
cg2021		263	unknown	2.2	9.9	2.7	1.0	1.0	1.5	14.5	12.3	8.8	11.3	10.4	6.3
cg2030		586	543	1.0	7.1	1.5	1.0	1.0	1.0	64.2	60.5	38.4	44.1	43.9	33.2
cg2031		181	unknown	1.6	5.3	2.7	1.4	1.0	1.0	88.6	108.3	74.9	91.0	68.5	59.7
cg2037		19	unknown	2.3	7.1	3.9	1.0	2.1	1.0	86.6	89.5	77.9	77.0	93.3	66.6
cg2045		222	unknown	1.3	6.3	2.1	1.0	0.8	1.0	15.4	12.4	42.4	24.0	24.3	46.5
cg2047		13	78	1.0	4.0	1.3	1.0	1.0	1.0	49.3	121.5	78.9	237.2	467.6	61.3
cg2051		33	14	4.5	24.2	8.9	2.1	1.0	1.7	180.3	286.1	140.0	197.9	206.5	116.7
cg2059		156	unknown	1.7	11.8	2.3	1.0	1.0	1.5	13.7	7.8	12.8	20.5	9.4	11.6
cg2061	*psp3*	155	121	1.0	3.1	1.0	1.0	1.0	1.0	39.0	35.2	40.1	45.1	37.0	49.1
cg2063		40	unknown	1.0	4.9	2.4	1.0	1.9	1.0	22.3	16.9	10.8	15.7	12.0	6.9
cg2069	*psp1*	33	17	1.0	4.4	2.9	1.0	1.0	1.0	69.4	49.0	45.8	71.8	52.7	37.9
cg2071	*int2*	82	618	3.5	10.3	4.3	2.7	1.0	3.3	86.7	90.1	137.1	94.0	191.0	217.9
cg2077	*aftC*	268	268	2.3	14.3	2.9	1.0	1.0	1.0	248.8	302.5	120.8	147.5	239.3	103.9
cg2078	*msrB*	282	unknown	1.0	3.0	1.0	1.2	1.0	1.0	538.4	1894.3	303.9	438.3	1183.0	327.1
cg2079		134	15	8.6	22.2	9.9	5.5	6.7	7.5	170.0	104.9	436.1	593.0	731.7	1573.5
cg2091	*ppgK*	202	202	58.9	174.4	105.8	35.7	2.7	6.3	453.5	426.4	833.1	464.8	475.5	476.9
cg2092	*sigA (rpoD)*	29	115	1.0	3.9	1.7	1.3	1.0	1.0	687.2	1215.9	598.1	541.9	774.5	573.4
cg2103	*dtxR*	579	310	1.0	3.3	1.6	1.0	2.4	1.0	666.9	702.5	468.0	548.9	529.8	318.5
cg2121	*ptsH*	31	unknown	1.9	4.2	1.9	1.0	1.0	1.0	2665.7	2945.4	2311.5	3242.5	1233.2	1896.9
cg2155		333	333	3.6	15.8	4.8	2.0	1.0	1.0	442.3	353.3	372.1	600.7	598.2	312.7
cg2171	*pptA*	448	unknown	1.0	5.4	1.6	1.0	1.0	1.6	98.1	111.7	86.0	123.5	97.4	74.6
cg2181	*oppA*	274	217	4.1	6.7	6.3	2.6	4.7	4.1	1255.6	128.3	1864.6	407.8	129.1	1460.9
cg2187		221	unknown	1.8	5.7	1.8	1.3	1.0	1.0	84.8	53.1	39.5	34.7	37.1	38.6
cg2188		55	2	1.0	3.0	1.0	1.0	1.0	1.0	119.0	93.3	60.9	60.8	67.1	51.4
cg2195		166	61	2.7	11.7	4.0	2.0	2.4	2.0	6384.2	8528.4	11102.6	8391.4	11066.7	11490.2
cg2197		0	1	1.0	6.5	1.7	1.0	1.5	1.0	244.5	126.1	333.4	170.0	196.4	311.8
cg2199	*pbp2a*	131	131	1.0	30.7	21.0	1.0	1.0	1.0	233.9	358.9	121.4	124.6	255.1	112.0
cg2200	*chrA (cgtR8)*	326	unknown	29.2	140.9	47.7	20.5	1.0	1.0	79.3	770.3	69.2	31.6	578.3	116.5

cg2201	*chrS (cgtS8)*	32	unknown	29.4	141.1	40.5	21.8	1.0	29.7	36.6	481.4	23.3	11.0	352.6	56.6
cg2201	*chrS (cgtS8)*	424	unknown	1.0	27.7	21.2	1.0	1.0	1.0	36.6	481.4	23.3	11.0	352.6	56.6
cg2206	*ispG*	236	190	2.1	3.9	1.5	1.4	1.0	1.0	524.6	842.9	566.4	398.5	585.2	449.4
cg2221	*tsf*	4	4	1.0	4.2	1.9	1.5	1.0	1.0	694.7	580.5	2069.5	795.7	774.8	2124.6
cg2224	*xerC*	134	31	15.5	49.1	28.4	10.6	4.4	9.4	41.0	25.6	29.6	40.5	39.7	32.0
cg2241	*tex*	149	149	1.4	9.7	3.2	1.0	1.0	1.0	96.4	46.4	119.9	70.3	72.2	98.4
cg2247		534	464	1.0	4.0	1.9	1.3	1.0	1.4	415.5	1108.7	264.4	352.6	724.0	270.6
cg2274		58	55	1.0	10.4	2.0	1.5	1.0	1.0	247.5	244.8	420.6	204.8	271.1	360.2
cg2290		221	unknown	1.0	3.8	1.8	1.0	1.0	1.0	93.3	60.5	35.0	58.2	47.9	27.7
cg2305	*hisD*	383	290	1.7	7.1	3.0	1.0	1.5	1.7	215.3	200.9	347.8	234.3	362.7	419.5
cg2310	*glgX*	307	307	1.0	3.1	1.0	1.0	1.0	1.0	206.5	178.4	297.4	175.5	175.1	203.8
cg2311		88	88	4.4	19.9	5.6	3.0	2.7	1.0	96.2	48.4	128.1	44.3	45.9	156.6
cg2337		421	379	1.0	9.9	3.1	1.0	1.0	1.0	799.6	894.0	371.9	858.6	1230.5	533.7
cg2337		264	222	1.0	9.0	1.0	1.0	1.0	1.0	799.6	894.0	371.9	858.6	1230.5	533.7
cg2338	*dnaE1*	607	607	1.2	4.0	1.0	1.0	1.3	1.0	269.0	389.3	216.5	382.3	383.6	179.0
cg2343		26	unknown	5.2	24.9	9.5	3.0	1.3	1.0	122.9	154.6	85.8	113.5	123.1	62.2
cg2373	*murF*	133	unknown	1.4	23.1	1.9	1.3	0.8	1.0	200.5	160.2	175.8	194.8	141.7	151.9
cg2403	*qcrB*	221	unknown	1.6	4.8	2.1	1.0	1.2	1.0	1474.9	4043.9	1898.9	501.6	1147.1	1176.0
cg2406	*ctaE*	324	324	20.3	52.9	28.1	11.0	20.7	23.3	3792.2	4388.5	1723.4	907.8	1375.2	995.2
cg2406	*ctaE*	616	616	1.0	29.3	1.0	1.0	1.0	1.0	3792.2	4388.5	1723.4	907.8	1375.2	995.2
cg2406	*ctaE*	27	27	1.0	17.9	1.0	1.0	1.0	1.0	3792.2	4388.5	1723.4	907.8	1375.2	995.2
cg2409	*ctaC*	259	73	5.7	16.1	8.6	4.0	6.2	5.9	2600.7	3428.4	2548.1	976.8	1329.5	1313.3
cg2423	*lipA*	163	69	1.0	18.4	1.0	1.0	1.0	1.0	652.1	1614.9	429.7	638.5	1617.6	442.8
cg2445	*hmuO*	150	44	3.1	10.4	4.5	1.0	1.0	3.7	178.5	77.0	249.1	7.8	9.1	18.2
cg2445	*hmuO*	587	481	1.0	4.3	1.0	1.6	1.0	1.0	178.5	77.0	249.1	7.8	9.1	18.2
cg2473	*acpM*	593	593	4.8	31.4	9.7	3.1	1.0	1.0	181.4	134.9	234.0	238.8	263.1	169.2
cg2478	*pbp6*	26	26	1.5	5.0	2.1	1.0	1.0	1.0	537.8	475.3	154.5	218.9	259.2	106.0
cg2491		162	unknown	1.0	4.0	1.0	1.0	1.0	1.0	94.1	86.0	125.1	89.9	129.9	123.2
cg2496		1	1	3.2	11.4	4.3	2.3	1.0	2.6	123.4	105.0	132.8	115.5	137.1	108.5
cg2523	*malQ*	94	94	1.8	4.7	2.9	1.0	1.0	1.0	1568.4	1124.7	1268.4	1040.2	947.1	996.7
cg2537	*brnQ*	336	unknown	2.9	6.6	1.0	1.6	1.7	3.2	171.9	129.2	143.0	148.8	177.7	163.3
cg2542		546	unknown	1.0	3.8	1.0	1.3	1.0	1.0	51.0	56.1	43.9	50.1	46.7	36.4
cg2546		194	173	4.3	18.3	6.8	2.2	3.8	2.6	5.2	4.0	11.4	3.1	3.5	15.5
cg2557		538	unknown	1.6	3.4	1.4	1.0	1.1	1.0	24.4	19.5	109.0	14.6	20.6	121.2
cg2566		132	unknown	1.4	5.5	2.3	1.0	1.0	1.3	29.8	19.4	59.3	21.2	13.6	29.5
cg2579		13	unknown	1.0	6.0	2.1	1.0	1.0	1.0	246.1	167.2	229.7	135.4	150.9	169.5
cg2592		140	140	1.0	4.8	1.8	1.0	1.0	1.0	91.1	82.9	130.9	129.4	173.5	144.4
cg2593		170	91	1.6	3.5	1.0	1.0	2.1	1.0	124.3	101.4	120.9	100.0	122.8	91.9
cg2601		327	unknown	3.5	3.6	2.8	2.9	1.0	3.6	57.7	26.4	31.3	38.9	29.3	21.2
cg2641	*benR*	229	229	6.3	20.8	6.8	2.8	1.0	1.0	22.8	25.0	42.9	20.6	22.6	19.4
cg2675		34	unknown	1.0	89.9	22.9	7.2	4.3	4.4	549.6	1308.3	17.1	808.4	378.7	58.5
cg2675		9	unknown	13.4	89.9	22.9	7.2	4.3	1.0	549.6	1308.3	17.1	808.4	378.7	58.5
cg2680	*argD2*	271	229	2.8	6.5	3.3	1.3	1.9	1.0	157.7	179.9	202.2	104.3	126.0	168.1
cg2685		13	16	7.0	25.0	13.0	5.0	10.3	8.3	142.6	68.6	76.2	108.2	115.4	123.9
cg2701	*musI*	523	523	1.0	4.4	2.1	1.7	1.0	1.5	578.8	391.0	635.7	362.6	413.2	664.5
cg2745		455	455	2.2	3.2	2.3	1.0	1.0	1.0	62.8	54.5	71.9	86.6	62.1	34.4
cg2747	*mepA*	69	unknown	1.4	4.1	2.1	1.0	1.5	1.0	94.6	118.3	173.8	305.9	102.2	67.7

cg2761	*cpdA*	310	310	4.4	11.8	4.7	1.7	1.0	1.0	98.2	165.2	166.3	87.0	209.8	117.7
cg2766		555	555	1.8	4.2	2.0	1.4	1.0	1.0	313.6	243.4	159.0	292.3	273.4	122.6
cg2780	*ctaD*	314	202	10.9	21.8	11.6	5.7	11.8	10.0	2992.2	5262.4	3087.5	1582.8	2519.5	1714.3
cg2786	*nrdE*	8	unknown	2.8	13.5	4.3	1.0	1.0	1.0	249.5	300.9	390.7	225.0	214.1	389.7
cg2823		347	unknown	1.0	9.9	2.8	1.4	1.0	1.4	2.6	1.7	1.5	2.1	1.4	0.9
cg2829	*murA2*	269	unknown	2.0	3.6	1.0	1.0	1.0	1.3	218.5	132.8	260.0	205.1	186.0	208.8
cg2831	*ramA*	42	19	1.8	5.0	2.3	1.0	1.9	2.9	223.2	240.4	130.2	148.6	173.8	195.4
cg2857	*purF*	19	19	1.0	8.1	1.0	1.4	1.3	1.2	404.9	374.1	261.5	455.7	791.0	346.2
cg2867	*mpx*	56	56	1.4	5.6	1.0	1.0	1.0	1.2	273.5	469.1	295.1	184.5	162.8	199.3
cg2944	*ispF*	540	unknown	4.7	3.8	2.9	1.0	1.0	2.0	190.6	131.5	199.8	155.2	170.0	165.7
cg2949		122	60	6.7	22.3	12.7	5.7	7.1	5.2	707.2	979.7	1539.3	483.6	833.9	937.9
cg2953	*vdh*	42	unknown	1.5	7.0	2.4	1.0	1.6	1.6	57.0	29.0	144.7	42.5	47.4	102.4
cg2977		408	408	1.0	4.4	1.0	1.0	1.0	1.0	444.0	424.7	281.2	406.6	432.4	218.9
cg3054	*purT*	241	205	1.0	3.3	2.6	1.6	1.0	1.2	187.4	190.9	212.9	136.2	132.6	147.7
cg3068	*fda*	20	9	3.1	20.5	7.7	2.7	1.0	1.0	978.6	631.5	1696.7	1271.8	1048.7	1758.1
cg3068	*fda*	423	305	1.0	6.3	2.2	1.0	1.0	1.0	978.6	631.5	1696.7	1271.8	1048.7	1758.1
cg3069		54	5	5.4	22.5	12.5	3.6	2.6	3.3	234.1	217.7	310.7	352.7	309.8	220.6
cg3097	*hspR*	393	unknown	1.0	3.1	1.0	1.0	1.0	1.0	87.0	419.1	271.5	69.3	227.8	248.3
cg3101		626	unknown	1.0	7.1	1.0	2.2	1.0	2.7	378.5	414.6	309.7	99.9	120.0	171.0
cg3101		25	unknown	1.8	7.1	3.5	2.2	1.0	2.1	378.5	414.6	309.7	99.9	120.0	171.0
cg3115	*cysD*	106	unknown	1.0	6.7	2.6	1.0	1.0	1.0	4453.1	5001.1	35.0	3477.3	3194.4	397.8
cg3118	*cysI*	498	446	1.0	3.7	1.0	1.5	1.0	1.0	5918.5	6455.9	54.8	4787.0	3972.1	476.6
cg3127	*tctC*	37	unknown	2.3	3.4	1.0	1.0	1.0	1.0	7.3	9.2	26.4	8.1	8.3	14.0
cg3156	*htaD*	151	unknown	5.7	17.3	8.6	3.9	7.3	4.2	6.3	0.9	48.1	2.6	0.7	23.5
cg3170		66	unknown	1.6	10.4	3.6	1.0	1.0	1.0	24.2	20.6	16.4	20.7	17.2	12.6
cg3173		0	unknown	2.7	6.6	3.4	2.2	1.0	2.1	322.9	203.0	303.9	238.8	206.5	267.7
cg3175		217	unknown	3.1	9.2	4.1	1.0	1.0	1.4	61.4	45.0	70.9	55.5	65.0	60.7
cg3182	*cop1*	198	13	1.0	4.0	3.1	1.0	1.0	1.0	537.5	663.0	1163.6	974.8	1214.0	923.4
cg3194		369	unknown	2.9	5.1	3.3	1.0	2.6	2.5	21.5	7.6	41.0	15.4	10.4	27.8
cg3199		158	unknown	2.7	5.0	1.0	2.1	2.8	1.9	49.2	28.5	77.5	31.7	41.6	67.2
cg3226		213	140	2.0	3.7	2.2	1.0	1.0	2.0	2480.6	547.0	79.3	1092.9	169.4	145.6
cg3226		622	549	4.2	5.5	3.3	1.0	6.2	2.0	2480.6	547.0	79.3	1092.9	169.4	145.6
cg3245		695	unknown	1.0	24.9	22.9	1.0	1.0	1.0	12.0	10.7	10.9	8.4	11.1	6.7
cg3247	*hrrA (cgtR11)*	108	26	60.4	271.4	107.2	34.1	1.0	30.8	78.8	50.7	214.3	0.1	0.0	0.2
cg3248	*hrrS (cgtS11)*	474	unknown	1.0	33.4	26.7	1.0	1.0	1.0	67.3	65.5	47.7	59.3	60.2	35.3
cg3249		419	419	1.0	20.5	18.6	15.8	1.0	1.0	28.2	17.3	27.5	18.2	25.5	21.0
cg3283		58	unknown	1.0	7.3	1.0	1.0	1.0	2.5	750.3	943.5	21.9	446.8	416.9	19.7
cg3315	*malR*	91	23	1.5	5.2	1.6	1.0	1.0	1.0	114.2	200.8	877.2	234.4	440.1	582.5
cg3317		29	unknown	2.5	9.5	4.8	2.1	1.0	2.6	132.1	204.2	212.7	208.5	322.2	352.1
cg3323	*ino1*	156	100	4.9	7.6	4.5	2.3	5.2	2.6	433.9	210.2	1216.8	283.8	674.5	1848.2
cg3357	*trpP*	91	91	1.3	4.0	1.0	1.0	1.0	1.0	184.5	426.6	114.2	172.7	338.6	121.4
cg3378	*cg3378*	60	unknown	1.0	3.8	2.6	1.0	1.0	1.9	6.6	16.4	18.4	16.9	34.6	13.3
cg3389		143	34	1.0	3.2	1.0	2.0	1.0	1.9	111.7	24.0	59.5	84.1	15.4	47.2
cg3402		13	5	2.8	18.4	7.5	2.9	1.0	2.5	1413.6	2492.6	27.0	1756.9	1175.2	23.0
cg3411		18	2	2.0	10.3	3.8	1.5	1.0	1.4	1511.1	5172.0	121.8	2499.8	3220.4	98.1
cg3422	*trxB*	5	11	1.0	5.8	1.0	1.0	1.0	1.0	839.4	1791.5	546.6	819.4	1000.3	460.0
cg4002		564	unknown	1.0	4.8	1.0	1.0	1.9	1.0	9.4	10.5	24.5	11.6	9.1	8.3

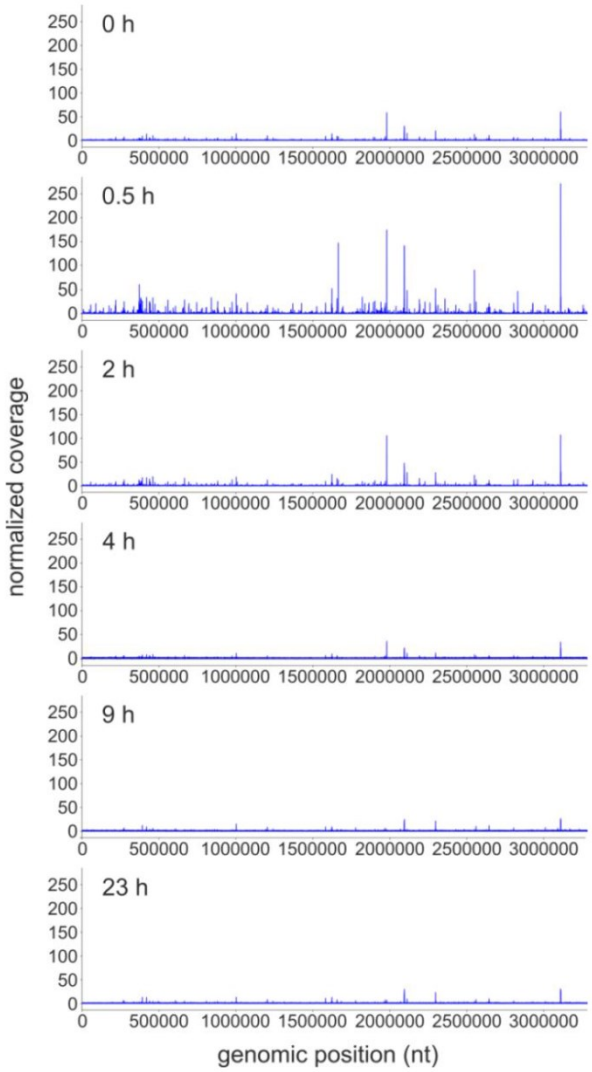

Figure S1: Global binding pattern of HrrA in the *C. glutamicum* genome in response to hemin addition. Genomic coverage (number of reads covering a particular genomic position) was normalized to the average coverage of the regions not harbouring binding peaks. Thus, depicted peak intensities are comparable between different time points. The strain *C. glutamicum* Δ*hrrSA* Δ*chrSA* harbouring the plasmid pJC1_P$_{hrrSA}$-*hrrSA-twin-strep*_P$_{chrSA}$-*chrSA-his* was cultivated in CGXII minimal medium (lacking $FeSO_4$) supplemented with 2% (w/v) glucose and 4 µM hemin was added at 0 h. Cells were harvested at different time points as described in Figure 1.

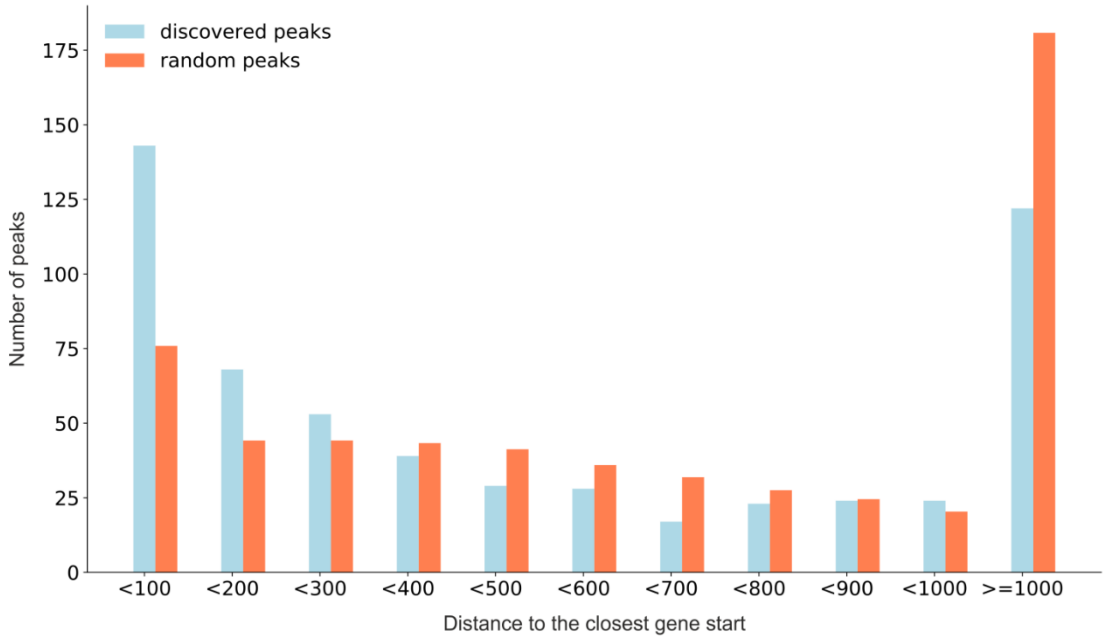

Figure S2: Distribution of distances from HrrA binding peaks centers to the closest gene start site (translation start site, TLS). As a background (red color), random peaks of the same width as real ones were generated. Random peak generation was performed 100 times and resulting distance distributions were then averaged into a single background distribution.

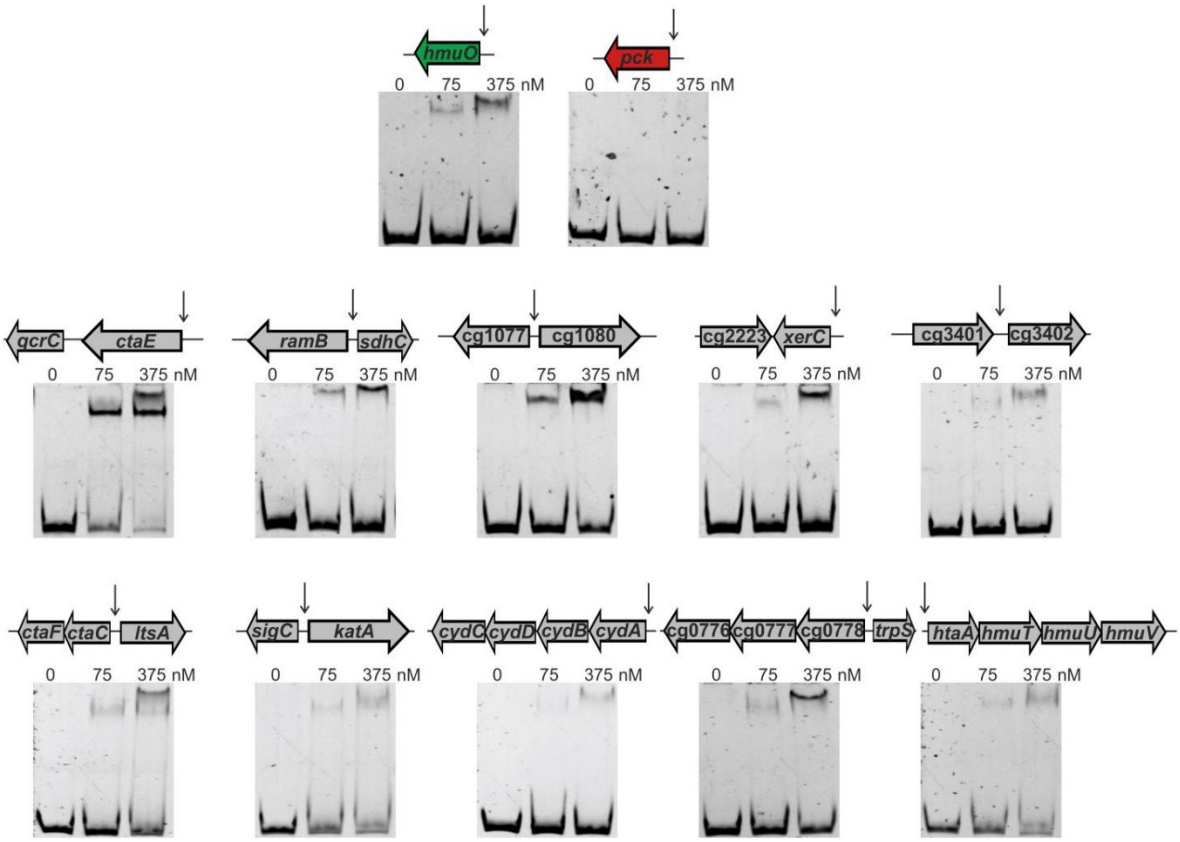

Figure S3: HrrA binding to selected target promotor regions. Protein-DNA interactions were validated by electrophoretic mobility shift assays (EMSA) using 15 nM DNA fragments covering 50 bp up- and downstream of the maximal ChAP-Seq peak height and an increasing protein monomer concentration of 0, 75 and 375 nM. The genomic location of the maximal peak height found in the ChAP-Seq experiments is indicated by an arrow. As control, the promoter regions of *hmuO* (positive control) and *pck* (negative control) were used.

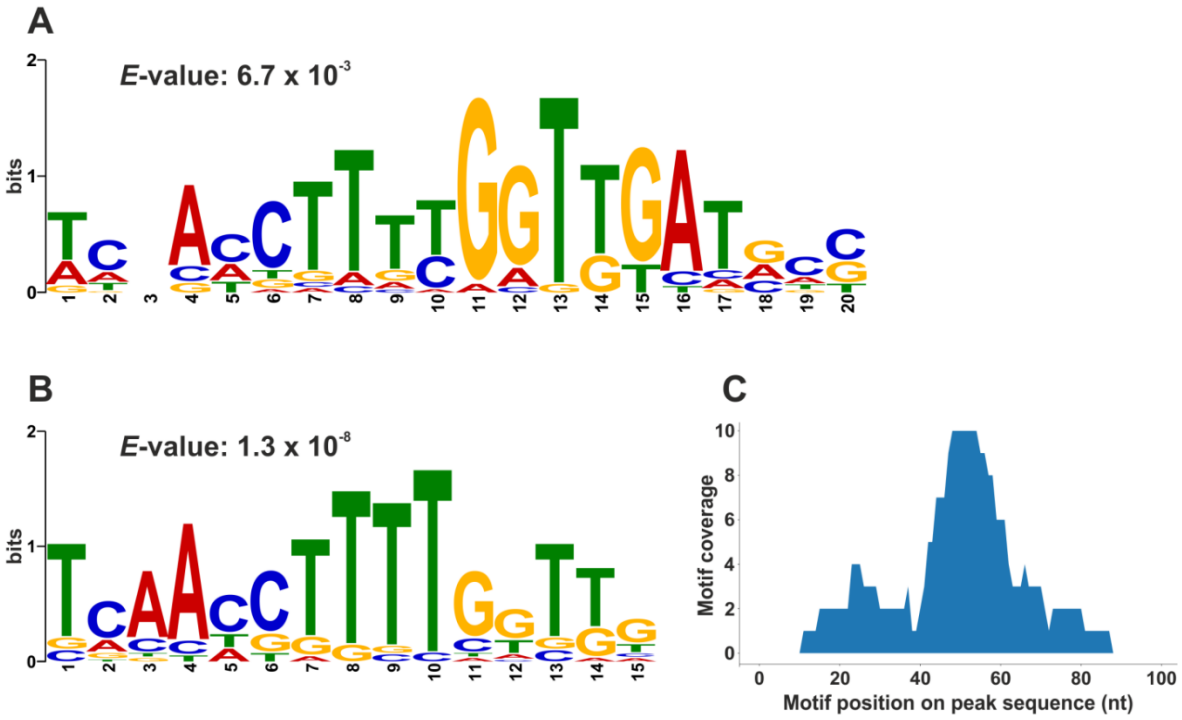

Figure S4: Derivation of a HrrA binding motif revealed a weakly conserved palindromic sequence. Sequences of the top 20 peaks (T_0) (A) or 100 bp of the tested EMSA DNA fragments (Figure S2) (B) were used for a MEME v.5 analysis (http://meme-suite.org). (C) Shown is the position of identified motif sequences within the analysed peak sequences used in (B). The majority of HrrA motifs centre at the position of the peak maximum (at 50 nt).

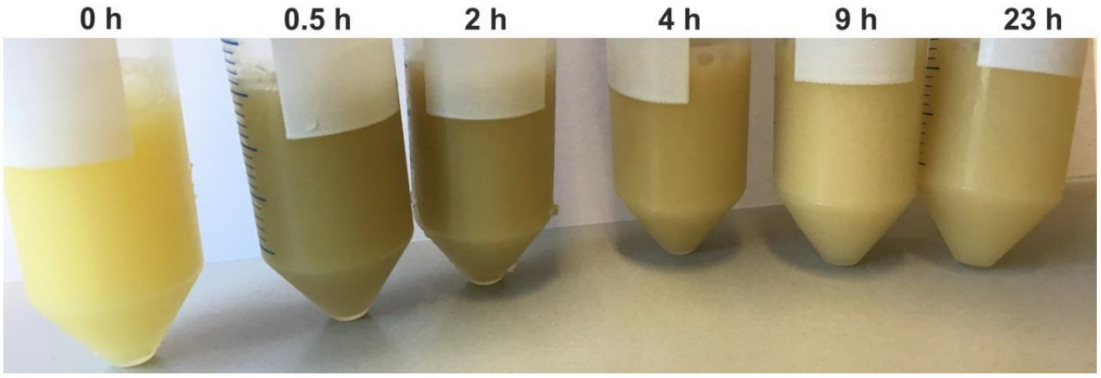

Figure S5: Visual inspection of *C. glutamicum* cells before and after addition of heme. Iron-starved *C. glutamicum* wild type cells were cultivated in CGXII medium (2 % (w/v) glucose, without $FeSO_4$) and cells were harvested at different time points before and after the addition of 4 µM heme. Cell pellets were subsequently resuspended in Tris-buffer (100 mM Tris-HCl, 1 mM EDTA, pH 8.0) and adjusted to an OD_{600} of 3.5.

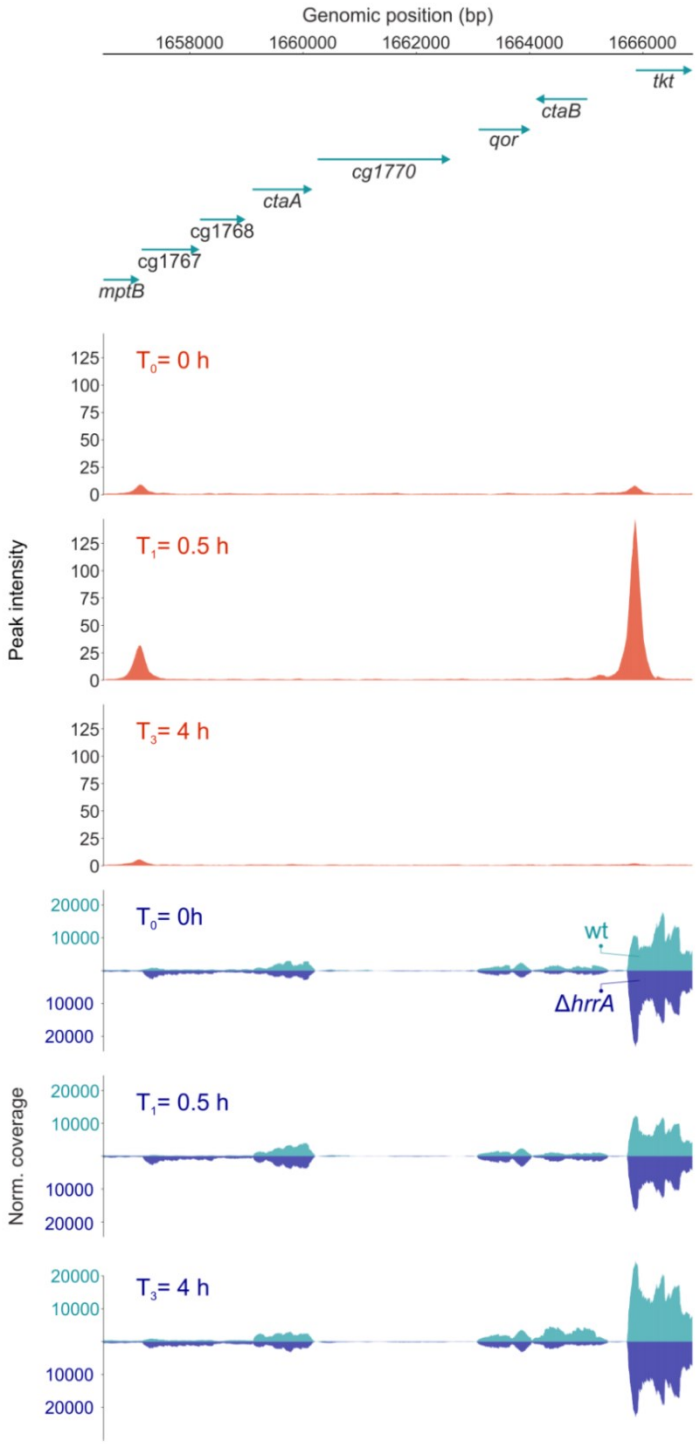

Figure S6: HrrA coordinates expression of *ctaA* and *ctaB* in response to heme. Shown are the ChAP-Seq (orange) and RNA-Seq (blue) results focusing on the *ctaA* and *ctaB* locus in the genome of *C. glutamicum.* Depicted is the genomic region between *mptb* (cg1766) and *tkt* (cg1774). For the cultivation, CGXII medium supplemented with 2% (w/v) glucose and 4 µM hemin was inoculated with iron starved cells from a stationary culture and adjusted to an OD_{600} of 3.5. Samples were analysed at the indicated time points as described in material and methods.

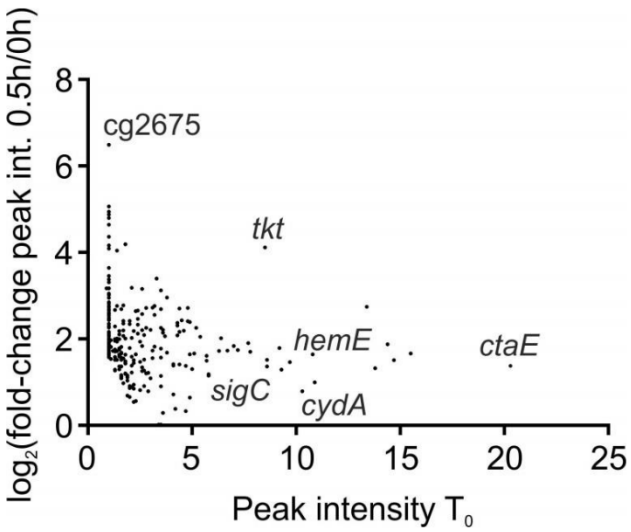

Figure S7: Dynamic range of HrrA association upon addition of external heme. ChAP-Seq analysis revealed that targets that are moderately bound before stimulus addition show a generally higher fold-change in HrrA association than targets sequences that showed already a high coverage at T_0. The $\log_2$ of the fold change of the normalized peak intensities was calculated ($T_{0.5}$ versus T_0) and plotted against the peak intensity at time point T_0 (before stimulus addition). For details on cultivation and ChAP-Sequencing, see material and methods and Figure 1.

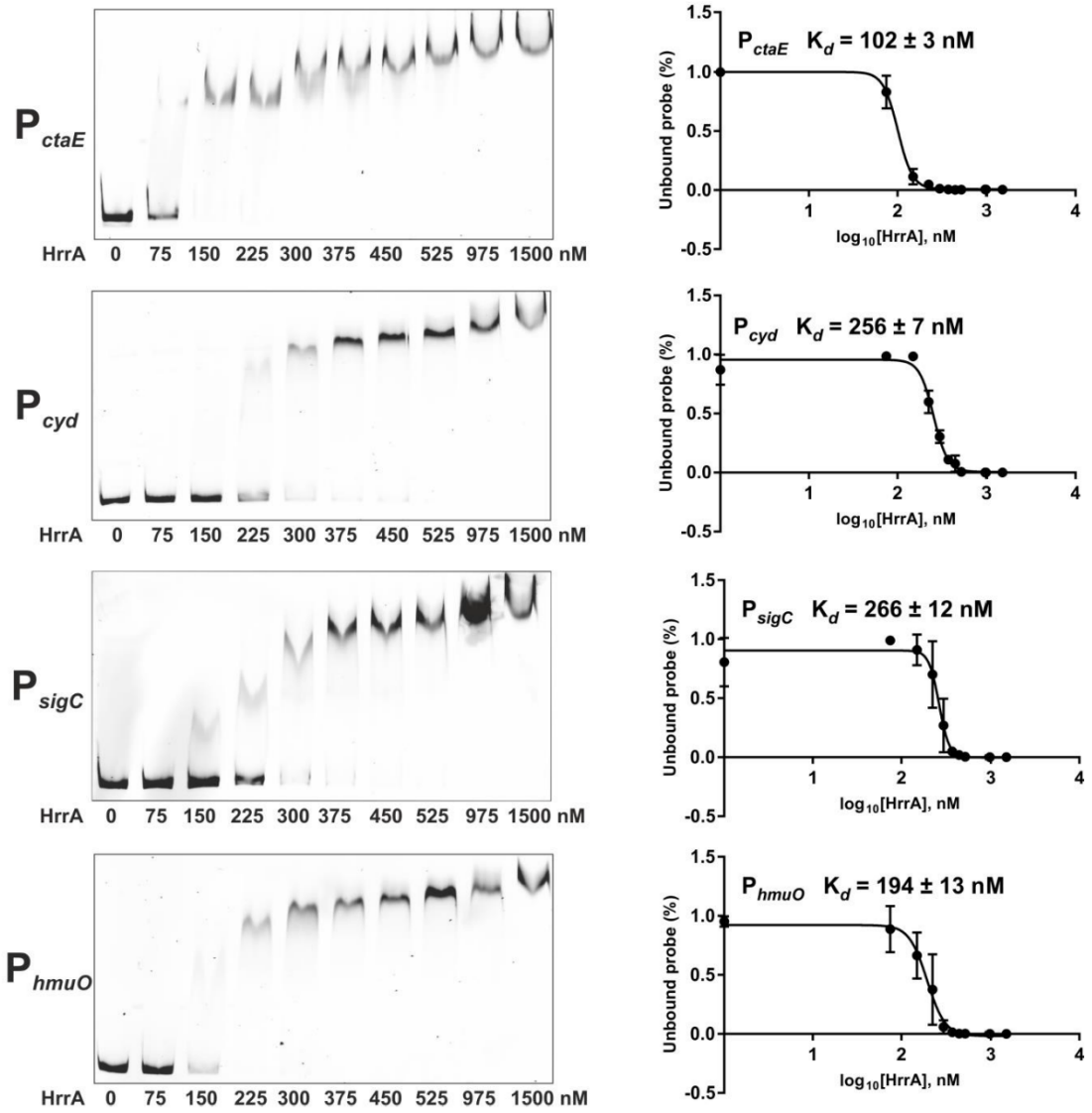

Figure S8: Binding affinity of HrrA to selected target promoters. Depicted are representative images of quantitative EMSAs used for analysis of protein-DNA interaction and the calculation of HrrA affinities to the different promoters. For the analyses, 15 nM DNA fragments covering 250 bp up- and downstream of the maximal ChAP-Seq peak height were used with an increasing monomeric protein concentration. Determination of unbound DNA in EMSA studies allowed the calculation of HrrA binding affinities to different target promoters. Quantification of unbound DNA band intensities was performed using AIDA v.4.15 (Raytest GmbH, Germany) and K_d values were calculated using GraphPad Prism 7.

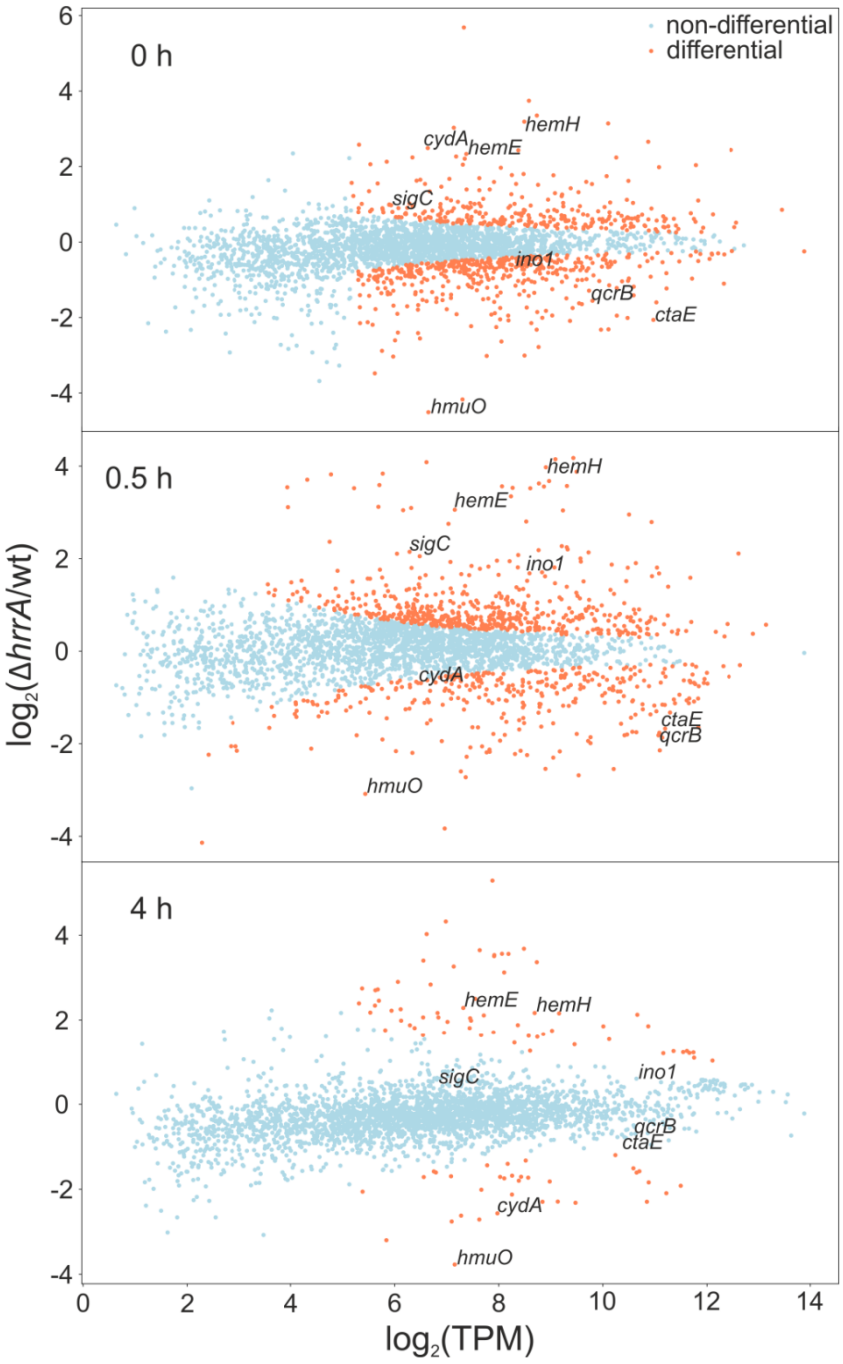

Figure S9: Time-resolved differential gene expression analysis. Shown is the $\log_2$ fold change in gene expression (Δ*hrrA* versus wild type) along with a $\log_2$ mean expression (expression averaged for Δ*hrrA* and WT samples) in transcripts per million (TPM). Orange dots represent significantly differentially expressed genes with an empirical FDR <0.05 (see material and methods). Wild type and Δ*hrrA C. glutamicum* strains were grown in CGXII medium (without $FeSO_4$) supplemented with 2% (w/v) glucose and 4 µM hemin (T_0 is prior addition of hemin; for details on cultivation and sample preparation see material and methods).

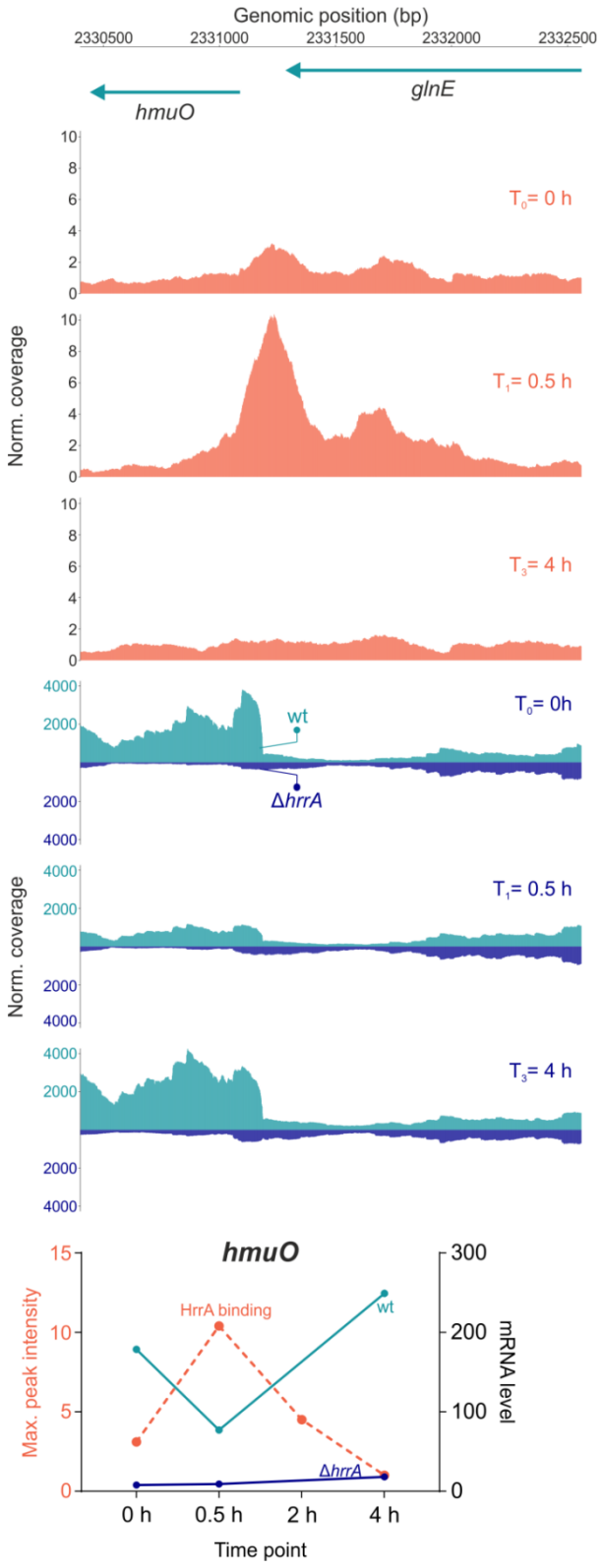

Figure S10: HrrA-dependent *hmuO* expression in response to heme. Shown are the ChAP-Seq (orange) and RNA-Seq (blue) results focusing on the *hmuO* locus in the genomic region between *hmuO* (cg2445) and *glnE* (cg2446). For the cultivation, CGXII medium supplemented with 2% (w/v) glucose and 4 µM hemin was inoculated with iron starved cells from a stationary culture and adjusted to an OD_{600} of 3.5. Samples were analysed at the indicated time points as described in material and methods.

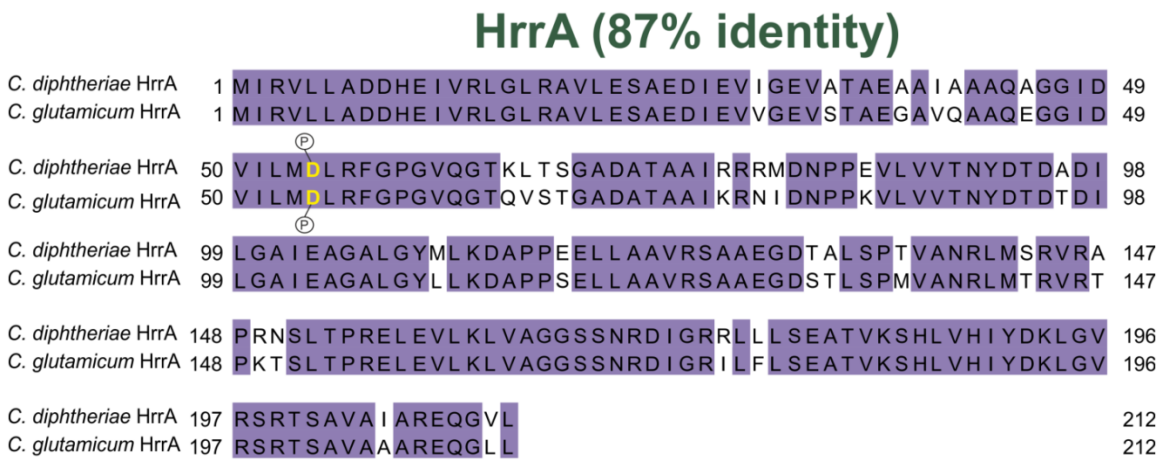

Figure S11: Alignment of HrrA orthologs of *C. glutamicum* and *C. diphtheria*. The aligment was generated with Clustal Omega (https://www.ebi.ac.uk/Tools/msa/clustalo/) and visualized using Jalview (http://www.jalview.org/). Indicated in purple are identical amino acids and in yellow are the aspartate residues which become phosphorylated by HrrS.

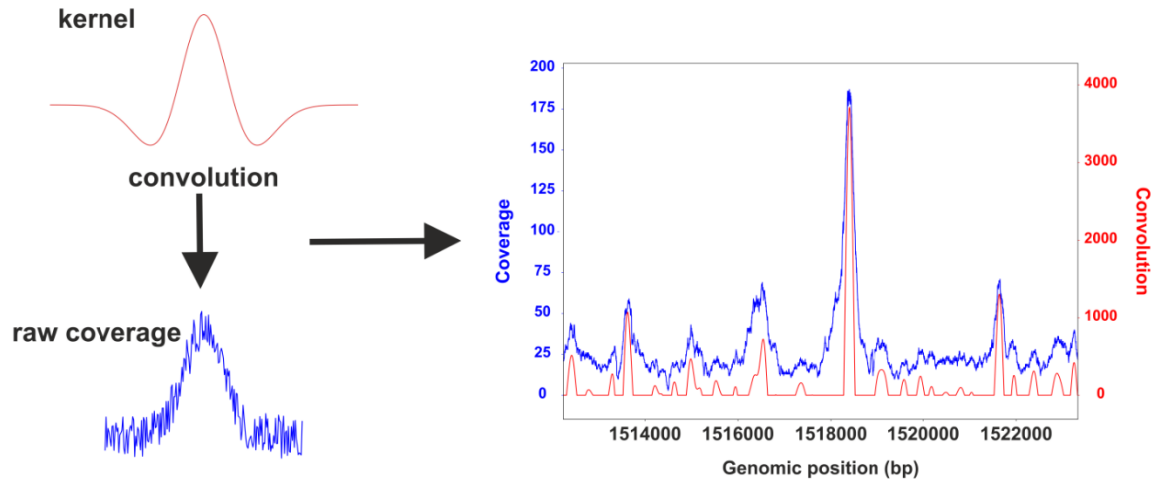

Figure S12: Schematic overview of the convolution profiling. Read coverage was convolved with negative second order Gaussian kernel. The convolved read coverage was then scanned to discover the local maxima (peaks).

References to the supplements to "HrrSA orchestrates a systemic response to heme and determines prioritisation of terminal cytochrome oxidase expression"

1 Studier, F. W. & Moffatt, B. A. Use of bacteriophage T7 RNA polymerase to direct selective high-level expression of cloned genes. *Journal of molecular biology* **189**, 113-130 (1986).

2 Kalinowski, J., Bathe, B., Bartels, D., Bischoff, N., Bott, M., Burkovski, A., Dusch, N., Eggeling, L., Eikmanns, B. J., Gaigalat, L., Goesmann, A., Hartmann, M., Huthmacher, K., Kramer, R., Linke, B., McHardy, A. C., Meyer, F., Mockel, B., Pfefferle, W., Puhler, A., Rey, D. A., Ruckert, C., Rupp, O., Sahm, H., Wendisch, V. F., Wiegrabe, I. & Tauch, A. The complete *Corynebacterium glutamicum* ATCC 13032 genome sequence and its impact on the production of L-aspartate-derived amino acids and vitamins. *Journal of biotechnology* **104**, 5-25 (2003).

3 Frunzke, J., Gatgens, C., Brocker, M. & Bott, M. Control of heme homeostasis in *Corynebacterium glutamicum* by the two-component system HrrSA. *Journal of bacteriology* **193**, 1212-1221, doi:10.1128/jb.01130-10 (2011).

4 Heyer, A., Gatgens, C., Hentschel, E., Kalinowski, J., Bott, M. & Frunzke, J. The two-component system ChrSA is crucial for haem tolerance and interferes with HrrSA in haem-dependent gene regulation in *Corynebacterium glutamicum*. *Microbiology (Reading, England)* **158**, 3020-3031, doi:10.1099/mic.0.062638-0 (2012).

5 Cremer, J., Eggeling, L. & Sahm, H. Cloning the *dapA dapB* cluster of the lysine-secreting bacterium *Corynebacterium glutamicum*. *Molecular and General Genetics MGG* **220**, 478-480, doi:10.1007/bf00391757 (1990).

6.4 Supplementary materials – Further characterization of Surf1

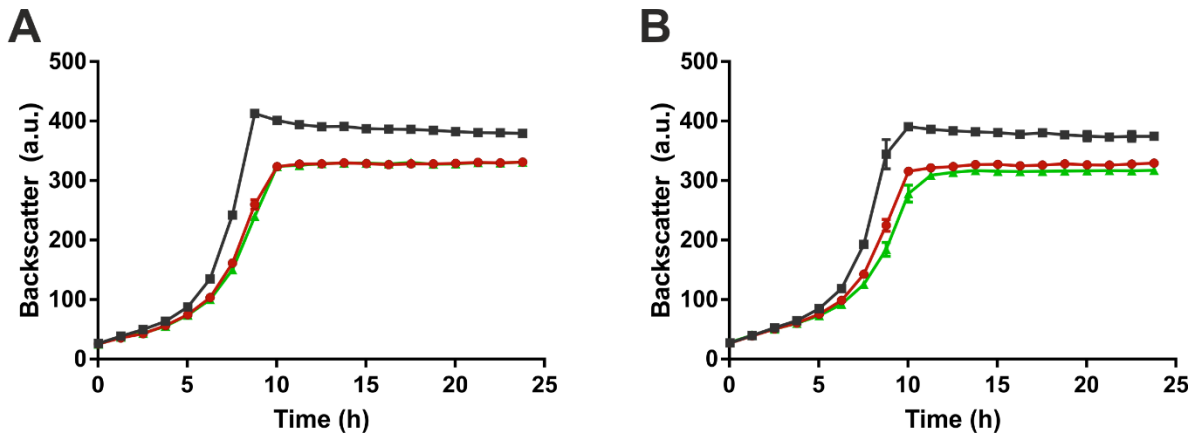

Figure S6.4.1. Impact of *ctaA* expression on the growth defect of *C. glutamicum* Δ*surf1*. The Δ*surf1* strain harboring the *ctaA* expression plasmid pAN6_*ctaA* (green triangles) was cultivated at 30 °C and 1200 rpm in a BioLector microcultivation system using FlowerPlates™ containing CGXII minimal medium with 2% (w/v) glucose and either devoid of (A) or with addition of 100 µM IPTG (B). As controls, the wt (black squares) and Δ*surf1* strain (red circles) harboring the empty plasmid were used. The Backscatter (620 nm) of biological triplicates was measured every hour.

Table S6.4. Identification of co-purified Surf1 interaction partners. Depicted are peptides (95% confidence) found in the elution fractions of purified Surf1-variants. Treatment of N- or C-terminally Strep-tagged Surf1 with 1 % formaldehyde (30 min) is indicated with a plus (+). Analysis of the proteins was performed by LC-MS. Not identified peptides are listed as n.a.

		Peptides (95%)			
Locus tag	**Annotated function**	**N-Surf1$_{St}$**	**N-Surf1$_{St}$ (+)**	**C-Surf1$_{St}$**	**C-Surf1$_{St}$ (+)**
cg2460	Hypothetical protein	64	33	14	10
cg1368	AtpD, ATP synthase subunit B	30	28	32	30
cg0811	DtsR2, acetyl/propionyl CoA carboxylase, beta subunit	24	23	22	18
cg1366	AtpA, ATP synthase subunit A	22	26	23	21
cg0802	AccBC, biotin carboxylase and biotin carboxyl carrier protein	24	24	34	37
cg2361	DivIVA, essential role in cell elongation	23	27	15	13
cg2833	CysK, *O*-acetylserine (thiol)-lyase	13	19	12	16
cg2444	Hypothetical protein	8	4	10	11
cg0601	RpsC, 30S ribosomal protein S3	11	13	12	10
cg0446	SdhA, succinate dehydrogenase	13	21	18	18
cg0598	RplB, 50S ribosomal protein L2	20	17	18	19
cg1365	AtpH, ATP synthase subunit D	9	12	8	10
cg1531	RpsA, 30S ribosomal protein S1	21	21	20	16
cg0631	RpsE, 30S ribosomal protein S5	22	13	12	10
cg3177	PccB, propionyl-CoA carboxylase beta chain	18	16	8	8
cg0654	RpsD, 30S ribosomal protein S4	15	11	13	13
cg0583	FusA, elongation factor EF-2	25	21	18	20
cg3100	DnaK, molecular chaperone Dnak	18	24	22	27
cg1556	Hypothetical protein	13	12	11	10
cg2675	ATPase component of ABC-type transport system, contains duplicated ATPase domains	18	20	11	11
cg0610	RplE, 50S ribosomal protein L5	6	9	7	7
cg1367	AtpG, ATP synthase subunit C	8	8	11	8
cg0957	Fas-IB, fatty acid synthase	59	50	34	45
cg1656	Ndh, NADH dehydrogenase	11	8	9	8
cg1737	Acn, aconitate hydratase	14	17	17	19
cg2151	sSmilar to phage shock protein A	17	12	9	10
cg2222	RpsB, 30S ribosomal protein S2	12	14	12	12
cg0417	CapD, probable dTDP-glucose 4,6-dehydratase transmembrane protein	18	12	6	6
cg0596	RplD, 50S ribosomal protein L4	9	7	8	7
cg2120	PtsF, sugar specific PTS system, fructose/mannitol-specific transport protein	17	13	9	9
cg0630	RplR, 50S ribosomal protein L18	3	5	4	4
cg0674	RpsI, 30S ribosomal protein S9	6	5	8	8
cg0414	Wzz, cell surface polysaccharide biosynthesis / chain length determinant protein	10	10	5	5
cg2421	SucB, dihydrolipoamide acetyltransferase	7	3	4	7
cg2466	AceE, pyruvate dehydrogenase subunit E1	21	21	21	25

cg1813	CarB, carbamoyl-phosphate synthase large subunit	31	11	12	17
cg2977	Hypothetical protein	11	10	n.a.	0
cg0791	Pyc, pyruvate carboxylase	39	28	40	39
cg1537	PtsG, glucose-specific enzyme II BC component of PTS	6	8	6	6
cg1586	ArgG, argininosuccinate synthase	13	8	5	7
cg1307	Superfamily II DNA and RNA helicase	20	11	10	12
cg3068	Fda, fructose-bisphosphate aldolase	3	7	5	7
cg0572	RplJ, 50S ribosomal protein L10	7	9	7	8
cg2404	QcrA1, rieske iron-sulfur protein	13	16	11	9
cg0652	RpsM, 30S ribosomal protein S13	7	6	9	6
cg0752	Putative secreted or membrane protein	21	18	7	8
cg0587	Tuf, elongation factor Tu	7	18	22	23
cg0438	Putative glycosyltransferase	10	5	3	3
cg0597	RplW, 50S ribosomal protein L23	4	3	3	3
cg2695	ABC-type transport system, ATPase component	12	9	8	9
cg2403	QcrB, cytochrome *b*, membrane protein	8	8	6	10
cg0594	RplC, 50S ribosomal protein L3	8	7	10	9
cg0573	RplL, 50S ribosomal protein L7/L12	12	10	8	9
cg2166	GpsI, putative polyribonucleotide phosphorylase / guanosine pentaphosphatesynthetase	16	11	15	16
cg0629	RplF, 50S ribosomal protein L6	4	6	9	8
cg0600	RplV, 50S ribosomal protein L22	7	7	7	7
cg2780	CtaD, cytochrome *c* oxidase polypeptide subunit	6	5	4	5
cg0602	RplP, 50S ribosomal protein L16	6	4	4	4
cg2262	FtsY, signal recognition particle GTPase	8	7	4	5
cg1280	kgd, alpha-ketoglutarate decarboxylase	17	15	25	31
cg2743	Fas-IA, fatty acid synthase	28	20	6	15
cg0628	RpsH, 30S ribosomal protein S8	6	4	4	3
cg0949	GltA, citrate synthase	3	6	6	5
cg0693	GroEL, 60 KDA chaperonin (protein CPN60) (groel protein) C-terminal fragment	8	12	7	8
cg2840	ActA, butyryl-CoA:acetate coenzyme A transferase	13	14	13	17
cg1046	Ppk2A, polyphosphate kinase	8	4	5	6
cg0867	Ribosome-associated protein Y (PSrp-1)	7	5	5	6
cg0420	Glycosyl transferase	11	5	1	n.a.
cg1787	Ppc, phosphoenolpyruvate carboxylase	16	9	10	12
cg1762	SufC, Fe-S cluster assembly ATPase	6	3	2	3
cg1730	Secreted protease subunit, stomatin/prohibitin homolog	10	8	7	8
cg1773	CtaB, heme *o* synthase	4	5	n.a.	n.a.
cg3018	Hypothetical protein	15	8	6	6
cg2429	GlnA, glutamine synthetase I	3	8	9	8
cg3114	CysN, sulfate adenyltransferase subunit 1	4	8	6	9
cg3219	Ldh, L-lactate dehydrogenase	7	8	7	6
cg0582	RpsG, 30S ribosomal protein S7	9	6	8	7
cg0564	RplA, 50S ribosomal protein L1	7	8	9	9
cg0737	ABC-type transport system, secreted lipoprotein component	4	6	1	1
cg0576	RpoB, DNA-directed RNA polymerase beta subunit	12	10	17	16

cg1111	Eno, phosphopyruvate hydratase	8	11	14	12
cg0812	DtsR1, acetyl/propionyl-CoA carboxylase beta chain	8	4	6	8
cg3011	GroEL, chaperonin groel	11	13	14	18
cg2708	MsiK1, ABC-type sugar transport system, ATPase component	5	10	8	7
cg0766	Icd, isocitrate dehydrogenase	4	16	10	11
cg0577	RpoC, DNA-directed RNA polymerase beta subunit	9	12	26	25
cg2963	ClpC, probable ATP-dependent protease (heat shock protein)	6	8	15	15
cg1606	PyrG, CTP synthetase	8	4	2	5
cg2862	PurL, phosphoribosylformylglycinamidine synthase subunit II	7	11	7	11
cg2958	ButA, L-2,3-butanediol dehydrogenase/acetoin reductase	4	6	5	7
cg0488	Ppx1, exopolyphosphatase	10	4	6	6
cg3191	Predicted glycosyltransferase	10	5	2	4
cg0603	RpmC, 50S ribosomal protein L29	6	4	5	5
cg2984	FtsH, cell-division protein (ATP-dependent Zn metallopeptidase)	12	10	2	4
cg2786	NrdE, ribonucleotide-diphosphate reductase alpha subunit	9	5	2	5
cg1348	Membrane protein containing CBS domain	9	8	n.a.	n.a.
cg0237	Short chain dehydrogenase	5	5	6	5
cg0868	SecA, translocase	8	13	20	13
cg1791	Gap, glyceraldehyde-3-phosphate dehydrogenase	6	4	8	7
cg1128	Similar to ribosomal protein S2	3	2	3	2
cg1409	PfkA, 6-phosphofructokinase	6	3	6	6
cg1437	IlvC, ketol-acid reductoisomerase	4	4	2	4
cg0655	RpoA, DNA-directed RNA polymerase alpha subunit	7	5	9	10
cg1354	Rho, transcription termination factor Rho	12	7	3	6
cg0424	Putative glycosyltransferase	6	4	2	2
cg0448	Hypothetical protein	1	1	1	1
cg0307	Asd, aspartate-semialdehyde dehydrogenase	2	2	5	6
cg0653	RpsK, 30S ribosomal protein S11	3	3	4	4
cg1725	MutA, methylmalonyl-CoA mutase, subunit	3	3	2	4
cg2167	RpsO, 30S ribosomal protein S15	3	3	4	3
cg1603	Hypothetical protein	8	6	4	2
cg2782	Ftn, ferritin-like protein	3	2	3	4
cg0928	ABC-type cobalamin/Fe^{3+}-siderophores transport system, ATPase component	5	1	3	0
cg3308	RpsF, 30S ribosomal protein S6	2	3	7	6
cg2705	AmyE, maltose-binding protein precursor	5	8	1	2
cg2678	ABC-type dipeptide/oligopeptide/nickel transport systems, secreted component	2	5	1	1
cg0165	ABC-2 type transporter	5	n.a.	n.a.	n.a.
cg0991	RpmB, 50S ribosomal protein L28	4	4	6	6
cg1451	SerA, phosphoglycerate dehydrogenase	4	10	6	10
cg2410	LtsA, glutamine-dependent amidotransferase	12	6	8	5

cg0435	UdgA1, UDP-glucose 6-dehydrogenase	5	3	3	2
cg0229	GltB, glutamine 2-oxoglutarate aminotransferase large SU	2	22	13	25
cg2091	PpgK, polyphosphate glucokinase	5	2	0	1
cg1369	AtpC, ATP synthase subunit epsilon	2	3	2	2
cg2496	Putative secreted protein	8	4	7	4
cg1408	Hypothetical protein	2	1	1	0
cg3255	UspA3, universal stress protein family	4	4	4	5
cg2141	RecA, recombinase A	6	3	1	2
cg2424	Hypothetical protein	6	6	5	3
cg0518	HemL, glutamate-1-semialdehyde aminotransferase	7	4	3	4
cg0418	Putative aminotransferase	5	3	1	0
cg2994	Putative secreted or membrane protein	1	2	2	2
cg3244	Hypothetical protein	6	3	5	5
cg2137	GluB, glutamate secreted binding protein	2	2	n.a.	0
cg3115	CysD, sulfate adenylyltransferase subunit 2	7	8	3	6
cg1841	AspS, aspartyl-tRNA synthetase	5	6	6	5
cg3049	FprA, putative ferredoxin/ferredoxin-NADP reductase	7	3	9	8
cg0156	CysR, transcriptional regulator involved in sulphonate utilisation	5	2	2	2
cg2366	FtsZ, cell division protein FtsZ	3	3	3	5
cg2647	Tig, trigger factor	1	7	7	5
cg1362	AtpB, ATP synthase subunit A	2	2	2	1
cg1269	GlgC, ADP-glucose pyrophosphorylase	6	5	1	3
cg2235	RplS, 50S ribosomal protein L19	7	5	4	5
cg0359	Hypothetical protein cg0359	4	5	3	3
cg2218	PyrH, uridylate kinase	3	2	3	1
cg0691	GroEL', 60 KDA chaperonin (protein CPN60) (HSP60)-N-terminal fragment	4	4	2	4
cg2291	Pyk, pyruvate kinase	11	13	13	14
cg3264	Hypothetical protein	13	9	4	4
cg2087	Hypothetical protein	5	3	2	2
cg2811	ABC-type transport system, involved in lipoprotein release, permease component	1	2	1	1
cg0528	Putative secreted protein	2	2	2	2
cg1629	SecA2, translocase	5	2	5	5
cg0248	Putative ABC-type polysaccharide/polyol phosphate export sytem, ATPase	2	4	1	0
cg1248	GTPase involved in stress response	4	8	9	10
cg1463	GltX, glutamyl-tRNA synthetase	5	4	1	2
cg1565	RplT, 50S ribosomal protein L20	5	5	6	5
cg0998	Trypsin-like serine protease	2	1	3	1
cg0781	Membrane protein	3	3	2	1
cg0161	Putative secreted or membrane protein	2	1	1	0
cg0810	Hypothetical protein	3	3	2	1
cg0683	Permease	5	5	2	2
cg0441	Lpd, dihydrolipoamide dehydrogenase	8	6	10	9
cg1838	AlaS, alanyl-tRNA synthetase	9	9	12	12

cg2176	InfB, translation initiation factor IF-2	6	6	7	13
cg3141	Hmp, flavohemoprotein	1	4	1	2
cg3017	Hypothetical protein	4	5	3	1
cg0783	Hypothetical protein	1	3	1	3
cg1867	SecD, protein export protein SecD	4	2	1	1
cg0007	GyrB, DNA topoisomerase IV subunit B	15	8	7	5
cg0952	Putative integral membrane protein	2	2	n.a.	n.a.
cg1344	NarG, nitrate reductase 2, alpha subunit	1	14	1	6
cg1121	Permease of the major facilitator superfamily	1	1	0	1
cg2474	NagD, putative phosphatase in N-acetylglucosamine metabolism	3	3	2	3
cg2428	Hypothetical protein	3	2	2	n.a.
cg2521	FadD15, long-chain fatty acid CoA ligase	11	6	8	7
cg2923	Putative rRNA methyltransferase TRMH family	5	4	3	4
cg3138	PpmA, putative membrane-bound protease modulator	4	5	3	0
cg2644	ClpP2, ATP-dependent Clp protease proteolytic subunit	4	2	2	1
cg3189	Hypothetical protein	5	2	0	n.a.
cg1551	UspA1, universal stress protein UspA and related nucleotide-binding proteins	2	4	5	6
cg0419	Glycosyltransferase	5	1	n.a.	n.a.
cg2861	Membrane protein, hemolysin III homolog	1	n.a.	0	n.a.
cg1133	GlyA, serine hydroxymethyltransferase	5	5	7	6
cg2812	ABC-type transport system, involved in lipoprotein release, ATPase component	4	4	2	2
cg2406	CtaE, cytochrome *c* oxidase subunit III	2	1	1	n.a.
cg2417	Short chain dehydrogenase	2	4	3	4
cg0673	RplM, 50S ribosomal protein L13	3	3	5	4
cg1141	Hypothetical protein	3	1	1	2
cg2280	Gdh, glutamate dehydrogenase	2	5	8	9
cg1165	Gamma-aminobutyrate permease or related permease	1	3	n.a.	n.a.
cg2192	Mqo, malate:quinone oxidoreductase	2	2	2	2
cg1338	ThrB, homoserine kinase	2	n.a.	0	n.a.
cg0845	Superfamily II DNA/RNA helicase, SNF2 family	5	n.a.	0	0
cg2160	Hydrolase of metallo-beta-lactamase superfamily	6	3	6	9
cg2498	Hypothetical protein	1	3	0	n.a.
cg3429	Putative inner membrane protein translocase component YidC	1	2	1	1
cg0838	Helicase	12	1	3	4
cg2779	SerB, phosphoserine phosphatase	3	1	n.a.	1
cg2214	Predicted Fe-S-cluster redox enzyme	5	n.a.	n.a.	1
cg2891	PoxB, pyruvate dehydrogenase	5	2	11	12
cg2594	RpmA, 50S ribosomal protein L27	1	n.a.	4	3
cg1109	PorB, anion-specific porin precursor	3	2	n.a.	0
cg2201	Signal transduction histidine kinase	4	n.a.	2	3
cg1433	Hypothetical protein	1	1	1	1
cg1844	Membrane protein	1	1	n.a.	n.a.
cg3192	Putative secreted or membrane protein	2	7	6	1

cg1763	SufD, Fe-S cluster assembly membrane protein	3	2	2	5
cg3020	Hypothetical protein	1	1	1	n.a.
cg2492	GlmS, D-fructose-6-phosphate amidotransferase	3	5	9	5
cg1007	Hypothetical protein	2	3	n.a.	n.a.
cg2467	ABC transporter ATP-binding protein	2	3	1	0
cg2657	Putative membrane protein-fragment	2	1	3	1
cg3365	UlaA, ascorbate-specific PTS system enzyme IIC	1	2	2	1
cg3079	ClpB, probable ATP-dependent protease (heat shock protein)	2	3	4	10
cg2781	NrdF, ribonucleotide-diphosphate reductase beta subunit	3	2	2	1
cg0593	RpsJ, 30S ribosomal protein S10	3	1	4	4
cg1404	GatA, glutamyl-tRNA amidotransferase subunit A	1	4	0	3
cg2412	Hypothetical protein	5	0	2	2
cg1283	AroE, shikimate 5-dehydrogenase	1	0	n.a.	n.a.
cg0063	Secreted protein	1	1	2	n.a.
cg1753	ATPase component of ABC transporters with duplicated ATPase domains	3	0	3	3
cg0047	Hypothetical protein	1	3	3	4
cg0841	Hypothetical protein	2	2	2	2
cg1075	PrsA, ribose-phosphate pyrophosphokinase	1	2	2	1
cg0840	Hypothetical protein	2	0	1	n.a.
cg1081	ABC-type multidrug transport system, ATPase component	1	1	1	1
cg1793	Hypothetical protein	2	1	1	1
cg3301	Permease of the major facilitator superfamily	1	1	n.a.	n.a.
cg2611	HscA, molecular chaperone, HSP70 family	2	0	n.a.	0
cg0375	CyaB, adenylate cyclase	1	0	n.a.	n.a.
cg2500	Bacterial regulatory proteins, ArsR family	1	0	0	1
cg1806	MetK, S-adenosylmethionine synthetase	1	0	n.a.	n.a.
cg0373	TopA, DNA topoisomerase I	3	0	3	1
cg3340	DadA, putative D-amino acid dehydrogenase (deaminating)	1	n.a.	n.a.	0
cg1865	SecF, protein export protein SecF	2	3	1	n.a.
cg2409	CtaC, cytochrome *c* oxidase chain II	3	2	1	1
cg3404	ABC-type cobalamin/Fe3+-siderophores transport system, secreted component	2	1	1	n.a.
cg2198	Map2, methionine aminopeptidase	5	1	4	3
cg2850	Hypothetical protein	2	1	2	3
cg0464	CtpA, copper-transporting ATPase	2	n.a.	0	0
cg3242	Hypothetical protein	4	0	n.a.	0
cg0310	KatA, catalase	2	2	4	2
cg2111	HrpA, put. ATP-dependent RNA helicase protein	1	n.a.	1	1
cg0848	WbbL, putative rhamnosyl transferase WbbL	1	n.a.	0	1
cg2597	Rne, probable ribonuclease E (RNase E) protein	1	n.a.	n.a.	2
cg2964	GuaB1, inositol-5-monophosphate dehydrogenase	6	n.a.	n.a.	n.a.
cg2321	DNA polymerase III epsilon subunit	1	1	1	1

6.5 Supplementary materials – Characterization of Cg2750 and σ^C

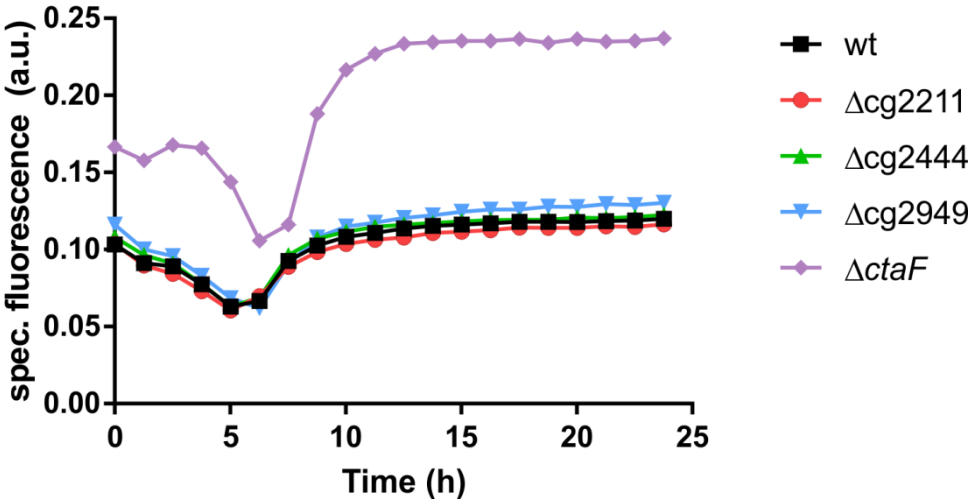

Figure S6.5.1. Activity analysis of the *cyd* promoter in *C. glutamicum* strains. Strains carrying the pJC1-P_{cyd}-*venus* reporter plasmid were cultivated in the BioLector microcultivation system at 30 °C and 1200 rpm using FlowerPlates™ in CGXII medium with 2% (w/v) glucose. Backscatter values (620 nm) and Venus fluorescence output (excitation 510 nm/emission 532 nm) of biological triplicates were measured every hour. Depicted is the mean and S.D. of the specific fluorescence (absolute fluorescence/backscatter).

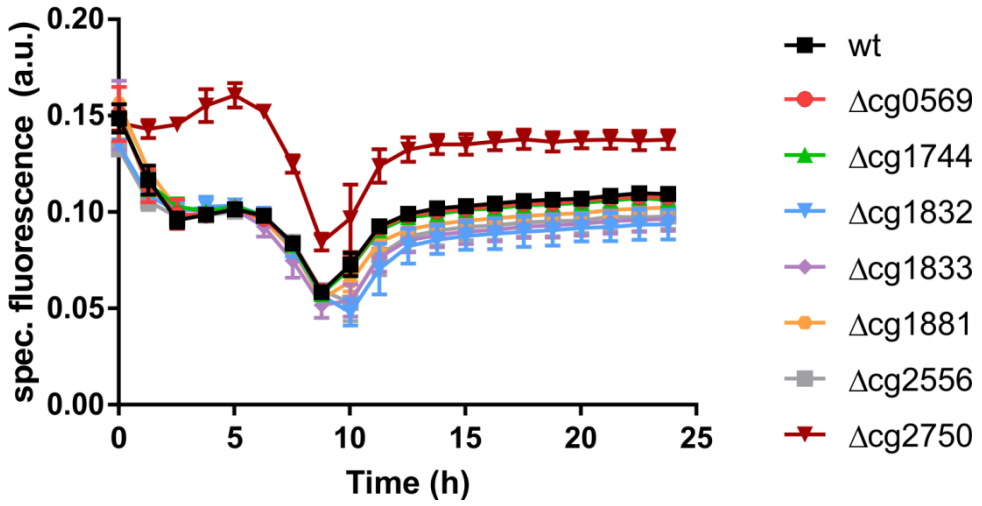

Figure S6.5.2. Activity analysis of the *cyd* promoter in *C. glutamicum* strains. Strains carrying the pJC1-P$_{cyd}$-*venus* reporter plasmid were cultivated in the BioLector microcultivation system at 30 °C and 1200 rpm using FlowerPlates™ in CGXII medium with 2% (w/v) glucose. Backscatter values (620 nm) and Venus fluorescence output (excitation 510 nm/emission 532 nm) of biological triplicates were measured every hour. Depicted is the mean and S.D. of the specific fluorescence (absolute fluorescence/backscatter).

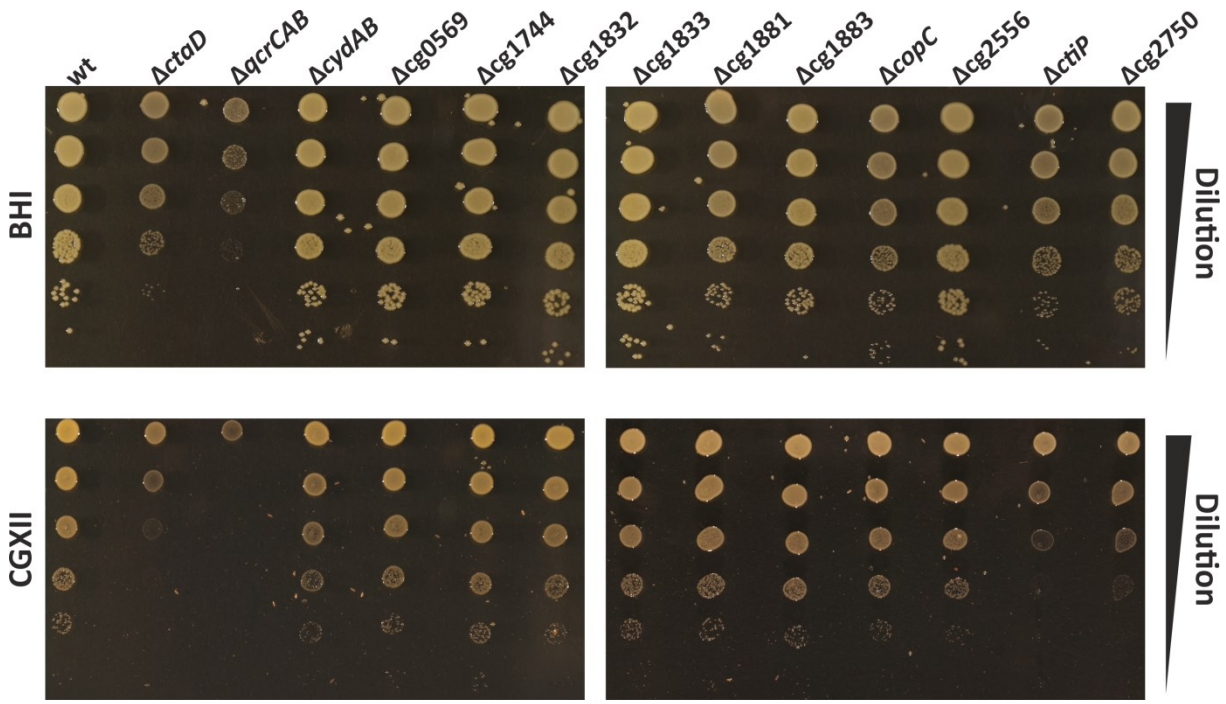

Figure S6.5.3. Growth properties of *C. glutamicum* copper-deprivation stimulon gene deletion strains. Construction of the deletion strains was based on a selection of an at least 3-fold increased gene expression level under copper-deprivation (150 µM BCS, 1 mM ascorbate) compared to copper-sufficiency (1.25 µM $CuSO_4$). Cells were spotted on BHI and CGXII agar plates with 2% (w/v) glucose in serial dilutions (3 µl each, 10^0 to 10^{-5}) adjusted to an OD_{600} of 1 and diluted in 0.9% (w/v) NaCl. The wt strain, Δ*ctaD*, Δ*qcrCAB* and Δ*cydAB* were used as controls. Incubation of the plates was performed at 30 °C for 48 h.

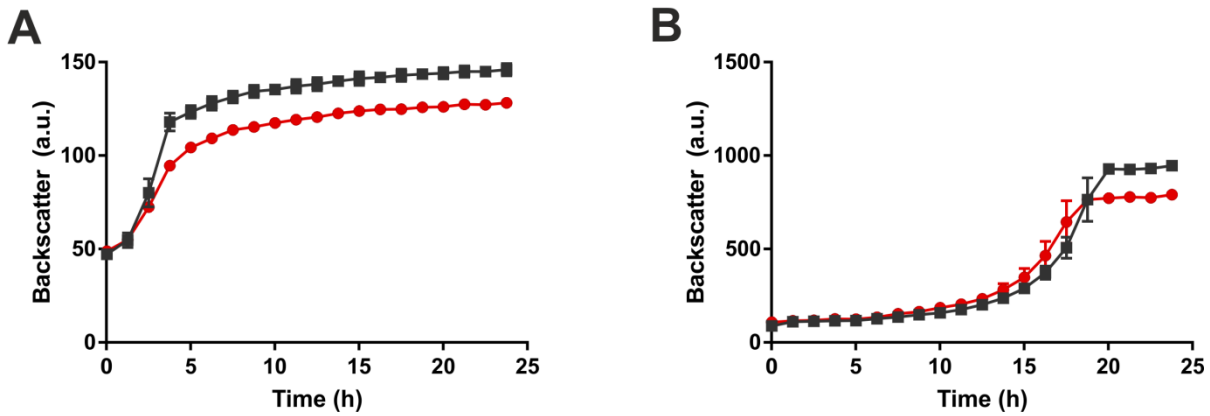

Figure S6.5.4. Growth properties of the *C. glutamicum* Δcg2750 strain (red circles) compared to the wt (black squares). The cultivations were performed at 30 °C and 1200 rpm in a BioLector microcultivation system using FlowerPlates™ containing BHI medium with 2% (w/v) glucose (A) or CGXII minimal medium (2 % (w/v) glucose) supplemented with 100 µM $CuSO_4$ (B). Mean and S.D. of hourly backscatter measurements at 620 nm of biological triplicates are depicted.

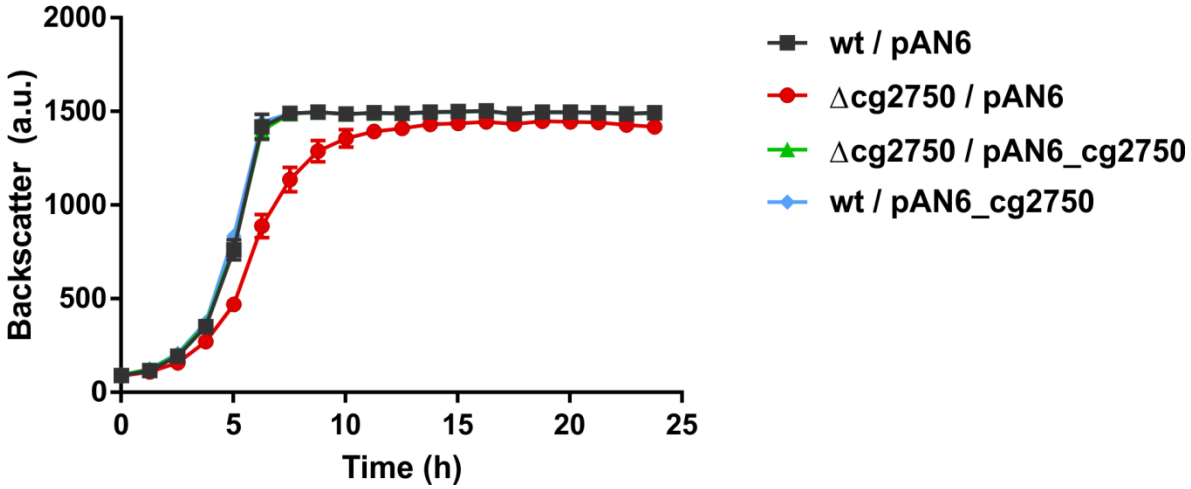

Figure S6.5.5. Complementation of the growth defect of the *C. glutamicum* Δcg2750 strain. The cultivations were performed at 30 °C and 1200 rpm in a BioLector microcultivation system using FlowerPlates™ containing CGXII minimal medium with 2% (w/v) glucose. Backscatter (620 nm) of biological triplicates was measured every hour.

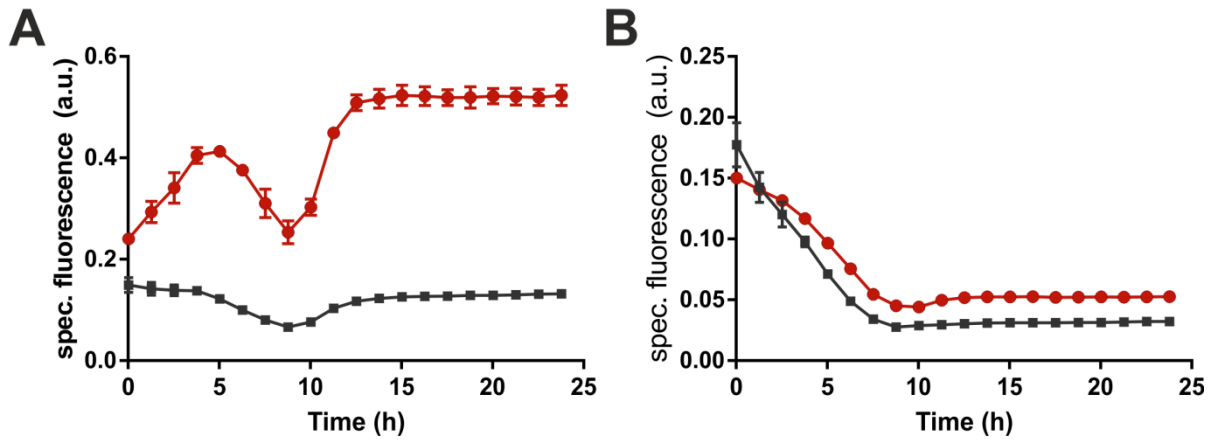

Figure S6.5.6. Activity analysis of the *copC* and cg2556 promoter in *C. glutamicum* Δcg2750. The Δcg2750 strain and wt carrying the (A) pJC1-P_{copC}-*venus* or (B) pJC1-P_{cg2556}-*venus* reporter plasmid were cultivated in the BioLector microcultivation system at 30 °C and 1200 rpm using FlowerPlates™ in CGXII medium with 2% (w/v) glucose. Backscatter values (620 nm) and Venus fluorescence output (excitation 510 nm/emission 532 nm) of biological triplicates were measured every hour. Depicted is the mean and S.D. of the specific fluorescence (absolute fluorescence/backscatter).

Table S6.5. Identification of co-purified Cg2750 interaction partners. Depicted are peptides (95% confidence) with 50% or 95% coverage found in cut out protein bands of N-terminally Strep-tagged Cg2750. Analysis of the proteins was performed by LC-MS.

Locus Tag	Annotated function	Peptides(95%)	%Cov(50)	%Cov(95)
cg1368	AtpD, ATP synthase subunit B	8	18.63	18.63
cg1366	AtpA, ATP synthase subunit A	4	6.58	6,58
cg0802	AccBC, biotin carboxylase and biotin carboxyl carrier	4	8.12	8.12
cg2403	QcrB, cytochrome B, membrane protein	2	6.12	3.90
cg1367	AtpG, ATP synthase subunit C	3	13.23	10.46
cg1368	AtpD, ATP synthase subunit B	4	10.35	8.28
cg1365	AtpH, ATP synthase subunit D	4	13.65	13.65
cg2444	Hypothetical protein	2	22.50	12.50
cg3186	Cmt2, trehalose corynomycolyl transferase	1	3.23	3.23
cg2052	Putative secreted protein	1	4.29	4.29
cg1364	AtpF, ATP synthase subunit B	0	6.92	0.00
cg2211	Hypothetical protein	2	14.29	14.29
cg2750	Hypothetical protein	3	19.87	19.23

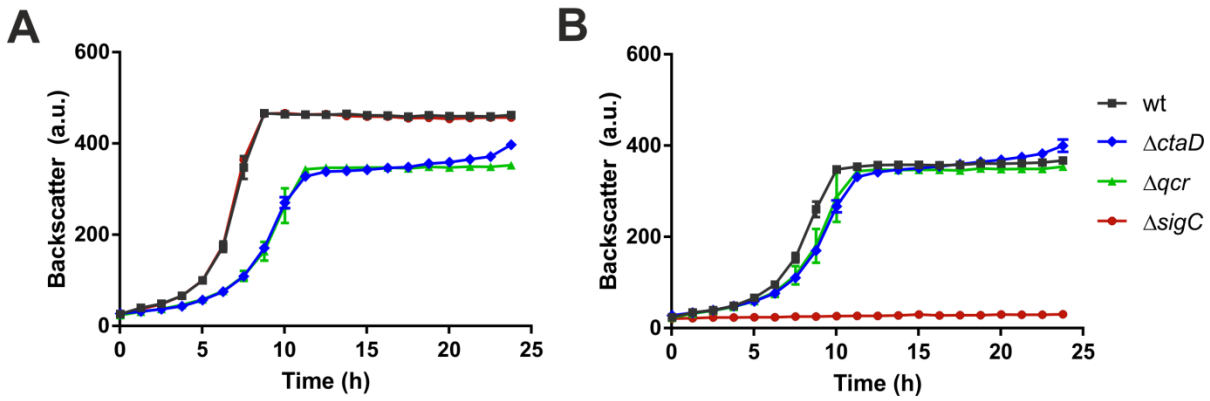

Figure S6.5.7. Growth properties of *C. glutamicum* deletion strains compared to the wt. The cultivations were performed at 30 °C and 1200 rpm in a BioLector microcultivation system using FlowerPlates™ containing 800 µl CGXII minimal medium with 2 % (w/v) glucose. In (A), standard medium with 1.25 µM $CuSO_4$ was used. For (B), the medium was devoid of added $CuSO_4$ and supplemented with 150 µM BCS and 1 mM ascorbic acid. Mean and S.D. of hourly backscatter measurements at 620 nm taken of biological triplicates are depicted.

Danksagung

Ein besonderer Dank gilt Prof. Dr. Michael Bott und Dr. Meike Baumgart, für die Überlassung des spannenden Themas, das große Interesse an meinem Thema und die vielen hilfreichen Diskussionen.

Auch bedanke ich mich bei Prof. Dr. Georg Groth für die freundliche Übernahme des Zweitgutachtens.

Des Weiteren will ich mich bei den Kollegen bedanken, die an den Projekten dieser Arbeit beteiligt waren: Prof. Dr. Julia Frunzke, Dr. Marc Keppel, Dr. Andrei Filipchyk und Ulrike Viets für die tolle Zusammenarbeit am HrrA-Projekt, sowie Dr. Tino Polen und Dr. Melanie Brocker für die große Hilfe am Kupfer-Chaperon Thema.

Natürlich will ich mich an dieser Stelle auch bei allen aktuellen und ehemaligen Mitgliedern der AG Bott/Baumgart (Alina, Andi, Brita, Karen, Ines, Johanna, Julia, Kim, Lingfeng, Lukas, dem anderen Lukas, Maike, Natalie, Paul, Sarah, Susana, Tina, Yannik) für die spaßige Arbeitsatmosphäre bedanken und dafür, dass ich durch euch meine Sucht für Kaffee entdeckt habe. Darüber hinaus bedanke ich mich bei nicht-AG Mitgliedern Max und Lion für die stets arbeitsfremden Unterhaltungen.

Darüber hinaus bedanke ich mich bei der großartigen Infrastruktur, insbesondere bei Marion Dreßen-Combach, Nina Böckmann, Marlene Lauer, Kirsten Bräker und Iris Eggeling, die mir oft ausgeholfen haben.

Ich bedanke mich auch bei meinen Eltern, insbesondere meinem Vater, ohne den ich nicht an dem Punkt in meinem Leben wäre an dem ich jetzt bin.

Der größte Dank gilt Eva, die meinem Leben eine Richtung gegeben und mir eine Familie geschenkt hat, und dem kleinen Phil, der neben dieser Doktorarbeit mein größter Stolz ist.

Erklärung

Ich versichere an Eides Statt, dass die vorgelegte Dissertation von mir selbständig und ohne unzulässige fremde Hilfe unter Beachtung der „Grundsätze zur Sicherung guter wissenschaftlicher Praxis an der Heinrich-Heine-Universität Düsseldorf“ erstellt worden ist. Die Dissertation wurde in der vorgelegten oder in ähnlicher Form noch bei keiner anderen Institution eingereicht. Ich habe bisher keine erfolglosen Promotionsversuche unternommen.

_____

Jülich, den 28.02.2019